



Development of Aircraft Gas Turbine Engine Design and Optimization

Software

**Phase I: Cycle Design and Analysis of Turbojet and Turbofan Engines for
Subsonic Aircraft**

Mr. Pathompong Toposit Student ID 6101003662020

Mr. Thitiwat Pinkaew Student ID 6101003663051

Project report submitted in partial fulfillment of requirement for the bachelor's degree

Department of Mechanical and Aerospace Engineering

Faculty of Engineering

King Mongkut's University of Technology North Bangkok

ACADEMIC YEAR 2022



Dissertation Certificate

Department of Mechanical and Aerospace Engineering
King Mongkut's University of Technology North Bangkok

Title Development of Aircraft Gas Turbine Engine Design and Optimization Software Phase I: Cycle Design and Analysis of Turbojet and Turbofan Engines for Subsonic Aircraft

By Pathompong TOPISTIT 6101003662020
 Thitiwat PINKAEW 6101003663051

Accepted by Department of Mechanical and Aerospace Engineering, King Mongkut's University of Technology North Bangkok in Partial Fulfilment of the Requirements for Bachelor of Engineering in Mechanical Engineering

Asst. Prof. Pongsak NIMDUM, Ph.D.

Head of Department of Mechanical and Aerospace Engineering

Examination committee

Chairperson

Asst. Prof. Dr. Boonchai WATJATRAJUL, Ph.D.

Member

Dr.-Ing. Oleksiy ANTOSHKIV, Ph.D.

Member

Mr. Thanapol POOJITGANONT

Member

Asst. Prof. Pumyos VALLIKUL, D.Sc.

Project Topic	Development of Aircraft Gas Turbine Engine Design and Optimization Software Phase I: Cycle Design and Analysis of Turbojet and Turbofan Engines for Subsonic Aircraft	
By	Mr. Pathompong Toposit	6101003662020
	Mr. Thitiwat Pinkaew	6101003663051
Department	Mechanical and Aerospace Engineering	
Academic Year	2022	

Accepted by Department of Mechanical and Aerospace Engineering, Faculty of Engineering, King Mongkut's University of Technology North Bangkok in Partial Fulfillment of the Requirements for the Bachelor's Degree in Aerospace Engineering, International Program

(Asst. Prof. Pongsak Nimendum, PhD)

Head of Department of Mechanical and Aerospace Engineering

Examination committee

Main advisor

(Asst. Prof. Dr. Boonchai Watjatrakul (MAE-KMUTNB))

Co-advisor

(Dr.-Ing. Oleksiy Antoshkiv (VFA-BTU-CS))

Co-advisor

(Mr. Thanapol Poojitanont (VFA-BTU-CS))

Examiner

(Asst. Prof. Pumyos Vallikul (MAE-KMUTNB))

Abstract

The objective of this project is to develop an in-house aircraft engine design software to study the aircraft engine design process as well as for educational purpose and further research. Parametric cycle analysis is performed with the purpose to determine the performance of aircraft engines at different flight conditions, design choices, and design limit parameters. With parametric cycle analysis, the design software, namely “GTA” or “Gas Turbine Analysis” is developed with Python. It can perform a parametric cycle analysis from the given user requirements for three engines namely 1. single spool turbojet, 2. double spool turbojet, and 3. high bypass ratio turbofan. GTA offers two main functions: 1. single point calculation 2. variation point calculation. The outputs are in the form of text file and plots. For the plots, flight performance parameters namely specific thrust, thrust-specific fuel consumption, fuel/air ratio, and efficiencies are printed out to study the behavior of the range of design choices of compressor pressure ratio, free stream Mach number, fan pressure ratio, and bypass ratio. The validation between GTA and AEDsys (ONX) was carried out and it was found that the results obtained from GTA are slightly different from AEDsys (ONX) because of different ideal gas model CSH and MSH for single spool turbojet engine. For double spool turbojet engine and high bypass ratio turbofan engine, the results comparison between AEDsys (ONX) and GTA are quite different because of the different ideal gas model and different approach on background equations specifically for compressor pressure ratios. The behaviors of variation of design choices that affect the performance of an engine are explained in details to exhibit the important of each parameter.

Keywords: Parametric cycle analysis / aircraft engine design software / Python / turbojet engine/ turbofan engine

Acknowledgement

We would like to express our deepest and sincerest gratitude to all the involved people who help made this project possible and complete.

First and foremost, we would like to express our appreciation to our advisors: Asst. Prof. Boonchai Watjatrakul, Dr.-Ing. Oleksiy Antoshkiv, and Mr. Thanapol Poojitganont for granting us the opportunity to exercise our knowledge in doing this project as well as all of the suggestions bestowed upon us which led to the success of this project.

We wish to show our greatest appreciation towards our university, King's Mongkut University of Technology North Bangkok for granting us the opportunities and knowledge and also for all the help from the staffs as well as the local committee members who encouraged and give us the strength and supporting us to complete this report.

We also want to offer our immensely gratitude to Mr. Poomsak Choochim who is not only a great friend to us but also helping us in Python programming and guiding us through all the problem related.

Last but not least, thanks to our families and friends for always providing us supportive and heartfelt encouragement and always be there for us even when the light is dim.

“Happiness resides not in possessions, and not in gold, happiness dwells in the soul” – Democritus

“One good test is worth a thousand expert opinions” – Wernher von Braun

Table of Contents

Abstract.....	C
Acknowledgement.....	D
LIST OF FIGURES	G
LIST OF TABLES	P
Nomenclature	Q
1. Introduction	1
1.1 Objectives	1
1.2 Scope of project	1
1.3 Methodology.....	1
1.4 Schedule	1
1.4.1 Work plan	1
2. Cycle Analysis of Gas Turbine Engines.....	2
2.1 Fundamental Equations Analysis	3
2.2 Cycle Analysis of Single-Spool Turbojet Engine	8
2.2.1 Single-Spool Turbojet Engine – Ideal case	9
2.2.2 Single-Spool Turbojet Engine – Real case	21
2.3 Cycle Analysis of Double-Spool Turbojet Engine.....	34
2.3.1 Double-Spool Turbojet Engine – Real case.....	34
2.3.2 Double-Spool Turbojet Engine with Afterburner – Real case	41
2.4 Cycle Analysis of High Bypass Ratio Turbofan Engine.....	48
2.4.1 Forward Fan Unmixed Single-Spool Configuration.....	50
2.4.2 Forward Fan Unmixed Two-Spool Engines	54

2.4.3 Cycle analysis steps of High Bypass Ratio Turbofan Engine – Ideal case.....	56
2.4.4 Cycle analysis steps of High Bypass Ratio Turbofan Engine – Real case.....	60
3. Methodology	65
3.1 Introduction.....	65
3.1.1 Python Application.....	65
3.2. Validation Software.....	76
3.2.1 AEDsys.....	76
3.2.2 GasTurb	77
4. Result and Discussion.....	78
4.1 Case study and Validation with the textbook.....	78
4.1.1 Single-Spool Turbojet Engine	78
4.1.2 High Bypass Ratio Turbofan Engine.....	102
4.2 Case study and validation with AEDsys (ONX)	126
4.2.1 Single Point Calculation	126
4.2.2 Variation Calculation.....	131
5. Conclusion and Perspectives	156
5.1 Conclusions	156
5.2 Perspectives.....	157
References	158
Appendix A: Example case for subsonic flight	159
Case 1: Height variation for subsonic flight, commercial airliners.....	159

LIST OF FIGURES

Figure 1 Single-Spool Turbojet Engine [7].....	8
Figure 2 Temperature-entropy diagram for (a) ideal turbojet and (b) inoperative afterburner [7]	9
Figure 3 Temperature-entropy diagram for ideal turbojet, operative afterburner [7]..	13
Figure 4 Station numbering of ideal turbojet engine [8]	14
Figure 5 T-s diagram of an ideal turbojet engine [8]	14
Figure 6 T-s diagram for an ideal afterburning turbojet engine [8]	19
Figure 7 T-s diagram for real single-spool inoperative afterburner [7]	21
Figure 8 T-s diagram for real single-spool operative afterburner [7]	21
Figure 9 T-s diagram for real single-spool turbojet engine [8]	28
Figure 10 T-s diagram for single-spool real afterburning turbojet engine [8]	31
Figure 11 Double-Spool Turbojet Engine station [7]	34
Figure 12 T-s cycle for inoperative Double-Spool Turbojet [7]	34
Figure 13 Stations for a Double-Spool Turbojet Engine with operative afterburner [7]	41
Figure 14 Cycle for a Double-Spool Turbojet Engine with operative afterburner [7]...	41
Figure 15 Dual-Spool Afterburning Turbojet Engine [7]	43
Figure 16 High-Bypass Ratio Turbofan Engine station [8].....	48
Figure 17 T-s diagram for core stream of ideal turbofan engine [8]	49
Figure 18 T-s diagram for core stream of ideal turbofan engine [8]	49
Figure 19 Layout of a two-spool turbofan engine (fan and compressor driven by an LPT) [7]	54
Figure 20 T-s diagram of a two-spool turbofan engine [7].....	54
Figure 21 T-s diagram for core stream of ideal turbofan engine [8]	56
Figure 22 T-s diagram for fan stream of ideal turbofan engine [8]	56

Figure 23 Station numbering of a turbofan engine [8].....	57
Figure 24 T-s diagram of turbofan engine with losses (not to scale) [8].....	60
Figure 25 GTA flowchart	66
Figure 26 Input file name.....	66
Figure 27 Output .txt files	67
Figure 28 Output .png files	67
Figure 29 Input files in case of High-Bypass ratio turbofan engine for GTA	71
Figure 30 Text file output High-Bypass Ratio Turbofan Engine (Single Point Calculation)	72
Figure 31 Text file output High-Bypass Ratio Turbofan Engine (Variation Calculation)	73
Figure 32 Plot the output parameters variation calculation High Bypass Ratio Turbofan Engine.....	74
Figure 33 Example plot of the problem with limit of the graph.....	75
Figure 34 Python, Single-Spool Turbojet Engine.....	78
Figure 35 SSTJE Ideal M_0 vs π_c : Specific Thrust [8]	79
Figure 36 SSTJE Ideal M_0 vs π_c : Specific Thrust from GTA	79
Figure 37 SSTJE Ideal M_0 vs π_c :Thrust-Specific Fuel Consumption [8]	80
Figure 38 SSTJE Ideal M_0 vs π_c : Thrust-Specific Fuel Consumption from GTA	80
Figure 39 SSTJE Ideal M_0 vs π_c : fuel/air ratio [8]	81
Figure 40 SSTJE Ideal M_0 vs π_c : fuel/air ratio from GTA.....	81
Figure 41 SSTJE Ideal M_0 vs π_c : efficiencies [8].....	82
Figure 42 SSTJE Ideal M_0 vs π_c : efficiencies from GTA.....	82
Figure 43 SSTJE Ideal π_c vs M_0 : Specific Thrust [8]	83
Figure 44 SSTJE Ideal π_c vs M_0 : Specific Thrust from GTA.....	83
Figure 45 SSTJE Ideal π_c vs M_0 : Thrust-Specific Fuel Consumption [8].....	84
Figure 46 SSTJE Ideal π_c vs M_0 : Thrust-Specific Fuel Consumption from GTA	84

Figure 47 SSTJE Ideal π_c vs M_0 : fuel/air ratio [8].....	85
Figure 48 SSTJE Ideal π_c vs M_0 : fuel/air ratio from GTA	85
Figure 49 SSTJE Ideal π_c vs M_0 : efficiencies [8].....	86
Figure 50 SSTJE Ideal π_c vs M_0 : efficiencies from GTA.....	86
Figure 51 SSTJE IdealAB π_c vs M_0 : Specific Thrust and Thrust-Specific Fuel Consumption [8].....	87
Figure 52 SSTJE IdealAB π_c vs M_0 : Specific Thrust and Thrust-Specific Fuel Consumption from GTA	87
Figure 53 SSTJE IdealAB M_0 vs π_c : Specific Thrust [8]	88
Figure 54 SSTJE IdealAB M_0 vs π_c : Specific Thrust from GTA.....	88
Figure 55 SSTJE IdealAB M_0 vs π_c : Thrust-Specific Fuel Consumption [8].....	89
Figure 56 SSTJE IdealAB M_0 vs π_c : Thrust-Specific Fuel Consumption from GTA	89
Figure 57 SSTJE IdealAB M_0 vs π_c : fuel/air ratios [8].....	90
Figure 58 SSTJE IdealAB M_0 vs π_c : fuel/air ratios from GTA	90
Figure 59 SSTJE IdealAB M_0 vs π_c : efficiencies [8].....	91
Figure 60 SSTJE IdealAB M_0 vs π_c : efficiencies from GTA	91
Figure 61 SSTJE Real M_0 vs π_c : Specific Thrust [8].....	92
Figure 62 SSTJE Real M_0 vs π_c : Specific Thrust from GTA.....	92
Figure 63 SSTJE Real M_0 vs π_c : Thrust-Specific Fuel Consumption [8].....	93
Figure 64 SSTJE Real M_0 vs π_c : Thrust-Specific Fuel Consumption from GTA	93
Figure 65 SSTJE Real M_0 vs π_c : fuel/air ratio [8]	94
Figure 66 SSTJE Real M_0 vs π_c : fuel/air ratio from GTA.....	94
Figure 67 SSTJE Real M_0 vs π_c : efficiencies [8].....	95
Figure 68 SSTJE Real M_0 vs π_c : efficiencies from GTA	95
Figure 69 SSTJE Real π_c vs M_0 : Specific Thrust [8]	96
Figure 70 SSTJE Real π_c vs M_0 : Specific Thrust from GTA.....	96

Figure 71 SSTJE Real π_c vs M_0 : Thrust-Specific Fuel Consumption [8]	97
Figure 72 SSTJE Real π_c vs M_0 : Thrust-Specific Fuel Consumption from GTA	97
Figure 73 SSTJE Real π_c vs M_0 : fuel/air ratio [8].....	98
Figure 74 SSTJE Real π_c vs M_0 : fuel/air ratio from GTA.....	98
Figure 75 SSTJE Real π_c vs M_0 : efficiencies [8].....	99
Figure 76 SSTJE Real π_c vs M_0 : efficiencies from GTA.....	99
Figure 77 SSTJE RealAB vs Real, π_c : Specific Thrust and Thrust-Specific Fuel Consumption [8]	100
Figure 78 SSTJE RealAB vs Real, π_c : Specific Thrust and Thrust-Specific Fuel Consumption from GTA.....	101
Figure 79 Python, High-Bypass ratio Turbofan Engine.....	102
Figure 80 HBPTFE Ideal α vs π_c for $\pi_f = 2, M_0 = 0.9$: Specific Thrust [8]	103
Figure 81 HBPTFE Ideal α vs π_c for $\pi_f = 2, M_0 = 0.9$: Specific Thrust from GTA.....	103
Figure 82 HBPTFE Ideal α vs π_c for $\pi_f = 2, M_0 = 0.9$: Thrust-Specific Fuel Consumption [8]	104
Figure 83 HBPTFE Ideal α vs π_c for $\pi_f = 2, M_0 = 0.9$: Thrust-Specific Fuel Consumption from GTA	104
Figure 84 HBPTFE Ideal α vs π_c for $\pi_f = 2, M_0 = 0.9$: fuel/air ratio and thermal efficiency [8].....	105
Figure 85 HBPTFE Ideal α vs π_c for $\pi_f = 2, M_0 = 0.9$: fuel/air ratio and thermal efficiency from GTA	105
Figure 86 HBPTFE Ideal α vs π_c for $\pi_f = 2, M_0 = 0.9$: propulsive and overall efficiencies [8]	106
Figure 87 HBPTFE Ideal α vs π_c for $\pi_f = 2, M_0 = 0.9$: propulsive and overall efficiencies from GTA	106
Figure 88 HBPTFE Ideal α vs π_c for $\pi_f = 2, M_0 = 0.9$: Thrust ratio [8].....	107
Figure 89 HBPTFE Ideal α vs π_c for $\pi_f = 2, M_0 = 0.9$: Thrust ratio from GTA	107

Figure 90 HBPTFE Ideal π_f vs π_c for $\alpha = 5, M_0 = 0.9$: Specific Thrust [8].....	108
Figure 91 HBPTFE Ideal π_f vs π_c for $\alpha = 5, M_0 = 0.9$: Specific Thrust from GTA	108
Figure 92 HBPTFE Ideal π_f vs π_c for $\alpha = 5, M_0 = 0.9$: Thrust-Specific Fuel Consumption [8]	
.....	109
Figure 93 HBPTFE Ideal π_f vs π_c for $\alpha = 5, M_0 = 0.9$: Thrust-Specific Fuel Consumption from GTA	109
Figure 94 HBPTFE Ideal π_f vs π_c for $\alpha = 5, M_0 = 0.9$: propulsive efficiency [8].....	110
Figure 95 HBPTFE Ideal π_f vs π_c for $\alpha = 5, M_0 = 0.9$: propulsive efficiency from GTA ..	110
Figure 96 HBPTFE Ideal π_f vs π_c for $\alpha = 5, M_0 = 0.9$: overall efficiency [8]	111
Figure 97 HBPTFE Ideal π_f vs π_c for $\alpha = 5, M_0 = 0.9$: overall efficiency from GTA.....	111
Figure 98 HBPTFE Ideal π_f vs π_c for $\alpha = 5, M_0 = 0.9$: Thrust ratio [8]	112
Figure 99 HBPTFE Ideal π_f vs π_c for $\alpha = 5, M_0 = 0.9$: Thrust ratio from GTA.....	112
Figure 100 HBPTFE Ideal α vs π_f for $\pi_c = 24, M_0 = 0.9$: Specific Thrust [8]	113
Figure 101 HBPTFE Ideal α vs π_f for $\pi_c = 24, M_0 = 0.9$: Specific Thrust from GTA.....	113
Figure 102 HBPTFE Ideal α vs π_f for $\pi_c = 24, M_0 = 0.9$: Thrust-Specific Fuel Consumption [8].....	114
Figure 103 HBPTFE Ideal α vs π_f for $\pi_c = 24, M_0 = 0.9$: Thrust-Specific Fuel Consumption from GTA	114
Figure 104 HBPTFE Ideal α vs π_f for $\pi_c = 24, M_0 = 0.9$: propulsive efficiency [8]	115
Figure 105 HBPTFE Ideal α vs π_f for $\pi_c = 24, M_0 = 0.9$: propulsive efficiency from GTA	
.....	115
Figure 106 HBPTFE Ideal α vs π_f for $\pi_c = 24, M_0 = 0.9$: Thrust ratio [8]	116
Figure 107 HBPTFE Ideal α vs π_f for $\pi_c = 24, M_0 = 0.9$: Thrust ratio from GTA	116
Figure 108 HBPTFE Ideal π_f vs α for $\pi_c = 24, M_0 = 0.9$: Specific Thrust [8]	117
Figure 109 HBPTFE Ideal π_f vs α for $\pi_c = 24, M_0 = 0.9$: Specific Thrust from GTA	117

Figure 110 HBPTFE Ideal π_f vs α for $\pi_c = 24, M_0 = 0.9$: Thrust-Specific Fuel Consumption [8]	118
Figure 111 HBPTFE Ideal π_f vs α for $\pi_c = 24, M_0 = 0.9$: Thrust-Specific Fuel Consumption from GTA	118
Figure 112 HBPTFE Ideal π_f vs α for $\pi_c = 24, M_0 = 0.9$: propulsive efficiency [8]	119
Figure 113 HBPTFE Ideal π_f vs α for $\pi_c = 24, M_0 = 0.9$: propulsive efficiency from GTA	119
Figure 114 HBPTFE Ideal π_f vs α for $\pi_c = 24, M_0 = 0.9$: Thrust ratio [8]	120
Figure 115 HBPTFE Ideal π_f vs α for $\pi_c = 24, M_0 = 0.9$: Thrust ratio from GTA	120
Figure 116 HBPTFE Ideal α vs π_c for $\pi_f = 2, M_0 = 0.9$: Specific Thrust [8]	121
Figure 117 HBPTFE Ideal α vs π_c for $\pi_f = 2, M_0 = 0.9$: Specific Thrust from GTA	121
Figure 118 HBPTFE Ideal α vs π_c for $\pi_f = 2, M_0 = 0.9$: fuel/air ratio [8]	122
Figure 119 HBPTFE Ideal α vs π_c for $\pi_f = 2, M_0 = 0.9$: fuel/air ratio from GTA	122
Figure 120 HBPTFE Ideal α vs π_c for $\pi_f = 2, M_0 = 0.9$: Thrust-Specific Fuel Consumption [8]	123
Figure 121 HBPTFE Ideal α vs π_c for $\pi_f = 2, M_0 = 0.9$: Thrust-Specific Fuel Consumption from GTA	123
Figure 122 HBPTFE Ideal α vs M_0 for $\pi_f = 2, \pi_c = 24$: Specific Thrust [8]	124
Figure 123 HBPTFE Ideal α vs M_0 for $\pi_f = 2, \pi_c = 24$: Specific Thrust from GTA	124
Figure 124 HBPTFE Ideal α vs M_0 for $\pi_f = 2, \pi_c = 24$: Thrust-Specific Fuel Consumption [8]	125
Figure 125 HBPTFE Ideal α vs M_0 for $\pi_f = 2, \pi_c = 24$: Thrust-Specific Fuel Consumption from GTA	125
Figure 126 Result single spool turbojet engine single point calculation subsonic flight from GTA	128
Figure 127 Result single spool turbojet engine single point calculation subsonic flight from ONX.....	128

Figure 128 Result double spool turbojet engine single point calculation subsonic flight from GTA	129
Figure 129 Result double spool turbojet engine single point calculation subsonic flight from ONX.....	129
Figure 130 Result high bypass ratio turbofan engine single point calculation subsonic flight from GTA.....	130
Figure 131 Result high bypass ratio turbofan engine single point calculation subsonic flight from ONX	130
Figure 132 Altitude variation calculation at sea level parameter input (SI).....	132
Figure 133 Altitude variation calculation at sea level parameter input (BE)	133
Figure 134 Altitude varaiton at sea level for Single Spool Turbojet Engine Specific Thrust plot from GTA.....	134
Figure 135 Altitude varaiton at sea level for Single Spool Turbojet Engine Specific Thrust plot from ONX.....	134
Figure 136 Altitude varaiton at sea level for Single Spool Turbojet Engine Thrust Specific Fuel Consumption plot from GTA	135
Figure 137 Altitude varaiton at sea level for Single Spool Turbojet Engine Thrust Specific Fuel Consumption plot from ONX.....	135
Figure 138 Altitude variation at sea level for Single Spool Turbojet Engine Fuel to Air Ratio plot from GTA	136
Figure 139 Altitude varaiton at sea level for Single Spool Turbojet Engine Fuel to Air Ratio plot from ONX	136
Figure 140 Altitude varaiton at sea level for Single Spool Turbojet Engine Propulsive Efficiencies plot from GTA	137
Figure 141 Altitude varaiton at sea level for Single Spool Turbojet Engine Propulsive Efficiencies plot from ONX.....	137

Figure 142 Altitude variation at sea level for Single Spool Turbojet Engine Thermal Efficiencies plot from GTA	138
Figure 143 Altitude variation at sea level for Single Spool Turbojet Engine Thermal Efficiencies plot from ONX.....	138
Figure 144 Altitude variation at sea level for Single Spool Turbojet Engine Overall Efficiencies plot from GTA	139
Figure 145 Altitude variation at sea level for Single Spool Turbojet Engine Overall Efficiencies plot from ONX.....	139
Figure 146 Altitude variation at sea level for Single Spool Turbojet Engine Efficiencies comparison plot from GTA.....	140
Figure 147 Altitude variation at sea level for Double Spool Turbojet Engine Specific Thrust plot from GTA.....	141
Figure 148 Altitude variation at sea level for Double Spool Turbojet Engine Specific Thrust plot from ONX.....	141
Figure 149 Altitude variation at sea level for Double Spool Turbojet Engine Thrust Specific Fuel Consumption plot from GTA	142
Figure 150 Altitude variation at sea level for Double Spool Turbojet Engine Thrust Specific Fuel Consumption plot from ONX.....	142
Figure 151 Altitude variation at sea level for Double Spool Turbojet Engine Fuel to Air Ratio plot from GTA	143
Figure 152 Altitude variation at sea level for Double Spool Turbojet Engine Fuel to Air Ratio plot from ONX	143
Figure 153 Altitude variation at sea level for Double Spool Turbojet Engine Propulsive Efficiencies plot from GTA	144
Figure 154 Altitude variation at sea level for Double Spool Turbojet Engine Propulsive Efficiencies plot from ONX.....	144

Figure 155 Altitude variation at sea level for Double Spool Turbojet Engine Thermal Efficiencies plot from GTA	145
Figure 156 Altitude variation at sea level for Double Spool Turbojet Engine Thermal Efficiencies plot from ONX.....	145
Figure 157 Altitude variation at sea level for Double Spool Turbojet Engine Overall Efficiencies plot from GTA	146
Figure 158 Altitude variation at sea level for Double Spool Turbojet Engine Overall Efficiencies plot from ONX.....	146
Figure 159 Altitude variation at sea level for Double Spool Turbojet Engine Efficiencies comparison plot from GTA.....	147
Figure 160 Altitude variation at sea level for High – Bypass Ratio Turbofan Engine Specific Thrust plot from GTA.....	149
Figure 161 Altitude variation at sea level for High – Bypass Ratio Turbofan Engine Specific Thrust plot from ONX.....	149
Figure 162 Altitude variation at sea level for High – Bypass Ratio Turbofan Engine Thrust Specific Fuel Consumption plot from GTA	150
Figure 163 Altitude variation at sea level for High – Bypass Ratio Turbofan Engine Thrust Specific Fuel Consumption plot from ONX.....	150
Figure 164 Altitude variation at sea level for High – Bypass Ratio Turbofan Engine Fuel to Air Ratio plot from GTA	151
Figure 165 Altitude variation at sea level for High – Bypass Ratio Turbofan Engine Fuel to Air Ratio plot from ONX	151
Figure 166 Altitude variation at sea level for High – Bypass Ratio Turbofan Engine Propulsive Efficiencies plot from GTA	152
Figure 167 Altitude variation at sea level for High – Bypass Ratio Turbofan Engine Propulsive Efficiencies plot from ONX	152

Figure 168 Altitude variation at sea level for High – Bypass Ratio Turbofan Engine Thermal Efficiencies plot from GTA.....	153
Figure 169 Altitude variation at sea level for High – Bypass Ratio Turbofan Engine Thermal Efficiencies plot from ONX	153
Figure 170 Altitude variation at sea level for High – Bypass Ratio Turbofan Engine Overall Efficiencies plot from GTA.....	154
Figure 171 Altitude variation at sea level for High – Bypass Ratio Turbofan Engine Overall Efficiencies plot from ONX	154
Figure 172 Altitude variation at sea level for High – Bypass Ratio Turbofan Engine Efficiencies comparison plot from GTA.....	155

LIST OF TABLES

Table 1 Work plan.....	1
Table 2 Temperature and Pressure Ratios [10].....	5
Table 3 Performance analysis variables for dual-spool afterburning turbojet engine [7]	45
Table 4 Input table single point calculation subsonic flight (10,000 m)	69
Table 5 Input table varation calculation subsonic flight (sea level)	70
Table 6 Input parameters subsonic flight Single point calculation GTA.....	127

Nomenclature

A	=	area
a	=	speed of sound
c	=	effective exhaust velocity; specific heat
c_p	=	specific heat at constant pressure
c_v	=	specific heat at constant volume
E	=	energy; modulus of elasticity
e	=	internal energy per unit mass; polytropic efficiency; exponential, 2.7183
F	=	force; uninstalled thrust; thrust
FR	=	thrust ratio
F / \dot{m}_0	=	specific thrust
f	=	fuel/air ratio
g	=	acceleration of gravity
g_c	=	Newton's constant
g_0	=	acceleration of gravity at sea level
h	=	enthalpy per unit mass (mass specific enthalpy)
h_{PR}	=	low heating value of fuel
M	=	Mach number; momentum
m	=	mass
\dot{m}	=	mass flow rate
N	=	number of moles; revolutions per minute
\hat{n}	=	normal vector
P	=	pressure
P_t	=	total pressure
Q	=	heat interaction
\dot{Q}	=	rate of heat interaction
q	=	heat interaction per unit mass; dynamic pressure
R	=	gas constant; extensive property
S	=	uninstalled thrust specific fuel consumption; entropy
T	=	temperature; installed thrust

T_t	=	total temperature
$TSFC$	=	thrust specific fuel consumption
t	=	time
u	=	velocity
V	=	absolute velocity; volume
v	=	volume per unit mass; velocity
W	=	weight; work
w	=	work interaction per unit mass; velocity; mass specific work
x, y, z	=	coordinate system
α	=	bypass ratio
β	=	bleed air fraction
γ	=	ratio of specific heats
Δ	=	change
δ	=	change; deviation
∂	=	partial differentiation
η	=	efficiency
λ	=	payload mass ratio
π	=	pressure ratio
ρ	=	density
Σ	=	summation
τ	=	temperature ratio
τ_λ	=	enthalpy ratio

Subscripts

A	=	air mass
a	=	air; atmosphere
AB	=	afterburner
b	=	burner or combustor; burning
C	=	core stream
c	=	compressor; chamber
cc	=	combustion chamber

cs = control surface
 cv = control volume
 d = diffuser or inlet; disk
 e = exit; exhaust
 F = fan stream
 f = fan; fuel; final
 fn = fan nozzle
 H = high-pressure
 h = hub
 hpc = high pressure compressor
 L = low-pressure
 lpc = low pressure compressor
 n = nozzle
 O = overall; output
 P = propulsive; products
 p = propellant
 R = reference; relative
 r = ram; reduced
 T = thermal
 t = total; turbine; throat; thermal
 x, y, z = directional component
 0, 1, 2, ..., 19 = different locations in space

Superscripts

$*$ = state corresponding to $M = 1$; corresponding to optimum state
 $-$ = average

1. Introduction

The aircraft engine has been designed and improved throughout the century. The first flight of the Wright brothers marked the beginning of the technological evolution of the mankind. The driving forces of this evolution have continuously driven us to consider the improvement in flight performance, cost-effective, safety, reliability, controls, and navigation. These demands have continuously driven the advancing of the aircraft system. The performance characteristics of air vehicle and propulsion systems are strongly dependent to each other. Therefore, to gain better understanding and improvement for further evolution, we have to be aware of the importance of the aircraft engine study and constantly gain insight of the advancements of the air vehicle technology. The focus of this project on this phase is the engine analysis and performance prediction specifically with parametric cycle analysis or on-design analysis. The good flight performance is correlated to that of a reliable propulsion system, hence, strengthen the importance to develop a software for designing aircraft gas turbine engines. For parametric cycle analysis, the atmospheric and flight condition parameters are defined as per cases. The performance of the engines for each case is then analyzed and presented in this report.

1.1 Objectives

1. To develop software for designing aircraft gas turbine engines that best match the aircraft performance requirements specifically for cycle analysis.
2. To fully understand the design process of aircraft gas turbine engines.
3. To obtain an in-house design software for teaching and further research.

1.2 Scope of project

1. Choice of cycle and type of turbomachinery layout -the single-spool turbojet, dual spool turbojet, and high bypass turbofan engines.

2. Engine cycle design point analysis -parametric analysis including performance parameters (primarily specific thrust and thrust specific fuel consumption) in terms of design limitations (such as maximum allowable turbine temperature and attainable component efficiencies), the flight conditions (the ambient pressure, temperature, and Mach number), and design choices (such as compressor pressure ratio, fan pressure ratio, bypass ratio, and theta break)
3. Comparison of engine performances associated with different design choices of several engines to select the most promising design that best balances performance for cycle analysis.

1.3 Methodology

1. Fundamental study and design approaches based on Mattingly [8] specifically focusing on the comparison between the ideal and real engine assumption to observe the changes behaviour with the variation of the engine parameters.
2. Developing an aircraft engine design software in Python for Single-Spool Turbojet, Dual-Spool Turbojet, and High Bypass Ratio Turbofan.
3. Validating the develop software with AEDsys (ONX).

1.4 Schedule

1.4.1 Work plan

Work plan activities as well as thesis milestones can be founded in the schedule below

Table 1 Work plan

Task (and numbered milestones)	January				February				9	March				April				May				June		
	1	2	3	4	5	6	7	8		10	11	12	13	14	15	16	17	18	19	20	21	22	23	
1. Study of aircraft gas turbine engine cycle design and analysis.																								
1.1 Parametric Cycle Analysis of Ideal Engines study																								
1.2 Parametric Cycle Analysis of Real Engines study																								
1.3 Engine Performance Analysis study																								
2. Develop a software using Python with user-friendly interfaces for designing aircraft gas turbine engines.																								
2.1 Single-spool turbojet layout																								
2.2 Dual-spool turbojet layout																								
2.3 High bypass turbofan layout																								
2.4 Debugging the program																								
3. Validate the developed software with available design software such as AEDsys and GasTurb																								
4. Trade-off study and implementation																								
5. Write a project report																								
Milestones in the thesis process																			2, 3		4			5

2. Cycle Analysis of Gas Turbine Engines

The cycle analysis aims to study the thermodynamic changes of the working fluid as it flows through the engine. For this phase of the project, we will be focusing on the parametric cycle analysis (also called on-design) to determine the performance of engines at different flight conditions, design choices, and design limit parameters that are specified by the user or designer. The main objective of parametric cycle analysis is to determine how the engine's performances, such as specific thrust and thrust specific fuel consumption, vary with the flight conditions, design limits, component performance, and design choices.

In this section, the fundamental equations and concepts are explained and used to derive the equations necessary for evaluating engine performance taken from various sources. [2, 7, 8, 10]. To demonstrate how the equations are derived, the process is presented as starting from section 2.1 Fundamental Equations Analysis.

2.1 Fundamental Equations Analysis

Conservation of Mass and Momentum

The most basic principle that govern the fluid interaction within the engine is the concepts of mass and momentum. The first term on the left-hand side represents the change of mass within the control volume with respect to time and the second term represents the flux of mass through the control surface

$$\frac{d}{dt} \int_{cv} \rho dV + \int_{cs} \rho(u \cdot \hat{n}) dA = 0 \quad (Eq. 1)$$

The flow is assumed to be one – dimensional steady state. The equation is reduced to

$$\rho_2 u_2 A_2 - \rho_1 u_1 A_1 = 0 \quad (Eq. 2)$$

For the conservation of momentum, the same assumption is applied

$$\frac{d}{dt} \int_{cv} u \rho dV + \int_{cs} u \rho(u \cdot \hat{n}) dA = \sum F \quad (Eq. 3)$$

The flow is assumed to be one – dimensional steady state. The sum of the forces is simply the difference between the pressure forces at the opposite ends of the control volume and any additional body forces. The equation is reduced to

$$\rho_2 u_2^2 A_2 - \rho_1 u_1^2 A_1 = P_1 A_1 - P_2 A_2 + F_{body} \quad (Eq. 4)$$

First Law of Thermodynamics or conservation of energy

Enthalpy is defined as the sum of the specific internal energy and flow work

$$h \equiv e + Pv \quad (Eq. 5)$$

The first law of thermodynamics states that the heat Q is the sum of the change in total energy ΔE_0 and the total work W_T

$$Q = \Delta E_0 + W_T \quad (Eq. 6)$$

Hence, the final form of the first law used is

$$q - w = \left(h + \frac{u^2}{2} + gz \right)_2 - \left(h + \frac{u^2}{2} + gz \right)_1 \quad (Eq. 7)$$

Ideal Gas

Adopted directly from the ideal gas law

$$Pv = RT \quad (\text{Eq. 8})$$

Specific Heats and Perfect Gas

Specific heat refers to the amount of energy needed to increase the temperature of a unit mass of a substance by one degree of temperature. There are two types of specific heat, the specific heat at constant volume and the specific heat at constant pressure. Any gas with constant specific heats is referred to as a perfect gas.

The specific heat at constant volume is defined as the change in internal energy relative to the change in temperature

$$c_v = \frac{de}{dT} \quad (\text{Eq. 9})$$

The specific heat at constant pressure is defined as the change in enthalpy relative to the change in temperature

$$c_p = \frac{dh}{dT} \quad (\text{Eq. 10})$$

From Eq 5, the relationship between specific heats and gas constant is derived as

$$c_p = c_v + R \quad (\text{Eq. 11})$$

Speed of Sound

From the relationship between the speed of sound to pressure and density

$$a^2 = \frac{dP}{d\rho} \quad (\text{Eq. 12})$$

Applying the ideal gas law, the speed of sound for a perfect gas becomes

$$a = \sqrt{\gamma RT} \quad (\text{Eq. 13})$$

Stagnation Properties

Stagnation values are obtained by bringing the flow to rest isentropically. Therefore, for a perfect gas

$$\frac{c_p}{c_v} = \gamma \quad (Eq. 14)$$

The stagnation relationship in terms of Mach number is obtained.

For temperature

$$\frac{T_t}{T} = 1 + \frac{\gamma - 1}{2} M^2 \quad (Eq. 15)$$

For pressure

$$\frac{P_t}{P} = \left(1 + \frac{\gamma - 1}{2} M^2 \right)^{\frac{\gamma}{\gamma - 1}} \quad (Eq. 16)$$

For density

$$\frac{\rho_t}{\rho} = \left(1 + \frac{\gamma - 1}{2} M^2 \right)^{\frac{1}{\gamma - 1}} \quad (Eq. 17)$$

Ratio Definitions

The temperature and pressure ratios based on the station numbering are summarized as shown in the Table 2 from Sung [10]

Table 2 Temperature and Pressure Ratios [10]

Temperature Ratio	Pressure Ratio
$\tau_r = 1 + \frac{\gamma - 1}{2} M_0^2$	$\pi_r = \left(1 + \frac{\gamma - 1}{2} M_0^2 \right)^{\frac{\gamma}{\gamma - 1}}$
$\tau_b = \frac{T_{t4}}{T_{t3}}$	$\pi_b = \frac{P_{t4}}{P_{t3}}$
$\tau_d = \frac{c_{pt} T_{t4}}{c_{pc} T_{t0}}$	$\pi_d = \frac{P_{t2}}{P_{t0}}$
$\tau_n = \frac{T_{t9}}{T_{t5}}$	$\pi_c = \frac{P_{t3}}{P_{t2}}$
$\tau_e = \frac{T_{t3}}{T_{t2}}$	$\pi_n = \frac{P_{t9}}{P_{t7}}$

Component Definitions

From Mattingly [8], the component-specific definitions are declared to properly calculate the engine performance.

Inlet Definitions

The inlets are assumed to be adiabatic, meaning $\tau_d = 1$. For calculating the pressure across the inlet, the property $\pi_{d\max}$ is defined as the pressure change due to wall friction and η_r as the ram recovery. The product of these two will result in the pressure ratio across the inlet

$$\pi_d = \pi_{d\max} \eta_r \quad (\text{Eq. 18})$$

The value of η_r varies with the Mach number (military specification 5008B)

$$\eta_r = \begin{cases} 1 & ; M_0 \leq 1 \\ 1 - 0.075(M_0 - 1)^{1.35} & ; 1 < M_0 < 5 \\ \frac{800}{M_0^4 + 935} & ; 5 < M_0 \end{cases} \quad (\text{Eq. 19})$$

Compressor Polytropic Efficiency

The polytropic efficiency is the ratio between ideal work and actual work per unit mass with respect to differential pressure change. It is used to calculate turbojet performance because the polytropic efficiency is essentially constant for highly efficient turbojets. It is an accurate estimation for modern engines from Sung [10]

$$e_c = \frac{dh_i}{dh_t} = \frac{RT \frac{dP}{P}}{c_p dT} \quad (\text{Eq. 20})$$

$$\tau_c = \pi_c^{\frac{\gamma-1}{e_c \gamma}} \quad (\text{Eq. 21})$$

Turbine Polytropic Efficiency

Similar to the compressor polytropic efficiency, the turbine polytropic efficiency can be considered as constant for a modern engine

$$e_t = \frac{dh_t}{dh_{ti}} = \frac{c_p dT}{RT \frac{dP}{P}} \quad (Eq. 22)$$

$$\pi_t = \tau_t^{\frac{\gamma}{e_t(\gamma-1)}} \quad (Eq. 23)$$

2.2 Cycle Analysis of Single-Spool Turbojet Engine

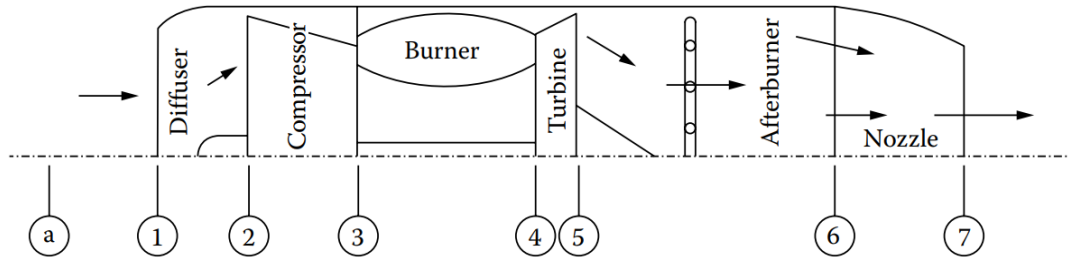


Figure 1 Single-Spool Turbojet Engine [7]

Single-spool turbojets may have either one or two compressors as well as a single driving turbine. It may or may not have an afterburner. As illustrated in Figure 1, a single-spool turbojet engine has a single compressor and an afterburner together with designations for each station.

The different processes encountered within the engine are described as follows:

Station (a) - (1): air flow far upstream where the velocity of air relative to engine is the flight velocity up to the intake, usually with some deceleration during cruise and acceleration during takeoff.

Station (2) - (3): air flows through the inlet diffuser and ducting system, where the air velocity is decreased as the air is carried to the compressor inlet. The air is compressed in a dynamic compressor.

Station (3) - (4): the air is heated by mixing and burning of fuel in the air.

Station (4) - (5): the air is expanded through a turbine to obtain power to drive the compressor.

Station (5) - (6): the air may or may not be further heated by the addition and burning of fuel in an afterburner.

Station (6) - (7): the air is accelerated and exhausted through the exhaust nozzle. If the engine is not fitted with an afterburner, then the station (5) and (6) are coincident. The amount of mass flow is usually set by flow choking in the nozzle throat.

2.2.1 Single-Spool Turbojet Engine – Ideal case

The components except the burners are assumed to be reversible adiabatic or isentropic. Moreover, the burners are replaced by a frictionless heater, so the velocities at station (2) through station (6) are negligible.

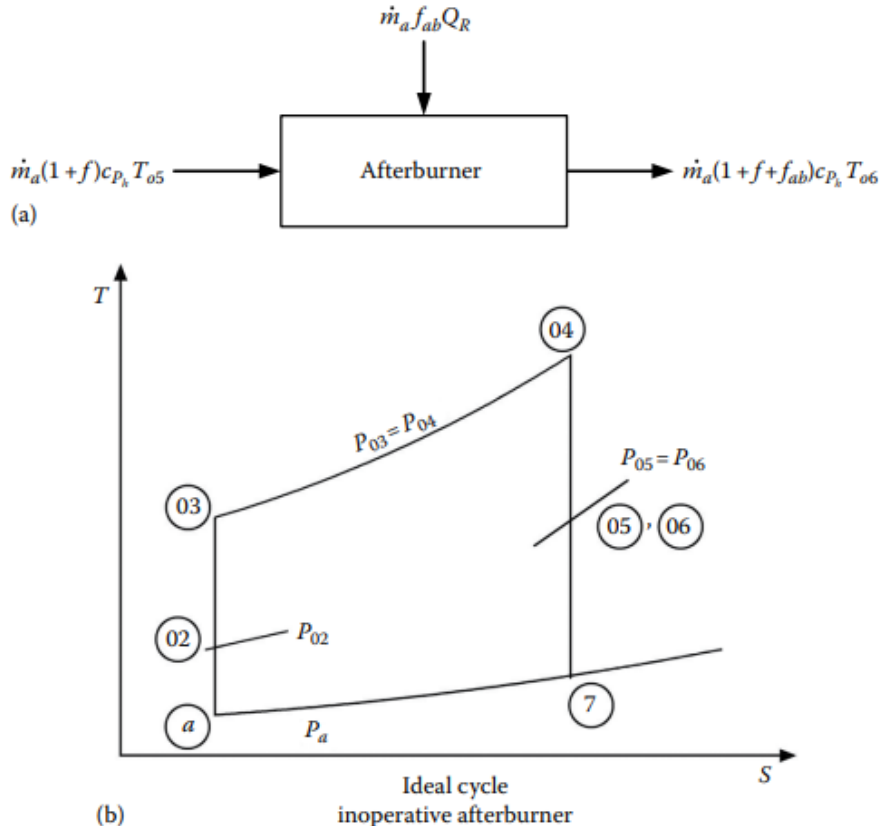


Figure 2 Temperature-entropy diagram for (a) ideal turbojet and (b) inoperative afterburner [7]

The different components of the engine would be analyzed as refer to Figure 2.

2.2.1.1 Intake or Inlet

During cruise, the static pressure rises from section (a) to station (1) outside the intake and from station (1) to station (2) inside the intake. The air is decelerated isentropically relative to the engine then the total or stagnation pressure at station (a), (1), and (2) are constant and equal

$$P_{02} = P_{01} = P_{0a} = P_a \left(1 + \frac{\gamma - 1}{2} M^2 \right)^{\gamma / \gamma - 1} \quad (\text{Eq. 24})$$

The stagnation temperatures for station (a), (1), (2) are also equal

$$T_{02} = T_{01} = T_{0a} = T_a \left(1 + \frac{\gamma - 1}{2} M^2 \right) \quad (\text{Eq. 25})$$

2.2.1.2 Compressor

The pressure ratio of the compressor π_c is assumed to be known, thus the pressure and temperature at the outlet of the compressor is evaluated from the corresponding values at the inlet of the compressor (outlet of the intake) from the relations below

$$P_{03} = (P_{02})(\pi_c) \quad (\text{Eq. 26})$$

$$T_{03} = T_{02} \left(\frac{P_{03}}{P_{02}} \right)^{\gamma-1/\gamma} \quad (\text{Eq. 27})$$

2.2.1.3 Combustion Chamber

The outlet conditions of the compressor will be those at the inlet to the combustion chamber. Combustion process takes place from station (3) to station (4). In this process, fuel is injected in an atomized form, evaporated and mixed with air. Spark plugs initiate the combustion process. Since no pressure drop is assumed for the ideal case, the pressures at the inlet and outlet of the combustion chamber are equal

$$P_{03} = P_{04} \quad (\text{Eq. 28})$$

The temperature at the outlet of the turbine is determined from metallurgical limits set by the turbine blade material and is known as the turbine-inlet temperature (TIT). Fuel is added to the combustion chamber and burnt. The mass flow rate of the burnt fuel is calculated from the energy balance of the combustion chamber

$$(\dot{m}_a + \dot{m}_f) c_{ph} T_{04} = \dot{m}_a c_{pc} T_{03} + \dot{m}_f Q_R \quad (\text{Eq. 29})$$

With

$$f = \dot{m}_f / \dot{m}_a \quad (\text{Eq. 30})$$

Then the fuel-to-air ratio is determined from the relation

$$f = \frac{c_{ph} T_{04} - c_{pc} T_{03}}{Q_R - c_{ph} T_{04}} \quad (\text{Eq. 31})$$

2.2.1.4 Turbine

The power consumed in the compression from station (2) to station (3) must be supplied through the turbine in expansion from station (4) to station (5). If the ratio

of the power needed to drive the compressor to the power available in the turbine is λ then, the energy balance for the compressor-turbine shaft is

$$W_c = \lambda W_t \quad (\text{Eq. 32})$$

Here λ is of the range 75% - 85%. Thus, in terms of the temperatures differences

$$c_{pc}(T_{03} - T_{02}) = \lambda(1+f)c_{ph}(T_{04} - T_{05}) \quad (\text{Eq. 33})$$

$$\frac{T_{05}}{T_{04}} = 1 - \frac{(c_{pc}/c_{ph})T_{02}}{\lambda(1+f)T_{04}} \left[\left(\frac{T_{03}}{T_{02}} \right)^{\gamma_c - 1/\gamma_c} - 1 \right] \quad (\text{Eq. 34})$$

Then the turbine and compressor pressure ratios are related by

$$\frac{P_{05}}{P_{04}} = \left\{ 1 - \frac{(c_{pc}/c_{ph})T_{02}}{\lambda(1+f)T_{04}} \left[\left(\frac{P_{03}}{P_{02}} \right)^{\gamma_c - 1/\gamma_c} - 1 \right] \right\}^{\gamma_h/\gamma_h - 1} \quad (\text{Eq. 35})$$

From substituting the equation Eq. 28

$$\frac{P_{05}}{P_{04}} = \left\{ 1 - \frac{(c_{pc}/c_{ph})T_a}{\lambda(1+f)T_{04}} \left(1 + \frac{\gamma - 1}{2} M^2 \right) \left[\left(\frac{P_{03}}{P_{02}} \right)^{\gamma_c - 1/\gamma_c} - 1 \right] \right\}^{\gamma_h/\gamma_h - 1} \quad (\text{Eq. 36})$$

If the pressure drop in the turbine is calculated prior to temperature drop calculation, the temperature at the turbine outlet T_{05} may be calculated from the isentropic relation

$$\frac{T_{05}}{T_{04}} = (P_{05}/P_{04})^{\gamma_h - 1/\gamma_h} \quad (\text{Eq. 37})$$

2.2.1.5 Afterburner

If the jet engine is without an afterburner, then no work or heat transfer occurs downstream of station (5). The stagnation enthalpy remains constant throughout the rest of the engine. However, if there is an afterburner, there are two possibilities:

1. The afterburner is inoperative, the station (5) and station (6) are coincident.
- Both of the temperatures and pressures are equal

$$T_{06} = T_{05} \quad (\text{Eq. 38})$$

$$P_{06} = P_{05} \quad (\text{Eq. 39})$$

2. The afterburner is operative, an additional amount of fuel is burnt which raises the temperature, which is much higher than the turbine-inlet temperature (TIT) because the downstream element is the nozzle, which is a non-rotating part. The walls are subjected only to thermal stresses rather than the combined thermal and mechanical stresses

$$T_{06A} = T_{\max} \quad (\text{Eq. 40})$$

$$P_{06A} = P_{05} \quad (\text{Eq. 41})$$

With additional fuel quantity added and burnt in the afterburner, the fuel-to-air ratio within the afterburner is declared

$$f_{ab} = \frac{(1+f)c_{p6A}T_{06A} - c_{p5}T_{05}}{Q_R - c_{p6A}T_{06A}} \quad (\text{Eq. 42})$$

2.2.1.6 Nozzle

The exhaust velocity is calculated from the conservation of energy in the nozzle. The hot gases expand in the nozzle from station (6) or (6A) to station (7) depending on the state of the afterburner: 1. inoperative and 2. operative.

1. Inoperative afterburner

The critical pressure is defined as

$$\frac{P_{06}}{P_c} = \left(\frac{\gamma_h + 1}{2} \right)^{\gamma_h / \gamma_h - 1} \quad (\text{Eq. 43})$$

The critical pressure is then compared with the ambient pressure. The nozzle is choked when the critical pressure is greater or equal to the ambient pressure. The nozzle outlet temperature is calculated from the relation

$$\frac{T_{06}}{T_7} = \left(\frac{\gamma_h + 1}{2} \right) \quad (\text{Eq. 44})$$

The exhaust velocity is calculated as

$$V_7 = \sqrt{\gamma_h R T_7} \quad (\text{Eq. 45})$$

If the ambient pressure is greater than the critical pressure, then the exhaust pressure is equal to the ambient pressure. The temperature of the exhaust gas is calculated from the relation

$$\frac{T_{06}}{T_7} = \left(\frac{P_{06}}{P_a} \right)^{\gamma_h - 1/\gamma_h} \quad (\text{Eq. 46})$$

The exhaust velocity is calculated as

$$V_7 = \sqrt{2c_{pn}(T_{06} - T_7)} = \sqrt{2c_{pn}T_{06} \left[1 - \left(P_a / P_{06} \right)^{\gamma_h - 1/\gamma_h} \right]} \quad (\text{Eq. 47})$$

2. Operative afterburner

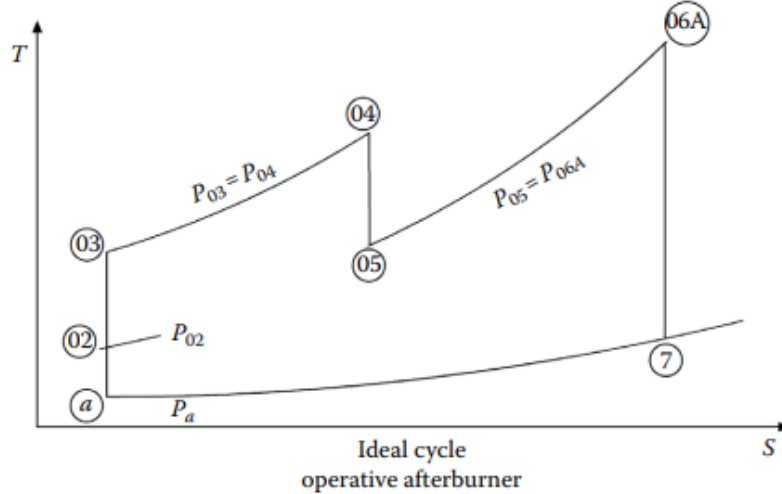


Figure 3 Temperature-entropy diagram for ideal turbojet, operative afterburner [7]

The expansion process in the nozzle starts from the station (6A) to station (7) as refer to Figure 3. The critical pressure calculation is performed to check the state of the nozzle

$$\frac{P_{06A}}{P_c} = \left(\frac{\gamma_h + 1}{2} \right)^{\gamma_h / \gamma_h - 1} \quad (\text{Eq. 48})$$

The outlet temperature (T_{7A}) is much greater than that in the case of inoperative afterburner and calculated as

$$\frac{T_{06A}}{T_{7A}} = \left(\frac{\gamma_h + 1}{2} \right) \quad (\text{Eq. 49})$$

If the nozzle is choked, then the exhaust velocity is calculated as

$$V_{7ab} = \sqrt{\gamma_h R T_{7A}} \quad (\text{Eq. 50})$$

If the nozzle is unchoked, then the exhaust pressure is ambient, and the velocity is calculated as

$$V_{7ab} = \sqrt{2c_{pn}T_{06A} \left[1 - \left(P_a / P_{06A} \right)^{\gamma_h - 1/\gamma_h} \right]} \quad (\text{Eq. 51})$$

The thrust force is expressed as

$$T = \dot{m}_a \left[(1 + f) V_e - V \right] + (P_e - P_a) A_e T \quad (\text{Eq. 52})$$

V_e is exhaust jet speed which maybe either V_7 or V_{7ab} depending on the state of afterburner (operative or inoperative).

2.2.1.8 Cycle analysis steps of Single-Spool Turbojet Engine – Ideal case

For this step, the engine stations for the single spool turbojet engine ideal case are changed in the figure 4.

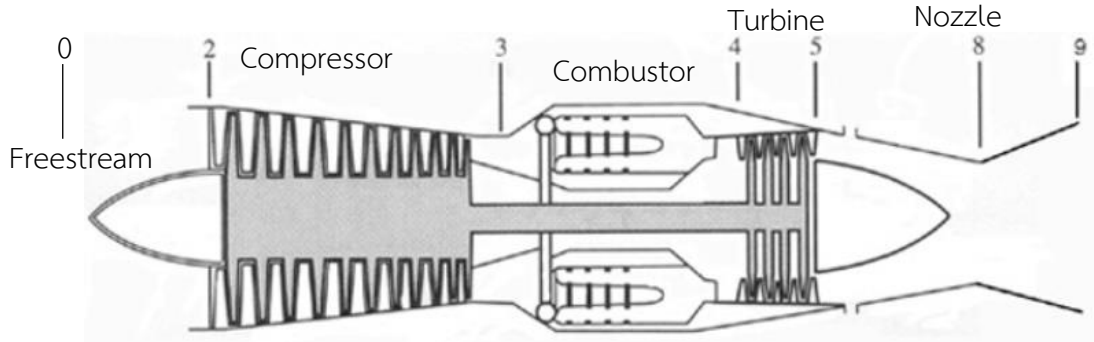


Figure 4 Station numbering of ideal turbojet engine [8]

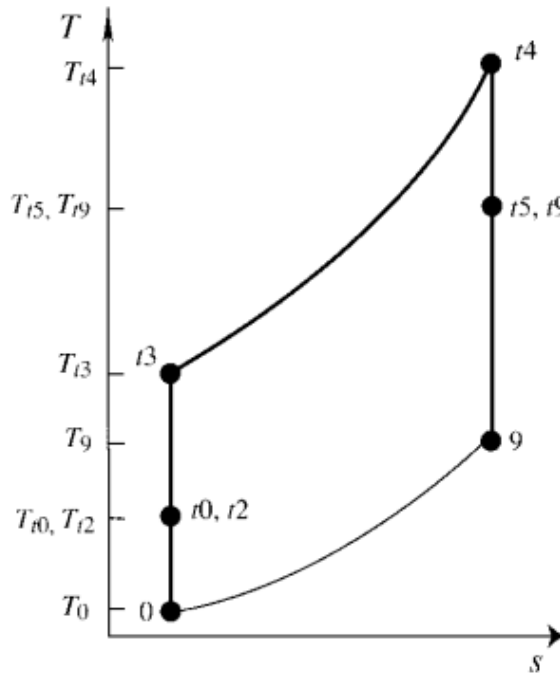


Figure 5 T-s diagram of an ideal turbojet engine [8]

Single-Spool Turbojet Engine cycle analysis for ideal case

Step 1:

$$\frac{F}{\dot{m}_0} = \frac{1}{g_c} (V_9 - V_0) = \frac{a_0}{g_c} \left(\frac{V_9}{a_0} - M_0 \right) \quad (\text{Eq. 53})$$

Step 2:

$$\left(\frac{V_9}{a_0} \right)^2 = \frac{a_0^2 M_9^2}{a_0^2} = \frac{\gamma R_9 g_c T_9 M_9^2}{\gamma_0 R_0 g_c T_0} = \frac{T_9}{T_0} M_9^2 \quad (\text{Eq. 54})$$

Step 3:

$$P_{t9} = P_9 \left(1 + \frac{\gamma - 1}{2} - M_9^2 \right)^{\gamma/(\gamma-1)} \quad (\text{Eq. 55})$$

And

$$P_{t9} = P_0 \frac{P_{t0}}{P_0} \frac{P_{t2}}{P_{t0}} \frac{P_{t3}}{P_{t2}} \frac{P_{t4}}{P_{t3}} \frac{P_{t5}}{P_{t4}} \frac{P_{t9}}{P_{t5}} = P_0 \pi_r \pi_d \pi_c \pi_b \pi_i \pi_n \quad (\text{Eq. 56})$$

However, $\pi_d = \pi_b = \pi_n = 1$ thus $P_{t9} = P_0 \pi_r \pi_c \pi_t$, and so

$$M_9^2 = \frac{2}{\gamma - 1} \left[\left(\frac{P_{t9}}{P_9} \right)^{(\gamma-1)/\gamma} - 1 \right] \quad (\text{Eq. 57})$$

Also

$$\frac{P_{t9}}{P_9} = \frac{P_{t9}}{P_9} \frac{P_0}{P_9} = \frac{P_0}{P_9} \pi_r \pi_c \pi_t = \pi_r \pi_c \pi_t \quad (\text{Eq. 58})$$

Then

$$M_9^2 = \frac{2}{\gamma - 1} \left[(\pi_r \pi_c \pi_t)^{(\gamma-1)/\gamma} - 1 \right] \quad (\text{Eq. 59})$$

However, $\pi_r^{(\gamma-1)/\gamma} = \tau_r$ and for an ideal turbojet and the same for compressor and turbine

$$M_9^2 = \frac{2}{\gamma - 1} [\tau_r \tau_c \tau_t - 1] \quad (\text{Eq. 60})$$

Step 4:

$$T_{t9} = T_0 \frac{T_{t0}}{T_0} \frac{T_{t2}}{T_{t0}} \frac{T_{t3}}{T_{t2}} \frac{T_{t4}}{T_{t3}} \frac{T_{t5}}{T_{t4}} \frac{T_{t9}}{T_{t5}} = T_0 \tau_r \tau_d \tau_c \tau_b \tau_t \tau_n = T_0 \tau_r \tau_c \tau_b \tau_t \quad (\text{Eq. 61})$$

Then

$$\frac{T_9}{T_0} = \frac{T_{t9}/T_0}{T_{t9}/T_9} \quad (\text{Eq. 62})$$

Thus

$$\frac{T_9}{T_0} = \tau_b \quad (\text{Eq. 63})$$

Step 5: Application of the steady flow energy equation to the burner gives,

$$\dot{m}_0 h_{t3} + \dot{m}_f h_{PR} = (\dot{m}_0 + \dot{m}_f) h_{t4} \quad (\text{Eq. 64})$$

For an ideal cycle, $\dot{m}_0 + \dot{m}_f \cong \dot{m}_0$ and $c_{p3} = c_{p4} = c_p$

Thus

$$\dot{m}_0 c_p T_{t3} + \dot{m}_f h_{PR} = \dot{m}_0 c_p T_{t4} \quad (\text{Eq. 65})$$

$$\dot{m}_f h_{PR} = \dot{m}_0 c_p (T_{t4} - T_{t3}) = \dot{m}_0 c_p T_0 \left(\frac{T_{t4}}{T_0} - \frac{T_{t3}}{T_0} \right) \quad (\text{Eq. 66})$$

Or

$$f = \frac{\dot{m}_f}{\dot{m}_0} = \frac{c_p T_0}{h_{PR}} \left(\frac{T_{t4}}{T_0} - \frac{T_{t3}}{T_0} \right) \quad (\text{Eq. 67})$$

However, since

$$\tau_\lambda = \frac{T_{t4}}{T_0} \quad (\text{Eq. 68})$$

$$\tau_r \tau_c = \frac{T_{t3}}{T_0} \quad (\text{Eq. 69})$$

Then

$$f = \frac{\dot{m}_f}{\dot{m}_0} = \frac{c_p T_0}{h_{PR}} (\tau_\lambda - \tau_r \tau_c) \quad (\text{Eq. 70})$$

or

$$f = \frac{\dot{m}_f}{\dot{m}_0} = \frac{c_p \tau_r \tau_c}{h_{PR}} (\tau_b - 1) \quad (\text{Eq. 71})$$

Step 6: The power out of the turbine is

$$\begin{aligned}\dot{W}_t &= (\dot{m}_0 + \dot{m}_f)(h_{t4} - h_{t5}) \equiv \dot{m}_0 c_p (T_{t4} - T_{t5}) \\ &= \dot{m}_0 c_p T_{t4} \left(1 - \frac{T_{t5}}{T_{t4}} \right) = \dot{m}_0 c_p T_{t4} (1 - \tau_t)\end{aligned}\quad (\text{Eq. 72})$$

The power required to drive the compressor is

$$\begin{aligned}\dot{W}_c &= \dot{m}_0 (h_{t3} - h_{t2}) = \dot{m}_0 c_p (T_{t3} - T_{t2}) \\ &= \dot{m}_0 c_p T_{t2} \left(\frac{T_{t3}}{T_{t2}} - 1 \right) = \dot{m}_0 c_p T_{t2} (\tau_c - 1)\end{aligned}\quad (\text{Eq. 73})$$

Since $\dot{W}_c = \dot{W}_t$ for the ideal turbojet, then

$$\dot{m}_0 c_p T_{t2} (\tau_c - 1) = \dot{m}_0 c_p T_{t4} (1 - \tau_t) \quad (\text{Eq. 74})$$

Or

$$\tau_t = 1 - \frac{T_{t2}}{T_{t4}} (\tau_c - 1) \quad (\text{Eq. 75})$$

Thus

$$\tau_t = 1 - \frac{\tau_r}{\tau_\lambda} (\tau_c - 1) \quad (\text{Eq. 76})$$

Step 7:

$$\frac{F}{\dot{m}_0} = \frac{a_0}{g_c} \left[\sqrt{\frac{2}{\gamma-1} \frac{\tau_\lambda}{\tau_r \tau_c} (\tau_r \tau_c \tau_t - 1)} - M_0 \right] \quad (\text{Eq. 77})$$

Step 8:

$$S = \frac{f}{F / \dot{m}_0} \quad (\text{Eq. 78})$$

The thrust specific fuel consumption S can be calculated by first calculating the fuel/air ratio f and the thrust per unit of air flow F / \dot{m}_0 using Eq. 70 and 77 respectively. Then substituting these values into the preceding equation. An analytical expression for S can be obtained by substituting Eq. 70 and Eq. 71 into Eq. 78 to get the following equation

$$S = \frac{c_p T_0 g_c (\tau_\lambda - \tau_r \tau_c)}{a_0 h_{PR} \left[\sqrt{\frac{2}{\gamma-1} \frac{\tau_\lambda}{\tau_r \tau_c} (\tau_r \tau_c \tau_t - 1)} - M_0 \right]} \quad (\text{Eq. 79})$$

Step 9:

Thermal efficiency:

$$\eta_T = 1 - \frac{1}{\tau_r \tau_c} \quad (\text{Eq. 80})$$

Propulsive efficiency:

$$\eta_P = \frac{2M_0}{V_9 / a_0 + M_0} \quad (\text{Eq. 81})$$

Overall efficiency:

$$\eta_O = \eta_P \eta_T \quad (\text{Eq. 82})$$

Summary of Equations of Single – Spool Turbojet Engine – Ideal Turbojet

Input parameters for single-spool turbojet engine – ideal turbojet

$$M_0, T_0(\text{K}, \text{°R}), \gamma, c_p \left(\frac{\text{kJ}}{\text{kg} \cdot \text{K}}, \frac{\text{Btu}}{\text{lbm} \cdot \text{°R}} \right), h_{PR} \left(\frac{\text{kJ}}{\text{kg}}, \frac{\text{Btu}}{\text{lbm}} \right), T_{t4}(\text{K}, \text{°R}), \pi_c$$

Expected outputs for single-spool turbojet engine – ideal turbojet

$$\frac{F}{\dot{m}_0} \left(\frac{\text{N}}{\text{kg} / \text{s}}, \frac{\text{lbf}}{\text{lbm} / \text{s}} \right), f, S \left(\frac{\text{mg} / \text{s}}{\text{N}}, \frac{\text{Ibm} / \text{h}}{\text{lbf}} \right), \eta_T, \eta_P, \eta_O$$

From equations (50 to 82)

$$\begin{aligned} R &= \frac{\gamma - 1}{\gamma} c_p & a_0 &= \sqrt{\gamma R g_c T_0} & \tau_r &= 1 + \frac{\gamma - 1}{2} M_0^2 & \tau_\lambda &= \frac{T_{t4}}{T_0} \\ \tau_c &= (\pi_c)^{(\gamma-1)/\gamma} & \tau_t &= 1 - \frac{\tau_r}{\tau_\lambda} (\tau_c - 1) & \frac{V_9}{a_0} &= \sqrt{\frac{2}{\gamma - 1} \frac{\tau_\lambda}{\tau_r \tau_c} (\tau_r \tau_c \tau_t - 1)} \\ \frac{F}{\dot{m}_0} &= \frac{a_0}{g_c} \left(\frac{V_9}{a_0} - M_0 \right) & f &= \frac{c_p T_0}{h_{PR}} (\tau_\lambda - \tau_r \tau_c) & S &= \frac{f}{F / \dot{m}_0} \\ \eta_T &= 1 - \frac{1}{\tau_r \tau_c} & \eta_P &= \frac{2M_0}{\frac{V_9}{a_0} + M_0} & \eta_O &= \eta_P \eta_T \end{aligned}$$

2.2.1.9 Cycle analysis steps of Single-Spool Turbojet Engine with Afterburner – Ideal case

From the Figure 4, an additional combustion chamber called an afterburner is added at the station 7. The thrust of a turbojet can be increased. The total temperature leaving the afterburner has a higher limiting value than the total temperature leaving the main combustor because the gases leaving the afterburner do not have a turbine to pass through.

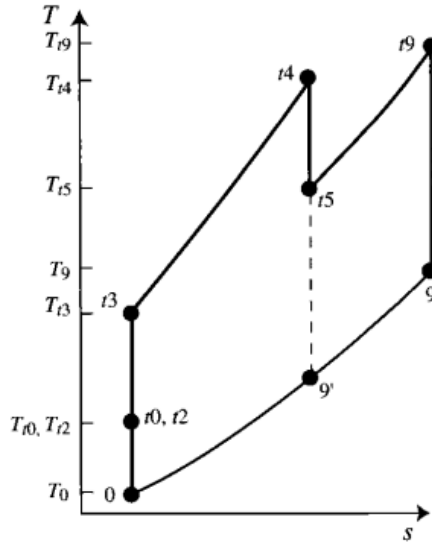


Figure 6 T-s diagram for an ideal afterburning turbojet engine [8]

By adopting the results of the ideal turbojet, the cycle analysis can be carried out by modify the equations to include afterburning phenomenon.

The gas velocity at the nozzle exit is given by

$$\frac{V_9^2}{2g_c c_p} = T_{t9} - T_9 = T_{t9} \left[1 - \left(\frac{P_9}{P_{t9}} \right)^{(\gamma-1)/\gamma} \right] \quad (\text{Eq. 83})$$

The temperature ratio $\tau_{\lambda AB}$ is defined as

$$\tau_{\lambda AB} = \frac{\tau_{t7}}{\tau_0} \quad (\text{Eq. 84})$$

The total temperature ratio of the afterburner is defined as

$$\frac{\tau_{t9}}{\tau_{t5}} = \frac{(\tau_{t9} / \tau_{t7})(\tau_{t7} / \tau_0)}{(\tau_{t5} / \tau_{t4})(\tau_{t4} / \tau_0)} = \frac{\tau_{\lambda AB}}{\tau_\lambda \tau_t} \quad (\text{Eq. 85})$$

The expression for (V_9 / a_0) is represented as shown

$$\left(\frac{V_9}{a_0} \right)^2 = \frac{2}{\gamma - 1} \tau_{\lambda AB} \left[1 - \frac{\tau_\lambda / (\tau_r / \tau_c)}{\tau_\lambda - \tau_r (\tau_c - 1)} \right] \quad (Eq. 86)$$

The total fuel-to-air ratio is defined as

$$f_t = \frac{\dot{m}_f}{\dot{m}_0} = \frac{c_p T_0}{h_{PR}} (\tau_{\lambda AB} - \tau_r) \quad (Eq. 87)$$

The thermal efficiency is given by

$$\eta_T = \frac{(\gamma - 1) c_p T_0 [(V_9 / a_0)^2 - M_0^2]}{2 f_t h_{PR}} \quad (Eq. 88)$$

Summary of equations of Single – Spool Turbojet Engine with Afterburner – Ideal Turbojet

Input parameters for single-spool turbojet engine – ideal turbojet

$$M_0, T_0 (K, ^\circ R), \gamma, c_p \left(\frac{kJ}{kg \cdot K}, \frac{Btu}{lbm \cdot ^\circ R} \right), h_{PR} \left(\frac{kJ}{kg}, \frac{Btu}{lbm} \right), T_{t4} (K, ^\circ R), T_{t7} (K, ^\circ R), \pi_c$$

Expected outputs for single-spool turbojet engine – ideal turbojet

$$\frac{F}{\dot{m}_0} \left(\frac{N}{kg/s}, \frac{lbf}{lbm/s} \right), f_{tot}, S \left(\frac{mg/s}{N}, \frac{lbm/h}{lbf} \right), \eta_T, \eta_P, \eta_O$$

From equations (50 to 88)

$$\begin{aligned} R &= \frac{\gamma - 1}{\gamma} c_p & a_0 &= \sqrt{\gamma R g_c T_0} & \tau_r &= 1 + \frac{\gamma - 1}{2} M_0^2 & \tau_\lambda &= \frac{T_{t4}}{T_0} \\ \tau_c &= (\pi_c)^{(\gamma-1)/\gamma} & \tau_t &= 1 - \frac{\tau_r}{\tau_\lambda} (\tau_c - 1) & \frac{V_9}{a_0} &= \sqrt{\frac{2}{\gamma - 1} \tau_{\lambda AB} \left[1 - \frac{\tau_\lambda / (\tau_r \tau_c)}{\tau_\lambda - \tau_r (\tau_c - 1)} \right]} \\ \frac{F}{\dot{m}_0} &= \frac{a_0}{g_c} \left(\frac{V_9}{a_0} - M_0 \right) & f_t &= \frac{c_p T_0}{h_{PR}} (\tau_{\lambda AB} - \tau_r) & S &= \frac{f_t}{F / \dot{m}_0} \end{aligned}$$

$$\eta_T = \frac{(\gamma - 1)c_p T_0 \left[(V_9 / a_0)^2 - M_0^2 \right]}{2 f_t h_{PR}} \quad \eta_P = \frac{2M_0}{\frac{V_9}{a_0} + M_0} \quad \eta_O = \eta_P \eta_T$$

2.2.2 Single-Spool Turbojet Engine – Real case

From the Figure 1, the temperature-entropy diagram for the real case is shown in Figure 7 for an inoperative afterburner and in Figure 8 for an operative afterburner.

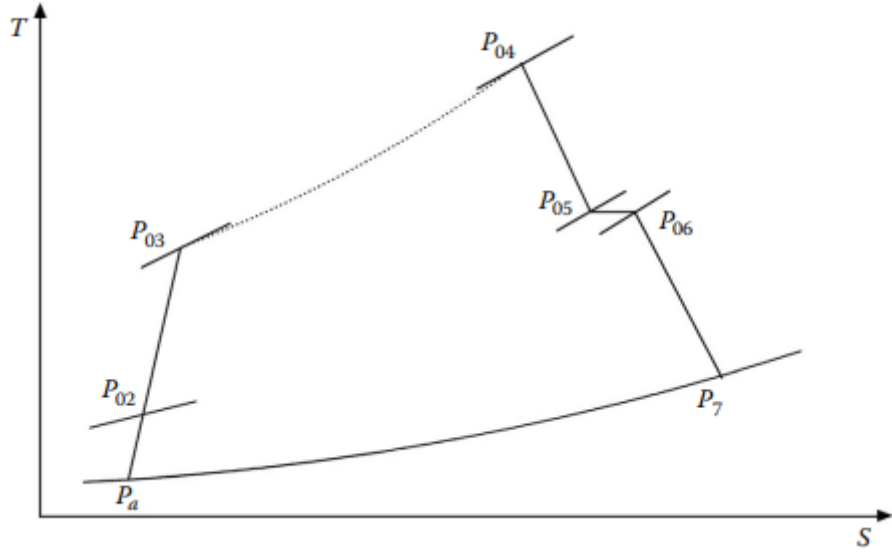


Figure 7 T-s diagram for real single-spool inoperative afterburner [7]

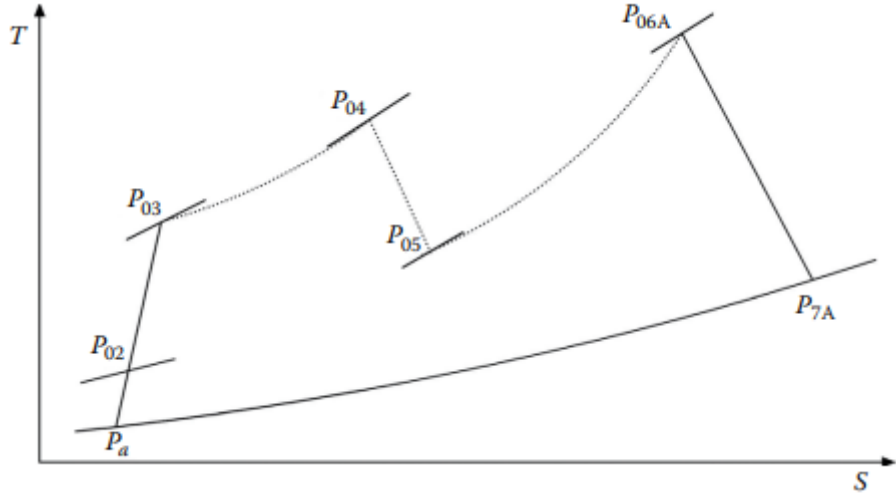


Figure 8 T-s diagram for real single-spool operative afterburner [7]

The general characteristics of single-spool turbojet real engine is as described,

1. All components are irreversible, but they are adiabatic (except burners), thus isentropic efficiencies for the intake, compressor, turbine, and nozzle are employed.
2. Friction in the air intake (or diffuser) reduces the total pressure from its free stream value and increases its entropy. The total temperature at the outlet of the intake is higher than the isentropic case, which depends on the intake or diffuser efficiency η_d .
3. The compression of the air in the compressor is accompanied by losses due to friction, turbulence, separation, shocks, and so on. Consequently, the entropy of the air also increases during its flow through the compressor. Moreover, at the outlet of the compressor, the temperature is higher than the corresponding isentropic temperature. Such an increase in temperature depends on the compressor efficiency η_c .
4. A portion of the compressed air is utilized in cooling the turbine disks, blades, and the supporting bearings through an air-bleed system. Thus, the air mass flow rate in the succeeding modules is somewhat smaller than that entering the compressor.
5. The burners are not simple heaters and the chemical composition of the working fluid changes during the combustion process. The larger the fuel-to-air ratio f , the greater the deviation in the chemical composition of the products of combustion from that of the air. Losses in the combustion process are encountered due to many factors including imperfect combustion, physical characteristics of the fuel as well as thermal losses due to conduction and radiation. Such losses are handled by introducing the burner efficiency η_b . Pressure drops due to skin friction and pressure drag in the combustors (normally 3%–6% of the total pressure of the entering air) must be also taken into account.
6. The expansion process in the turbine is nearly adiabatic. However, due to friction an increase in entropy is encountered. Moreover, the outlet temperature is higher than that of the isentropic case. Thus, the available power from the turbine is less than that in the isentropic case. The expansion process is associated with the turbine efficiency η_t .

7. The expansion process in the nozzle is similar to that in the turbine and influenced by skin friction. It is also governed by the adiabatic efficiency η_n .

8. The air/gas velocities within the gas generator are ignored. The velocities at the inlet to intake and outlet of nozzle are only calculated.

The engine performance is estimated by defining the adiabatic efficiencies as follows:

Diffuser efficiency: $0.7 < \eta_d < 0.9$ (depending strongly on flight Mach number)

Compressor efficiency: $0.85 < \eta_c < 0.90$

Burner efficiency: $0.97 < \eta_b \leq 0.99$ (same value applies for the efficiency of afterburner)

Turbine efficiency: $0.90 < \eta_t < 0.95$

Nozzle efficiency: $0.95 < \eta_n < 0.98$

The different processes through the engine modules are described as

2.2.2.1 Intake

The pressure ratio within the inlet is given and the outlet pressure is obtained

$$\pi_d = \frac{P_{02}}{P_{0a}} \quad (\text{Eq. 89})$$

Alternatively, the efficiency of the inlet (η_d) is given, the outlet pressure is given by

$$P_{02} = P_a \left(1 + \eta_d \frac{\gamma_c - 1}{2} M_a^2 \right)^{\gamma_c / \gamma_c - 1} \quad (\text{Eq. 90})$$

From the Eq. 25

$$T_{02} = T_{0a} = T_a \left(1 + \frac{\gamma_c - 1}{2} M_a^2 \right)$$

From the Eq. 24, outside the engine, the total pressure remains constant

$$P_{01} = P_{0a} = P_a \left(1 + \frac{\gamma - 1}{2} M^2 \right)^{\gamma / \gamma - 1}$$

2.2.2.2 Compressor

From the station (2) to station (3), an irreversible adiabatic compression process takes place, which is associated with the isentropic efficiency of the compressor η_c .

The outlet conditions are

$$P_{03} = (P_{02})(\pi_c) \quad (Eq. 91)$$

$$T_{03} = T_{02} \left(1 + \frac{\pi_c^{\gamma_c - 1/\gamma_c} - 1}{\eta_c} \right) \quad (Eq. 92)$$

2.2.2.3 Combustion chamber

The stagnation pressure at the outlet of combustion chamber at station (4) is less than its value at inlet of station (3) because of fluid friction. The pressure drop is either given as a definite value or as a percentage. Thus, the outlet pressure from the combustion chamber P_{cc} is expressed either as

$$P_{04} = P_{03} - \Delta P_{cc} \quad (Eq. 93)$$

Or

$$P_{04} = P_{03} (1 - \Delta P_{cc} \%) \quad (Eq. 94)$$

The outlet temperature of the combustion chamber is defined as high as the turbine material limitations will allow. The fuel-to-air ratio is calculated, taking into consideration the efficiency of burners η_b from the relation

$$f = \frac{c_{ph} T_{04} - c_{pc} T_{03}}{\eta_b Q_R - c_{ph} T_{04}} \quad (Eq. 95)$$

2.2.2.4 Turbine

From station (4) to station (5), the fluid expands through the turbine, providing shaft power input to the compressor plus any mechanical losses or accessory power. The outlet temperature to the turbine T_{05} is calculated. However, the outlet pressure is calculated considering the adiabatic efficiency of the turbine η_t as

$$\frac{P_{05}}{P_{04}} = \left[1 - \frac{1}{\eta_t} \left(1 - \frac{T_{05}}{T_{04}} \right) \right]^{\gamma_h / \gamma_h - 1} \quad (Eq. 96)$$

Alternatively, for evaluating the pressure ratio are

$$\frac{P_{05}}{P_{04}} = \left\{ 1 - \frac{(c_{pc} / c_{ph}) T_{02}}{\lambda (1 + f) T_{04}} \left[\left(\frac{P_{03}}{P_{02}} \right)^{\gamma_c - 1/\gamma_c} - 1 \right] \right\}^{\gamma_h / \gamma_h - 1} \quad (Eq. 97)$$

Substitute Eq. 25, then the equation becomes

$$\frac{P_{05}}{P_{04}} = \left\{ 1 - \frac{(c_{pc} / c_{ph}) T_a}{\lambda(1+f) \eta_c \eta_t T_{04}} \left(1 + \frac{\gamma-1}{2} M^2 \right) \left[\left(\frac{P_{03}}{P_{02}} \right)^{\gamma_c - 1/\gamma_c} - 1 \right] \right\}^{\gamma_h / \gamma_h - 1} \quad (Eq. 98)$$

2.2.2.5 Afterburner

As station (6) depends on the geometry of the engine. The pressure at the outlet of the afterburner will be less than its value at the inlet whether the afterburner is operative or inoperative.

1. The afterburner is inoperative, a treatment similar to the combustion chamber is considered. Thus, based on the value of the pressure drop within the afterburner due to the skin friction and the drag from the flame holders

From Eq. 38

$$T_{06} = T_{05}$$

$$P_{06} = P_{05} - \Delta P_{ab} \quad (Eq. 99)$$

2. The afterburner is operative, an additional amount of fuel is burnt which raises the temperature, which is much higher than the turbine-inlet temperature (TIT) because the downstream element is the nozzle, which is a non-rotating part. The walls are subjected only to thermal stresses rather than the combined thermal and mechanical stresses

From Eq. 40

$$T_{06A} = T_{\max}$$

Considered from Eq. 99

$$P_{06A} = P_{05} - \Delta P_{ab}$$

With additional fuel quantity added and burnt in the afterburner, the fuel-to-air ratio within the afterburner is declared

$$f_{ab} = \frac{(1+f)(c_{p6A} T_{06A} - c_{p5} T_{05})}{\eta_{ab} Q_R - c_{p6A} T_{06A}} \quad (Eq. 100)$$

2.2.2.6 Nozzle

A check for nozzle choking is also performed first by calculating the critical pressure depending on the state of the afterburner: 1. inoperative and 2. operative.

1. Inoperative afterburner

The critical pressure is obtained as

$$\frac{P_{06}}{P_c} = \frac{1}{\left[1 - \frac{1}{\eta_n} \left(\frac{\gamma_h - 1}{\gamma_h + 1}\right)\right]^{\gamma_h/\gamma_h - 1}} \quad (\text{Eq. 101})$$

If the nozzle is unchoked when the outlet pressure is equal to the ambient pressure, the jet speed is evaluated as

$$V_7 = \sqrt{2c_{ph}(T_{06} - T_7)} = \sqrt{2c_{ph}\eta_n T_{06} \left[1 - (P_a - P_{06})^{\gamma_h - 1/\gamma_h}\right]} \quad (\text{Eq. 102})$$

Or

$$V_7 = \sqrt{\frac{2}{\gamma_h - 1} \left[1 - (P_a - P_{06})^{\gamma_h - 1/\gamma_h}\right]} \quad (\text{Eq. 103})$$

If the ambient pressure is greater than the critical pressure, then the exhaust pressure is equal to the ambient pressure, the temperature of the exhaust gas is calculated from the relation

$$\frac{T_{06}}{T_7} = \left(\frac{P_{06}}{P_a}\right)^{\gamma_h - 1/\gamma_h} \quad (\text{Eq. 104})$$

The exhaust velocity is calculated as

$$V_7 = \sqrt{2c_{ph}(T_{06} - T_7)} = \sqrt{2c_{ph}T_{06} \left[1 - (P_a - P_{06})^{\gamma_h - 1/\gamma_h}\right]} \quad (\text{Eq. 105})$$

2. Operative afterburner

The expansion process in the nozzle starts from the station (6A) to station (7).

The critical pressure calculation is performed to check the state of the nozzle as

$$\frac{P_{06A}}{P_c} = \frac{1}{\left[1 - \frac{1}{\eta_n} \left(\frac{\gamma_h - 1}{\gamma_h + 1}\right)\right]^{\gamma_h/\gamma_h - 1}} \quad (\text{Eq. 106})$$

If the nozzle is choked, then the velocity is calculated as

$$V_{7ab} = \sqrt{\gamma_n R T_{7A}} \quad (\text{Eq. 107})$$

If the nozzle is unchoked, then the velocity is calculated as

$$V_{7ab} = \sqrt{2c_{ph}\eta_n T_{06A} \left[1 - \left(P_7 / P_{06A} \right)^{\gamma_h - 1/\gamma_h} \right]} \quad (Eq. 108)$$

The two engine parameters defining the performance of the engine are the specific thrust and the specific fuel consumption.

The specific thrust is expressed by the relation

$$\frac{T}{\dot{m}_a} = \left[(1 + f + f_{ab}) V_7 - V \right] + \frac{A_7}{\dot{m}_a} (P_7 - P_a) \quad (Eq. 109)$$

The thrust-specific fuel consumption (TSFC) is given by

$$TSFC = \frac{\dot{m}_f + \dot{m}_{fab}}{T} \quad (Eq. 110)$$

Or

$$TSFC = \frac{f + f_{ab}}{(1 + f + f_{ab}) V_7 - V + \frac{A_7}{\dot{m}_a} (P_7 - P_a)} \quad (Eq. 111)$$

For an inoperative afterburner, the specific thrust, thrust-specific fuel consumption equations above are also applied to use but the afterburner fuel-to-air ratio f_{ab} is set equal to zero.

For an inoperative afterburner, both the specific thrust T / \dot{m}_a and the TSFC are dependent on

1. Compressor pressure ratio π_c
2. Flight Mach number M
3. Maximum temperature or turbine-inlet temperature T_{04}

For an operative afterburner or in the case of augmented thrust, an additional parameter is considered, namely, the maximum temperature in the engine T_{06A} .

2.2.2.8 Cycle analysis steps of Single-Spool Turbojet Engine – Real case

For the real case, the behaviour of the turbojet engine is now including component losses, the mass flow rate of fuel through the components, and the variation of specific heats. The flow is assumed to be one-dimensional flow at the entrance and exit of each component. The station numbering can be seen in Figure 4. Single-spool turbojet engine cycle analysis for real case

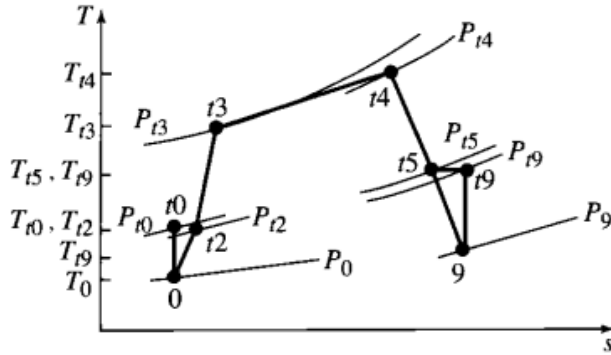


Figure 9 T-s diagram for real single-spool turbojet engine [8]

Step 1: For uninstalled thrust

$$\frac{F}{\dot{m}_0} = \frac{a_0}{g_c} \left[(1+f) \frac{V_9}{a_0} - M_0 + (1+f) \frac{R_t}{R_c} \frac{T_9/T_0}{V_9/a_0} \frac{1 - P_0/P_9}{\gamma_c} \right] \quad (\text{Eq. 112})$$

Step 2:

$$\left(\frac{V_9}{a_0} \right)^2 = \frac{\gamma_t R_t T_9}{\gamma_c R_c T_0} M_9^2 \quad (\text{Eq. 113})$$

From the definition of τ_λ

$$\tau_\lambda = \frac{c_{pt} T_{t4}}{c_{pc} T_0} \quad (\text{Eq. 114})$$

Step 3:

$$M_9^2 = \frac{2}{\gamma_t - 1} \left[\left(\frac{P_{t9}}{P_9} \right)^{(\gamma_t-1)/\gamma_t} - 1 \right] \quad (\text{Eq. 115})$$

Also

$$\frac{P_{t9}}{P_9} = \frac{P_0}{P_9} \pi_r \pi_d \pi_c \pi_b \pi_t \pi_n \quad (\text{Eq. 116})$$

Step 4:

$$\frac{T_{t9}}{T_0} = \tau_r \tau_d \tau_c \tau_b \tau_t \tau_n \quad (\text{Eq. 117})$$

Step 5:

$$f = \frac{\tau_\lambda - \tau_r \tau_c}{\eta_b h_{PR} / (c_{pc} T_0) - \tau_\lambda} = \tau_r \tau_d \tau_c \tau_b \tau_t \tau_n \quad (\text{Eq. 118})$$

Step 6:

Turbine temperature ratio is defined as

$$\tau_t = 1 - \frac{1}{\eta_m (1 + f)} \frac{\tau_r}{\tau_\lambda} (\tau_c - 1) \quad (\text{Eq. 119})$$

Turbine pressure ratio is defined as

$$\pi_t = \tau_t^{\gamma_t / [(\gamma_t - 1)e_t]} \quad (\text{Eq. 120})$$

Turbine efficiency is defined as

$$\eta_t = \frac{1 - \tau_t}{1 - \tau_t^{1/e_t}} \quad (\text{Eq. 121})$$

Compressor temperature ratio is defined as

$$\tau_c = \pi_c^{(\gamma_c - 1) / (\gamma_t e_t)} \quad (\text{Eq. 122})$$

Compressor efficiency is defined as

$$\eta_c = \frac{\pi_c^{(\gamma_c - 1) / \gamma_c} - 1}{\tau_c - 1} \quad (\text{Eq. 123})$$

Step 7: The equation for the thrust specific fuel consumption is

$$S = \frac{f}{F / \dot{m}_0} \quad (\text{Eq. 124})$$

Step 8: The propulsive and thermal efficiency are defined as

$$\eta_p = \frac{2g_c V_0 (F / \dot{m}_0)}{a_0^2 \left[(1 + f) (V_9 / a_0)^2 - M_0^2 \right]} \quad (\text{Eq. 125})$$

And

$$\eta_t = \frac{a_0^2 \left[(1 + f) (V_9 / a_0)^2 - M_0^2 \right]}{2g_c f h_{PR}} \quad (\text{Eq. 126})$$

Summary of Equations of Single – Spool Turbojet Engine – Real Turbojet

Input parameters for single-spool turbojet engine – real turbojet

$$M_0, T_0 \left(\text{K}, {}^\circ\text{R} \right), \gamma_c, c_{pc} \left(\frac{\text{kJ}}{\text{kg} \cdot \text{K}}, \frac{\text{Btu}}{\text{lbf} \cdot {}^\circ\text{R}} \right), \gamma_t, c_{pt} \left(\frac{\text{kJ}}{\text{kg} \cdot \text{K}}, \frac{\text{Btu}}{\text{lbf} \cdot {}^\circ\text{R}} \right), h_{PR} \left(\frac{\text{kJ}}{\text{kg}}, \frac{\text{Btu}}{\text{lbf}} \right), \\ \pi_{dmax}, \pi_c, \pi_b, \pi_n, e_c, e_t, \eta_b, \eta_m, P_0 / P_9, T_{t4} \left(\text{K}, {}^\circ\text{R} \right)$$

Expected outputs for single-spool turbojet engine – real turbojet

$$\frac{F}{\dot{m}_0} \left(\frac{\text{N}}{\text{kg} / \text{s}}, \frac{\text{Ibf}}{\text{lbf} / \text{s}} \right), f, S \left(\frac{\text{mg} / \text{s}}{\text{N}}, \frac{\text{lbf} / \text{h}}{\text{Ibf}} \right), \eta_T, \eta_P, \eta_O, \eta_c, \eta_t$$

From equations (102 to 126)

$$R_c = \frac{\gamma_c - 1}{\gamma_c} c_{pc} \quad R_t = \frac{\gamma_t - 1}{\gamma_t} c_{pt} \quad a_0 = \sqrt{\gamma_c R_c g_c T_0} \quad V_0 = a_0 M_0 \\ \tau_r = 1 + \frac{\gamma_c - 1}{2} M_0^2 \quad \pi_r = \tau_r^{\gamma_t / (\gamma_t - 1)} \quad \pi_d = \pi_{dmax} \eta_r \quad \tau_\lambda = \frac{c_{pt} T_{t4}}{c_{pc} T_0} \\ \eta_r = 1 \text{ for } M_0 \leq 1 \quad \eta_r = 1 - 0.075 (M_0 - 1)^{1.35} \text{ for } M_0 > 1 \\ \tau_c = \pi_c^{(\gamma_c - 1) / (\gamma_c e_c)} \quad \eta_c = \frac{\pi_c^{(\gamma_c - 1) / \gamma_c} - 1}{\tau_c - 1} \quad f = \frac{\tau_\lambda - \tau_r \tau_c}{h_{PR} \eta_b / (c_{pc} T_0) - \tau_\lambda} \\ \tau_t = 1 - \frac{1}{\eta_m (1 + f)} \frac{\tau_r}{\tau_\lambda} (\tau_c - 1) \quad \pi_t = \tau_t^{\gamma_t [(\gamma_t - 1) e_t]} \quad \eta_t = \frac{1 - \tau_t}{1 - \tau_t^{1/e_t}} \\ \frac{P_{t9}}{P_9} = \frac{P_0}{P_9} \pi_r \pi_d \pi_c \pi_b \pi_t \pi_n \quad M_9 = \sqrt{\frac{2}{\gamma_t - 1} \left[\left(\frac{P_{t9}}{P_9} \right)^{\frac{\gamma_t - 1}{\gamma_t}} - 1 \right]} \\ \frac{T_9}{T_0} = \frac{\tau_\lambda \tau_t}{(P_{t9} / P_9)^{(\gamma_t - 1) / \gamma_t}} \frac{c_{pc}}{c_{pt}} \quad \frac{V_9}{a_0} = M_9 \sqrt{\frac{\gamma_t R_t T_9}{\gamma_c R_c T_0}} \quad S = \frac{f}{F / \dot{m}_0} \\ \frac{F}{\dot{m}_0} = \frac{a_0}{g_c} \left[(1 + f) \frac{V_9}{a_0} - M_0 + (1 + f) \frac{R_t T_9 / T_0}{R_c V_9 / a_0} \frac{(1 - P_0 / P_9)}{\gamma_c} \right] \quad \eta_o = \eta_P \eta_T \\ \eta_T = \frac{a_0^2 \left[(1 + f) (V_9 / a_0)^2 - M_0^2 \right]}{2 g_c f h_{PR}} \quad \eta_P = \frac{2 g_c V_0 (F / \dot{m}_0)}{a_0^2 \left[(1 + f) (V_9 / a_0)^2 - M_0^2 \right]}$$

2.2.2.9 Cycle analysis steps of Single-Spool Turbojet Engine with Afterburner – Real case

From the Figure 4, the afterburner is added at the station 7.

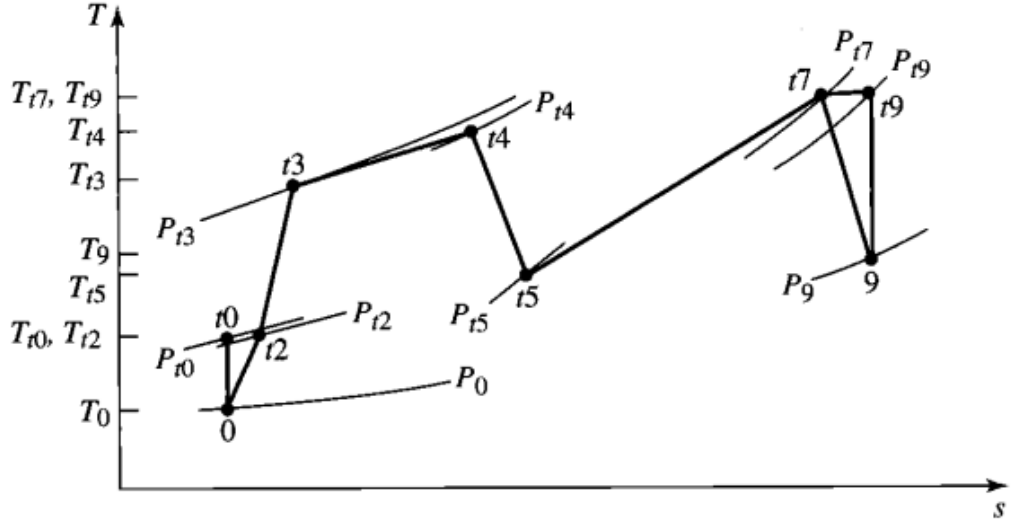


Figure 10 T-s diagram for single-spool real afterburning turbojet engine [8]

The afterburner definitions are defined as

$$\pi_{AB} = \frac{P_{t7}}{P_{t6}} \quad (\text{Eq. 127})$$

$$f_{AB} = \frac{\dot{m}_{fAB}}{\dot{m}_0} \quad (\text{Eq. 128})$$

$$\tau_{AB} = \frac{T_{t7}}{T_{t6}} \quad (\text{Eq. 129})$$

$$\tau_{\lambda AB} = \frac{c_{pAB}}{c_{pc}} \frac{T_{t7}}{T_0} = \frac{c_{pAB}}{c_{pc}} \tau_{\lambda} \tau_i \tau_{AB} \quad (\text{Eq. 130})$$

$$\eta_{AB} = \frac{(\dot{m}_0 + \dot{m}_f + \dot{m}_{fAB}) c_{pAB} T_{t7} - (\dot{m}_0 + \dot{m}_f) c_{pt} T_{t6}}{\dot{m}_{fAB} h_{PR}} \quad (\text{Eq. 131})$$

$$\frac{\dot{m}_9}{\dot{m}_0} = \frac{\dot{m}_0 + \dot{m}_f + \dot{m}_{fAB}}{\dot{m}_0} = 1 + f + f_{AB} \quad (\text{Eq. 132})$$

Step 1: The specific thrust equation becomes

$$\frac{F}{\dot{m}_0} = \frac{a_0}{g_c} \left[(1 + f + f_{AB}) \frac{V_9}{a_0} - M_0 + (1 + f + f_{AB}) \frac{R_{AB}}{R_c} \frac{T_9 / T_0}{V_9 / a_0} \frac{1 - P_0 / P_9}{\gamma_c} \right] \quad (\text{Eq. 133})$$

Step 2:

$$\left(\frac{V_9}{a_0} \right)^2 = \frac{\gamma_{AB} R_{AB} T_9}{\gamma_c R_c T_0} M_9^2 \quad (Eq. 134)$$

Step 3:

$$M_9^2 = \frac{2}{\gamma_{AB} - 1} \left[\left(\frac{P_{t9}}{P_9} \right)^{(\gamma_{AB}-1)/\gamma_{AB}} - 1 \right] \quad (Eq. 135)$$

Also

$$\frac{P_{t9}}{P_9} = \frac{P_0}{P_9} \pi_r \pi_d \pi_c \pi_b \pi_t \pi_{AB} \pi_n \quad (Eq. 136)$$

Step 4:

$$\frac{T_9}{T_0} = \frac{T_{t9} / T_0}{\left(P_{t9} / P_9 \right)^{(\gamma_{AB}-1)/\gamma_{AB}}} \quad (Eq. 137)$$

And

$$\frac{T_{t9}}{T_0} = \tau_{\lambda AB} \frac{c_{pc}}{c_{pAB}} \quad (Eq. 138)$$

Step 5:

$$f_{AB} = (1 + f) \frac{\tau_{\lambda AB} - \tau_{\lambda} \tau_t}{\eta_{AB} h_{PR} / (c_{pc} T_0) - \tau_{\lambda AB}} \quad (Eq. 139)$$

Step 6:

The power balance between the turbine and compressor is unaffected by the addition of the afterburner. Thus, equations for $\tau_t, \pi_t, \eta_t, \tau_c, \eta_c$ are applied to this engine cycle.

Step 7: The equation for the thrust specific fuel consumption is

$$S = \frac{f + f_{AB}}{F / \dot{m}_0} \quad (Eq. 140)$$

Step 8: The propulsive and thermal efficiency are defined as

$$\eta_p = \frac{2 g_c V_0 (F / \dot{m}_0)}{a_0^2 \left[(1 + f + f_{AB}) (V_9 / a_0)^2 - M_0^2 \right]} \quad (Eq. 141)$$

$$\eta_c = \frac{a_0^2 \left[(1 + f + f_{AB}) (V_9 / a_0)^2 - M_0^2 \right]}{2 g_c (f + f_{AB}) h_{PR}} \quad (Eq. 142)$$

Summary of Equations of Single-Spool Turbojet Engine with Afterburner – Real Turbojet

Input parameters for single-spool turbojet engine with afterburner – real turbojet

$$M_0, T_0 \left(K, {}^{\circ}R \right), \gamma_c, c_{pc} \left(\frac{kJ}{kg \cdot K}, \frac{Btu}{lbm \cdot {}^{\circ}R} \right), \gamma_t, c_{pt} \left(\frac{kJ}{kg \cdot K}, \frac{Btu}{lbm \cdot {}^{\circ}R} \right), h_{PR} \left(\frac{kJ}{kg}, \frac{Btu}{lbm} \right), \\ \gamma_{AB}, c_{pAB} \left(\frac{kJ}{kg \cdot K}, \frac{Btu}{lbm \cdot {}^{\circ}R} \right), \pi_{dmax}, \pi_c, \pi_b, \pi_{AB}, \pi_n, e_c, e_t, \eta_b, \eta_m, \eta_{AB}, \\ P_0 / P_9, T_{t4} \left(K, {}^{\circ}R \right), T_{t7} \left(K, {}^{\circ}R \right)$$

Expected outputs for single-spool turbojet engine with afterburner – real turbojet

$$\frac{F}{\dot{m}_0} \left(\frac{N}{kg / s}, \frac{Ibf}{Ibm / s} \right), f, f_{AB}, S \left(\frac{mg / s}{N}, \frac{Ibm / h}{Ibf} \right), \eta_T, \eta_P, \eta_O, \eta_c, \eta_t$$

From equations (102 to 142)

The equations for single-spool turbojet real engine with afterburner can be mostly adopted from the single-spool turbojet real engine without afterburner with modification of some equations as listed below

$$R_{AB} = \frac{\gamma_{AB} - 1}{\gamma_{AB}} c_{pAB} \quad \tau_{\lambda AB} = \frac{c_{pAB}}{c_{pc}} \frac{T_{t7}}{T_0} \quad \frac{T_9}{T_0} = \frac{T_{t7} / T_0}{(P_{t9} / P_9)^{(\gamma_{AB} - 1) / \gamma_{AB}}} \\ f_{AB} = (1 + f) \frac{\tau_{\lambda AB} - \tau_{\lambda} \tau_t}{\eta_{AB} h_{PR} / (c_{pc} T_0) - \tau_{\lambda AB}} \quad \frac{P_{t9}}{P_9} = \frac{P_0}{P_9} \pi_r \pi_d \pi_c \pi_b \pi_t \pi_{AB} \pi_n \\ M_0^2 = \frac{2}{\gamma_{AB} - 1} \left[\left(\frac{P_{t9}}{P_9} \right)^{\gamma_{AB} - \frac{1}{\gamma_{AB}}} \right] \quad \frac{V_9}{a_0} = M_0 \sqrt{\frac{\gamma_{AB} R_{AB} T_9}{\gamma_c R_c T_0}} \\ \frac{F}{\dot{m}_0} = \frac{a_0}{g_c} \left[\begin{array}{l} \left(1 + f + f_{AB} \right) \frac{V_9}{a_0} - M_0 + \left(1 + f + f_{AB} \right) \\ \times \frac{R_{AB}}{R_c} \frac{T_9 / T_0}{V_9 / a_0} \frac{1 - P_0 / P_9}{\gamma_c} \end{array} \right] \quad S = \frac{f + f_{AB}}{F / \dot{m}_0} \\ \eta_O = \eta_P \eta_T \quad \eta_P = \frac{2 g_c V_0 F / \dot{m}_0}{a_0^2 \left[\left(1 + f + f_{AB} \right) \left(V_9 / a_0 \right)^2 - M_0^2 \right]} \\ \eta_T = \frac{a_0^2 \left[\left(1 + f + f_{AB} \right) \left(V_9 / a_0 \right)^2 - M_0^2 \right]}{2 g_c (f + f_{AB}) h_{PR}}$$

2.3 Cycle Analysis of Double-Spool Turbojet Engine

2.3.1 Double-Spool Turbojet Engine – Real case

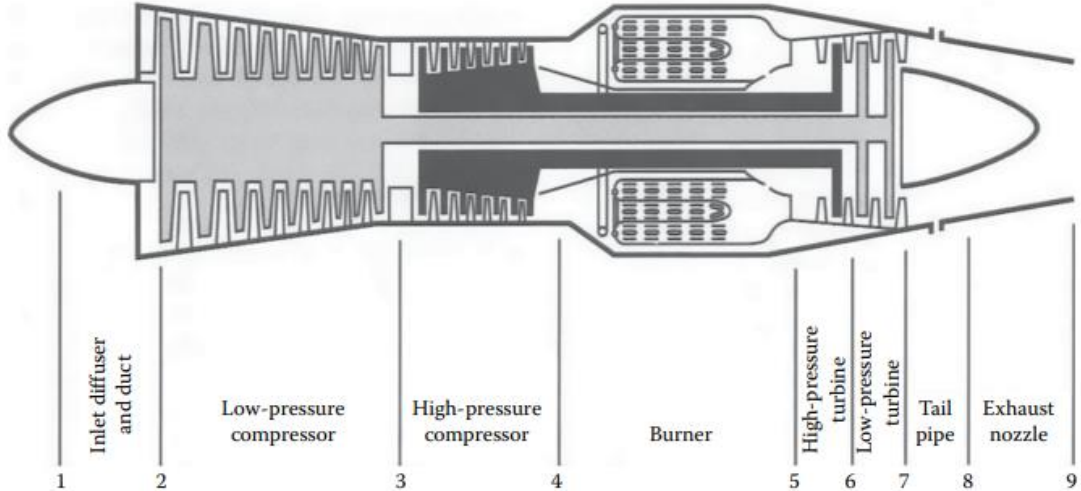


Figure 11 Double-Spool Turbojet Engine station [7]

The two-spool engines are composed of two compressors coupled to two turbines through two spools or shafts. As in the case of single spool with afterburner turbojet, the afterburning engines have two combustors, namely, the conventional combustion chamber and the afterburner installed downstream the LPT.

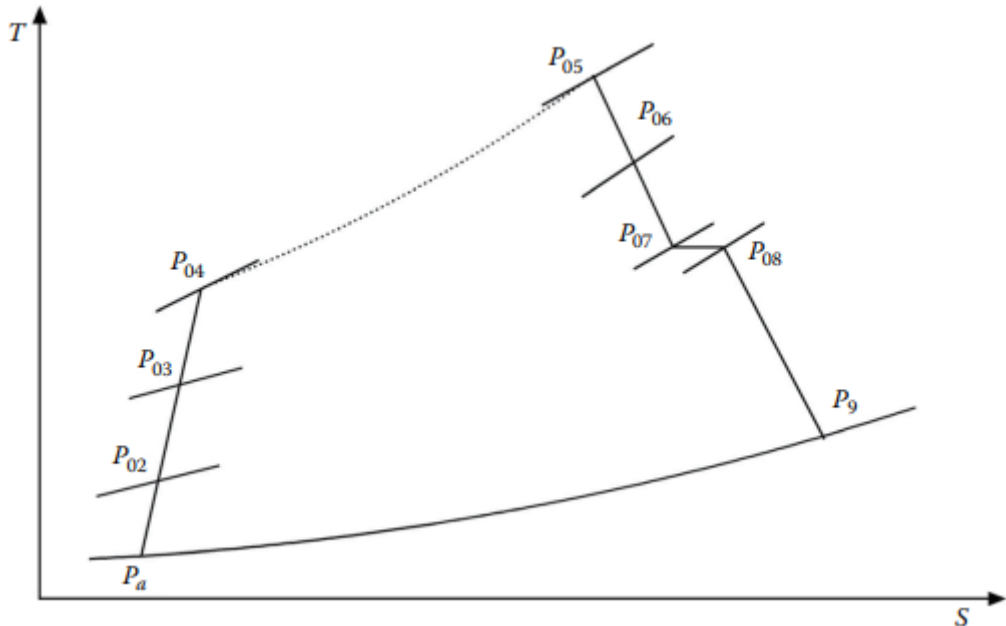


Figure 12 T-s cycle for inoperative Double-Spool Turbojet [7]

As for the ideal case, the efficiencies are set equal to unity and no pressure losses.

2.3.1.1 Intake or inlet

The inlet conditions of the air entering the inlet are the ambient pressure and temperature P_a and T_a respectively. The intake has an isentropic efficiency η_d . For a flight Mach number M_a , the temperature and pressure at the outlet of the intake are T_{02} and P_{02} given by the same relations as the single spool engine

$$P_{02} = P_a \left(1 + \eta_d \frac{\gamma_c - 1}{2} M_a^2 \right)^{\gamma/\gamma-1} \quad (\text{Eq. 143})$$

The stagnation temperatures for stations (a), (1), (2) are also equal, as represented in Eq. 28

$$T_{02} = T_{0a} = T_a \left(1 + \frac{\gamma_c - 1}{2} M_a^2 \right)$$

2.3.1.2 Low-pressure compressor

For a known compressor pressure ratio π_{c1} and isentropic efficiency η_{c1} , the temperature and pressure at the outlet of the low-pressure compressor are given by

$$P_{03} = (P_{02})(\pi_{c1}) \quad (\text{Eq. 144})$$

$$T_{03} = T_{02} \left[1 + \frac{\pi_{c1}^{\gamma_c-1/\gamma_c} - 1}{\eta_{c1}} \right] \quad (\text{Eq. 145})$$

2.3.1.3. High-pressure compressor

Similarly, both the pressure ratio π_{c2} and its isentropic efficiency η_{c2} are known. Thus, the temperature and pressure at the outlet of the high-pressure compressor are given as

$$P_{04} = (P_{03})(\pi_{c2}) \quad (\text{Eq. 146})$$

$$T_{04} = T_{03} \left[1 + \frac{\pi_{c2}^{\gamma_c-1/\gamma_c} - 1}{\eta_{c2}} \right] \quad (\text{Eq. 147})$$

2.3.1.4. Combustion Chamber

The temperature at the end of combustion process T_{05} is generally known. It is the maximum temperature in the cycle if the afterburner is inoperative. The pressure at the end of the combustion depends on the pressure drop in the combustion process

itself. Thus, depending on the known expression for the pressure drop in the combustion chamber, it may be expressed as

$$P_{05} = P_{04} - \Delta P_{cc} \quad (Eq. 148)$$

Or

$$P_{05} = P_{04} (1 - \Delta P_{cc} \%) \quad (Eq. 149)$$

The energy balance for the combustion chamber yields the following relation for the fuel-to-air ratio (f) defined as the ratio between the mass of fuel burnt to the air mass flow rate through the gas generator

$$\dot{m}_a (1 + f) c_{ph} T_{05} = \dot{m}_a c_{pc} T_{04} + \eta_b \dot{m}_f Q_R \quad (Eq. 150)$$

Then the fuel-to-air ratio is determined from the relation

$$f = \frac{(c_{ph} / c_{ph})(T_{05} / T_{04}) - 1}{\eta_b (Q_R / c_{pc} T_{04}) - (c_{ph} / c_{ph})(T_{05} / T_{04})} \quad (Eq. 151)$$

2.3.1.5. High-pressure turbine

The power generated in the high-pressure turbine is used in driving the high-pressure compressor in addition to some of the accessories. If the ratio of the power needed to drive the high-pressure compressor to the power available from the high-pressure turbine is λ_1 , then the energy balance for the compressor-turbine shaft is

$$W_{HPC} = \lambda_1 W_{HPT} \quad (Eq. 152)$$

Here λ is of the range 75% - 85%. Thus, in terms of the temperature's differences

$$c_{pc} (T_{04} - T_{03}) = \lambda_1 (1 + f) c_{ph} (T_{05} - T_{06}) \quad (Eq. 153)$$

$$\frac{T_{06}}{T_{05}} = 1 - \frac{(c_{pc} / c_{ph}) T_{03}}{\lambda_1 (1 + f) T_{05}} \left[\left(\frac{T_{04}}{T_{03}} \right) - 1 \right] \quad (Eq. 154)$$

The pressure ratios of the high-pressure turbine and high-pressure compressor are related by

$$\frac{P_{06}}{P_{05}} = \left\{ 1 - \frac{(c_{pc} / c_{ph}) T_{03}}{\lambda_1 (1 + f) \eta_{c2} \eta_{t2} T_{05}} \left[\left(\frac{P_{04}}{P_{03}} \right)^{\gamma_c - 1/\gamma_c} - 1 \right] \right\}^{\gamma_h / \gamma_h - 1} \quad (Eq. 155)$$

2.3.1.6. Low-pressure turbine

The power consumed in the compression from station (2) to station (3) must be supplied through the low-pressure turbine in expansion from station (6) to station (7). If the ratio of the power needed to drive the compressor to the power available in the turbine is λ_2 , then the energy balance for the low-pressure spool is

$$W_{LPC} = \lambda_2 W_{LPT} \quad (\text{Eq. 156})$$

The power available in the turbine λ_2 is of the range 75% - 85%. In terms of the temperature differences

$$c_{pc}(T_{03} - T_{02}) = \lambda_2(1+f)c_{ph}(T_{06} - T_{07}) \quad (\text{Eq. 157})$$

$$\frac{T_{07}}{T_{06}} = 1 - \frac{(c_{pc}/c_{ph})T_{02}}{\lambda_2(1+f)T_{06}} \left[\left(\frac{T_{03}}{T_{02}} \right)^{\gamma_c - 1/\gamma_c} - 1 \right] \quad (\text{Eq. 158})$$

Then the turbine and compressor pressure ratios are related by

$$\frac{P_{07}}{P_{06}} = \left\{ 1 - \frac{(c_{pc}/c_{ph})T_{02}}{\lambda_2(1+f)\eta_{c1}\eta_{t1}T_{06}} \left[\left(\frac{P_{03}}{P_{02}} \right)^{\gamma_c - 1/\gamma_c} - 1 \right] \right\}^{\gamma_h/\gamma_h - 1} \quad (\text{Eq. 159})$$

From the diffuser part, the equation can be defined as

$$\frac{P_{07}}{P_{06}} = \left\{ 1 - \frac{(c_{pc}/c_{ph})T_a}{\lambda_2(1+f)\eta_{c1}\eta_{t1}T_{06}} \left(1 + \frac{\gamma - 1}{2} M^2 \right) \left[\left(\frac{P_{03}}{P_{02}} \right)^{\gamma_c - 1/\gamma_c} - 1 \right] \right\}^{\gamma_h/\gamma_h - 1} \quad (\text{Eq. 160})$$

2.3.1.7. Jet pipe

The jet pipe following the low-pressure turbine and preceding the nozzle is associated with a slight pressure drop, while the total temperature remains unchanged

$$P_{08} = P_{07} - \Delta P_{jet\ pipe} \quad (\text{Eq. 161})$$

$$T_{08} = T_{07} \quad (\text{Eq. 162})$$

2.3.1.8. Nozzle

Nozzle choking checking is performed. Thus, for an isentropic efficiency of the nozzle η_n , the critical pressure is obtained from the relation

$$\frac{P_{08}}{P_c} = \frac{1}{\left[1 - \frac{1}{\eta_n} \left(\frac{\gamma_h - 1}{\gamma_h + 1} \right) \right]^{\gamma_h / \gamma_h - 1}} \quad (\text{Eq. 163})$$

If the nozzle is unchoked, then the outlet pressure is equal to the ambient pressure. The speed is now evaluated from the relation

$$V_9 = \sqrt{2c_{ph}\eta_n T_{08} \left[1 - \left(P_a / P_{08} \right)^{\gamma_h - 1 / \gamma_h} \right]} \quad (\text{Eq. 164})$$

If the nozzle is choked

$$\frac{T_{08}}{T_9} = \left(\frac{\gamma_h + 1}{2} \right) \quad (\text{Eq. 165})$$

The velocity is expressed as

$$V_9 = \sqrt{\gamma_h R T_9} \quad (\text{Eq. 166})$$

Summary of Equations of Double-Spool Turbojet Engine – Real Turbojet

Input parameters for double-spool turbojet engine – real turbojet

Choices

Flight parameters: $M_0, T_0(K, {}^\circ R), P_0(kPa, psia)$

Throttle setting: $T_{t4}(K, {}^\circ R), T_{t7}(K, {}^\circ R)$

Exhaust nozzle setting: P_0 / P_9

Design constants

π : $\pi_{dmax}, \pi_b, \pi_{tH}, \pi_{tL}, \pi_{AB}, \pi_n$

τ : τ_{tH}, τ_{tL}

η : $\eta_{cL}, \eta_{cH}, \eta_b, \eta_{AB}, \eta_{mL}, \eta_{mH}$

Gas properties: $\gamma_c, \gamma_t, \gamma_{AB}, c_{pc}, c_{pt}, c_{pAB} [kJ / (kg \cdot K), Btu / (lbm \cdot {}^\circ R)]$

Fuel: $h_{PR}(kJ / kg, Btu / lbm)$

Reference conditions

Flight parameters: $M_{0R}, T_{0R}(K, {}^\circ R), P_{0R}(kPa, psia), \tau_{rR}, \pi_{rR}$

Throttle setting: $T_{t4}(K, {}^\circ R)$

Component behavior: $\pi_{dR}, \pi_{cLR}, \pi_{cHR}, \tau_{cLR}, \tau_{cHR}$

Expected outputs for double-spool turbojet engine – real turbojet

Overall performance:

$$F(N, lbf), \dot{m}_0(kg / s, lbm / s), f_0, S\left(\frac{mg / s}{N}, \frac{lbm / h}{lbf}\right), \eta_p, \eta_t, \eta_o$$

Design constants

π : $\pi_{dmax}, \pi_b, \pi_{tH}, \pi_{tL}, \pi_{AB}, \pi_n$

τ : τ_{tH}, τ_{tL}

η : $\eta_{cL}, \eta_{cH}, \eta_b, \eta_{AB}, \eta_{mL}, \eta_{mH}$

Gas properties: $\gamma_c, \gamma_t, \gamma_{AB}, c_{pc}, c_{pt}, c_{pAB} [kJ / (kg \cdot K), Btu / (lbm \cdot {}^\circ R)]$

Fuel: $h_{PR}(kJ / kg, Btu / lbm)$

Reference conditions

Flight parameters: $M_{0R}, T_{0R}(K, {}^\circ R), P_{0R}(kPa, psia), \tau_{rR}, \pi_{rR}$

Throttle setting: $T_{t4}(K, {}^\circ R)$

Component behavior:

$$\pi_{cL}, \pi_{cH}, \tau_{cL}, \tau_{cH}, f, f_{AB}, M_9, (N / N_R)_{LPspool}, (N / N_R)_{HPspool}$$

From equations (143 to 166)

$$\begin{aligned}
R_{AB} &= R_t, c_{pAB} = c_{pt}, \gamma_{AB} = \gamma_t, T_{t7} = T_{t4}\tau_{tH}\tau_{tL}, \pi_{AB} = 1, f_{AB} = 0 \\
R_c &= \frac{\gamma_c - 1}{\gamma_c} c_{pc} \quad R_t = \frac{\gamma_t - 1}{\gamma_t} c_{pt} \quad a_0 = \sqrt{\gamma_c R_c g_c T_0} \quad V_0 = a_0 M_0 \\
\tau_r &= 1 + \frac{\gamma_c - 1}{2} M_0^2 \quad \pi_r = \tau_r^{\gamma_c/(\gamma_c-1)} \quad \pi_d = \pi_{max} \eta_r \\
\eta_r &= 1 \text{ for } M_0 \leq 1, \quad \eta_r = 1 - 0.075(M_0 - 1)^{1.35} \text{ for } M_0 > 1 \\
\tau_{cL} &= 1 + \frac{T_{t4}/T_0}{(T_{t4}/T_0)_R} \frac{(\tau_r)_R}{\tau_r} (\tau_{cL} - 1)_R \quad \pi_{cL} = [1 + \eta_{cL} (\tau_{cL} - 1)]^{\gamma_c/(\gamma_c-1)} \\
\tau_{cH} &= 1 + \frac{T_{t4}/T_0}{(T_{t4}/T_0)_R} \frac{(\tau_r \tau_{cL})_R}{\tau_r \tau_{cL}} (\tau_{cH} - 1)_R \quad \pi_{cH} = [1 + \eta_{cH} (\tau_{cH} - 1)]^{\gamma_c/(\gamma_c-1)} \\
\tau_\lambda &= \frac{c_{pt} T_{t4}}{c_{pc} T_0} \quad f = \frac{\tau_\lambda - \tau_r \tau_{cL} \tau_{cH}}{h_{PR} \eta_b / (c_{pc} T_0) - \tau_\lambda} \quad \dot{m}_0 = \dot{m}_{0R} \frac{P_0 \pi_r \pi_d \pi_{cL} \pi_{cH}}{(P_0 \pi_r \pi_d \pi_{cL} \pi_{cH})_R} \sqrt{\frac{T_{t4R}}{T_{t4}}} \\
\frac{P_{t9}}{P_9} &= \frac{P_0}{P_9} \pi_r \pi_d \pi_{cL} \pi_{cH} \pi_b \pi_{tL} \pi_{tH} \pi_{AB} \pi_n \quad M_9 = \sqrt{\frac{2}{\gamma_{AB} - 1} \left[\left(\frac{P_{t9}}{P_9} \right)^{(\gamma_{AB}-1)/\gamma_{AB}} - 1 \right]} \\
\frac{T_9}{T_0} &= \frac{T_{t7}/T_0}{(P_{t9}/P_9)^{(\gamma_{AB}-1)/\gamma_{AB}}} \quad \frac{V_9}{a_0} = M_9 \sqrt{\frac{\gamma_{AB} R_{AB}}{\gamma_c R_c} \frac{T_9}{T_0}} \quad f_o = f + f_{AB} \\
\frac{F}{\dot{m}_0} &= \frac{a_0}{g_c} \left[(1 + f_o) \frac{V_9}{a_0} - M_0 + (1 + f_o) \frac{R_{AB}}{R_c} \frac{T_9/T_0}{V_9/a_0} \frac{1 - P_0/P_9}{\gamma_c} \right] \quad S = \frac{f_o}{F/\dot{m}_0} \\
\eta_T &= \frac{a_0^2 \left[(1 + f_o) \left(V_9/a_0 \right)^2 - M_0^2 \right]}{2 g_c f_o h_{PR}} \quad \eta_P = \frac{2 g_c V_0 (F/\dot{m}_0)}{a_0^2 \left[(1 + f_o) \left(V_9/a_0 \right)^2 - M_0^2 \right]} \\
\eta_o &= \eta_P \eta_T \\
\left(\frac{N}{N_R} \right)_{LPspool} &= \sqrt{\frac{T_0 \tau_r \pi_{cL}^{(\gamma-1)/\gamma} - 1}{T_{0R} \tau_{rR} \pi_{cLR}^{(\gamma-1)/\gamma} - 1}} \quad \left(\frac{N}{N_R} \right)_{HPspool} = \sqrt{\frac{T_0 \tau_r \tau_{cL} \pi_{cH}^{(\gamma-1)/\gamma} - 1}{T_{0R} \tau_{rR} \tau_{cLR} \pi_{cHR}^{(\gamma-1)/\gamma} - 1}} \\
\frac{A_9}{A_{9R}} &= \left[\frac{P_{t9}/P_9}{(P_{t9}/P_9)_R} \right]^{(\gamma_t+1)/(2\gamma_t)} \sqrt{\frac{\left(P_{t9}/P_9 \right)_R^{(\gamma_t-1)/\gamma_t} - 1}{\left(P_{t9}/P_9 \right)^{(\gamma_t-1)/\gamma_t} - 1}}
\end{aligned}$$

2.3.2 Double-Spool Turbojet Engine with Afterburner – Real case

The diagrammatic sketch for the engine is shown in Figure 8 and the cycle plotted on the T-s diagram is shown in Figure 13. The low-pressure compressor is driven by the low-pressure turbine whereas the high-pressure compressor is driven by the high-pressure turbine. Considering the afterburner, due to fuel addition in the afterburner, a steep rise in temperature than that obtained in the combustion chamber.

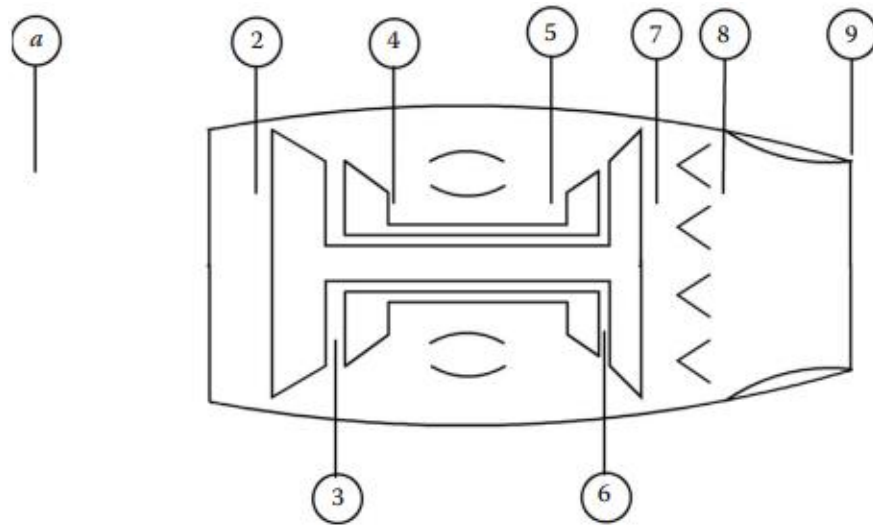


Figure 13 Stations for a Double-Spool Turbojet Engine with operative afterburner [7]

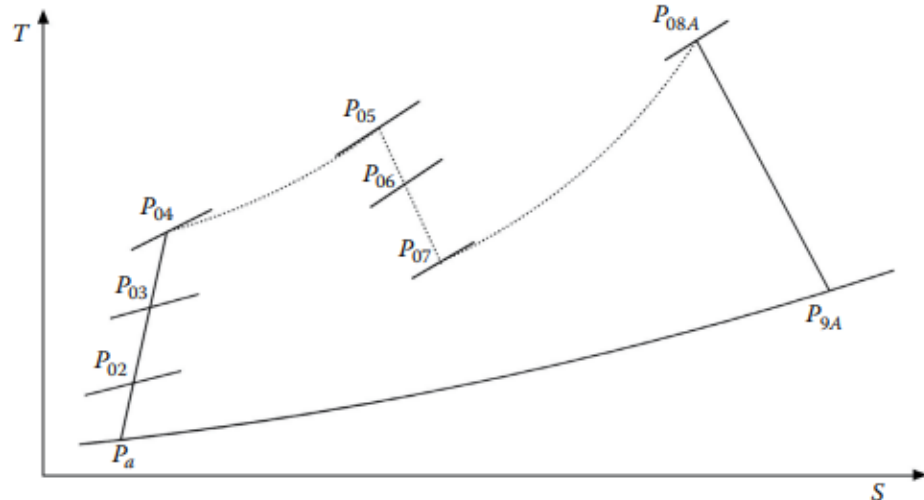


Figure 14 Cycle for a Double-Spool Turbojet Engine with operative afterburner [7]

Due to the fuel lines, igniters, and flameholders, a pressure drop is encountered in the afterburner

$$P_{08A} = P_{07} - \Delta P_{ab} \quad (\text{Eq. 167})$$

Or

$$P_{08A} = P_{07} (1 - \Delta P_{ab} \%) \quad (\text{Eq. 168})$$

The maximum temperature in the cycle is obtained at the end of the combustion process

$$T_{08A} = T_{max} \quad (\text{Eq. 169})$$

The afterburner fuel-to-air ratio is calculated from the energy balance in the afterburner

$$f_{ab} = \frac{(1+f)(c_{p8A}T_{08A} - c_{p7}T_{07})}{\eta_{ab}Q_R - c_{p8A}T_{08A}} \quad (\text{Eq. 170})$$

As the hot gases leaving the afterburner expand in the nozzle from the station (08A) to station (9), a nozzle choking checking is performed

$$\frac{P_{08A}}{P_c} = \frac{1}{\left[1 - \frac{1}{\eta_n} \left(\frac{\gamma_h - 1}{\gamma_h + 1}\right)\right]^{\gamma_h / (\gamma_h - 1)}} \quad (\text{Eq. 171})$$

If the nozzle is unchoked, the speed is expressed as

$$V_{9ab} = \sqrt{2c_{ph}\eta_n T_{08A} \left[1 - \left(P_a / P_{08A}\right)^{\gamma_h - 1 / \gamma_h}\right]} \quad (\text{Eq. 172})$$

If the nozzle is choked, the exhaust gases leave the nozzle with a temperature T_{9A} , from Eq. 165

$$\frac{T_{08}}{T_{9A}} = \left(\frac{\gamma_h + 1}{2}\right)$$

The exhaust speed is expressed as

$$V_{9ab} = \sqrt{\gamma_h R T_{9A}} \quad (\text{Eq. 173})$$

The performance parameters are the specific thrust and the specific fuel consumption as well as the three efficiencies as usual, the specific thrust is expressed by the relation

$$\frac{T}{\dot{m}_a} = \left[(1 + f + f_{ab}) V_9 - V \right] + \frac{A_9}{\dot{m}_a} (P_9 - P_a) \quad (\text{Eq. 174})$$

The thrust-specific fuel consumption (TSFC) is expressed by the relation

$$TSFC = \frac{\dot{m}_f + \dot{m}_{fab}}{T} \quad (Eq. 175)$$

Or

$$TSFC = \frac{f + f_{ab}}{(1 + f + f_{ab})V_9 - V + \frac{A_9}{\dot{m}_a}(P_9 - P_a)} \quad (Eq. 176)$$

For an inoperative afterburner, the same equations for specific thrust and thrust-specific fuel consumption are applied but the afterburner fuel-to-air ratio f_{ab} is set equal to zero.

As the turbojet engines resemble a one-stream flow engine, the propulsive efficiency is expressed as

$$\eta_p = \frac{TV}{TV + \frac{1}{2}\dot{m}_e(V_e - V)^2} \quad (Eq. 177)$$

The mass and velocity of the gases leaving the nozzle are exposed and the thermal efficiency is obtained from the relation

$$\eta_{th} = \frac{TV + \frac{1}{2}\dot{m}_a(1+f)(V_e - V)^2}{\dot{m}_f Q_R} \quad (Eq. 178)$$

The overall efficiency is then expressed as

$$\eta_o = \eta_p \times \eta_{th} \quad (Eq. 179)$$

From the Figure 15

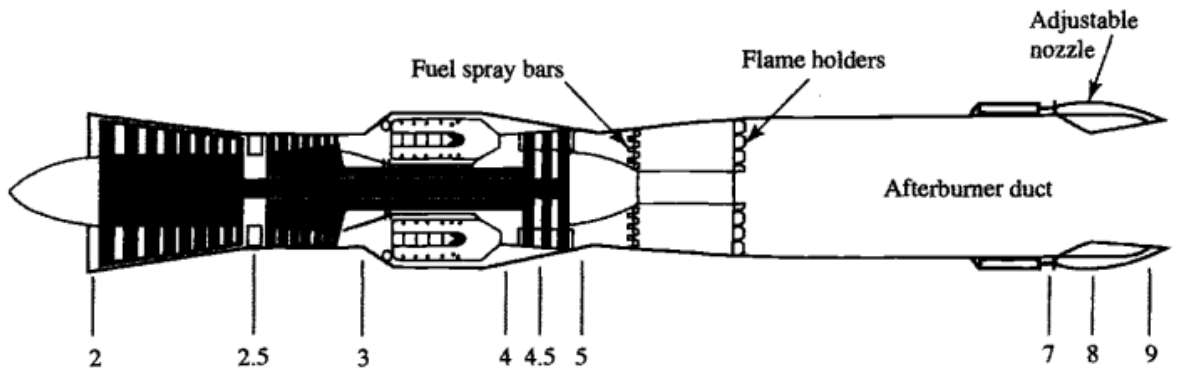


Figure 15 Dual-Spool Afterburning Turbojet Engine [7]

High-pressure turbine

The mass flow rate at the entrance to the high-pressure turbine equals to that entering the low-pressure turbine

$$\dot{m}_4 = \frac{P_{t4}}{\sqrt{T_{t4}}} A_4(M_4) = \dot{m}_{4.5} = \frac{P_{t4.5}}{\sqrt{T_{t4.5}}} A_{4.5}(M_{4.5}) \quad (\text{Eq. 180})$$

The areas are constant, and the flow is choked at stations 4 and 4.5 then

$$\frac{P_{t4}/P_{t4.5}}{\sqrt{T_{t4}/T_{t4.5}}} = \frac{\sqrt{\tau_{tH}}}{\pi_{tH}} = \text{constant} \quad (\text{Eq. 181})$$

Thus, $\eta_{tH}, \pi_{tH}, \tau_{tH}, \dot{m}_{c4}, \dot{m}_{c4.5}$ are also constant values.

Low-pressure turbine

The mass flow rate at the entrance to the low-pressure turbine equals to that at the exit nozzle throat

$$\pi_{tL} = \pi_{tLR} \sqrt{\frac{\tau_{tL}}{\tau_{tLR}}} \frac{(M_{8R})}{(M_8)} \quad (\text{Eq. 182})$$

$$\tau_{tL} = 1 - \eta_{tL} (1 - \pi_{tL}^{(\gamma_t-1)/\gamma_t}) \quad (\text{Eq. 183})$$

High-pressure compressor

$$\tau_{cH} = 1 + \frac{T_{t4}/T_0}{(T_{t4}/T_0)_R} \frac{(\tau_r \tau_{cL})_R}{\tau_r \tau_{cL}} (\tau_{cH} - 1)_R \quad (\text{Eq. 184})$$

$$\pi_{cH} = [1 + \eta_{cH} (\tau_{cH} - 1)]^{\gamma_c/(\gamma_c-1)} \quad (\text{Eq. 185})$$

Low-pressure compressor

$$\tau_{cL} = 1 + \frac{T_{t4}/T_0}{(T_{t4}/T_0)_R} \frac{(\tau_r)_R}{\tau_r} (\tau_{cL} - 1)_R \quad (\text{Eq. 186})$$

$$\pi_{cL} = [1 + \eta_{cL} (\tau_{cL} - 1)]^{\gamma_c/(\gamma_c-1)} \quad (\text{Eq. 187})$$

Mass Flow Rate

$$\frac{\dot{m}_0}{\dot{m}_{0R}} = \frac{P_0 \pi_r \pi_d \pi_{cL} \pi_{cH}}{(P_0 \pi_r \pi_d \pi_{cL} \pi_{cH})_R} \sqrt{\frac{T_{t4R}}{T_{t4}}} \quad (\text{Eq. 188})$$

Performance analysis variables for dual-spool afterburning turbojet engine

Table 3 Performance analysis variables for dual-spool afterburning turbojet engine [7]

	Variables		
Component	Independent	Constant or known	Dependent
Engine	M_0, T_0, P_0	\dot{m}_0	
Diffuser		$\pi_d = f(M_0)$	
Fan		η_{cL}	π_{cL}, τ_{cL}
High-pressure compressor		η_{cH}	π_{cH}, τ_{cH}
Burner	T_{t4}	π_b, η_b	f
High-pressure turbine		π_{tH}, τ_{tH}	
Low-pressure turbine		π_{tL}, τ_{tL}	
Afterburner	T_{t7}	π_{AB}, η_{AB}	f_{Ab}
Nozzle	$\frac{P_9}{P_0}$	π_n	$M_9, \frac{T_9}{T_0}$
Total number	6		9

Summary of Equations of Double-Spool Turbojet Engine with Afterburner – Real Turbojet

Input parameters for double-spool turbojet engine with afterburner – real turbojet Choices

Flight parameters: $M_0, T_0(K, {}^\circ R), P_0(kPa, psia)$

Throttle setting: $T_{t4}(K, {}^\circ R), T_{t7}(K, {}^\circ R)$

Exhaust nozzle setting: P_0 / P_9

Design constants

π : $\pi_{dmax}, \pi_b, \pi_{tH}, \pi_{tL}, \pi_{AB}, \pi_n$

τ : τ_{tH}, τ_{tL}

η : $\eta_{cL}, \eta_{cH}, \eta_b, \eta_{AB}, \eta_{mL}, \eta_{mH}$

Gas properties: $\gamma_c, \gamma_t, \gamma_{AB}, c_{pc}, c_{pt}, c_{pAB} [kJ/(kg \cdot K), Btu/(lbm \cdot {}^\circ R)]$

Fuel: $h_{PR}(kJ/kg, Btu/lbm)$

Reference conditions

Flight parameters $M_{0R}, T_{0R}(K, {}^\circ R), P_{0R}(kPa, psia), \tau_{rR}, \pi_{rR}$

Throttle setting: $T_{t4}(K, {}^\circ R)$

Component behavior: $\pi_{dR}, \pi_{cLR}, \pi_{cHR}, \tau_{cLR}, \tau_{cHR}$

Expected outputs for double-spool turbojet engine with afterburner – real turbojet

Overall performance:

$$F(N, lbf), \dot{m}_0(kg/s, lbm/s), f_0, S\left(\frac{mg/s}{N}, \frac{lbf}{lbm}\right), \eta_p, \eta_T, \eta_o$$

Component behavior:

Design constants

π : $\pi_{dmax}, \pi_b, \pi_{tH}, \pi_{tL}, \pi_{AB}, \pi_n$

τ : τ_{tH}, τ_{tL}

η : $\eta_{cL}, \eta_{cH}, \eta_b, \eta_{AB}, \eta_{mL}, \eta_{mH}$

Gas properties: $\gamma_c, \gamma_t, \gamma_{AB}, c_{pc}, c_{pt}, c_{pAB} [kJ/(kg \cdot K), Btu/(lbm \cdot {}^\circ R)]$

Fuel: $h_{PR}(kJ/kg, Btu/lbm)$

Reference conditions

Flight parameters: $M_{0R}, T_{0R}(K, {}^\circ R), P_{0R}(kPa, psia), \tau_{rR}, \pi_{rR}$

Throttle setting: $T_{t4}(K, {}^\circ R)$

Component behavior:

$$\pi_{cL}, \pi_{cH}, \tau_{cL}, \tau_{cH}, f, f_{AB}, M_9, (N/N_R)_{LPspool}, (N/N_R)_{HPspool}$$

From equations (167 to 188)

$$\begin{aligned}
R_{AB} &= \frac{\gamma_{AB} - 1}{\gamma_{AB}} c_{pAB} & \tau_{\lambda AB} &= \frac{c_{pAB} T_{t7}}{c_{pc} T_0} & f_{AB} &= \frac{\tau_{\lambda AB} - \tau_\lambda \tau_{tH} \tau_{tL}}{h_{PR} \eta_{AB} / (c_{pc} T_0) - \tau_{\lambda AB}} \\
R_c &= \frac{\gamma_c - 1}{\gamma_c} c_{pc} & R_t &= \frac{\gamma_t - 1}{\gamma_t} c_{pt} & a_0 &= \sqrt{\gamma_c R_c g_c T_0} & V_0 &= a_0 M_0 \\
\tau_r &= 1 + \frac{\gamma_c - 1}{2} M_0^2 & \pi_r &= \tau_r^{\gamma_c / (\gamma_c - 1)} & \pi_d &= \pi_{max} \eta_r \\
\eta_r &= 1 \text{ for } M_0 \leq 1, \quad \eta_r = 1 - 0.075(M_0 - 1)^{1.35} \text{ for } M_0 > 1 \\
\tau_{cL} &= 1 + \frac{T_{t4} / T_0}{(T_{t4} / T_0)_R} \frac{(\tau_r)_R}{\tau_r} (\tau_{cL} - 1)_R & \pi_{cL} &= [1 + \eta_{cL} (\tau_{cL} - 1)]^{\gamma_c / (\gamma_c - 1)} \\
\tau_{cH} &= 1 + \frac{T_{t4} / T_0}{(T_{t4} / T_0)_R} \frac{(\tau_r \tau_{cL})_R}{\tau_r \tau_{cL}} (\tau_{cH} - 1)_R & \pi_{cH} &= [1 + \eta_{cH} (\tau_{cH} - 1)]^{\gamma_c / (\gamma_c - 1)} \\
\tau_\lambda &= \frac{C_{pt} T_{t4}}{C_{pc} T_0} & f &= \frac{\tau_\lambda - \tau_r \tau_{cL} \tau_{cH}}{h_{PR} \eta_b / (c_{pc} T_0) - \tau_\lambda} & \dot{m}_0 &= \dot{m}_{0R} \frac{P_0 \pi_r \pi_d \pi_{cL} \pi_{cH}}{(P_0 \pi_r \pi_d \pi_{cL} \pi_{cH})_R} \sqrt{\frac{T_{t4R}}{T_{t4}}} \\
\frac{P_{t9}}{P_9} &= \frac{P_0}{P_9} \pi_r \pi_d \pi_{cL} \pi_{cH} \pi_b \pi_{tL} \pi_{tH} \pi_{AB} \pi_n & M_9 &= \sqrt{\frac{2}{\gamma_{AB} - 1} \left[\left(\frac{P_{t9}}{P_9} \right)^{(\gamma_{AB} - 1) / \gamma_{AB}} - 1 \right]} \\
\frac{T_9}{T_0} &= \frac{T_{t7} / T_0}{(P_{t9} / P_9)^{(\gamma_{AB} - 1) / \gamma_{AB}}} & \frac{V_9}{a_0} &= M_9 \sqrt{\frac{\gamma_{AB} R_{AB}}{\gamma_c R_c} \frac{T_9}{T_0}} & f_o &= f + f_{AB} \\
\frac{F}{\dot{m}_0} &= \frac{a_0}{g_c} \left[(1 + f_o) \frac{V_9}{a_0} - M_0 + (1 + f_o) \frac{R_{AB}}{R_c} \frac{T_9 / T_0}{V_9 / a_0} \frac{1 - P_0 / P_9}{\gamma_c} \right] & S &= \frac{f_o}{F / \dot{m}_0} \\
\eta_T &= \frac{a_0^2 \left[(1 + f_o) (V_9 / a_0)^2 - M_0^2 \right]}{2 g_c f_o h_{PR}} & \eta_p &= \frac{2 g_c V_0 (F / \dot{m}_0)}{a_0^2 \left[(1 + f_o) (V_9 / a_0)^2 - M_0^2 \right]} \\
\eta_o &= \eta_p \eta_T \\
\left(\frac{N}{N_R} \right)_{LPspool} &= \sqrt{\frac{T_0 \tau_r}{T_{0R} \tau_{rR}} \frac{\pi_{cL}^{(\gamma-1)/\gamma} - 1}{\pi_{cLR}^{(\gamma-1)/\gamma} - 1}} & \left(\frac{N}{N_R} \right)_{HPspool} &= \sqrt{\frac{T_0 \tau_r \tau_{cL}}{T_{0R} \tau_{rR} \tau_{cLR}} \frac{\pi_{cH}^{(\gamma-1)/\gamma} - 1}{\pi_{cHR}^{(\gamma-1)/\gamma} - 1}} \\
\frac{A_9}{A_{9R}} &= \left[\frac{P_{t9} / P_9}{(P_{t9} / P_9)_R} \right]^{(\gamma_t + 1) / (2\gamma_t)} \sqrt{\frac{(P_{t9} / P_9)_R^{(\gamma_t - 1) / \gamma_t} - 1}{(P_{t9} / P_9)^{(\gamma_t - 1) / \gamma_t} - 1}}
\end{aligned}$$

2.4 Cycle Analysis of High Bypass Ratio Turbofan Engine

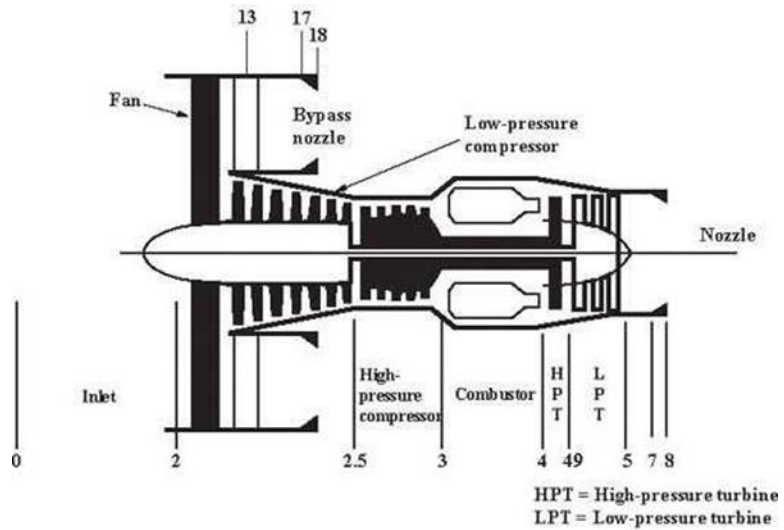


Figure 16 High-Bypass Ratio Turbofan Engine station [8]

High bypass turbofan engine consists of an inlet, fan, gas generator, nozzle as a schematic diagram of high bypass turbofan is shown in Figure 16.

The different processes encountered within the engine are described in stages:

Station (0) to (2): the free stream from ambient conduct into the fan and separate into bypass and core.

Station (2) to (2.5): the air flow through into the core, the low-pressure compressor will compress the air that encounters the compressed air fins to increase the pressure higher than the air ambient.

Station (2.5) to (3): the airflow that compresses by the low-pressure compressor through into a High-pressure compressor. The high-pressure compressor will increase the air pressure more than the low-pressure compressor. During this time, the air pressure will be very high, ready to be sent to the next combustion chamber.

Station (3) to (4): there will be air channels that have been compressed by high-pressure compressor and then pressurized air in the combustion chamber and will have fuel injectors and the ignition plug, which is only used to ignite the ignition during the first start. At the end of the combustion chamber, there will be a channel for the combustion air to exit to be sent to the next turbine section.

Station (4) to (4.5): the hot gases from combustion chamber through the fins of high-pressure turbine drive the outer shaft, which couples the high-pressure turbine to the high-pressure compressor (high-spool).

Station (4.5) to (5): the hot gas from high-pressure turbine through the fins of to low-pressure turbine to drive the inner shaft, which connects the low-pressure turbine to the booster and fan (low-spool).

Station (5) to (8): the hot gas races out through the exhaust nozzle at the back of the engine to be accelerated the speed at which this gas exits the nozzle is call (jet-velocity) and hot gases are discharged from the nozzle and encounter with the secondary flow into the atmosphere, they generate thrust, which moves the airplane forward.

Station (8) to (19): the hot gas then flows backward to the fan station to create forward thrust.

Ideal High Bypass Ratio Turbofan Engine

Ideal high bypass ratio turbofan, the efficiencies are set equal to unity as well as no component losses and no pressure losses.

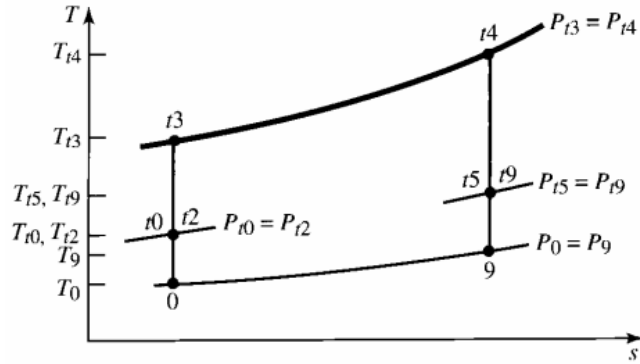


Figure 17 T-s diagram for core stream of ideal turbofan engine [8]

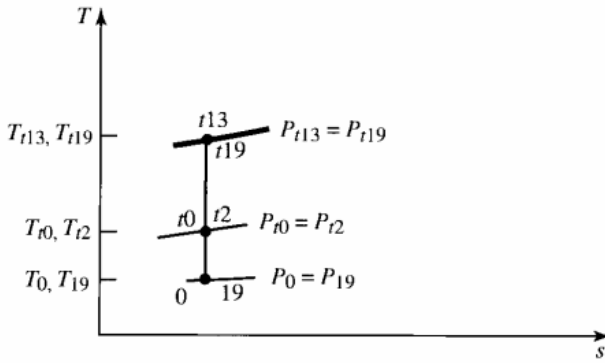


Figure 18 T-s diagram for core stream of ideal turbofan engine [8]

2.4.1 Forward Fan Unmixed Single-Spool Configuration

2.4.1.1 Intake

The inlet condition of the air entering the inlet are the ambient temperature and pressure. The intake has an isentropic efficiency. For a flight Mach number, the temperature and pressure at the outlet of the intake are given by the relations

$$P_{02} = P_a \left(1 + \eta_d \frac{\gamma_{c-1}}{2} M_a^2 \right)^{\gamma_c/\gamma_{c-1}} \quad (\text{Eq. 189})$$

$$T_{02} = T_{0a} = T_a \left(1 + \frac{\gamma_{c-1}}{2} M_a^2 \right) \quad (\text{Eq. 190})$$

2.4.1.2 Fan

Fan pressure ratio and isentropic efficiency the temperature and pressure at the outlet of the fan are given by the relations

$$P_{08} = (P_{02})(\pi_f) \quad (\text{Eq. 191})$$

$$T_{08} = T_{02} \left[1 + \frac{1}{\eta_f} (\pi_f^{\gamma-1/\gamma} - 1) \right] \quad (\text{Eq. 192})$$

2.4.1.3 Compressor

The compressor pressure ratio and isentropic efficiency are given. The temperature and pressure at the outlet of the compressor are given by the relations

$$P_{03} = (P_{08})(\pi_c) \quad (\text{Eq. 193})$$

$$T_{03} = T_{08} \left[1 + \frac{1}{\eta_c} (\pi_c^{\gamma-1/\gamma} - 1) \right] \quad (\text{Eq. 194})$$

2.4.1.4 Combustion Chamber

The temperature at the end of the combustion chamber process is T_{04} . It is the maximum temperature in the cycle. The process at the end of combustion depends on the pressure drop in combustion process. The pressure drop is given by the relations

$$P_{03} = P_{03} - \Delta P_{cc} \quad (\text{Eq. 195})$$

or

$$P_{04} = P_{03} (1 - \Delta P_{cc} \%) \quad (\text{Eq. 196})$$

The energy balance for combustion chamber is expressed by the relation of fuel to air ratio f , which is defined as the ratio between the mass of fuel burn to the air mass flow rate through the core as expressed in the following relations

$$f = \frac{\dot{m}_f}{\dot{m}_a} \quad (Eq. 197)$$

$$\dot{m}_a(1+f)c_{ph}T_{04} = \dot{m}_a c_{pc} T_{03} + \eta_b \dot{m}_f Q_R \quad (Eq. 198)$$

$$f = \frac{(c_{ph}/c_{pc})(T_{05}/T_{04}) - 1}{\eta_b(Q_R/c_{pc}T_{04}) - (c_{ph}/c_{pc})(T_{05}/T_{04})} \quad (Eq. 199)$$

2.4.1.5 Turbine

The energy balance for this spool per unit air mass flow rate is given by

$$W_t = W_c + W_f \quad (Eq. 200)$$

From the relation, the temperature ratio across the turbine is deduced as shown

$$\dot{m}_a(1+f)c_{ph}(T_{04}-T_{05}) = \dot{m}_a c_{pc}(T_{03}-T_{08}) + (1+\beta)\dot{m}_a c_{pc}(T_{08}-T_{02}) \quad (Eq. 201)$$

$$T_{04}/T_{05} = \frac{c_{pc}\{(T_{03}-T_{08})\] + (1+\beta)[(T_{08}-T_{02})\]}{c_{ph}(1+f)} \quad (Eq. 202)$$

$$\frac{T_{05}}{T_{04}} = 1 - \frac{[(T_{03}-T_{08})\] + (1+\beta)[(T_{08}-T_{02})\]}{(T_{04})(c_{ph}/c_{pc})(1+f)} \quad (Eq. 203)$$

From the relation, can be derived as

$$\frac{T_{05}}{T_{04}} = 1 - \frac{[(T_{03}-T_{02})\] + \beta[(T_{08}-T_{02})\]}{(T_{04})(c_{ph}/c_{pc})(1+f)} \quad (Eq. 204)$$

The temperature ratio can be further expressed as

$$\frac{T_{05}}{T_{04}} = \left\{ 1 - \frac{(1/\eta_c)[(P_{03}/P_{02})^{\gamma_{c-1/\gamma_c}}] + (\beta/\eta_f)[(P_{08}/P_{02})^{\gamma_{c-1/\gamma_c}} - 1]}{(1+f)(c_{ph}/c_{pc})(T_{04}/P_{02})} \right\} \quad (Eq. 205)$$

2.4.1.6 Turbine Nozzle

It is assumed that no changes occurred for the total pressure and total temperature. Thus, a nozzle isentropic efficiency critical pressure is calculated by this relation

$$\frac{P_{06}}{P_c} = \frac{1}{\left[1 - \frac{1}{\eta_{n_t}} \left(\frac{\gamma_h - 1}{\gamma_h + 1} \right) \right]^{\gamma_h/\gamma_h-1}} \quad (Eq. 206)$$

If the nozzle is an ideal, then $\eta_{n_t} = 1$

$$\left(\frac{P_{06}}{P_c} \right) = \left(\frac{\gamma_h + 1}{2} \right)^{\gamma_h/\gamma_h-1} \quad (Eq. 207)$$

If $P_c \geq P_a$, then the nozzle is choked. The temperature of the gases leaving the nozzle is obtained by this relation from Eq. 44 as,

$$\left(\frac{T_{06}}{T_7} \right) = \left(\frac{\gamma_h + 1}{2} \right)$$

Then

$$V_7 = \sqrt{\gamma_h R T_7} \quad (Eq. 208)$$

The pressure ratio in the nozzle is obtained by the relation

$$\frac{P_{06}}{P_a} = \frac{P_{06}}{P_{05}} \frac{P_{05}}{P_{04}} \frac{P_{04}}{P_{03}} \frac{P_{03}}{2} \frac{P_{02}}{P_{0a}} \frac{P_{0a}}{P_a} \quad (Eq. 209)$$

$$T_{07} = T_{06} - \left(\frac{1+\beta}{1+f} \right) \left(\frac{c_{pc}}{c_{ph}} \right) (T_{010} - T_{02}) - \left(\frac{c_{pc}}{c_{ph}} \right) \left(\frac{T_{03} - T_{010}}{1+f} \right) \quad (Eq. 210)$$

The pressure at the outlet can be obtained by the relation

$$P_{07} = P_{06} \left(1 - \frac{T_{06} - T_{07}}{\eta_{t2} T_{06}} \right)^{\gamma_h/\gamma_h-1} \quad (Eq. 211)$$

2.4.1.7 Fan Nozzle

The fan nozzle critical pressure can be calculated by the relation

$$\frac{P_{08}}{P_c} = \frac{1}{\left[1 - \frac{1}{\eta_{fn}} \left(\frac{\gamma_c - 1}{\gamma_c + 1} \right) \right]^{\gamma_c/\gamma_c-1}} \quad (Eq. 212)$$

If the flow in nozzle is an ideal, then $\eta_{fn} = 1$

$$\left(\frac{P_{08}}{P_c} \right) = \left(\frac{\gamma_c + 1}{2} \right)^{\gamma_c/\gamma_c - 1} \quad (Eq. 213)$$

If $P_c \geq P_a$, then the fan nozzle is choked. The temperature of the gases leaving can be obtained by the relation by Eq. 165

$$\left(\frac{T_{08}}{T_9} \right) = \left(\frac{\gamma_c + 1}{2} \right)$$

From Eq. 169 for the outlet velocity

$$V_9 = \sqrt{\gamma_c RT_9}$$

If $P_9 = P_a$, then the fan nozzle is unchoked. The temperature of the gases leaving can be obtained by the relation

$$V_9 = \sqrt{\frac{2\gamma_c RT_{08} \eta_{fn}}{(\gamma_c - 1)} \left[1 - \left(\frac{P_a}{P_{08}} \right)^{\gamma_c - 1/\gamma_c} \right]} \quad (Eq. 214)$$

$$\frac{P_{08}}{P_a} = \frac{P_{08}}{P_{02}} \frac{P_{02}}{P_a} \quad (Eq. 215)$$

The thrust force can be obtained by the relation

$$\begin{aligned} \frac{T}{\dot{m}_a} &= (1 + f)V_7 + \beta V_9 - u(1 + \beta) + \frac{1}{\dot{m}_a} [A_7(P_7 - P_a) + A_9(P_7 - P_a)] = \\ &= (1 + f)V_7 + \beta(V_9 - u) - u + \frac{1}{\dot{m}_a} [A_7(P_7 - P_a) + A_9(P_7 - P_a)] \end{aligned} \quad (Eq. 216)$$

The specific thrust, the thrust force per total air mass flow rate is further evaluated by the relation

$$\begin{aligned} \frac{T}{\dot{m}_{at}} &= \frac{T}{\dot{m}_h + \dot{m}_c} = \frac{T}{\dot{m}_h(1 + \beta)} = \frac{(1 + f)}{(1 + \beta)} V_7 + \frac{\beta}{(1 + \beta)} V_9 - \\ &\quad u + \frac{1}{\dot{m}_a(1 + \beta)} [A_7(P_7 - P_a) + A_9(P_7 - P_a)] \end{aligned} \quad (Eq. 217)$$

The TSFC is expressed as

$$TSFC = \frac{\dot{m}_f}{T} = \frac{\dot{m}_f}{\dot{m}_a} \frac{\dot{m}_a}{T} = \frac{f}{T / m_a} \quad (Eq. 218)$$

2.4.2 Forward Fan Unmixed Two-Spool Engines

2.4.2.1 Intake

Intake implemented the same governing equation in single spool configuration.

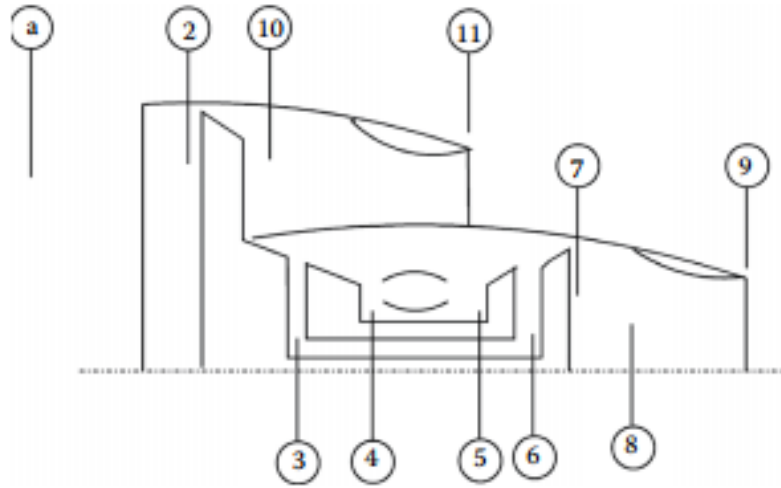


Figure 19 Layout of a two-spool turbofan engine (fan and compressor driven by an LPT) [7]

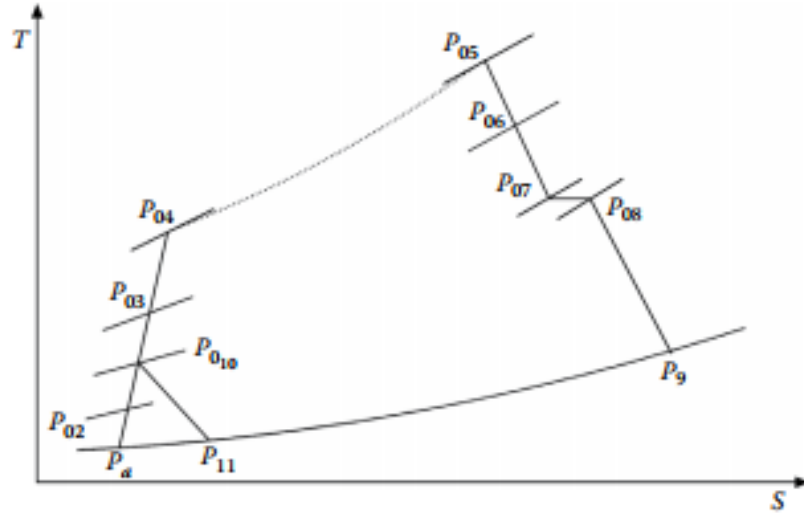


Figure 20 T-s diagram of a two-spool turbofan engine [7]

2.4.2.2 Fan

The following equations are applied

$$P_{0_{10}} = (P_{02}) (\pi_f) \quad (Eq. 219)$$

$$T_{0_{10}} = T_{02} \left[1 + \frac{1}{\eta_f} (\pi_f^{\gamma-1/\gamma} - 1) \right] \quad (Eq. 220)$$

2.4.2.3 Low-pressure compressor (LPC)

The pressure ratio achieved in this compressor is less than two and expressed as

$$P_{03} = (P_{0_{10}}) (\pi_{lpc}) \quad (Eq. 221)$$

$$T_{03} = T_{0_{10}} \left[1 + \frac{1}{\eta_{lpc}} (\pi_{lpc}^{\gamma-1/\gamma} - 1) \right] \quad (Eq. 222)$$

2.4.2.4 High-pressure compressor (HPC)

$$P_{04} = (P_{03}) (\pi_{hpc}) \quad (Eq. 223)$$

$$T_{04} = T_{03} \left[1 + \frac{1}{\eta_{hpc}} (\pi_{hpc}^{\gamma-1/\gamma} - 1) \right] \quad (Eq. 224)$$

2.4.2.5 Combustion Chamber

The pressure at the outlet of the combustion chamber is obtained from the pressure drop in the combustion chamber as

From Eq. 148

$$P_{05} = P_{04} - \Delta P_{cc}$$

Or from Eq. 149

$$P_{05} = P_{04} (1 - \Delta P_{cc} \%)$$

The temperature at the outlet of the combustion chamber is the maximum temperature in the engine. Thus, the fuel-to-air ratio is calculated from the relation

$$f = \frac{(c_{ph} / c_{pc})(T_{05} / T_{04}) - 1}{\eta_b (Q_R / c_{pc} T_{04}) - (c_{ph} / c_{pc})(T_{05} / T_{04})} \quad (Eq. 225)$$

2.4.2.6 High-pressure turbine (HPT)

To calculate the temperature and pressure at the outlet of the HPT, an energy balance between the HPC and HPT is performed as follow

$$\dot{m}_a c_{pc} (T_{04} / T_{03}) = \dot{m}_a (1 + f) c_{ph} (T_{05} / T_{06}) \quad (Eq. 226)$$

From this relation, the temperature at the outlet of the turbine T_{06} is defined. Moreover, from the known isentropic efficiency of the HPT η_{hpt} , the outlet pressure from the HPT P_{06} is calculated as explained previously in the single spool turbofan.

2.4.2.7 Low-pressure turbine (LPT)

An energy balance between the fan and LPC from one side and the LPT on the other side is expressed by the relation

$$T_{07} = T_{06} - \left(\frac{1+\beta}{1+f} \right) \left(\frac{c_{pc}}{c_{ph}} \right) (T_{010} - T_{02}) - \left(\frac{c_{pc}}{c_{ph}} \right) \left(\frac{T_{03} - T_{010}}{1+f} \right) \quad (\text{Eq. 227})$$

The pressure at the outlet can be obtained by the relation

$$P_{07} = P_{06} \left(1 - \frac{T_{06} - T_{07}}{\eta_{t2} \times T_{06}} \right)^{\frac{\gamma_h - 1}{\gamma_h}} \quad (\text{Eq. 228})$$

Now, if there is an air bleed from the HPC at a station where the pressure is P_{03b} , the flow in the jet pipe is frequently associated with a pressure drop, mainly due to skin friction. Thus, the pressure upstream of the turbine nozzle is slightly less than the outlet pressure from the turbine. The temperature, however, is the same.

Thus

$$P_{08} = P_{07} (1 - \Delta P_{jetpipe}) \quad (\text{Eq. 229})$$

$$T_{08} = T_{07} \quad (\text{Eq. 230})$$

2.4.3 Cycle analysis steps of High Bypass Ratio Turbofan Engine – Ideal case

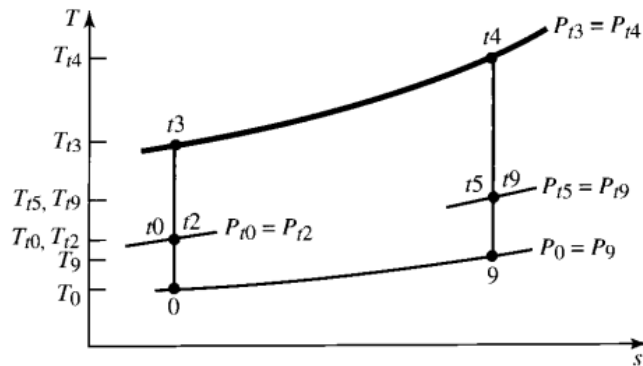


Figure 21 T-s diagram for core stream of ideal turbofan engine [8]

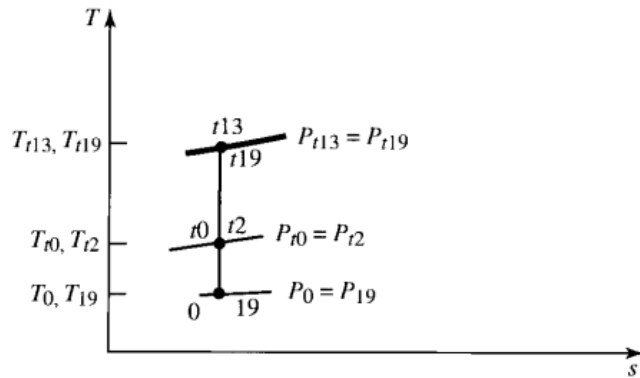


Figure 22 T-s diagram for fan stream of ideal turbofan engine [8]

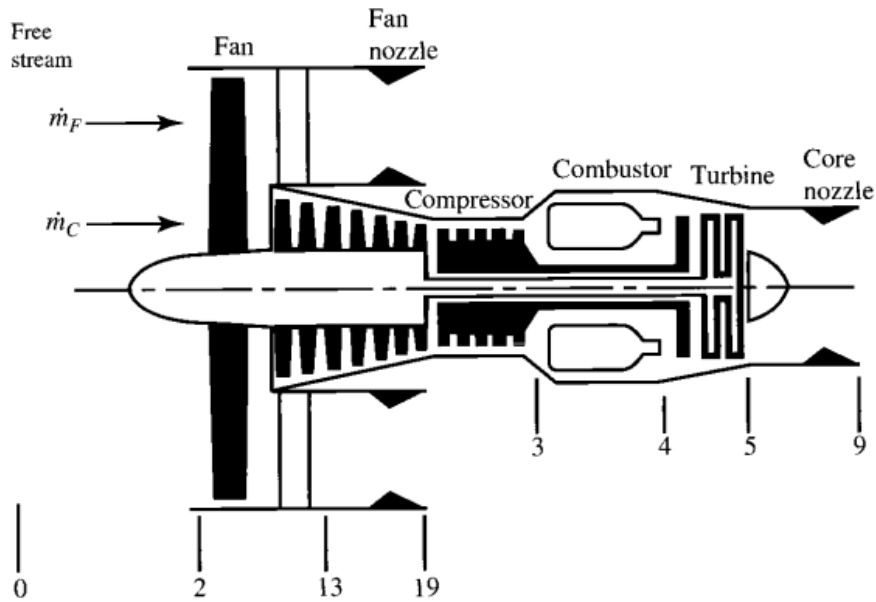


Figure 23 Station numbering of a turbofan engine [8]

From the Figure 23, the station numbering of a turbofan engine for cycle analysis for both ideal and real cases is shown.

High Bypass Ratio Turbofan Engine cycle analysis for ideal case,

Step 1: The thrust of the ideal turbofan engine is defined as

$$\frac{F}{\dot{m}_0} = \frac{a_0}{g_c} \frac{1}{1+\alpha} \left[\frac{V_9}{a_0} - M_0 + \alpha \left(\frac{V_{19}}{a_0} - M_0 \right) \right] \quad (\text{Eq. 231})$$

Step 2 - 4: Since the core stream of the turbofan engine encounters the same engine components as the ideal turbojet, its result can be adopted

$$\left(\frac{V_9}{a_0} \right)^2 = \frac{T_9}{T_0} M_9^2, \quad \frac{T_9}{T_0} = \tau_b = \frac{\tau_\lambda}{\tau_r \tau_c}, \quad \text{and} \quad M_9^2 = \frac{2}{\gamma-1} (\tau_r \tau_c \tau_t - 1)$$

Thus

$$\left(\frac{V_9}{a_0} \right)^2 = \frac{2}{\gamma-1} (\tau_r \tau_c \tau_t - 1) \quad (\text{Eq. 232})$$

As for the fan stream, the turbofan contains a fan rather than a compressor and does not have either a combustor or a turbine. The preceding equations for the core stream of the ideal turbofan can be adapted for the fan stream as

$$\left(\frac{V_{19}}{a_0}\right)^2 = \frac{T_{19}}{T_0} M_{19}^2, \quad T_{19} = T_0, \quad \text{and} \quad M_{19}^2 = \frac{2}{\gamma - 1} (\tau_r \tau_f - 1)$$

Thus

$$\left(\frac{V_{19}}{a_0}\right)^2 = \frac{2}{\gamma - 1} (\tau_r \tau_f - 1) \quad (Eq. 233)$$

Step 5: The fuel/air ratio is defined as

$$f = \frac{c_p T_0}{h_{PR}} (\tau_\lambda - \tau_r \tau_c) \quad (Eq. 234)$$

Step 6:

$$\tau_t = 1 - \frac{\tau_r}{\tau_\lambda} [\tau_c - 1 + \alpha (\tau_f - 1)] \quad (Eq. 235)$$

Step 7:

$$\left(\frac{V_9}{a_0}\right)^2 = \frac{2}{\gamma - 1} \left\{ \tau_\lambda - \tau_r [\tau_c - 1 + \alpha (\tau_f - 1)] - \frac{\tau_\lambda}{\tau_r \tau_c} \right\} \quad (Eq. 236)$$

Step 8:

$$S = \frac{f}{(1 + \alpha)(F / \dot{m}_0)} \quad (Eq. 237)$$

$$\eta_p = 2 \frac{V_9 / V_0 - 1 + \alpha (V_{19} / V_0 - 1)}{V_9^2 / V_0^2 - 1 + \alpha (V_{19}^2 / V_0^2 - 1)} \quad (Eq. 238)$$

$$FR = \frac{F_c / \dot{m}_c}{F_f / \dot{m}_f} = \frac{V_9 / a_0 - M_0}{V_{19} / a_0 - M_0} \quad (Eq. 239)$$

Step 9: The thermal efficiency is defined as

$$\eta_T = 1 - \frac{1}{\tau_r \tau_c} \quad (Eq. 240)$$

Summary of Equations of High Bypass Ratio Turbofan Engine – Ideal Turbofan

Input parameters for high bypass ratio turbofan engine – ideal turbofan

$$M_0, T_0(\text{K}, \text{°R}), \gamma, c_p \left(\frac{\text{kJ}}{\text{kg} \cdot \text{K}}, \frac{\text{Btu}}{\text{lbf} \cdot \text{°R}} \right), h_{PR} \left(\frac{\text{kJ}}{\text{kg}}, \frac{\text{Btu}}{\text{lbf}} \right), T_{t4}(\text{K}, \text{°R}), \pi_c, \pi_f, \alpha$$

Expected outputs for high bypass ratio turbofan engine – ideal turbofan

$$\frac{F}{\dot{m}_0} \left(\frac{\text{N}}{\text{kg/s}}, \frac{\text{Ibf}}{\text{lbf/s}} \right), f, S \left(\frac{\text{mg/s}}{\text{N}}, \frac{\text{Ibm/h}}{\text{Ibf}} \right), \eta_T, \eta_P, \eta_O, FR$$

From equations (214 to 240)

$$\begin{aligned} R &= \frac{\gamma - 1}{\gamma} c_p & a_0 &= \sqrt{\gamma R g_c T_0} & \tau_r &= 1 + \frac{\gamma - 1}{2} M_0^2 & \tau_\lambda &= \frac{T_{t4}}{T_0} \\ \tau_c &= (\pi_c)^{(\gamma-1)/\gamma} & \tau_f &= (\pi_f)^{(\gamma-1)/\gamma} & \frac{V_{19}}{a_0} &= \sqrt{\frac{2}{\gamma - 1} (\tau_r \tau_f - 1)} \\ \frac{V_9}{a_0} &= \sqrt{\frac{2}{\gamma - 1} \left\{ \tau_\lambda - \tau_r [\tau_c - 1 + \alpha(\tau_f - 1)] - \frac{\tau_\lambda}{\tau_r \tau_c} \right\}} \\ \frac{F}{\dot{m}_0} &= \frac{a_0}{g_c} \frac{1}{1 + \alpha} \left[\frac{V_9}{a_0} - M_0 + \alpha \left(\frac{V_{19}}{a_0} - M_0 \right) \right] & S &= \frac{f}{(1 + \alpha)(F / \dot{m}_0)} \\ f &= \frac{c_p T_0}{h_{PR}} (\tau_\lambda - \tau_r \tau_c) & FR &= \frac{V_9 / a_0 - M_0}{V_{19} / a_0 - M_0} & \eta_O &= \eta_P \eta_T \\ \eta_P &= 2 M_0 \frac{V_9 / a_0 - M_0 + \alpha(V_{19} / a_0 - M_0)}{V_9^2 / a_0^2 - M_0^2 + \alpha(V_{19}^2 / a_0^2 - M_0^2)} & \eta_T &= 1 - \frac{1}{\tau_r \tau_c} \end{aligned}$$

The turbofan engine has three design variables:

1. Compressor pressure ratio,
2. Fan pressure ratio, π_f
3. Bypass ratio, α

Therefore, the variation of these three variables would be required to perform a checking for engine performance.

2.4.4 Cycle analysis steps of High Bypass Ratio Turbofan Engine – Real case

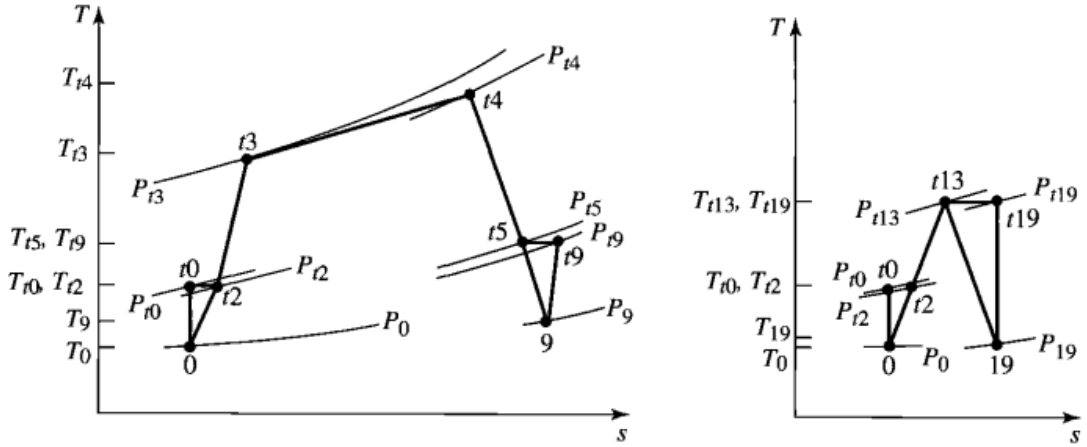


Figure 24 T-s diagram of turbofan engine with losses (not to scale) [8]

High bypass ratio turbofan engine cycle analysis for real case,

The assumptions for the analysis of the turbofan engine cycle with losses are as follows:

1. Perfect gas upstream of main burner with constant properties γ_c, R_c, c_{pc} .
2. Perfect gas downstream of main burner with constant properties γ_t, R_t, c_{pt} .
3. All components are adiabatic (no turbine cooling).
4. The efficiencies of the compressor, fan, and turbine are described through the use of constant polytropic efficiencies respectively.

For engine fan stream,

Step 1: Uninstalled thrust of fan stream F_F

$$\frac{F_F}{\dot{m}_F} = \frac{a_0}{g_c} \left(\frac{V_{19}}{a_0} - M_0 + \frac{T_{19}/T_0}{V_{19}/a_0} \frac{1 - P_0/P_{19}}{\gamma_c} \right) \quad (\text{Eq. 241})$$

Step 2:

$$\left(\frac{V_{19}}{a_0} \right)^2 = \frac{T_{19}}{T_0} M_{19}^2 \quad (\text{Eq. 242})$$

Step 3:

$$M_{19}^2 = \frac{2}{\gamma_c - 1} \left[\left(\frac{P_{t19}}{P_{19}} \right)^{(\gamma_c-1)/\gamma_c} - 1 \right] \quad (\text{Eq. 243})$$

And

$$\frac{P_{t19}}{P_{19}} = \frac{P_0}{P_{19}} \pi_r \pi_d \pi_f \pi_{fn} \quad (Eq. 244)$$

Step 4:

$$\frac{T_{19}}{T_0} = \frac{T_{t19} / T_0}{(P_{t19} / P_{19})^{(\gamma_c - 1) / \gamma_c}} \quad (Eq. 245)$$

And

$$\frac{T_{t19}}{T_0} = \tau_r \tau_f \quad (Eq. 246)$$

For engine core stream,

Step 1: Uninstalled thrust

$$\frac{F_c}{\dot{m}_c} = \frac{a_0}{g_c} \left[(1+f) \frac{V_9}{a_0} - M_0 + (1+f) \frac{R_t}{R_c} \frac{T_9 / T_0}{V_9 / a_0} \frac{1 - P_0 / P_9}{\gamma_c} \right] \quad (Eq. 247)$$

Step 2:

$$\left(\frac{V_9}{a_0} \right)^2 = \frac{\gamma_t R_t T_9}{\gamma_c R_c T_0} M_9^2 \quad (Eq. 248)$$

Step 3:

$$M_9^2 = \frac{2}{\gamma_t - 1} \left[\left(\frac{P_{t9}}{P_9} \right)^{(\gamma_t - 1) / \gamma_t} - 1 \right] \quad (Eq. 249)$$

And

$$\frac{P_{t9}}{P_9} = \frac{P_0}{P_9} \pi_r \pi_d \pi_c \pi_b \pi_t \pi_n \quad (Eq. 250)$$

Step 4:

$$\frac{T_9}{T_0} = \frac{T_{t9} / T_0}{(P_{t9} / P_9)^{(\gamma_t - 1) / \gamma_t}} \quad (Eq. 251)$$

$$\frac{T_{t9}}{T_0} = \tau_r \tau_d \tau_c \tau_b \tau_t \tau_n = \frac{c_{pc}}{c_{pt}} \tau_\lambda \tau_t \quad (Eq. 252)$$

Step 5:

$$f = \frac{\tau_\lambda - \tau_r \tau_c}{\eta_b h_{PR} / (c_{pc} T_0) - \tau_\lambda} \quad (Eq. 253)$$

Step 6:

$$\tau_t = 1 - \frac{1}{\eta_m (1 + f)} \frac{\tau_r}{\tau_\lambda} \left[\tau_c - 1 + \alpha (\tau_f - 1) \right] \quad (Eq. 254)$$

$$\tau_f = \pi_f^{(\gamma_c - 1)/(\gamma_c e_f)} \quad (Eq. 255)$$

$$\eta_f = \frac{\pi_f^{(\gamma_c - 1)/\gamma_c} - 1}{\tau_f - 1} \quad (Eq. 256)$$

Step 7:

$$\frac{F}{\dot{m}_0} = \frac{1}{1 + \alpha} \frac{a_0}{g_c} \left[(1 + f) \frac{V_9}{a_0} - M_0 + (1 + f) \frac{R_t}{R_c} \frac{T_9 / T_0}{V_9 / a_0} \frac{1 - P_0 / P_9}{\gamma_c} \right] + \frac{\alpha}{1 + \alpha} \frac{a_0}{g_c} \left[\frac{V_{19}}{a_0} - M_0 + \frac{T_{19} / T_0}{V_{19} / a_0} \frac{1 - P_0 / P_9}{\gamma_c} \right] \quad (Eq. 257)$$

Step 8:

$$S = \frac{f}{(1 + \alpha) F / \dot{m}_0} \quad (Eq. 258)$$

Step 9:

$$\eta_p = \frac{2M_0 \left[(1 + f)(V_9 / a_0) + \alpha (V_{19} / a_0) - (1 + \alpha)M_0 \right]}{(1 + f)(V_9 / a_0)^2 + \alpha (V_{19} / a_0)^2 - (1 + \alpha)M_0^2} \quad (Eq. 259)$$

$$\eta_T = \frac{2a_0^2 \left[(1 + f)(V_9 / a_0)^2 + \alpha (V_{19} / a_0)^2 - (1 + \alpha)M_0^2 \right]}{2g_c f h_{PR}} \quad (Eq. 260)$$

Summary of Equations of High Bypass Ratio Turbofan Engine – Real Turbofan

Input parameters for high bypass ratio turbofan engine – real turbofan

$$M_0, T_0 (\text{K}, \text{°R}), \gamma_c, c_{pc} \left(\frac{\text{kJ}}{\text{kg} \cdot \text{K}}, \frac{\text{Btu}}{\text{lbm} \cdot \text{°R}} \right), \gamma_t, C_{pt} \left(\frac{\text{kJ}}{\text{kg} \cdot \text{K}}, \frac{\text{Btu}}{\text{lbm} \cdot \text{°R}} \right), h_{PR} \left(\frac{\text{kJ}}{\text{kg}}, \frac{\text{Btu}}{\text{lbm}} \right), \pi_{dnax}, \pi_b, \pi_n, \pi_{fn}, e_c, e_f, e_i, \eta_b, \eta_m, P_0 / P_9, P_0 / P_{19}, T_{t4} (\text{K}, \text{°R}), \pi_c, \pi_f, \alpha$$

Expected outputs for high bypass ratio turbofan engine – real turbofan

$$\frac{F}{\dot{m}_0} \left(\frac{\text{N}}{\text{kg} / \text{s}}, \frac{\text{lbf}}{\text{lbm} / \text{s}} \right), f, S \left(\frac{\text{mg} / \text{s}}{\text{N}}, \frac{\text{lbm} / \text{h}}{\text{lbf}} \right), \eta_T, \eta_P, \eta_O, \eta_c, \eta_t, FR$$

From equations (241 to 260)

$$R_c = \frac{\gamma_c - 1}{\gamma_c} c_{pc} \quad R_t = \frac{\gamma_t - 1}{\gamma_t} c_{pt} \quad a_0 = \sqrt{\gamma_c R_c g_c T_0} \quad V_0 = a_0 M_0$$

$$\tau_r = 1 + \frac{\gamma_c - 1}{2} M_0^2 \quad \pi_r = \tau_r^{\gamma_c / (\gamma_c - 1)} \quad \pi_d = \pi_{max} \eta_r$$

$$\eta_r = 1 \text{ for } M_0 \leq 1 \text{ or } \eta_r = 1 - 0.075 (M_0 - 1)^{1.35} \text{ for } M_0 > 1$$

$$\tau_\lambda = \frac{C_{pt} T_{t4}}{C_{pc} T_0} \quad \tau_c = (\pi_c)^{(\gamma_c - 1) / \gamma_c e_c} \quad \eta_c = \frac{(\pi_c)^{(\gamma_c - 1) / \gamma_c} - 1}{\tau_c - 1}$$

$$\tau_f = (\pi_f)^{(\gamma_c - 1) / \gamma_c e_f} \quad \eta_f = \frac{(\pi_f)^{(\gamma_c - 1) / \gamma_c} - 1}{\tau_f - 1} \quad f = \frac{\tau_\lambda - \tau_r \tau_c}{h_{PR} \eta_b / (c_{pc} T_0) - \tau_\lambda}$$

$$\tau_t = 1 - \frac{1}{\eta_m (1 + f)} \frac{\tau_r}{\tau_\lambda} \left[\tau_c - 1 + \alpha (\tau_f - 1) \right] \quad \pi_t = \tau_t^{\frac{\gamma_t}{[(\gamma_t - 1) e_t]}}$$

$$\eta_t = \frac{1 - \tau_t}{1 - \tau_t^{\frac{1}{e_t}}} \quad \frac{P_{t9}}{P_9} = \frac{P_0}{P_9} \pi_r \pi_d \pi_c \pi_b \pi_t \pi_n \quad \frac{P_{t19}}{P_{19}} = \frac{P_0}{P_{19}} \pi_r \pi_d \pi_f \pi_{fn}$$

$$\frac{T_9}{T_0} = \frac{\tau_\lambda \tau_t}{(P_{t9} / P_9)^{(\gamma_t - 1) / \gamma_t}} \frac{C_{pc}}{C_{pt}} \quad \frac{T_{19}}{T_0} = \frac{\tau_r \tau_f}{(P_{t19} / P_{19})^{(\gamma_c - 1) / \gamma_c}}$$

$$M_9 = \sqrt{\frac{2}{\gamma_t - 1} \left[\left(\frac{P_{t9}}{P_9} \right)^{(\gamma_t - 1) / \gamma_t} - 1 \right]} \quad M_{19} = \sqrt{\frac{2}{\gamma_c - 1} \left[\left(\frac{P_{t19}}{P_{19}} \right)^{(\gamma_c - 1) / \gamma_c} - 1 \right]}$$

$$\frac{V_9}{a_0} = M_9 \sqrt{\frac{\gamma_t R_t T_9}{\gamma_c R_c T_0}} \quad \frac{V_{19}}{a_0} = M_{19} \sqrt{\frac{T_{19}}{T_0}}$$

$$\begin{aligned}
\frac{F}{\dot{m}_0} &= \frac{1}{1+\alpha} \frac{a_0}{g_c} \left[\frac{(1+f) \frac{V_9}{a_0} - M_0 + (1+f)}{\frac{R_t}{R_c} \frac{T_9/T_0}{V_9/a_0} \frac{1-P_0/P_9}{\gamma_c}} \right] + \frac{\alpha}{1+\alpha} \frac{a_0}{g_c} \left(\frac{V_{19}}{a_0} - M_0 + \frac{T_{19}/T_0}{V_{19}/a_0} \frac{1-P_0/P_{19}}{\gamma_c} \right) \\
S &= \frac{f}{(1+\alpha)F/\dot{m}_0} \quad FR = \frac{(1+f) \frac{V_9}{a_0} - M_0 + (1+f) \frac{R_t T_9 / T_0}{R V_9 / a_0} \frac{1-P_0/P_9}{\gamma_c}}{\frac{V_{19}}{a_0} - M_0 + \frac{T_{19}/T_0}{V_{19}/a_0} \frac{1-P_0/P_9}{\gamma_c}} \\
\eta_o &= \eta_p \eta_t \quad \eta_p = \frac{2M_0 \left[(1+f) V_9 / a_0 + \alpha (V_{19} / a_0) - (1+\alpha) M_0 \right]}{(1+f) (V_9 / a_0)^2 + \alpha (V_{19} / a_0)^2 - (1+\alpha) M_0^2} \\
\eta_t &= \frac{a_0^2 \left[(1+f) (V_9 / a_0)^2 + \alpha (V_{19} / a_0)^2 - (1+\alpha) M_0^2 \right]}{2g_c f h_{PR}}
\end{aligned}$$

3. Methodology

3.1 Introduction

For the methodology part, the Python framework for the developed software is introduced and explain in detail including input and output parts and also the introduction to the validation software is also included. For instance, only the AEDsys is being simulated to compare with this project developed software namely GTA (Gas Turbine Analysis) and for GasTurb, it would be studied in the later phase.

3.1.1 Python Application

In doing this project, Python which is a powerful general-purpose programming language designed to be interactive and object-oriented. With its high-level built-in data structure, modules and packages. The Python module packages that are being used are NumPy, and Matplotlib. NumPy is used in doing this project for array sequencing and mathematical procedure purpose. NumPy is the fundamental package for scientific computing in Python that provides a multidimensional array object, various derived objects, and an assortment of routines for fast operations on arrays. Also, with NumPy the calculation would be much faster as well as more sorting. In addition, NumPy also acts as a main package for other modules. Matplotlib is a plotting library for the Python programming language and its numerical mathematics extension NumPy. Matplotlib provides an object-oriented API for embedding plots into applications using GUI toolkits such as Tkinter, wxPython, and GTK for user friendly interface developing. Matplotlib is mainly used to construct a plot for representing the results. The Matplotlib can display mathematical formulas, Greek letters, and mathematical symbols using a math rendering module known as mathtext which is applied in the symbol of plots in this program namely “GTA”.

The program “GTA” is designed and developed in Python, and its working sequences are described as follow.

The function procedure in Python of GTA is as shown in the flowchart below,

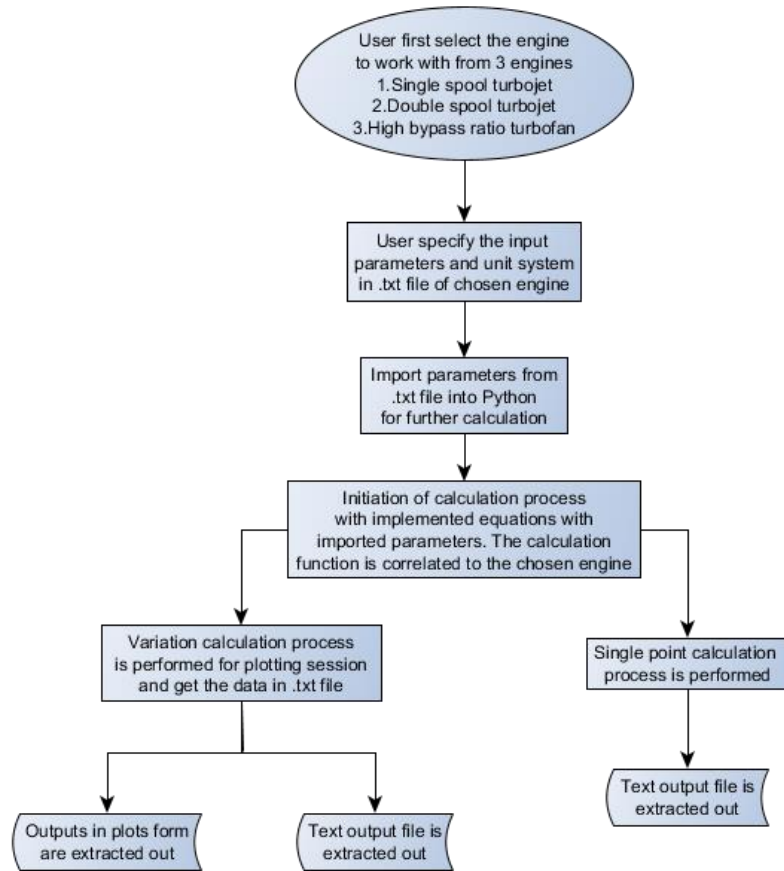


Figure 25 GTA flowchart

The first step to work with GTA is to select the engine. There are three engines for user to choose namely 1. Single spool turbojet 2. Double spool turbojet 3. High bypass ratio turbofan. The input files for three engines are as shown in the Figure 26.



Figure 26 Input file name

DSTBJE stands for double spool turbojet engine, HBPTFE stands for high bypass ratio turbofan engine, and SSTJE stands for single spool turbojet engine. After choosing an engine, user needs to specify the input parameters according to user requirement.

GTA would perform the calculation from the imported parameters correlate to the chosen engine with the equations implemented in itself.

The outputs are categorized into 2 main categories:

1. text output .txt file from single point and variation point calculation

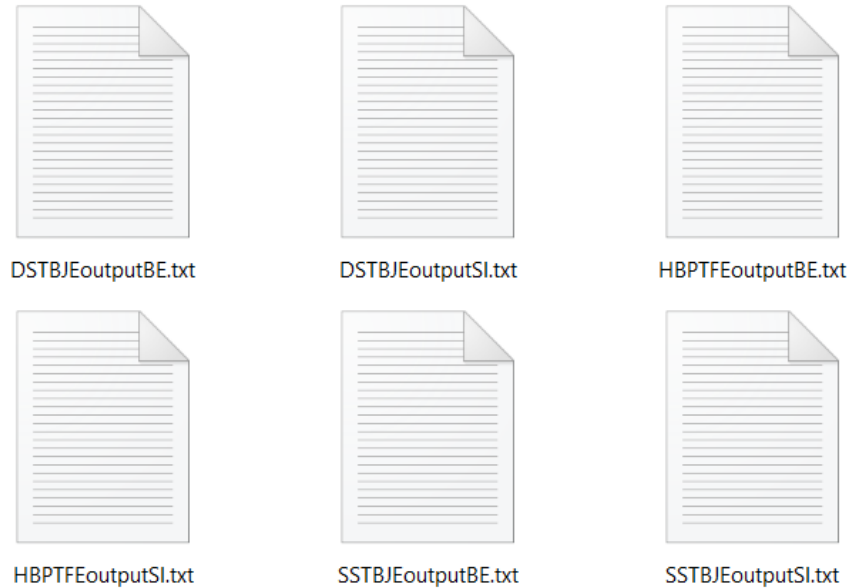


Figure 27 Output .txt files

2. plot output .png file from variation point calculation

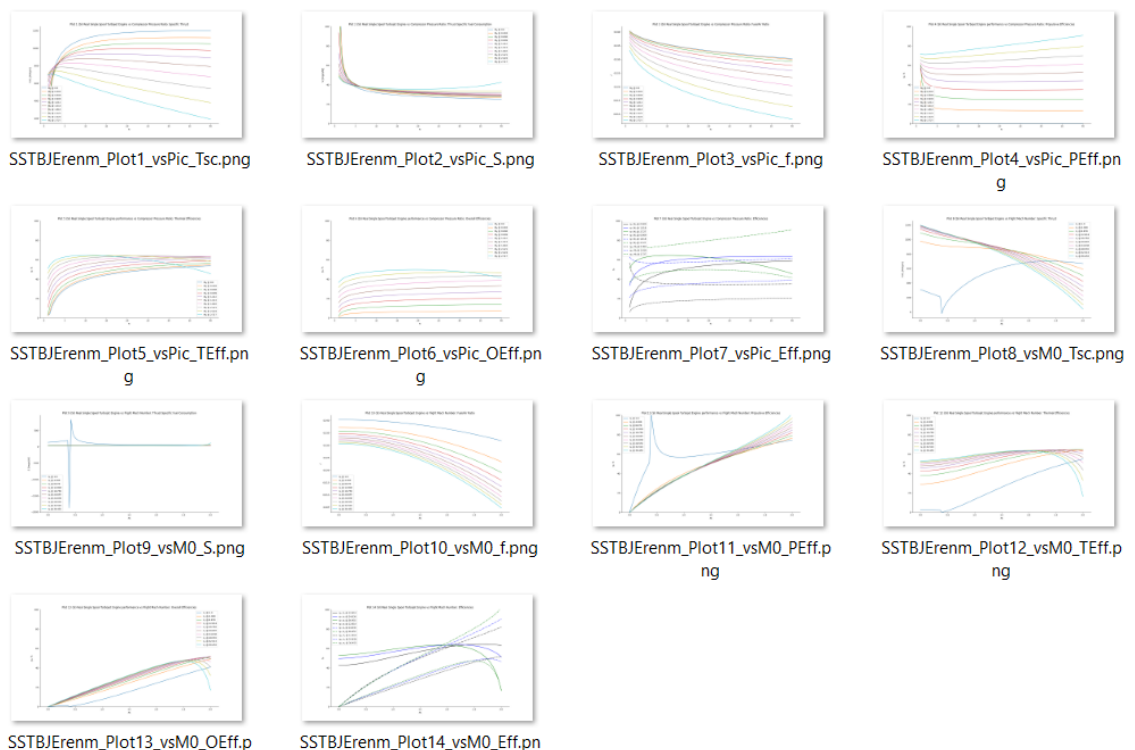


Figure 28 Output .png files

3.1.1.1 Input data for GTA

To determine the input parameters and its format, first we need to take a look at the categories of the input. The design inputs can be classified into four categories

- 1) Flight conditions

For example: $P_0, T_0, M_0, c_p, \tau_r, \pi_r$ etc.

- 2) Design limits

For example: $(c_p T_t)_{\text{burner exit}}, T_{t4}, h_{PR}$ etc.

- 3) Component performance

For example: $\pi_d, \pi_b, \pi_n, e_c, e_t$ etc.

- 4) Design choices

For example: π_c, π_f etc.

The input format for GTA can be either in SI unit or BE unit as the implemented background code can automatically identifies the system unit and proceed the calculation process in according to the unit system.

There are two major sections in the input file

- 1) Variation calculation input data
- 2) Single point calculation input data

The detailed explanation for the input file of GTA is described as follow,

The example case that is taken into consideration is the subsonic flight at the altitude of 10,000 m for single point calculation and height variation at sea level for variation calculation.

For the single point calculation, to reduce the size of the input file, some of the parameters that are listed in the variation calculation section are also adopted for single point calculation.

Example input table for single point calculation,

SSTJE = single spool turbojet engine, DSTJE = double spool turbojet engine,
HBPTFE = high bypass ratio turbofan engine.

Case 1: Subsonic flight (10,000 m)

Table 4 Input table single point calculation subsonic flight (10,000 m)

Parameter, Unit: SI	SSTJE	DSTJE	HBPTFE
\dot{m} (kg/s)	100	100	100
M_0	0.8	0.8	0.8
π_c	24	24	24
α	-	-	5
π_f	-	-	2
h (m)	10000	10000	10000
g_c ($(kg * m)/(N * s^2)$)	1	1	1
T_{t4} (K)	1666.67	1666.67	1666.67
γ	1.4	1.4	1.4
c_p ($kJ/(kg * K)$)	1.004	1.004	1.004
h_{PR} (kJ/kg)	42800	42800	42800
T_{t7} (K)	2222.22	2222.22	-
γ_c	1.4	1.4	1.4
c_{pc} ($kJ/(kg * K)$)	1.004	1.004	1.004
γ_t	1.35	1.35	1.35
c_{pt} ($kJ/(kg * K)$)	1.0969	1.0969	1.0969
$\pi_{d_{max}}$	0.98	0.98	0.98
π_b	0.98	0.98	0.98
π_n	0.98	0.98	0.98
π_{fn}	-	-	0.98
π_t	-	-	0.89
e_c	0.92	0.92	0.92
e_f	-	-	0.88
e_t	0.91	0.91	0.91
η_b	0.99	0.99	0.99
η_m	0.98	0.98	0.98
η_{cL}	-	0.8755	-
η_{cH}	-	0.8791	-
P_0/P_9	1	1	1
P_0/P_{19}	-	-	1
γ_{AB}	1.3	1.3	-
c_{pAB} ($kJ/(kg * K)$)	1.24	1.24	-
π_{AB}	0.98	0.98	-
η_{AB}	0.96	0.96	-
P_0 (kPa)	-	101.33	-
π_{tH}	-	0.5466	-
π_{tL}	-	0.6127	-

For variation calculation, the input parameters are shown in table 5.

SSTJE = single spool turbojet engine, DSTJE = double spool turbojet engine,
HBPTFE = high bypass ratio turbofan engine.

Case 1.1: Altitude at sea level

Table 5 Input table variation calculation subsonic flight (sea level)

Parameter, Unit: SI	SSTJE	DSTJE	HBPTFE
$g_c ((kg * m)/(N * s^2))$	1	1	1
$h (m)$	0	0	0
$T_{t4} (K)$	1666.67	1666.67	1666.67
γ	1.4	1.4	1.4
$c_p (kJ/(kg * K))$	1.004	1.004	1.004
$h_{PR} (kJ/kg)$	42800	42800	42800
$T_{t7} (K)$	2222.22	2222.22	-
γ_c	1.4	1.4	1.4
$c_{pc} (kJ/(kg * K))$	1.004	1.004	1.004
γ_t	1.35	1.35	1.35
$c_{pt} (kJ/(kg * K))$	1.0969	1.0969	1.0969
$\pi_{d_{max}}$	0.98	0.98	0.98
π_b	0.98	0.98	0.98
π_n	0.98	0.98	0.98
π_{fn}	-	-	0.98
π_t	-	-	0.89
e_c	0.92	0.92	0.92
e_f	-	-	0.88
e_t	0.91	0.91	0.91
η_b	0.99	0.99	0.99
η_m	0.98	0.98	0.98
η_{cL}	-	0.8755	-
η_{cH}	-	0.8791	-
P_0/P_9	1	1	1
P_0/P_{19}	-	-	1
γ_{AB}	1.3	1.3	-
$c_{pAB} (kJ/(kg * K))$	1.24	1.24	-
π_{AB}	0.98	0.98	-
η_{AB}	0.96	0.96	-
$P_0 (kPa)$	-	101.33	-
π_{tH}	-	0.5466	-
π_{tL}	-	0.6127	-
$M_{0,fix}$	-	-	0.5
$\pi_{c,fix}$	-	-	10
α_{fix}	-	-	5
$\pi_{f,fix}$	-	-	2
M_0	0 – 3	0 – 3	0 – 3
Iteration step of M_0	0.5	0.5	0.5
π_c	1 – 40	1 – 40	1 – 40
Iteration step of π_c	1	1	1
α	-	-	0 – 40
Iteration step of α	-	-	0.5

As compare to that of the table data, the input files in case of High-Bypass ratio turbofan engine for GTA is as shown in the figure below

```

HBPTBFEinputSI.txt - Notepad
File Edit Format View Help
Unit:SI
Gc((kg*m)/(N*(s^2))),Gravitational_constant: 1
h(m,Altitude): 0
It4(K,total_Temperature_at_station_4): 1666.67
Gamma(-,Ratio_of_specific_heats): 1.4
Cp(kJ/(kg*K)),Specific_heats(constant_pressure): 1.004
Hpr((kJ/kg),Low_heating_value_of_fuel): 42800
Gammac(-,Ratio_of_specific_heats(compressor)): 1.4
Cpc(kJ/(kg*K)),Specific_heats(compressor): 1.004
Gammat(-,Ratio_of_specific_heats(turbine)): 1.35
Cpt((kJ/(kg*K)),Specific_heats(turbine)): 1.0969
Pidmax(-,Diffuser_pressure_ratio_(Max)): 0.98
Pib(-,Burner_pressure_ratio): 0.98
Pin(-,Nozzle_pressure_ratio): 0.98
Pifn(-,Fan_Nozzle_pressure_ratio): 0.98
Pit(-,Turbine_pressure_ratio): 0.89
Ec(-,Polytropic_efficiency_Compressor): 0.92
Ef(-,Polytropic_efficiency_fan): 0.88
Et(-,Polytropic_efficiency_Turbine): 0.91
Nb(-,Component_efficiency_Burner): 0.99
Nm(-,Component_efficiency_Mechanical): 0.98
Pratio09(-,Exhaust_Nozzle(pressure_0_9)): 1.0
Pratio19(-,Exhaust_Nozzle(pressure_1_9)): 1.0
M0fix(-,free_stream_Mach_number): 0.5
Picfix(-,compressor_pressure_ratio): 10
Alphafix(-,Bypass_ratio): 5
Piffix(-,Fan_pressure_ratio): 2
M0min(-,Minimum_free_stream_Mach_number): 0
M0max(-,Maximum_free_stream_Mach_number): 3
IterM0(-,Iteration_variable_M0): 0.5
Picmin(-,Minimum_compressor_pressure_ratio): 1
Picmax(-,Maximum_compressor_pressure_ratio): 40
IterPic(-,Iteration_variable_Pic): 1
Pifmin(-,Minimum_fan_pressure_ratio): 0
Pifmax(-,Maximum_fan_pressure_ratio): 40
IterPif(-,Iteration_variable_Pif): 0.5
Alphamin(-,Minimum_bypass_ratio): 0
Alphamax(-,Maximum_bypass_ratio): 40
IterAlpha(-,Iteration_variable_Alpha): 0.5

Single_point_calculation_input_data (some_parameters_are_adopted_from_list_above)
mdot(kg/s,mass_flow_rate): 100
M0sp(-,free_stream_Mach_number): 0.8
Picsp(-,compressor_pressure_ratio): 24
hsp(m,altitude): 0
Pifsp(-,fan_pressure_ratio): 2
Alphasp(-,bypass_ratio): 5

```

Figure 29 Input files in case of High-Bypass ratio turbofan engine for GTA

From the figure above, the area of circle no.1 or solid square indicates the unit system in which the user specifies between SI and BE unit system, the area of circle no.3 or long dash square indicates the variation calculation input data section which the requirements are different for each engine, the area of circle no.4 or long dash and dot square indicates the single point calculation input data. The variation and single point calculation proceed in order. Therefore, some of the input data from variation section are also applied for single point calculation as in the area of circle no.2 or round point square.

3.1.1.2 Output data for GTA

GTA outputs are consisted of

1. Text file
2. Plots (Graphs)

For the single point calculation, the text file output is represented as shown in the figure below,

```
***** Table of Unit (Single Point Calculation)
      SI          BE
R       kJ/(kg*K)   ft*lbf/(lbm*R)
Rc      kJ/(kg*K)   ft*lbf/(lbm*R)
Rt      kJ/(kg*K)   ft*lbf/(lbm*R)
A0      m/s         ft/s
V0      m/s         ft/s
M02     m/s         ft/s
Tauram -           -
TauR    -           -
Pir     -           -
Nr      %           %
Pid     -           -
TauC    -           -
Nc      %           %
Tauf    -           -
Nf      %           %
Taut    -           -
Pit     -           -
Nt      %           %
Pt9P9   -           -
M9      -           -
T9T0    -           -
V9A0    -           -
Pt19P19 -           -
M19    -           -
T19T0   -           -
V19A0   -           -
V9      m/s         ft/s
V19     m/s         ft/s
Tsc     N/(kg/s)   lbf/(lbm/s)
Thrust  N           lbf
f       -           -
S       (mg/s)/N   lbf/(lbm/s)
NT      %           %
NP      %           %
NO      %           %
FR      -           -

#####
Results for Ideal High-Bypass Ratio Turbofan Engine (Single Point Calculation)

R_idsphBPTFE:0.28686
A0_idsphBPTFE:340.18
Tauram_idsphBPTFE:5.784
TauR_idsphBPTFE:1.2
TauC_idsphBPTFE:1.931
Tauf_idsphBPTFE:1.219
V9_idsphBPTFE:704.051
V19_idsphBPTFE:517.476
Tsc_idsphBPTFE:208.392
Thrust_idsphBPTFE:20839.2
f_idsphBPTFE:0.02343
S_idsphBPTFE:18.739
NT_idsphBPTFE:56.844
NP_idsphBPTFE:74.605
NO_idsphBPTFE:42.408
FR_idsphBPTFE:2.052

#####
Results for Real High-Bypass Ratio Turbofan Engine (Single Point Calculation)

Rc_resphBPTFE:0.28686
Rt_resphBPTFE:0.28438
A0_resphBPTFE:340.18
V0_resphBPTFE:340.18
M02_resphBPTFE:1.0
TauR_resphBPTFE:1.2
Pir_resphBPTFE:1.893
Nr_resphBPTFE:1
Pid_resphBPTFE:0.98
Tauram_resphBPTFE:6.319
TauC_resphBPTFE:2.044
Nc_resphBPTFE:89.147
Tauf_resphBPTFE:1.252
Nf_resphBPTFE:86.91
f_resphBPTFE:0.02759
Taut_resphBPTFE:0.566
Pit_resphBPTFE:0.08959
Nt_resphBPTFE:93.337
Pt9P9_resphBPTFE:15.857
M9_resphBPTFE:2.446
T9T0_resphBPTFE:1.599
V9A0_resphBPTFE:3.024
Pt19P19_resphBPTFE:3.636
M19_resphBPTFE:1.493
T19T0_resphBPTFE:1.039
V19A0_resphBPTFE:1.522
Tsc_resphBPTFE:267.463
Thrust_resphBPTFE:26746.3
S_resphBPTFE:17.192
FR_resphBPTFE:4.037
NT_resphBPTFE:73.398
NP_resphBPTFE:62.986
NO_resphBPTFE:46.23
*****:*****
```

Figure 30 Text file output High-Bypass Ratio Turbofan Engine (Single Point Calculation)

In the output file for single point calculation, the table of units for resultant parameters is declared then follow by the results for single point calculation resultant parameters for both ideal and real cases of an engine of choice.

For variation calculation, the text file output is also represented and with the addition of various plots that is aligned with the resultant parameters from the text section as listed,

- Specific Thrust (T_{sc})
- Thrust Specific Fuel Consumption (S)
- Fuel to air ratio (f)
- Propulsive, Thermal, Overall efficiency
- Thrust ratio (from High Bypass ratio turbofan engine)

***** Results for [Ideal High-Bypass Ratio Turbofan Engine] *****

***** Table of Units *****

	SI	BE
R	$\text{kJ}/(\text{kg} \cdot \text{K})$	$\text{ft} \cdot \text{lbf}/(\text{lbm} \cdot \text{R})$
Tauram	-	-
A ₀	m/s	ft/s
T _{sc}	N/(kg/s)	lbf/(lbm/s)
f	-	-
S	(mg/s)/N	lbf/(lbm/s)
NT	%	%
NP	%	%
NO	%	%
FR	-	-

```

R_id(SI , Specific Gas Constant)
R_id=0.2868571428571428

Tauram_id(SI , Burner Exit Enthalpy Ratio)
Tauram_id=5.784036092313032

A0_id(SI , Speed of Sound)
A0_id=340.1779534302598

M0 (x-axis) / Pif (y-axis)
Alpha, Bypass Ratio = 5.0
Pif, Fan Pressure Ratio = 2.0

Pif at: 8.08

```

Alpha	T _{sc} _id	f_id	S_id	NT_id	NP_id	NO_id	FR_id
0.0	893.11	0.02539	28.43	50.67	27.58	13.98	1.61
0.4	725.26	0.02539	24.94	50.67	31.45	15.94	1.43
0.81	626.13	0.02539	22.43	50.67	34.96	17.72	1.23
1.21	555.75	0.02539	20.66	50.67	37.97	19.24	1.0
1.62	496.64	0.02539	19.54	50.67	40.13	20.33	0.73
2.02	433.1	0.02539	19.41	50.67	40.4	20.47	0.34

Figure 31 Text file output High-Bypass Ratio Turbofan Engine (Variation Calculation)

The area of circle no.1 or solid square indicates the type of engine that the user selected, the area of circle no.2 or round point square indicates the table of units for

the variation output parameter, the area of circle no.3 or long dash square indicates the variation output parameters that are one dimension calculation and for the area of circle no.4 or long dash and dot square indicates the variation output parameters that are multi-dimension calculation.

As for the plot the output parameters that are shown in the plots are

- Specific thrust (T_{sc})
- Thrust specific fuel consumption (S)
- Fuel to air ratio (f)
- Propulsive, Thermal, Overall efficiency
- Thrust ratio (from high bypass ratio turbofan engine)

The example output plot is as shown below,

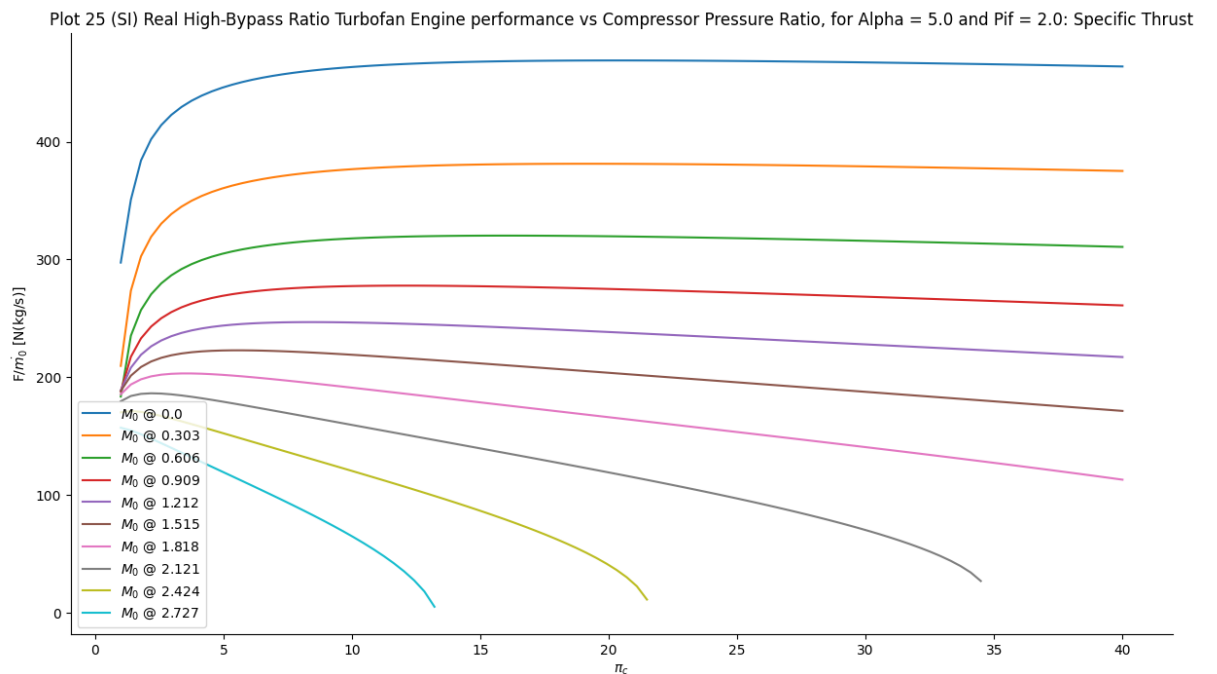


Figure 32 Plot the output parameters variation calculation High Bypass Ratio Turbofan Engine

The resultant plots are varied with compressor pressure ratio, free stream Mach number, fan pressure ratio, and bypass ratio (the last 2 parameters are for turbofan engine setting) with the previously mentioned parameters.

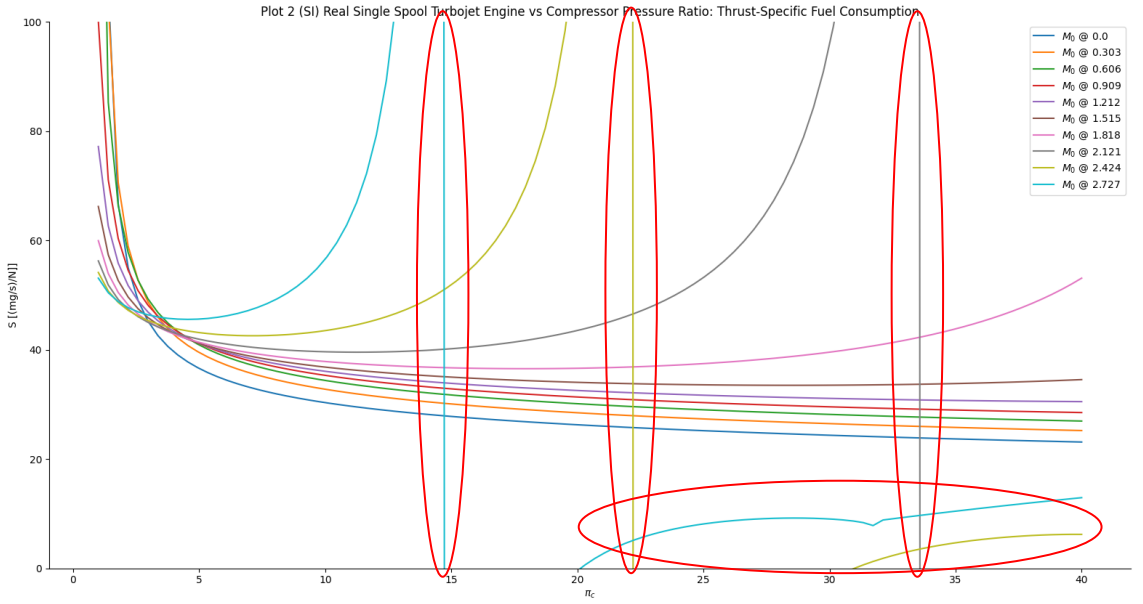


Figure 33 Example plot of the problem with limit of the graph

The graphs that would be represented as an output from both GTA and ONX in the later pages are exhibiting unusual phenomena as shown in the Figure 33 above with red oval. These lines indicate that the result of that line is reaching the critical point where the value reaching its highest or lowest possible and is regressed to normal or zero. Therefore, for the better result, study of this behavior should be carried out to define the limit of these parameters and impose limit to them.

3.2. Validation Software

To verify and validate the results from GTA, commercial software such as GasTurb and/or educational-purpose software such as AEDsys are simulated to obtain the results for the purpose of comparison.

3.2.1 AEDsys

AEDsys is based on the design tools in chapter 2 through 7 of Mattingly [8]. The program algorithm is as same as or similar to our project. Therefore, the expected outcome would be similar and comparable especially with the same input parameters. AEDsys offers,

1. 14 constraint types
2. 8 contour plots
3. 13 mission types
4. 7 aircraft drag models
5. 7 engine thrust models
6. 7 engine fuel consumption (TSFC) models

AEDsys can perform,

1. Constraint analysis
2. Contours of aircraft/engine performance
3. Mission analysis
4. Engine performance analysis

Which will specifically focus on its parametric cycle analysis function, namely ONX, its result will be introduced and study in chapter four.

3.2.2 GasTurb

GasTurb is a powerful and flexible gas turbine cycle program used by industry professionals and academic researchers. This commercial gas turbine engine performance simulation program uses a pseudo-perfect gas assumption in their calculations, where the specific heat is taken as a function of temperature and gas composition which is used for turbojet and turbofan engine design projects in the aspect of on-design parametric cycle analysis, off-design engine performance analysis, and on-design selection of cycle parameters. The input parameters are the same as using for GTA. Therefore, the expected outcome would be similar and comparable. With the help of GasTurb verification, the developed software could be verified at a certain level in the next phase.

GasTurb capabilities are as follow,

1. calculating design and off-design performance of gas turbines.
2. shows engine cross sections with station numbering and air system.
3. provides temperature-entropy, enthalpy-entropy, and pressure-volume diagrams.
4. performs model-based test analysis and engine performance monitoring.
5. does preliminary engine design and draws the general arrangement to scale.
6. defines a mission based on many operating conditions or a flight envelope and calculates all points in a single run.

4. Result and Discussion

4.1 Case study and Validation with the textbook

4.1.1 Single-Spool Turbojet Engine

The input parameters for all Single-Spool Turbojet Engine in Python are as represented in the figure below and each case is separated in its own defining function.

```
1  import numpy as np
2  import matplotlib.pyplot as plt
3  from scipy.interpolate import make_interp_spline
4  from scipy.optimize import curve_fit
5  from pathlib import Path
6
7  # in BE unit (ft)
8
9  # Input (Pic and M0 TBD)
10 Gc = 32.174
11 T0 = 390
12 Tt4 = 3000
13 Gamma = 1.4
14 Cp = 0.24
15 Hpr = 18400
16 Tt7 = 4000
17 Gammac = 1.4
18 Cpc = 0.24
19 Gammat = 1.35
20 Cpt = 0.262
21 Pidmax = 0.98
22 Pib = 0.98
23 Pin = 0.98
24 Ec = 0.92
25 Et = 0.91
26 Nb = 0.99
27 Nm = 0.98
28 Pratio09 = 1
29 GammaAB = 1.30
30 CpAB = 0.295
31 PiAB = 0.98
32 NAB = 0.96
33
34 def SSTJE_idnm():...
379
380     SSTJE_idnm()
381
382 def SSTJE_idab():...
785
786     SSTJE_idab()
787
788 def SSTJE_renm():...
1293
1294     SSTJE_renm()
1295
1296 def SSTJE_reab():...
1529
1530     SSTJE_reab()
```

Figure 34 Python, Single-Spool Turbojet Engine

Case study 1: Single-Spool Turbojet Engine – Ideal Turbojet

1. Input section

From the reference Mattingly [8],

$$T_0 = 390^\circ\text{R}, \gamma = 1.4, c_p = 0.24 \text{ Btu / (lbm} \cdot ^\circ\text{R}),$$

$$h_{PR} = 18,400 \text{ Btu / lbm}, T_{t4} = 3000^\circ\text{R}, M_0 = 0 - 3, \pi_c = 1 - 40$$

2. Results comparison

Variation of Mach number in comparison to compressor pressure ratio,

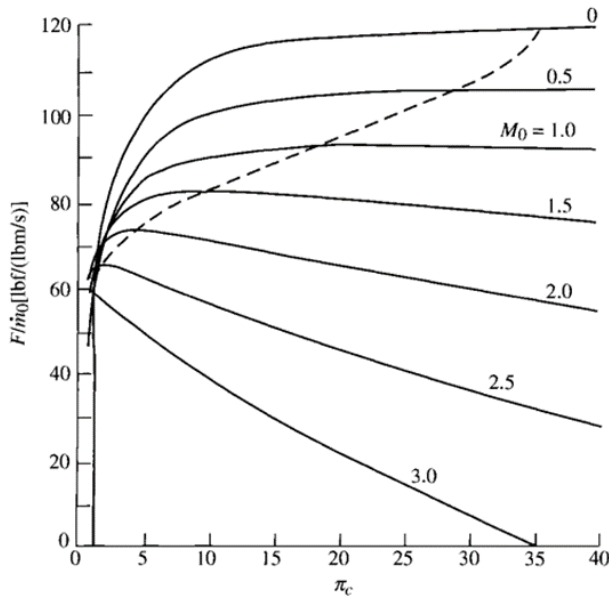


Figure 35 SSTJE Ideal M_0 vs π_c : Specific Thrust [8]

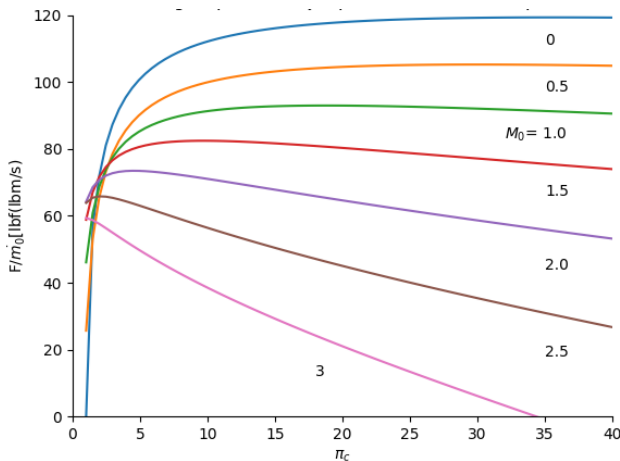


Figure 36 SSTJE Ideal M_0 vs π_c : Specific Thrust from GTA

From the Figure 35 and 36, it can be seen that for a fixed Mach number, there is a compressor pressure ratio that gives maximum specific thrust. The loci of the compressor pressure ratios that give maximum specific thrust are indicated by the

dashed line in Figure 35. Also, with a lower compressor ratio at a high Mach number, a reasonable specific thrust can be obtained.

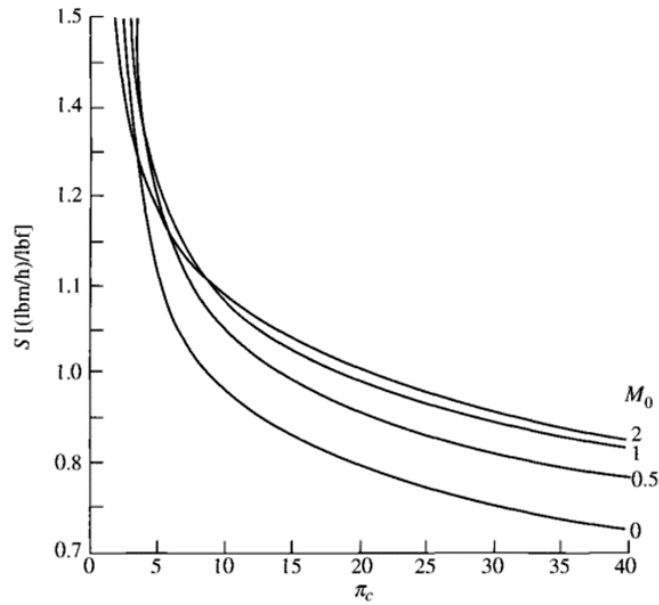


Figure 37 SSTJE Ideal M_0 vs π_c : Thrust-Specific Fuel Consumption [8]

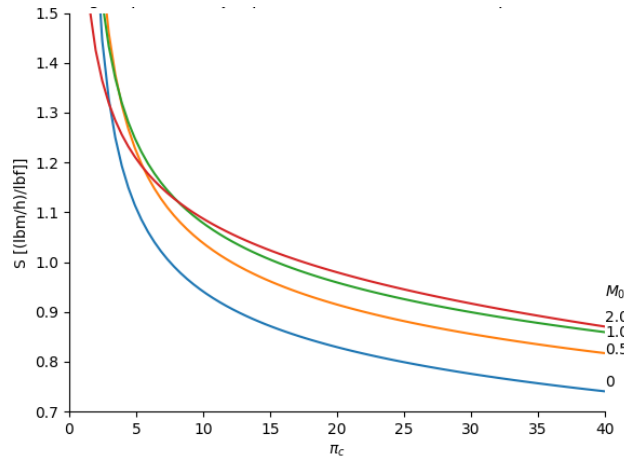


Figure 38 SSTJE Ideal M_0 vs π_c : Thrust-Specific Fuel Consumption from GTA

From the Figure 37 and 38, it can be seen that the increase in the compressor pressure ratio will give decrease the thrust-specific fuel consumption value in each Mach number respectively.

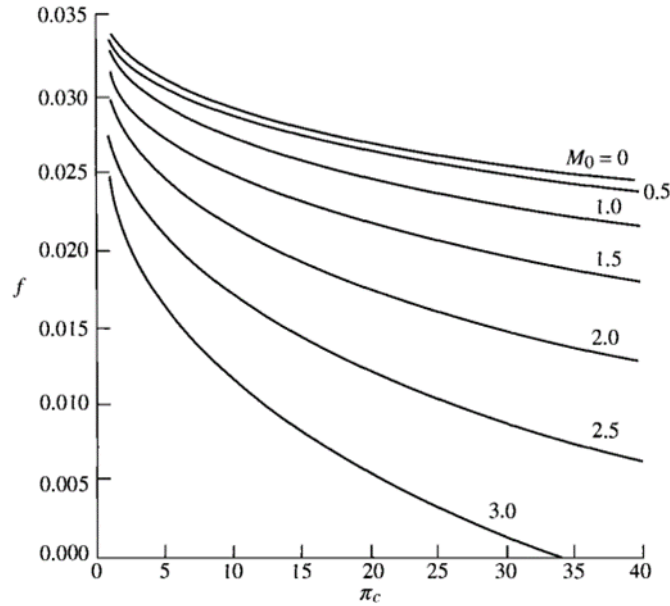


Figure 39 SSTJE Ideal M_0 vs π_c : fuel/air ratio [8]

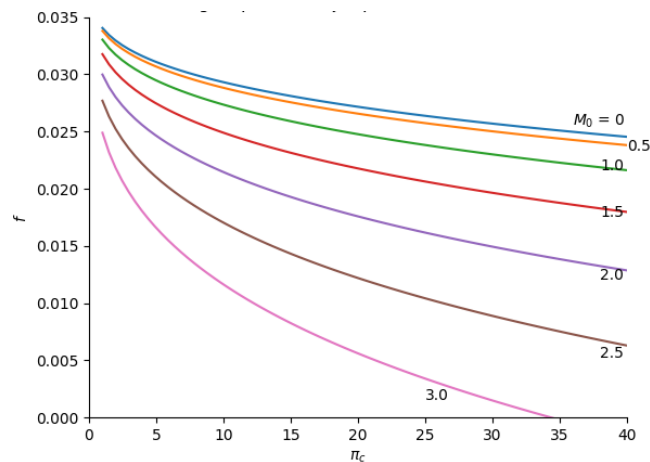


Figure 40 SSTJE Ideal M_0 vs π_c : fuel/air ratio from GTA

From the Figure 39 and 40, it can be seen that the increase in the compressor pressure ratio and Mach number will give a decrease in the Fuel/Air ratio respectively.

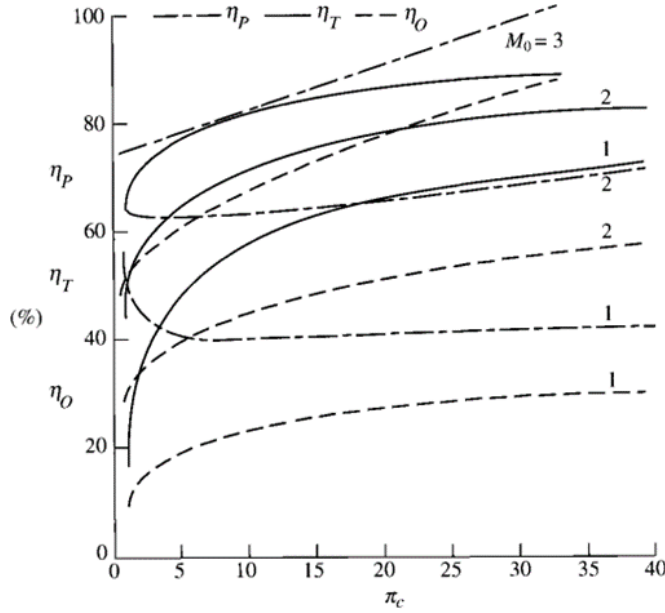


Figure 41 SSTJE Ideal M_0 vs π_c : efficiencies [8]

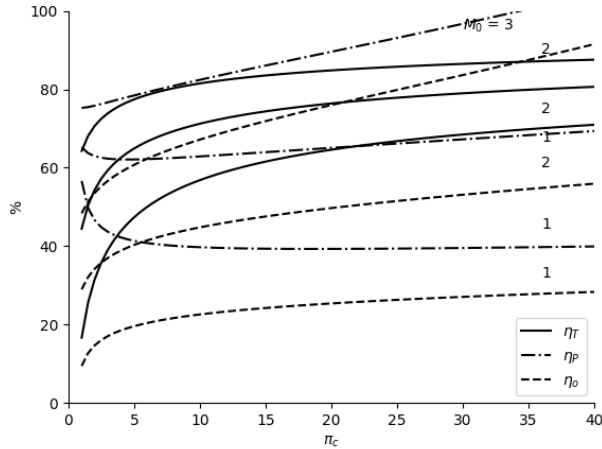


Figure 42 SSTJE Ideal M_0 vs π_c : efficiencies from GTA

From the Figure 41 and 42, it can be seen that the general increase in the compressor pressure ratio and Mach number will give an increase in the propulsive, thermal, and overall efficiencies respectively because of the dominant influence of both the compressor ratio and flight Mach number as one can see from the equation 80 – 82, for thermal efficiency as M_0 and π_c increase, τ_r and τ_c would increase respectively which result in the increase of thermal efficiency. The same go for propulsive efficiency as M_0 increase, as exhibit in equation 81, the propulsive will also increase. Thus, from the increasing of thermal and propulsive efficiency, the overall efficiency would also increase.

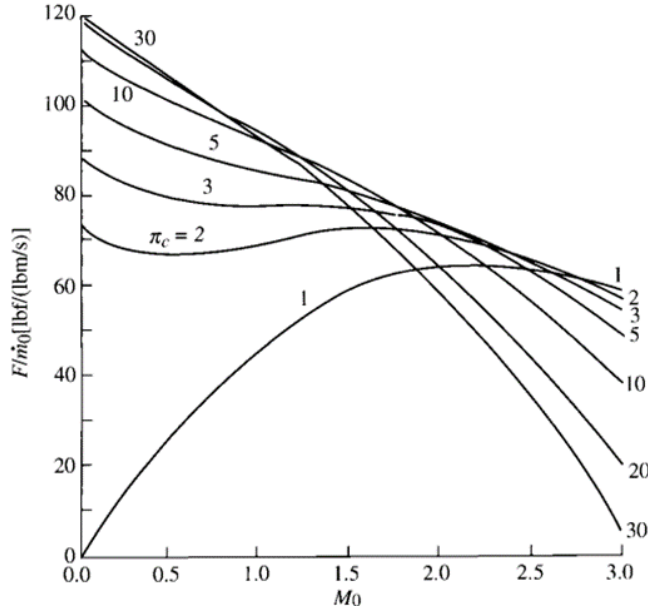


Figure 43 SSTJE Ideal π_c vs M_0 : Specific Thrust [8]

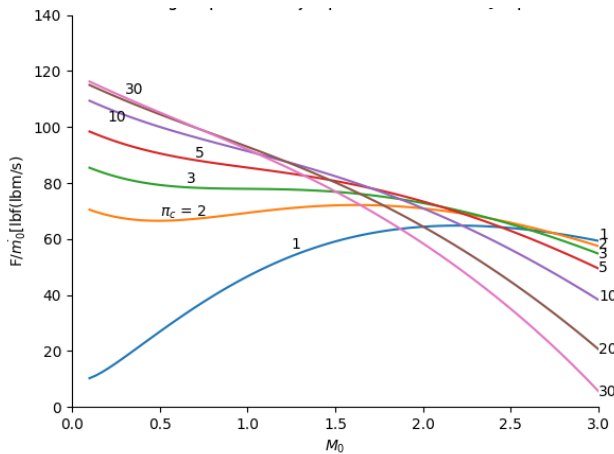


Figure 44 SSTJE Ideal π_c vs M_0 : Specific Thrust from GTA

From the Figure 43 and 44, it can be seen that the high value in the compressor pressure ratio and Mach number will give a decrease in the specific thrust respectively. The high compressor pressure ratio is desirable for subsonic flight for good specific thrust. However, the supersonic flight must be carefully used in the compressor pressure ratio because of the rapid falloff in specific thrust with the compressor pressure ratio.

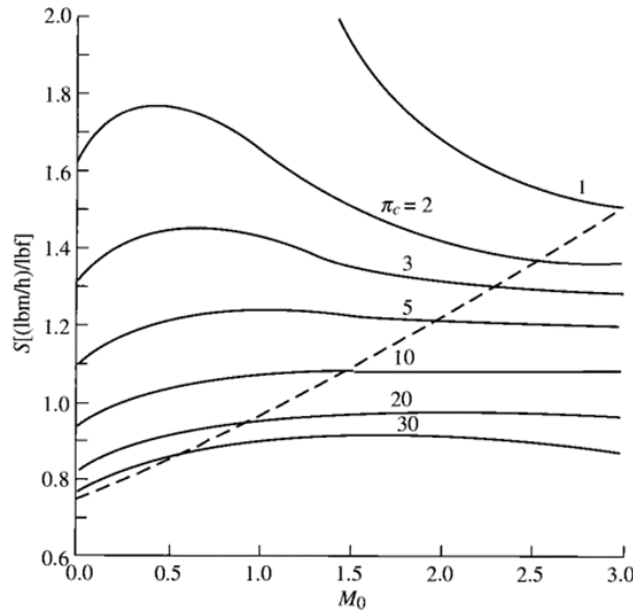


Figure 45 SSTJE Ideal π_c vs M_0 : Thrust-Specific Fuel Consumption [8]

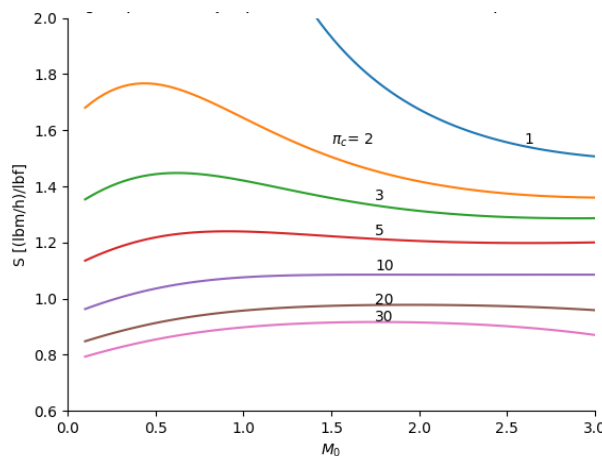


Figure 46 SSTJE Ideal π_c vs M_0 : Thrust-Specific Fuel Consumption from GTA

From the Figure 45 and 46, it can be seen that the increasing compressor pressure ratio and flight Mach number will give an increase in thrust specific fuel consumption then decrease and reach the constant point respectively. Also, a high compressor ratio is desirable for subsonic flight for low fuel consumption.

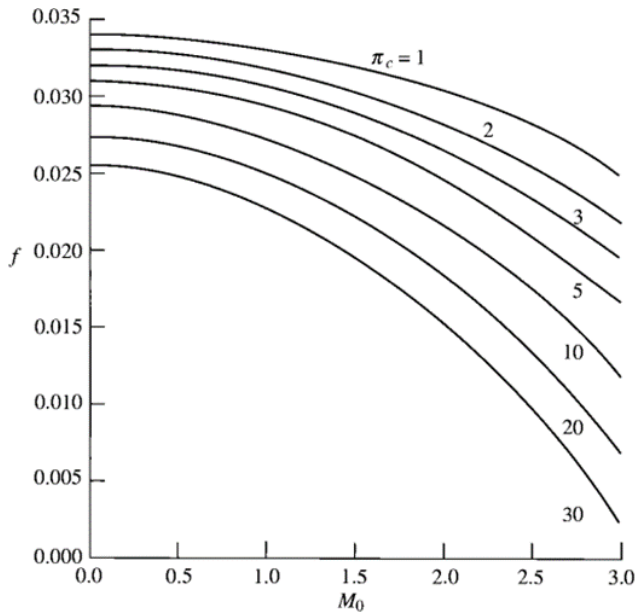


Figure 47 SSTJE Ideal π_c vs M_0 :fuel/air ratio [8]

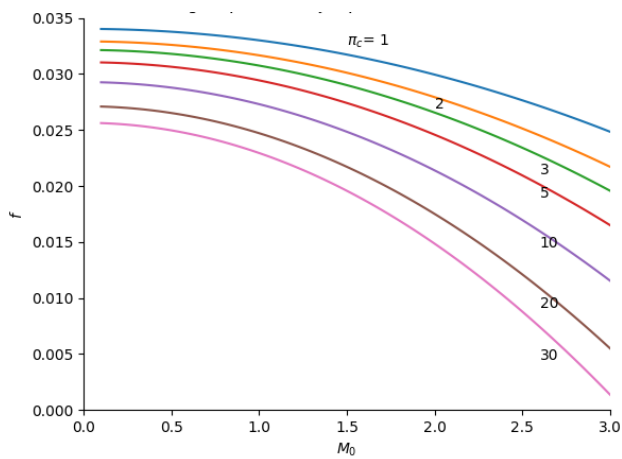


Figure 48 SSTJE Ideal π_c vs M_0 :fuel/air ratio from GTA

From the Figure 47 and 48, it can be seen that the increasing compressor pressor ratio and flight Mach number will give a decrease in fuel/air ratio respectively.

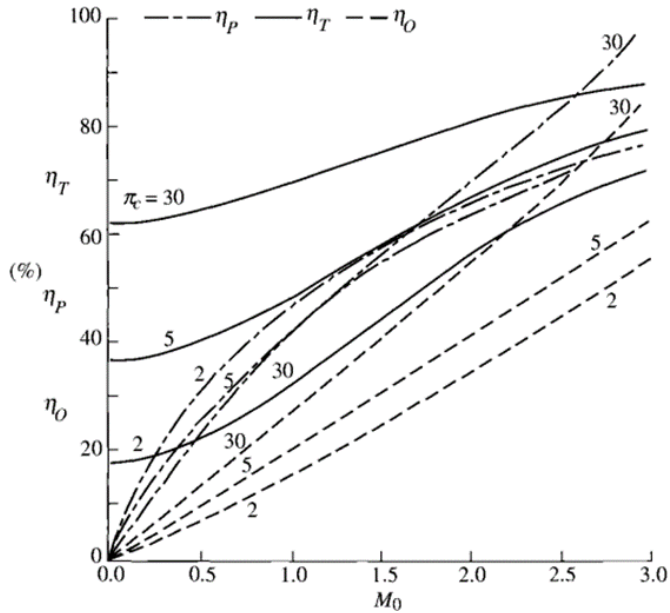


Figure 49 SSTJE Ideal π_c vs M_0 : efficiencies [8]

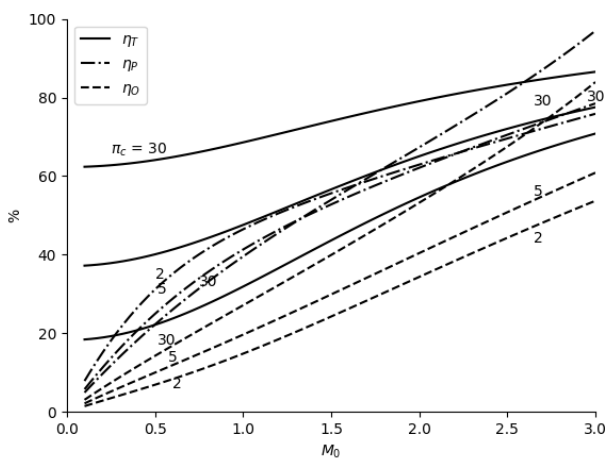


Figure 50 SSTJE Ideal π_c vs M_0 : efficiencies from GTA

From the Figure 49 and 50, it can be seen that the increasing compressor pressor ratio and flight Mach number are will give an increase in the propulsive, thermal, and overall efficiencies respectively.

Case study 2: Single-Spool Turbojet Engine with Afterburner – Ideal Turbojet

1. Input section

From the reference Mattingly [8],

$$T_0 = 390^\circ\text{R}, \gamma = 1.4, c_p = 0.24 \text{ Btu / (lbm} \cdot ^\circ\text{R}),$$

$$h_{PR} = 18,400 \text{ Btu / lbm}, T_{t4} = 3000^\circ\text{R}, T_{t7} = 4000^\circ\text{R}, M_0 = 0 - 3, \pi_c = 1 - 40$$

2. Results comparison

Variation of Mach number in comparison to compressor pressure ratio,

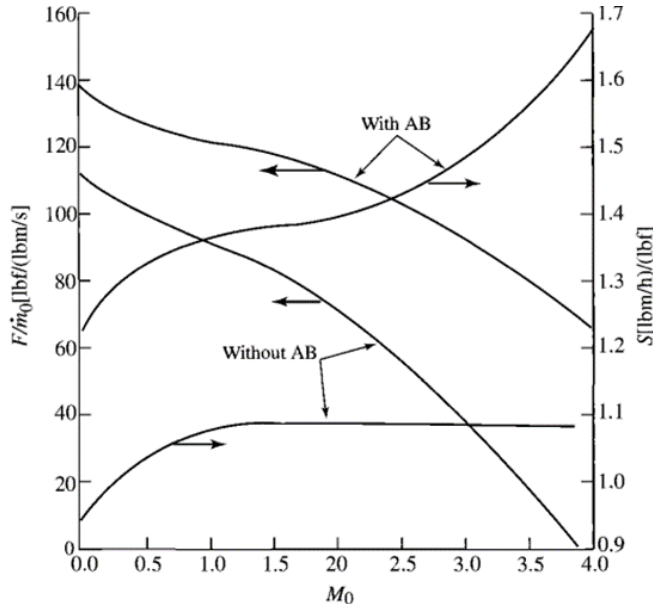


Figure 51 SSTJE IdealAB π_c vs M_0 : Specific Thrust and Thrust-Specific Fuel Consumption [8]

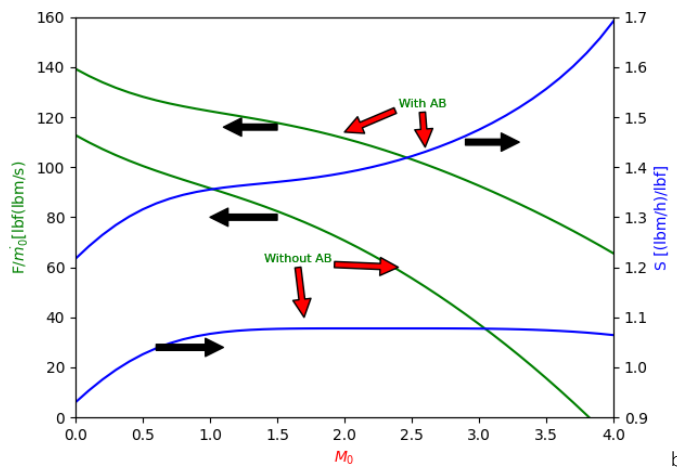


Figure 52 SSTJE IdealAB π_c vs M_0 : Specific Thrust and Thrust-Specific Fuel Consumption from GTA

From the Figure 51 and 52, it can be seen that Single Spool Turbojet Engine with Afterburning increases both the specific thrust and the thrust specific fuel consumption. Also, afterburning turbojet with moderate to high compressor pressure

ratios gives very good specific thrust at high flight Mach numbers. However, Single Spool Turbojet Engine with Afterburning at a higher flight Mach number will give a lower thrust specific fuel consumption and higher specific thrust than the without an afterburner.

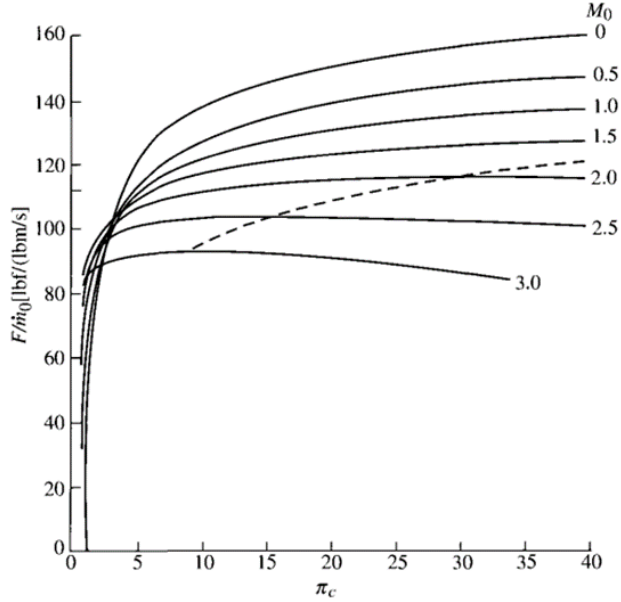


Figure 53 SSTJE IdealAB M_0 vs. π_c : Specific Thrust [8]

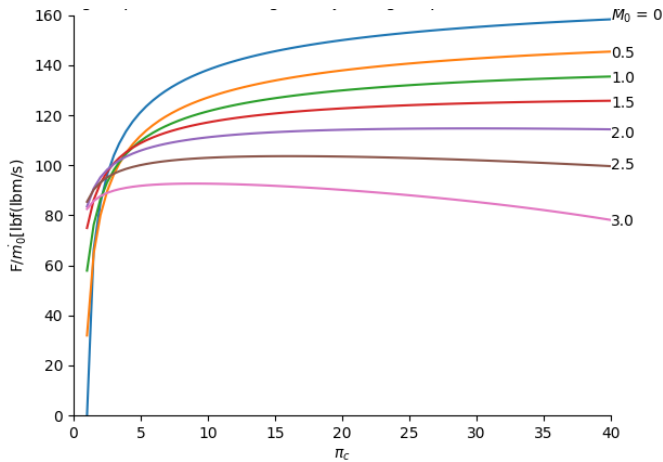


Figure 54 SSTJE IdealAB M_0 vs. π_c : Specific Thrust from GTA

From the Figure 53 and 54, it can be seen that the increasing compressor pressor ratio and flight Mach number will give a decrease in the Specific Thrust and reach a stagnation point respectively.

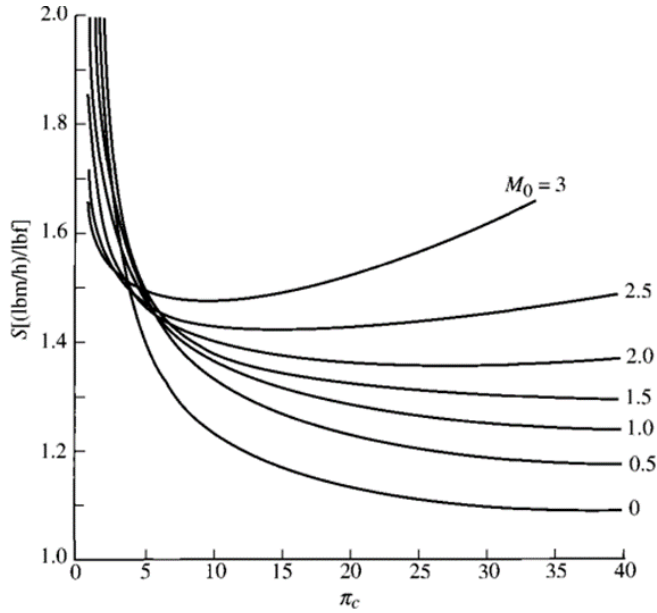


Figure 55 SSTJE IdealAB M_0 vs π_c : Thrust-Specific Fuel Consumption [8]

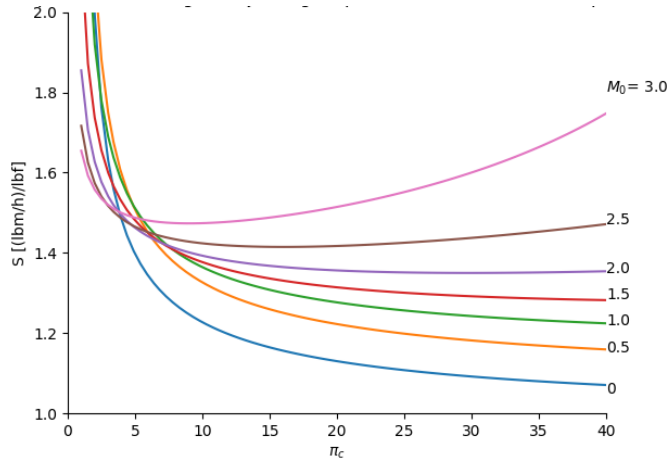


Figure 56 SSTJE IdealAB M_0 vs π_c : Thrust-Specific Fuel Consumption from GTA

From the Figure 55 and 56, it can be seen that the increasing compressor pressor ratio and flight Mach number will give a decrease in the Thrust Specific Fuel Consumption then it will increase at high compressor pressure ratio then reach a stagnation point respectively.

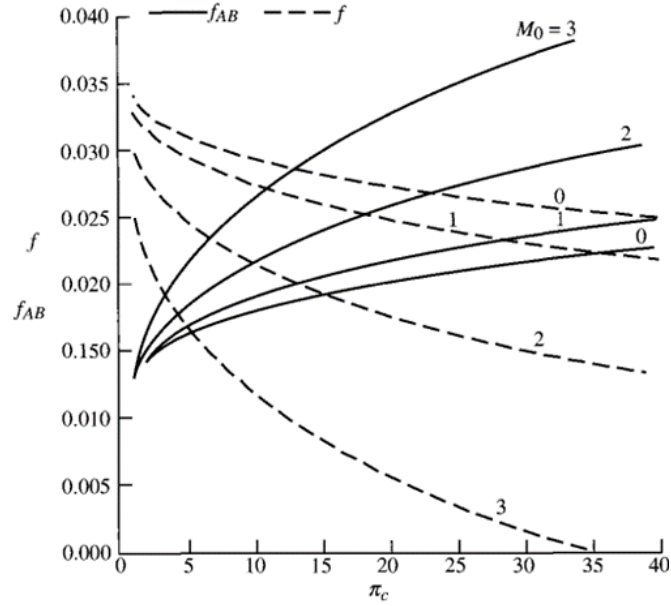


Figure 57 SSTJE IdealAB M_0 vs π_c : fuel/air ratios [8]

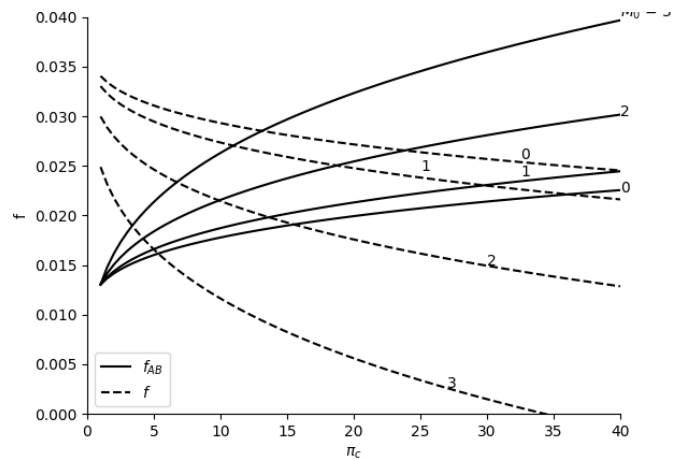


Figure 58 SSTJE IdealAB M_0 vs π_c : fuel/air ratios from GTA

From the Figure 57 and 58, it can be seen that Single Spool Turbojet Engine without Afterburning with increasing compressor pressor ratio and flight Mach number will give a decrease in the Fuel/Air ratio. And Single Spool Turbojet Engine with Afterburning with increasing compressor pressor ratio and flight Mach number will give an increase Fuel/Air ratio respectively.

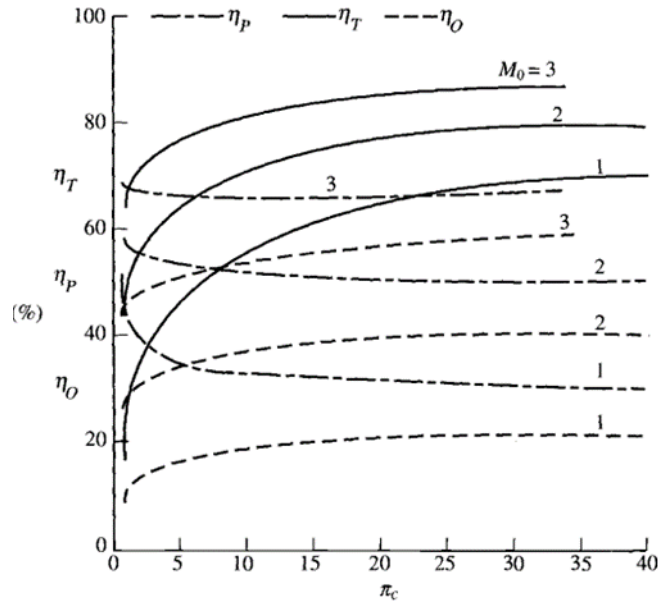


Figure 59 SSTJE IdealAB M_0 vs π_c : efficiencies [8]

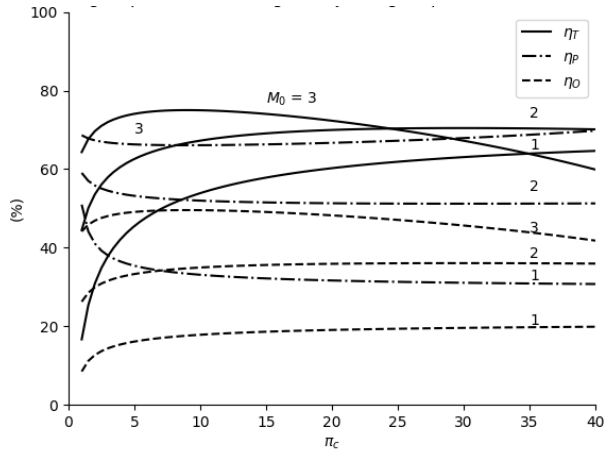


Figure 60 SSTJE IdealAB M_0 vs π_c : efficiencies from GTA

From the Figure 59 and 60, it can be seen that the thermal, propulsive, and overall efficiencies are reduced by afterburning. As represented in, the result obtained from Python, for the thermal and overall efficiencies for the Mach number equal to 3, the trend of the thermal efficiency graph line should go upward but it goes downward which also affects the trend line of overall efficiency. The problem may be resulted from the relation of the supersonic Mach number which still working on to solve this problem.

Case study 3: Single-Spool Turbojet Engine – Real Turbojet

1. Input section

From the reference Mattingly [8],

$$M_0 = 2, T_0 = 216.7 \text{ K}, \gamma_c = 1.4, c_{pc} = 1.004 \text{ kJ / (kg} \cdot \text{K}),$$

$$\gamma_t = 1.3, c_{pt} = 1.239 \text{ kJ / (kg} \cdot \text{K}), h_{PR} = 42,800 \text{ kJ / (kg} \cdot \text{K}),$$

$$\pi_{dmax} = 0.95, \pi_b = 0.94, \pi_n = 0.96, e_c = 0.9, e_t = 0.9, \eta_b = 0.98,$$

$$\eta_m = 0.99, P_0 / P_9 = 0.5, T_{t4} = 1800 \text{ K}, \pi_c = 10$$

2. Results comparison

Variation of Mach number in comparison to compressor pressure ratio,

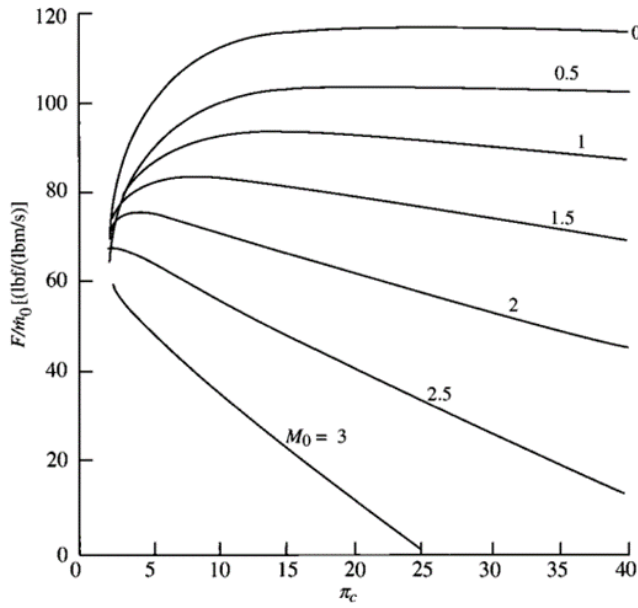


Figure 61 SSTJE Real M_0 vs π_c : Specific Thrust [8]

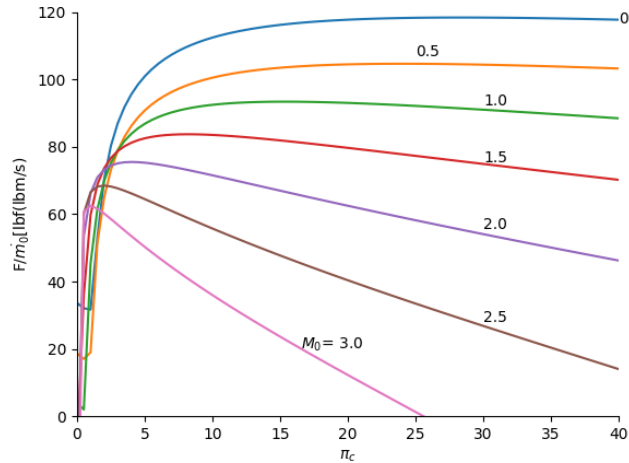


Figure 62 SSTJE Real M_0 vs π_c : Specific Thrust from GTA

From the Figure 61 and 62, at high Mach numbers, the effect of the losses causes the specific thrust to go to zero at a lower compressor pressure ratio. For a Mach number the compressor pressure ratio that gives the maximum specific thrust.

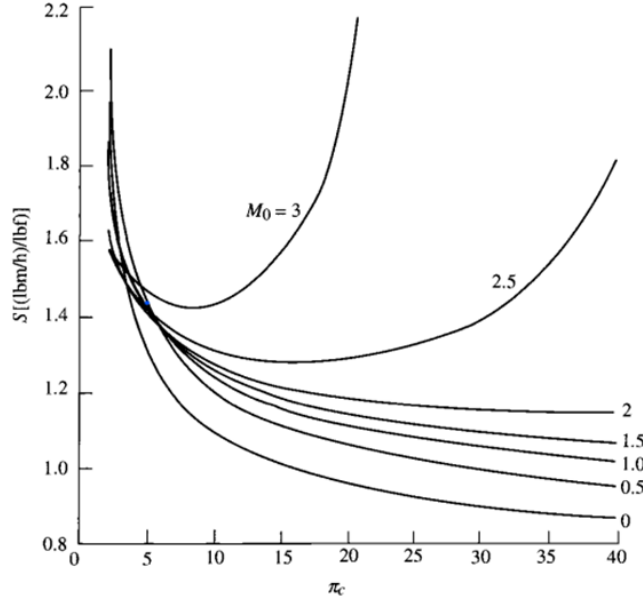


Figure 63 SSTJE Real M_0 vs π_c : Thrust-Specific Fuel Consumption [8]

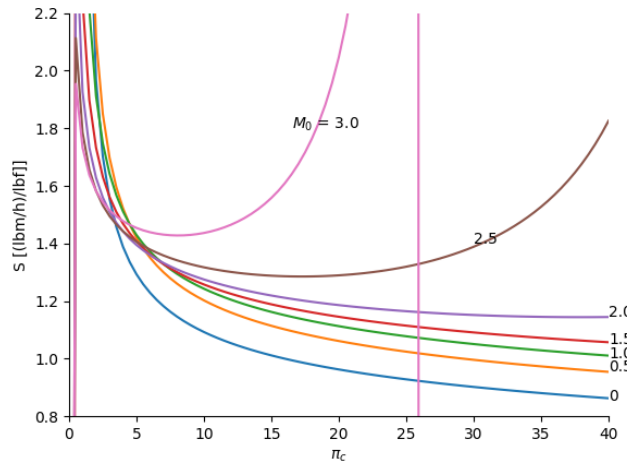


Figure 64 SSTJE Real M_0 vs π_c : Thrust-Specific Fuel Consumption from GTA

From the Figure 63 and 64, it can be seen that the values of fuel consumption are visibly larger for the real case. With increasing compressor pressure ratio, the thrust specific fuel consumption is no longer decreasing, and with a given Mach number, the minimum fuel consumption can be observed with a compressor pressure ratio.

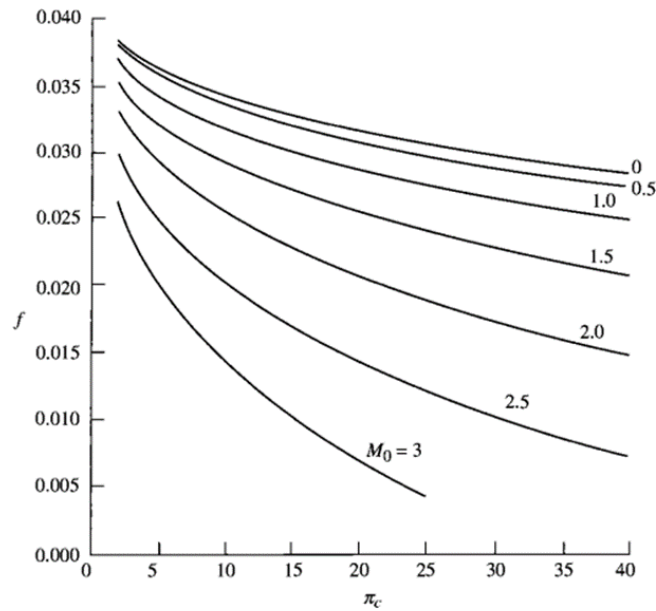


Figure 65 SSTJE Real M_0 vs π_c : fuel/air ratio [8]

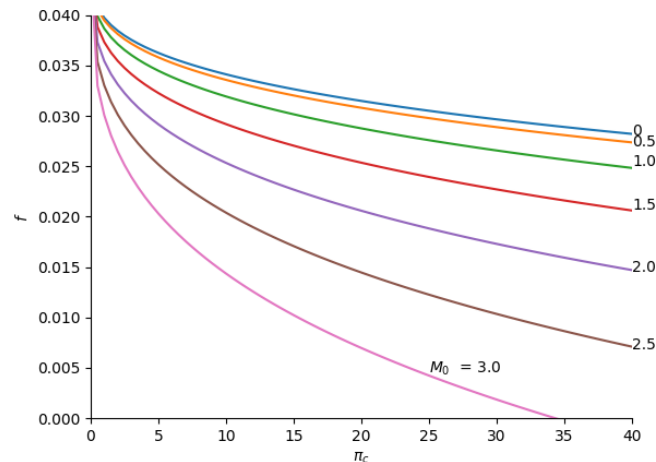


Figure 66 SSTJE Real M_0 vs π_c : fuel/air ratio from GTA

From the Figure 65 and 66, it can be seen that the increasing of compressor pressor ratio and flight Mach number will give a decrease in the Fuel/Air ratio then reach a stagnation point respectively.

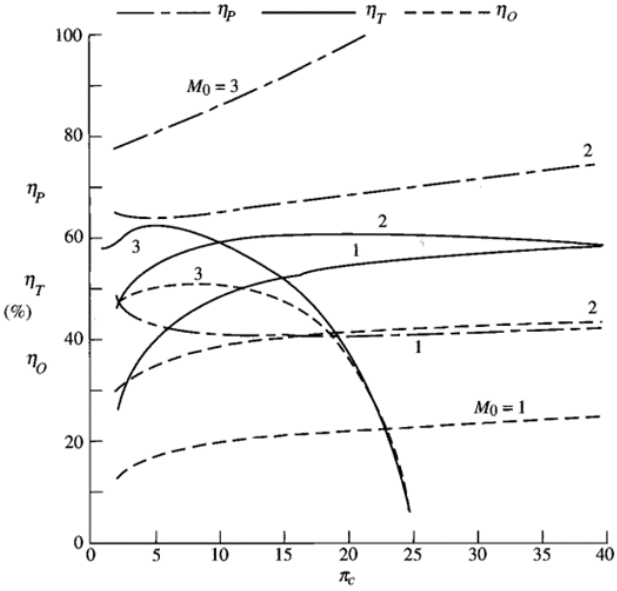


Figure 67 SSTJE Real M_0 vs π_c : efficiencies [8]

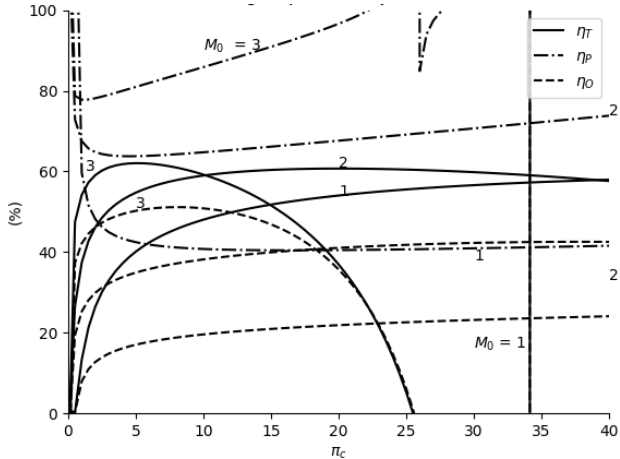


Figure 68 SSTJE Real M_0 vs π_c : efficiencies from GTA

From the Figure 67 and 68, it can be seen that the propulsive efficiencies are a little larger for the turbojet with losses as compare to ideal condition. This is due mainly to the decrease in exhaust velocity for the real engine. For thermal efficiency, the real engine with losses has lower thermal efficiency. Also, the thermal efficiency of high compressor pressure ratio engines at high Mach goes toward zero because thrust goes to zero before the fuel flow rate. The overall efficiencies are lower for real engine with losses due to the decrease in thermal efficiency.

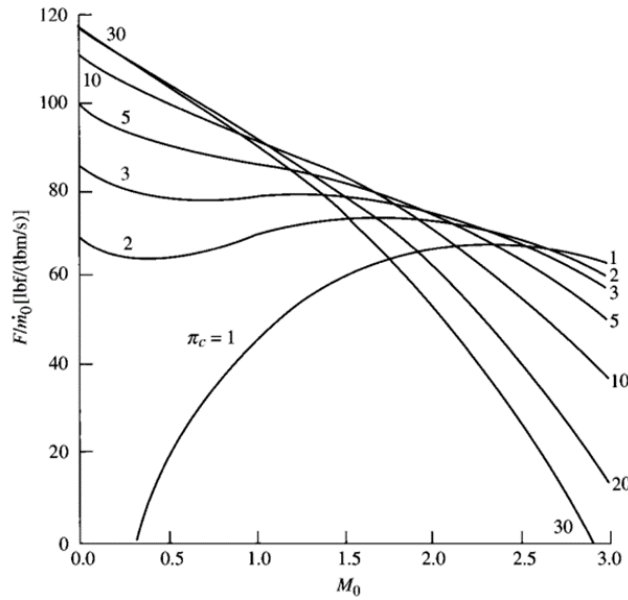


Figure 69 SSTJE Real π_c vs M_0 : Specific Thrust [8]

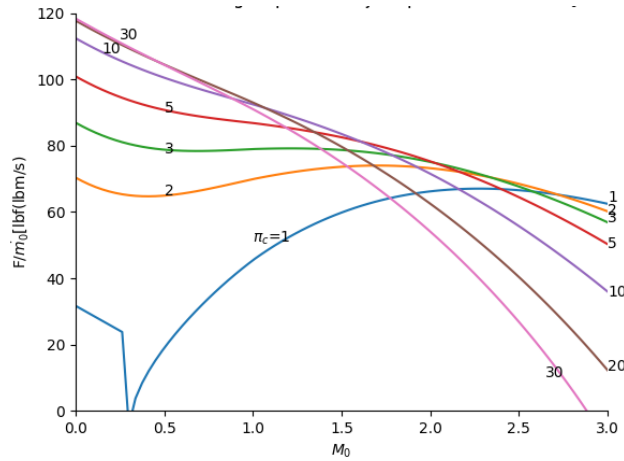


Figure 70 SSTJE Real π_c vs M_0 : Specific Thrust from GTA

From the Figure 69 and 70, it can be seen that the increasing of compressor pressure ratio and flight Mach number will give a decrease in the specific thrust then reach into zero respectively. However, compressor pressure ratio = 1 increase and then reach stagnation point and decrease respectively.

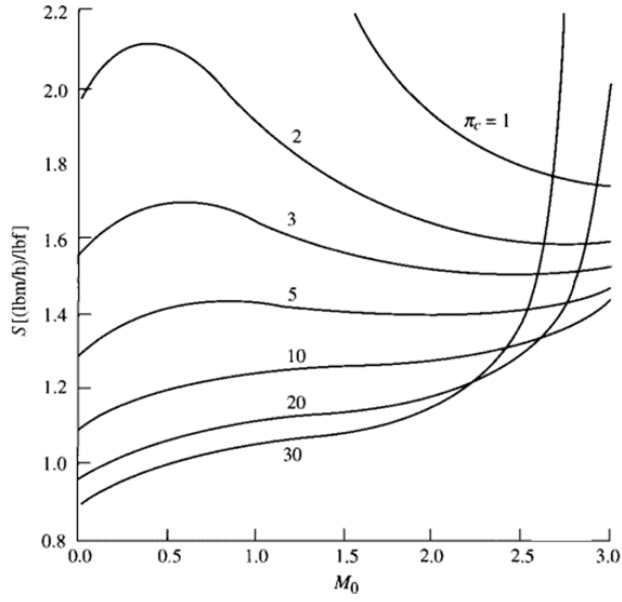


Figure 71 SSTJE Real π_c vs M_0 : Thrust-Specific Fuel Consumption [8]

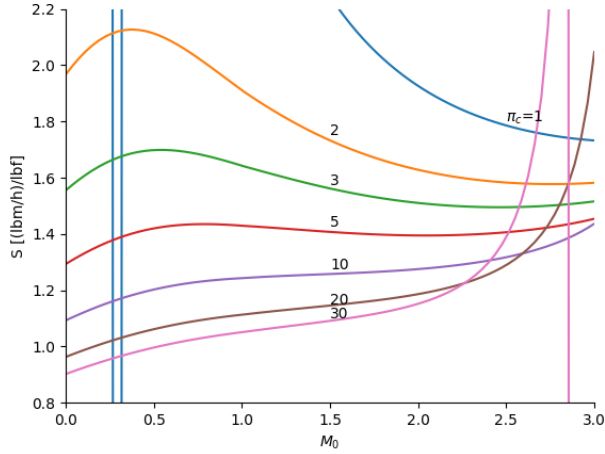


Figure 72 SSTJE Real π_c vs M_0 : Thrust-Specific Fuel Consumption from GTA

From the Figure 71 and 72, it can be seen that the increasing of compressor pressure ratio and flight Mach number will give a decrease in the specific thrust at low flight Mach number and then an increase in the thrust specific fuel consumption at high flight Mach number respectively.

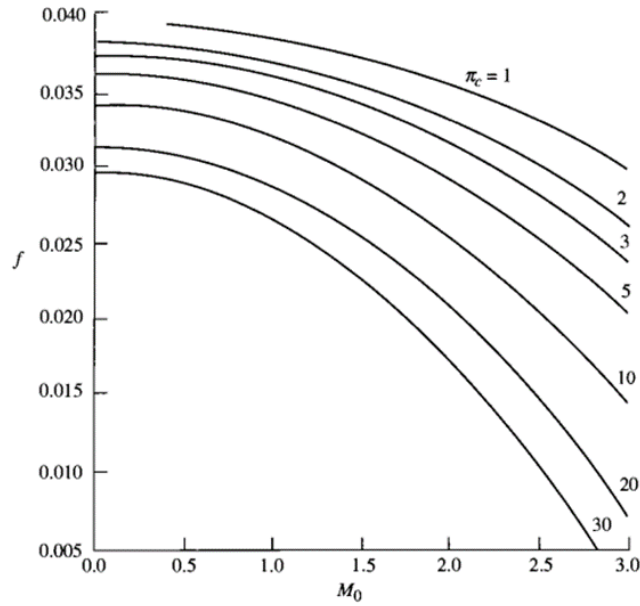


Figure 73 SSTJE Real π_c vs M_0 : fuel/air ratio [8]

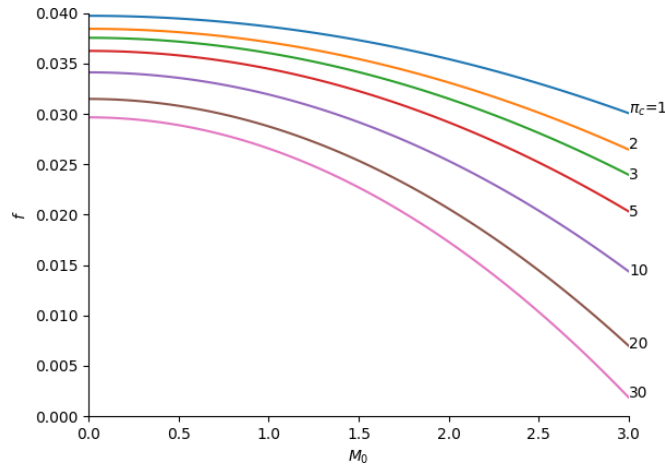


Figure 74 SSTJE Real π_c vs M_0 : fuel/air ratio from GTA

From the Figure 73 and 74, it can be seen that the increasing of compressor pressure ratio and flight Mach number will give a decrease in the fuel/air ratio go to zero respectively.

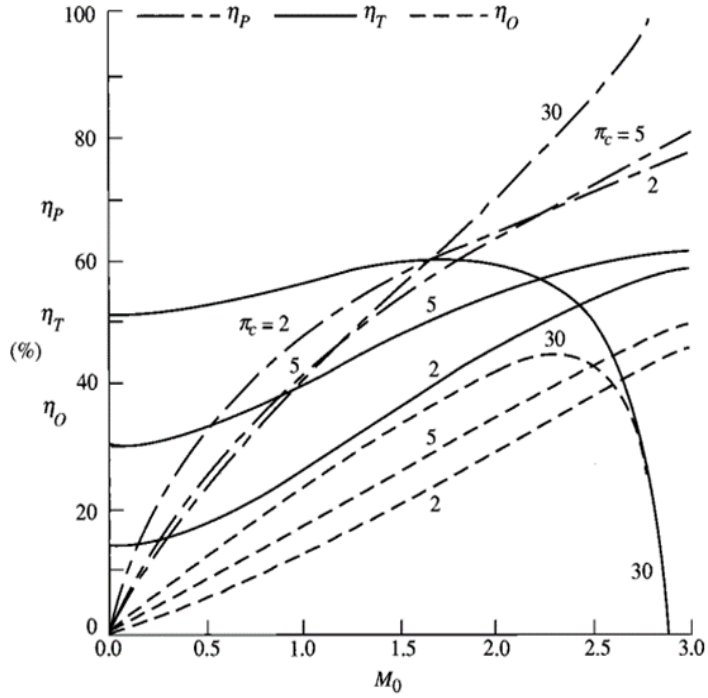


Figure 75 SSTJE Real π_c vs M_0 : efficiencies [8]

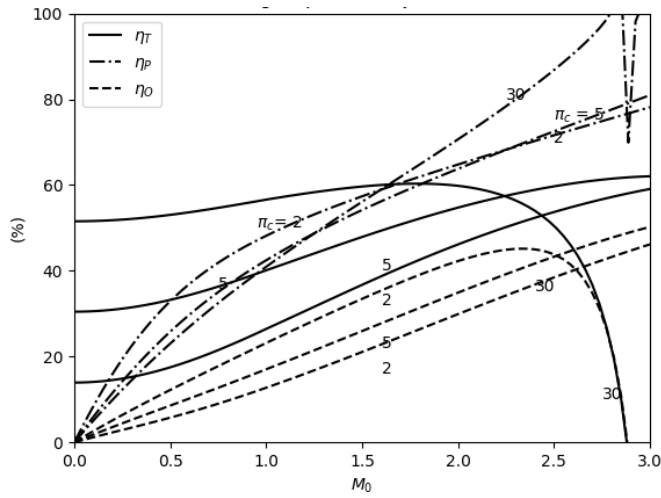


Figure 76 SSTJE Real π_c vs M_0 : efficiencies from GTA

From the Figure 75 and 76, it can be seen that the increasing of compressor pressure ratio and flight Mach number will give an increase in propulsive efficiency respectively. For thermal efficiency, increase and decrease respectively at high Mach number go toward zero because the thrust goes to zero before the fuel flow rate. Overall efficiency will increase and reach a stagnation point. However, the overall efficiency at compressor pressure ratio = 30 will decrease and go toward zero.

Case study 4: Single-Spool Turbojet Engine with Afterburner – Real Turbojet

1. Input section

From the reference Mattingly [8],

$$\begin{aligned}
 M_0 &= 2, \pi_c = 2 \rightarrow 14, T_0 = 390^\circ R, \gamma_c = 1.4, \\
 c_{pc} &= 0.24 \text{ Btu / (lbm} \cdot {}^\circ \text{R}), \gamma_t = 1.33, c_{pt} = 0.276 \text{ Btu / (lbm} \cdot {}^\circ \text{R}), \\
 h_{PR} &= 18,400 \text{ Btu / lbm}, \gamma_{AB} = 1.30, c_{pAB} = 0.295 \text{ Btu / (lbm} \cdot {}^\circ \text{R}), \\
 \pi_{dmax} &= 0.98, \pi_b = 0.98, \pi_{AB} = 0.98, \pi_n = 0.98, e_c = 0.89, \\
 e_t &= 0.91, \eta_b = 0.99, \eta_m = 0.98, \eta_{AB} = 0.96, P_0 / P_9 = 1, \\
 T_{t4} &= 3000^\circ R, T_{t7} = 3500^\circ R
 \end{aligned}$$

2. Results comparison

From the reference, the specific thrust and thrust-specific fuel consumption versus compressor pressure ratio are represented as shown,

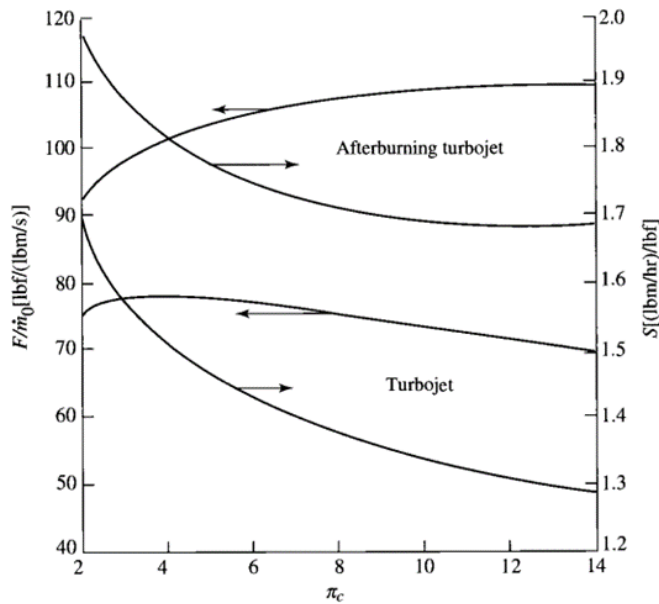


Figure 77 SSTJE RealAB vs Real, π_c : Specific Thrust and Thrust-Specific Fuel Consumption [8]

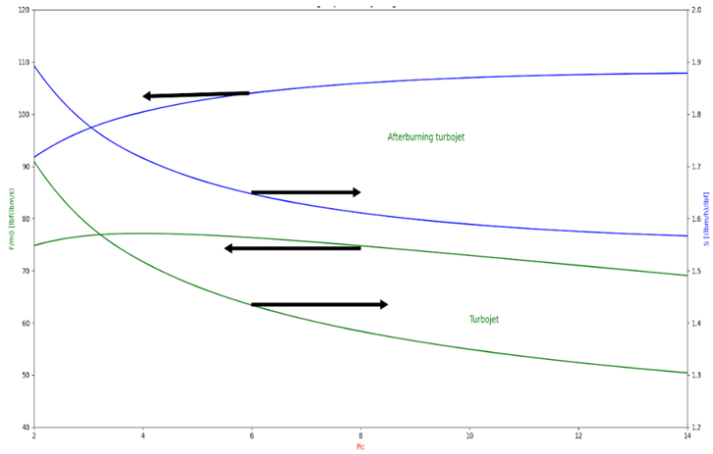


Figure 78 SSTJE RealAB vs Real, π_c : Specific Thrust and Thrust-Specific Fuel Consumption from GTA

From the Figure 77 and 78, it can be seen that the single spool turbojet engine with afterburning increases both the specific thrust and the thrust specific fuel consumption. Also, afterburning turbojet with moderate to high compressor pressure ratios gives very good specific thrust at high flight Mach numbers more than single spool turbojet engine without afterburning.

4.1.2 High Bypass Ratio Turbofan Engine

The input parameters for all High – Bypass ratio Turbofan Engine in Python are as represented in the figure below (for now), and each case is separated in its own defining

```
1  import numpy as np
2  import matplotlib.pyplot as plt
3  from scipy.interpolate import make_interp_spline
4  from scipy.optimize import curve_fit
5  from pathlib import Path
6
7  # in SI unit (m)
8
9  # Input (Pic, M0, Alpha, Pif TBD)
10 Gc = 1
11 T0 = 216.7
12 Tt4 = 1670
13 Gamma = 1.4
14 Gammac = 1.4
15 Gammat = 1.35
16 Hpr = 42800
17 M0 = 0.9
18 Cp = 1.004
19 Cpc = 1.004
20 Cpt = 1.096
21 Pidmax = 0.98
22 Pib = 0.98
23 Pin = 0.98
24 Pifn = 0.98
25 Ec = 0.90
26 Ef = 0.88
27 Et = 0.91
28 Pit = 0.89
29 Nb = 0.99
30 Nm = 0.99
31 Pif = 2
32 Pratio09 = 1
33 Pratio19 = 1
34
35 def HBP_id():
363
364     HBP_id()
37
386 def HBP_re():
392
393     HBP_re()
394
395
396
```

Figure 79 Python, High-Bypass ratio Turbofan Engine

Case study 7: High Bypass Ratio Turbofan Engine – Ideal Turbofan

1. Input section

From the reference Mattingly [8],

$$T_0 = 216.7^\circ K, \gamma = 1.4, c_p = 1.004 \text{ kJ / (Kg} \cdot ^\circ \text{K}),$$

$$H_{PR} = 42800 \text{ kJ / kg}, T_{t4} = 1670^\circ K, M_0 = 0.9, \pi_c = 1 - 40$$

2. Results comparison

Variation of bypass ratio in comparison to compressor pressure ratio with constant fan pressure ratio of 2 and flight Mach number of 0

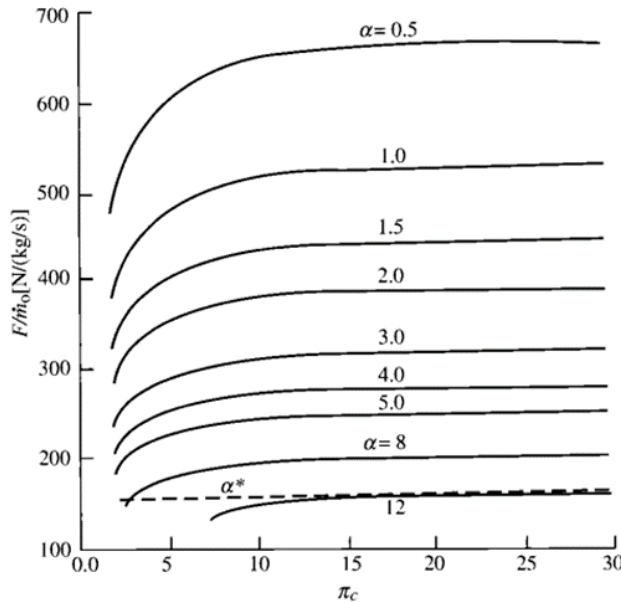


Figure 80 HBPTFE Ideal α vs π_c for $\pi_f = 2, M_0 = 0.9$: Specific Thrust [8]

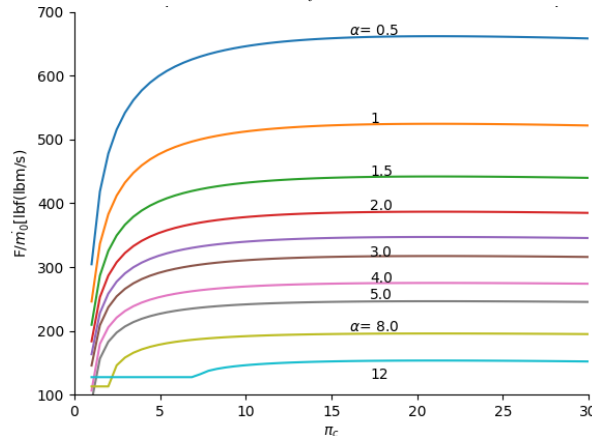


Figure 81 HBPTFE Ideal α vs π_c for $\pi_f = 2, M_0 = 0.9$: Specific Thrust from GTA

From the Figure 80 and 81, it can be seen that the increasing of compressor pressure ratio and bypass ratio will give an increase specific thrust remains essentially constant with respect to the compressor pressure ratio for values from 15 to 25, and that specific thrust decreases with increasing bypass ratio.

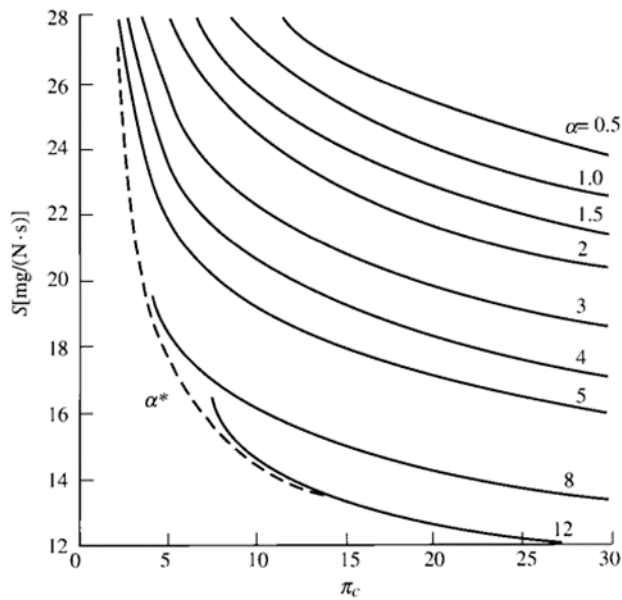


Figure 82 HBPTFE Ideal α vs π_c for $\pi_f = 2, M_0 = 0.9$: Thrust-Specific Fuel Consumption [8]

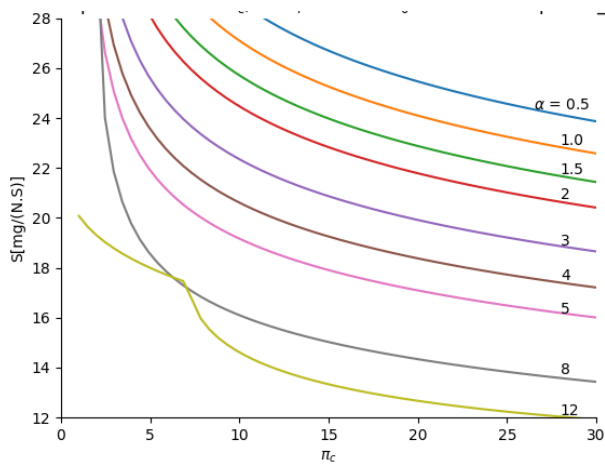


Figure 83 HBPTFE Ideal α vs π_c for $\pi_f = 2, M_0 = 0.9$: Thrust-Specific Fuel Consumption from GTA

From Figure 82 and 83, it can be seen that the increasing of compressor pressor ratio and bypass ratio will give a decrease thrust specific fuel consumption respectively.

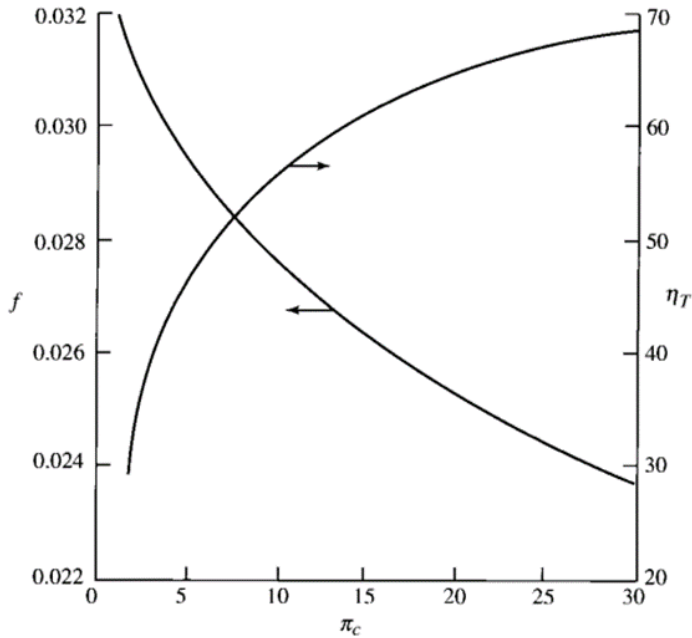


Figure 84 HBPTFE Ideal α vs π_c for $\pi_f = 2, M_0 = 0.9$: fuel/air ratio and thermal efficiency [8]

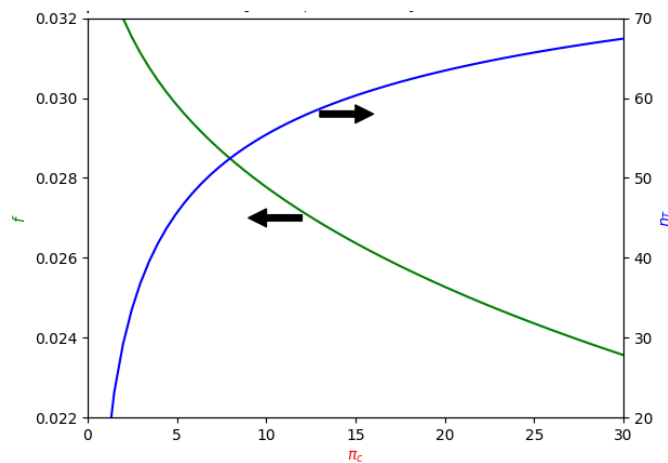


Figure 85 HBPTFE Ideal α vs π_c for $\pi_f = 2, M_0 = 0.9$: fuel/air ratio and thermal efficiency from GTA

From the Figure 84 and 85, it can be seen that the increasing of compressor pressor ratio and bypass ratio will give a decreasing fuel/air ratio respectively. As well as thermal efficiency increasing respectively.

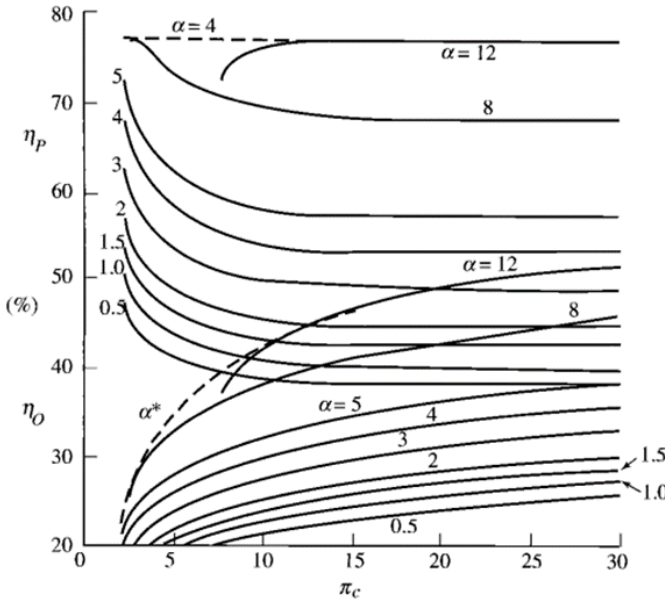


Figure 86 HBPTFE Ideal α vs π_c for $\pi_f = 2, M_0 = 0.9$: propulsive and overall efficiencies [8]

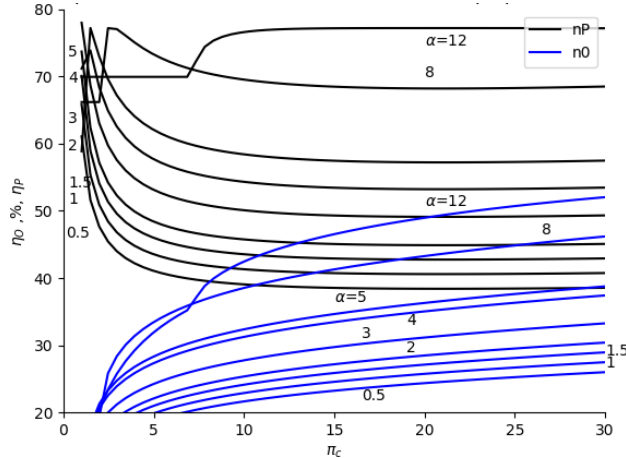


Figure 87 HBPTFE Ideal α vs π_c for $\pi_f = 2, M_0 = 0.9$: propulsive and overall efficiencies from GTA

From the Figure 86 and 87, it can be seen that the propulsive efficiency increases with engine bypass ratio and varies very little with compressor pressure ratio. The overall efficiency increases with both compressor pressure ratio and bypass ratio. From the comparison a fixed bypass ratio and variation of compressor pressure ratio, the propulsive efficiency increases with engine bypass ratio and varies very little with compressor pressure ratio. The overall efficiency increases with both compressor pressure ratio and bypass ratio.

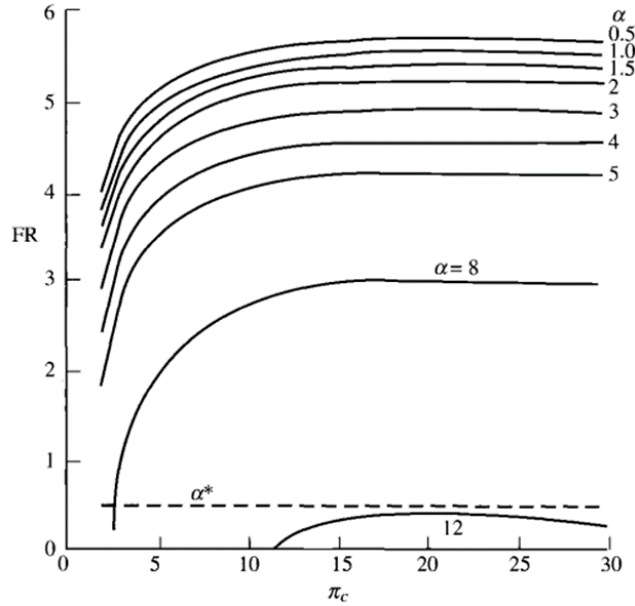


Figure 88 HBPTFE Ideal α vs π_c for $\pi_f = 2, M_0 = 0.9$: Thrust ratio [8]

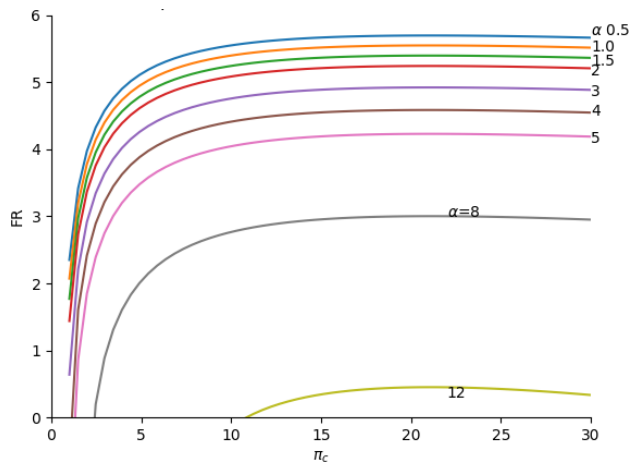


Figure 89 HBPTFE Ideal α vs π_c for $\pi_f = 2, M_0 = 0.9$: Thrust ratio from GTA

From the Figure 88 and 89, it can be seen that the thrust ratio decreases with increasing bypass ratio and varies very little with compressor pressure ratio.

Variation of fan pressure ratio in comparison to compressor pressure ratio with constant bypass ratio of 5 and flight Mach number of 0.9

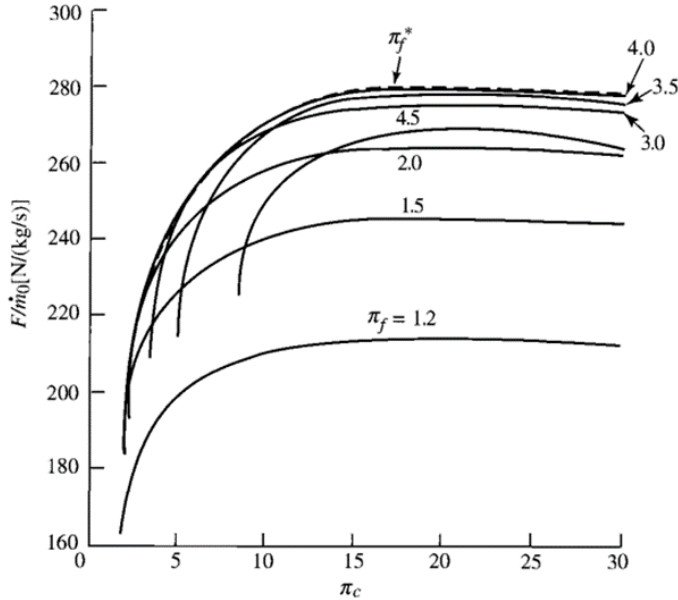


Figure 90 HBPTFE Ideal π_f vs π_c for $\alpha = 5, M_0 = 0.9$: Specific Thrust [8]

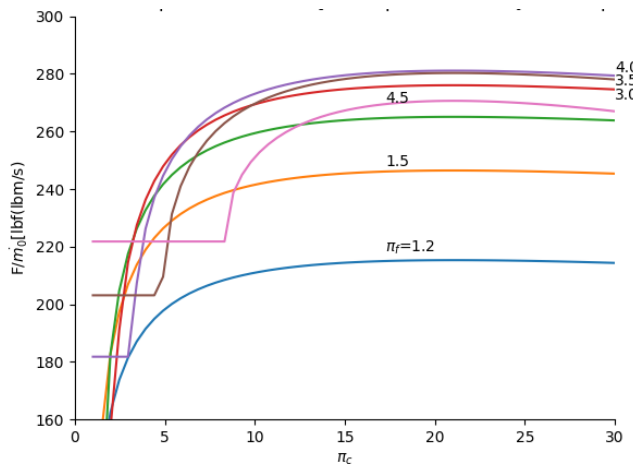


Figure 91 HBPTFE Ideal π_f vs π_c for $\alpha = 5, M_0 = 0.9$: Specific Thrust from GTA

From the Figure 90 and 91, it can be seen that the increasing of fan pressure ratio and variation of compressor pressure ratio will give an increase the specific thrust remains essentially constant with respect to the compressor pressure ratio from 15 to 25, and that the specific thrust has a maximum with respect to the fan pressure ratio

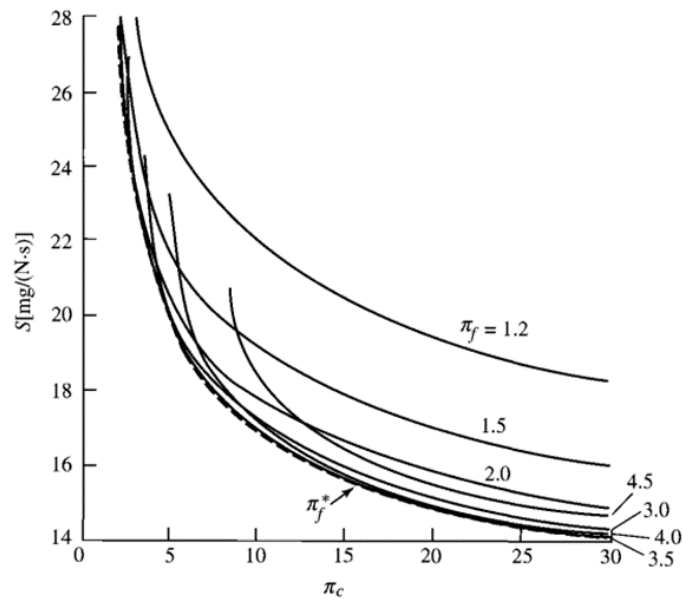


Figure 92 HBPTFE Ideal π_f vs π_c for $\alpha = 5, M_0 = 0.9$: Thrust-Specific Fuel Consumption [8]

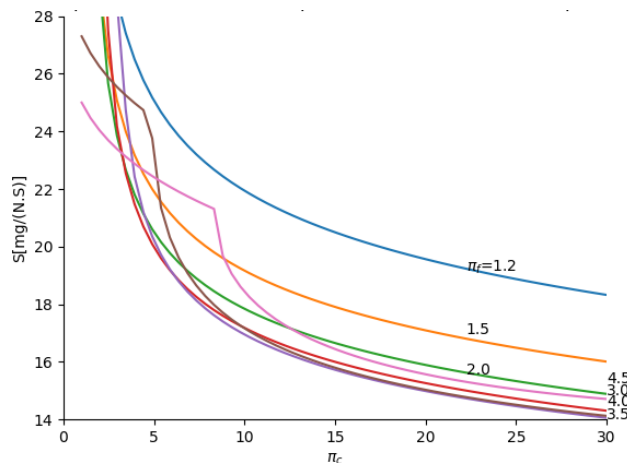


Figure 93 HBPTFE Ideal π_f vs π_c for $\alpha = 5, M_0 = 0.9$: Thrust-Specific Fuel Consumption from GTA

From the Figure 92 and 93, it can be seen that the increasing of fan pressure ratio and variation of compressor pressure ratio will give a thrust-specific fuel consumption decreases respectively.

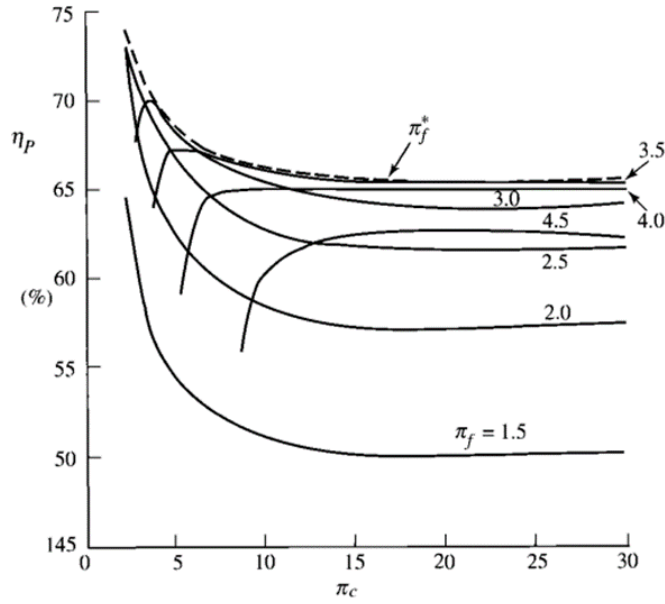


Figure 94 HBPTFE Ideal π_f vs π_c for $\alpha = 5, M_0 = 0.9$: propulsive efficiency [8]

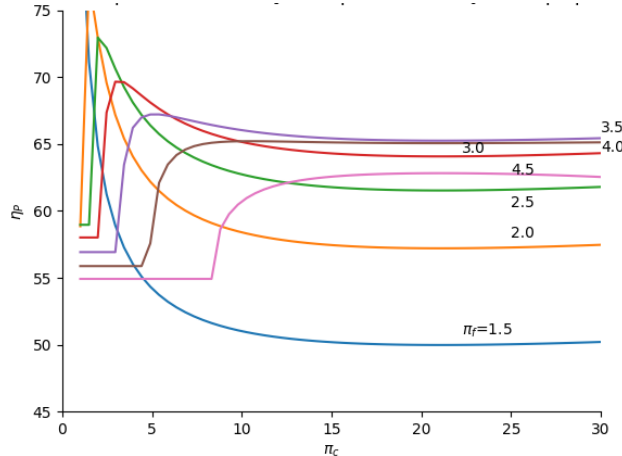


Figure 95 HBPTFE Ideal π_f vs π_c for $\alpha = 5, M_0 = 0.9$: propulsive efficiency from GTA

From the Figure 94 and 95, it can be seen that the increasing of fan pressure ratio and variation of compressor pressure ratio will give propulsive efficiency increases with fan pressure ratio until a value of 3.5 and then decreases. There is a fan pressure ratio giving maximum propulsive efficiency. Propulsive efficiency is essentially constant for values of the compressor pressure ratio above 15.

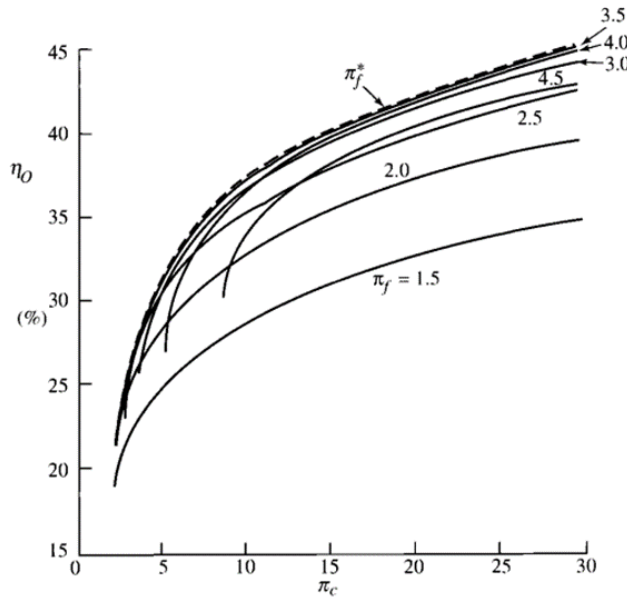


Figure 96 HBPTFE Ideal π_f vs π_c for $\alpha=5, M_0 = 0.9$: overall efficiency [8]

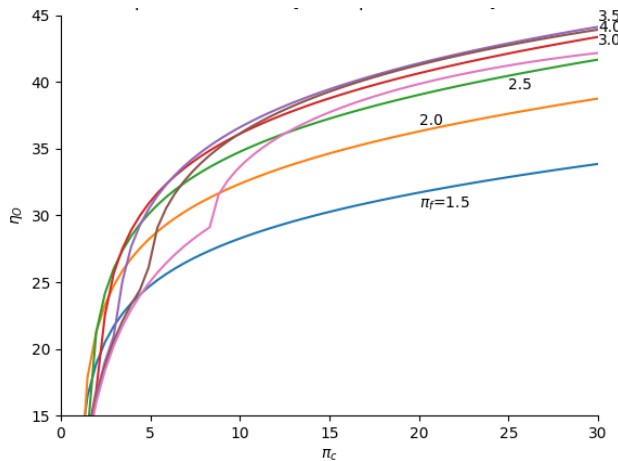


Figure 97 HBPTFE Ideal π_f vs π_c for $\alpha=5, M_0 = 0.9$: overall efficiency from GTA

From the Figure 96 and 97, it can be seen that the overall efficiency increases with compressor pressure ratio and increases with fan pressure ratio until a value of 3.5 and then decreases. There is a fan pressure ratio giving maximum overall efficiency.

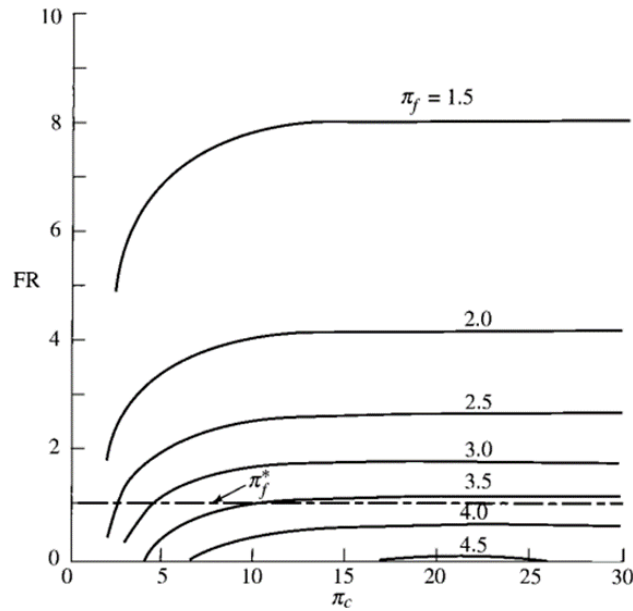


Figure 98 HBPTFE Ideal π_f vs π_c for $\alpha = 5, M_0 = 0.9$: Thrust ratio [8]

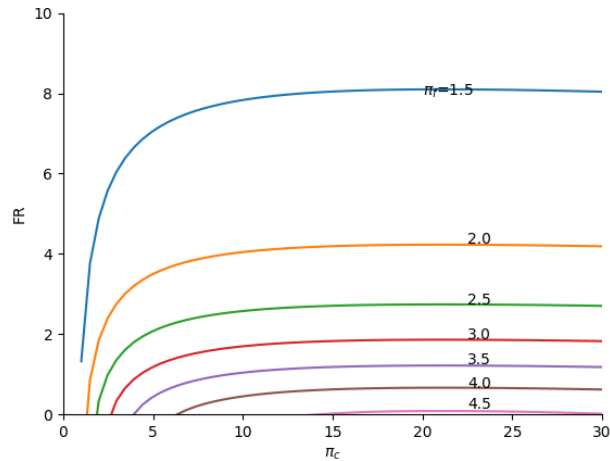


Figure 99 HBPTFE Ideal π_f vs π_c for $\alpha = 5, M_0 = 0.9$: Thrust ratio from GTA

From the Figure 98 and 99, it can be seen that the thrust ratio decreases with increasing fan pressure ratio and varies very little with compressor pressure ratio.

Variation of bypass ratio in comparison to fan pressure ratio with constant compressor pressure ratio of 24 and flight Mach number of 0.9,

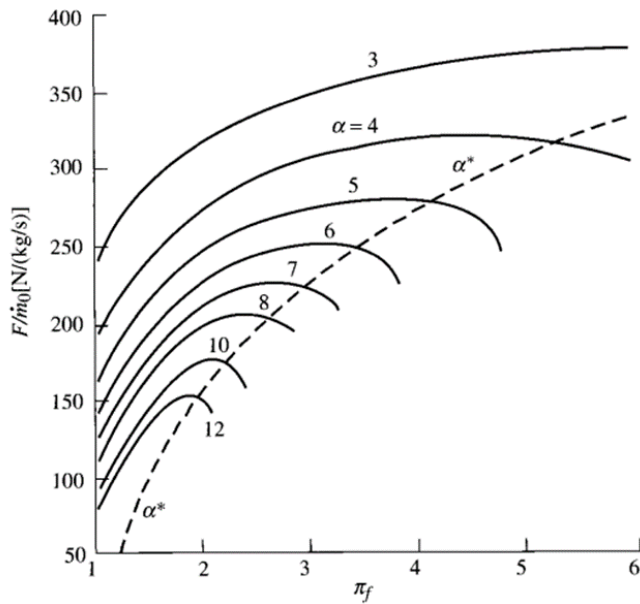


Figure 100 HBPTFE Ideal α vs π_f for $\pi_c = 24, M_0 = 0.9$: Specific Thrust [8]

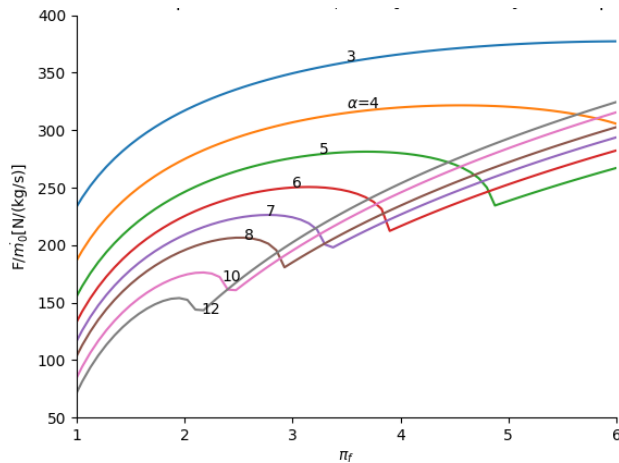


Figure 101 HBPTFE Ideal α vs π_f for $\pi_c = 24, M_0 = 0.9$: Specific Thrust from GTA

From the Figure 100 and 101, it can be seen that the increasing of bypass ratio and variation fan pressure ratio will give an increasing the specific thrust decrease respectively.

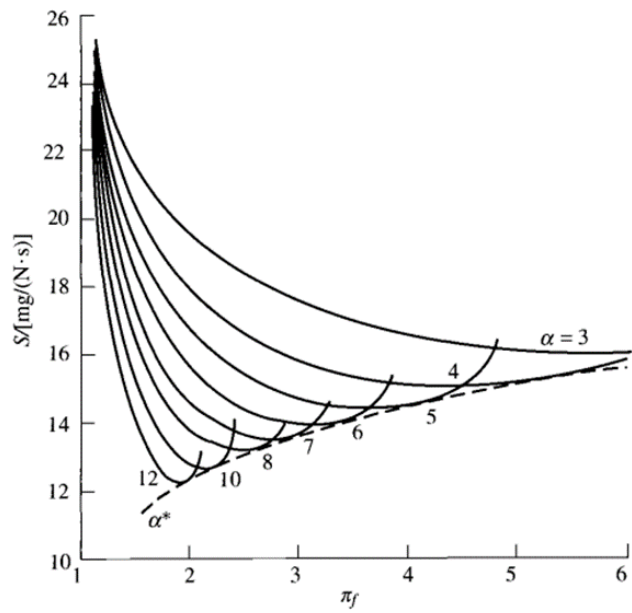


Figure 102 HBPTFE Ideal α vs π_f for $\pi_c = 24, M_0 = 0.9$: Thrust-Specific Fuel Consumption [8]

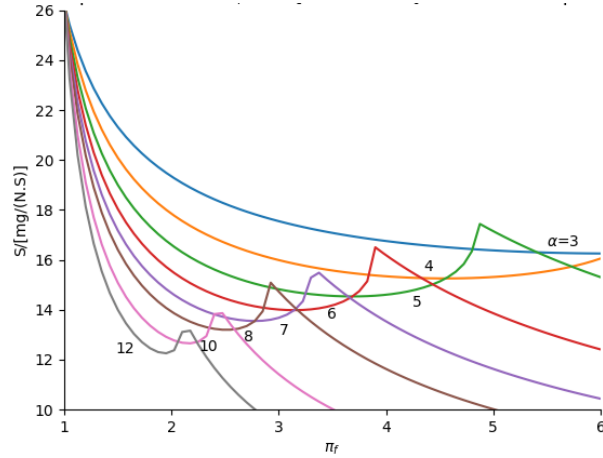


Figure 103 HBPTFE Ideal α vs π_f for $\pi_c = 24, M_0 = 0.9$: Thrust-Specific Fuel Consumption from GTA

From the Figure 102 and 103, it can be seen that the increasing of fan pressure ratio and variation of bypass ratio will give a thrust-specific fuel consumption decreases respectively.

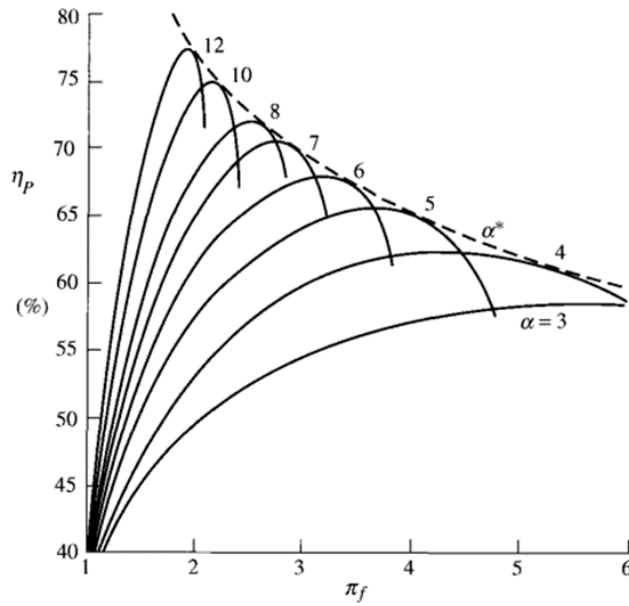


Figure 104 HBPTFE Ideal α vs π_f for $\pi_c = 24, M_0 = 0.9$: propulsive efficiency [8]

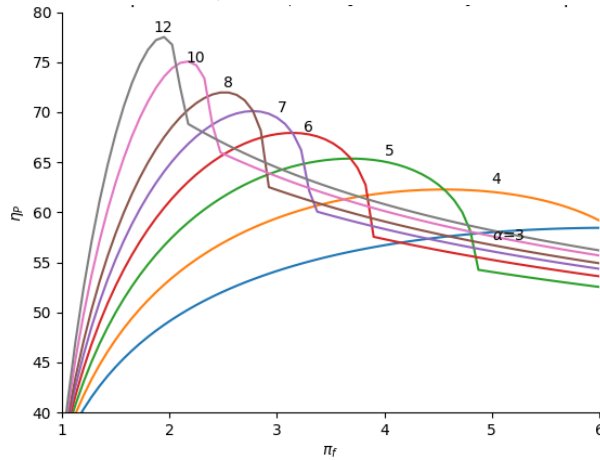


Figure 105 HBPTFE Ideal α vs π_f for $\pi_c = 24, M_0 = 0.9$: propulsive efficiency from GTA

From the Figure 104 and 105, it can be seen that the increasing of fan pressure ratio and variation of bypass ratio will give increasing a propulsive efficiency decreases respectively.

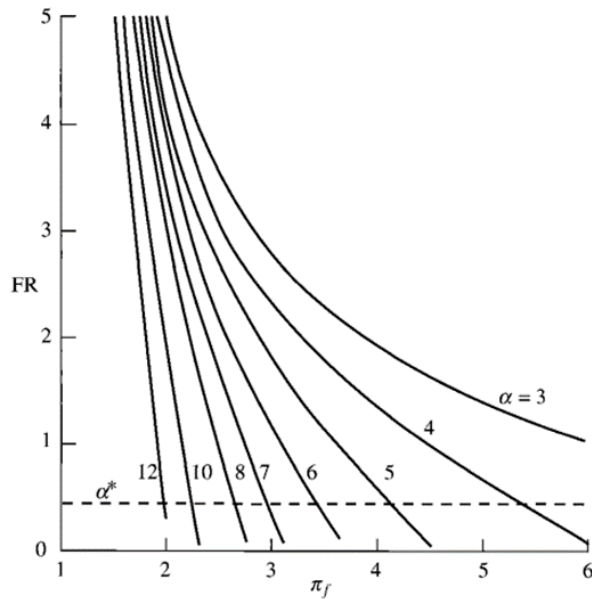


Figure 106 HBPTFE Ideal α vs π_f for $\pi_c = 24, M_0 = 0.9$: Thrust ratio [8]

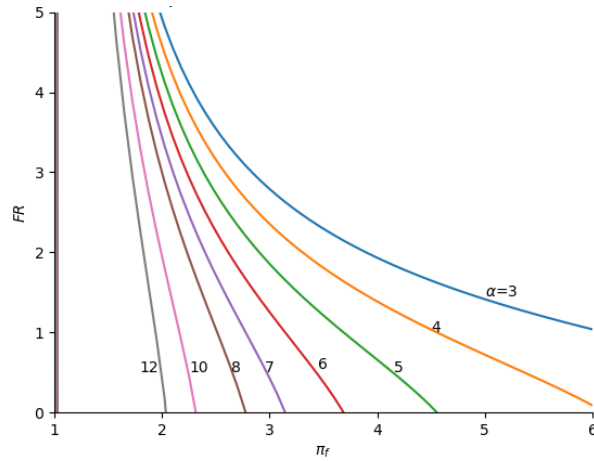


Figure 107 HBPTFE Ideal α vs π_f for $\pi_c = 24, M_0 = 0.9$: Thrust ratio from GTA

From the Figure 106 and 107, it can be seen that the increasing of fixed bypass ratio and variation of fan pressure ratio will give decreasing a thrust ratio respectively.

Variation of fan pressure ratio in comparison to bypass ratio with constant compressor pressure ratio of 24 and flight Mach number of 0.9,

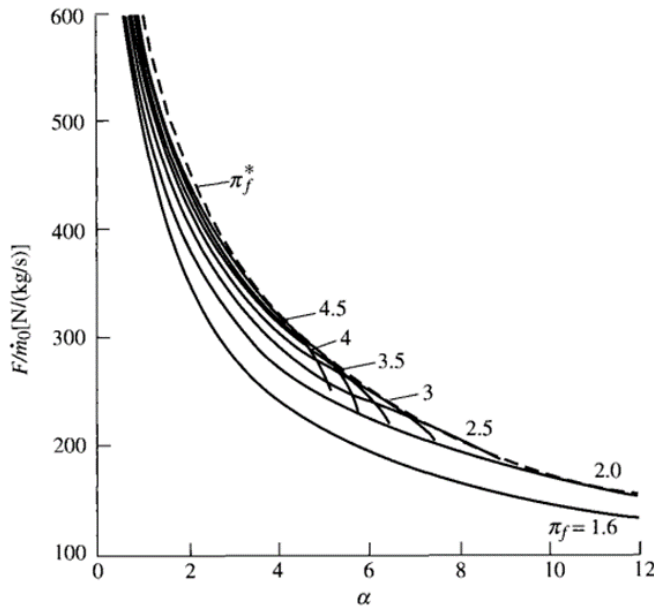


Figure 108 HBPTFE Ideal π_f vs α for $\pi_c = 24, M_0 = 0.9$: Specific Thrust [8]

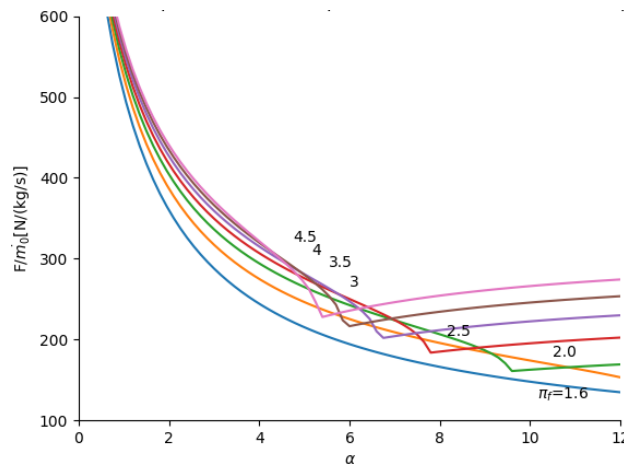


Figure 109 HBPTFE Ideal π_f vs α for $\pi_c = 24, M_0 = 0.9$: Specific Thrust from GTA

From the Figure 108 and 109, it can be seen that the increasing of fixed fan pressure ratio and variation of bypass ratio will give the decreasing trend in specific thrust that is characteristic of turbofan engines.

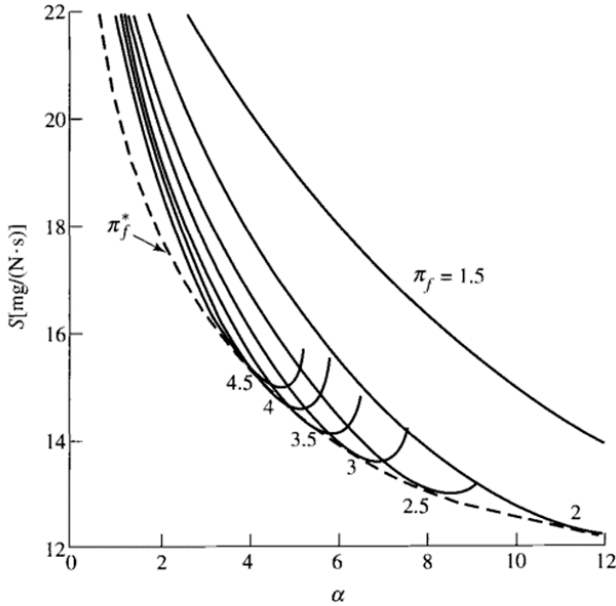


Figure 110 HBPTFE Ideal π_f vs α for $\pi_c = 24$, $M_0 = 0.9$: Thrust-Specific Fuel Consumption [8]

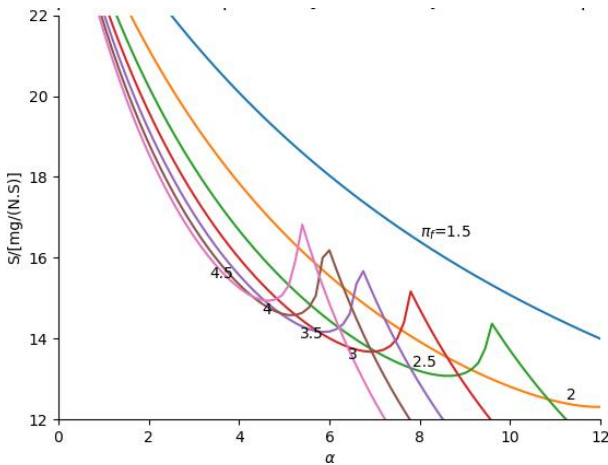


Figure 111 HBPTFE Ideal π_f vs α for $\pi_c = 24$, $M_0 = 0.9$: Thrust-Specific Fuel Consumption from GTA

From the Figure 110 and 111, it can be seen that the increasing of fixed fan pressure ratio and variation of bypass ratio will give the decreasing trend in Thrust Specific Fuel Consumption there is an optimum bypass ratio for each fan pressure ratio.

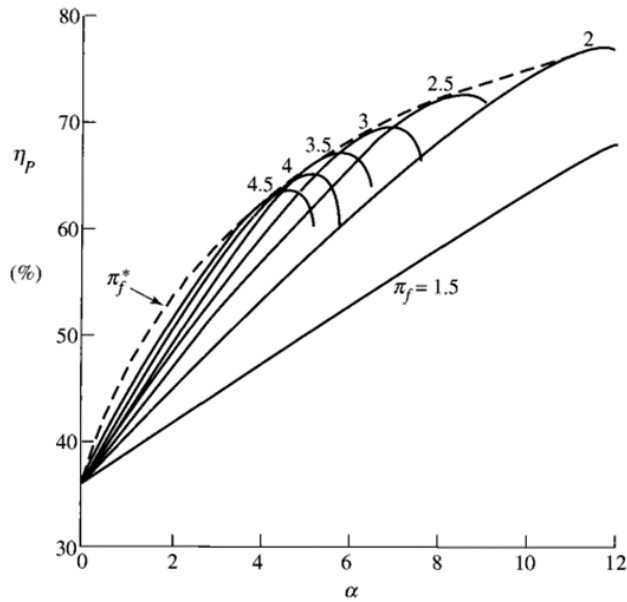


Figure 112 HBPTFE Ideal π_f vs α for $\pi_c = 24, M_0 = 0.9$: propulsive efficiency [8]

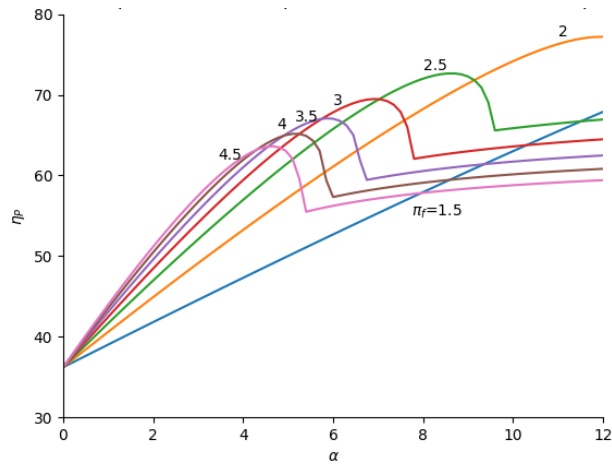


Figure 113 HBPTFE Ideal π_f vs α for $\pi_c = 24, M_0 = 0.9$: propulsive efficiency from GTA

From the Figure 112 and 113, it can be seen that the increasing of fixed fan pressure ratio and variation of bypass ratio will give the increasing trend in propulsive efficiency. there is an optimum bypass ratio for each fan pressure ratio that will maximize propulsive efficiency.

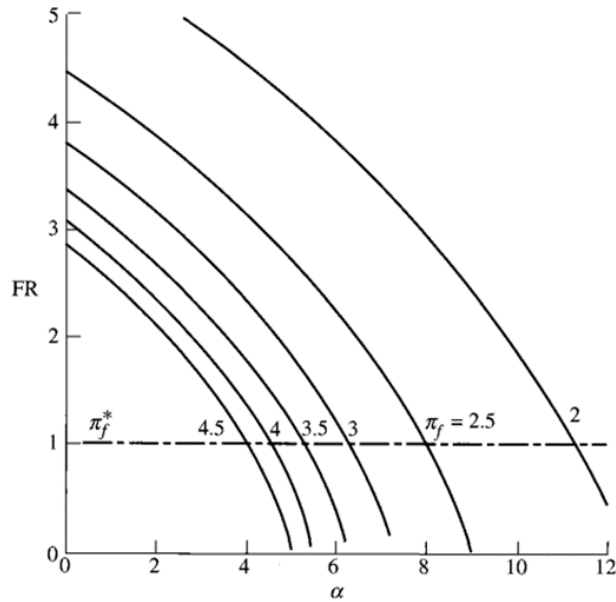


Figure 114 HBPTFE Ideal π_f vs α for $\pi_c = 24$, $M_0 = 0.9$: Thrust ratio [8]

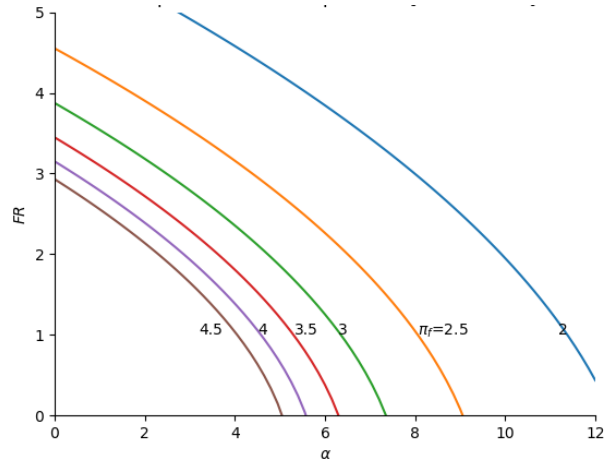


Figure 115 HBPTFE Ideal π_f vs α for $\pi_c = 24$, $M_0 = 0.9$: Thrust ratio from GTA

From the Figure 114 and 115, it can be seen that the increasing of fixed fan pressure ratio and variation of bypass ratio will give the decreasing trend in thrust ratio respectively.

Case study 8: High Bypass Ratio Turbofan Engine – Real Turbofan

1. Input section

From the reference Mattingly [8],

$$\begin{aligned}
 M_0 &= 0.9, \pi_c = 24, T_0 = 216.7^\circ K, \gamma_c = 1.4, \\
 c_{pc} &= 1.004 \text{ kJ / (kg} \cdot ^\circ \text{K}), \gamma_t = 1.35, c_{pt} = 1.096 \text{ kJ / (kg} \cdot ^\circ \text{K}), \\
 h_{PR} &= 42,800 \text{ kJ / kg}, \pi_{dmax} = 0.98, \pi_b = 0.98, \pi_{fn} = 0.98, \\
 \pi_n &= 0.98, e_c = 0.90, e_t = 0.91, e_f = 0.88, \eta_b = 0.99, \\
 \eta_m &= 0.98, P_0 / P_9 = 1, T_{t4} = 3000^\circ R, P_0 / P_9 = 1, P_0 / P_{19} = 1
 \end{aligned}$$

2. Results comparison

Variation of bypass ratio in comparison to compressor pressure ratio with constant fan pressure ratio of 2 and flight Mach number of 0.9,

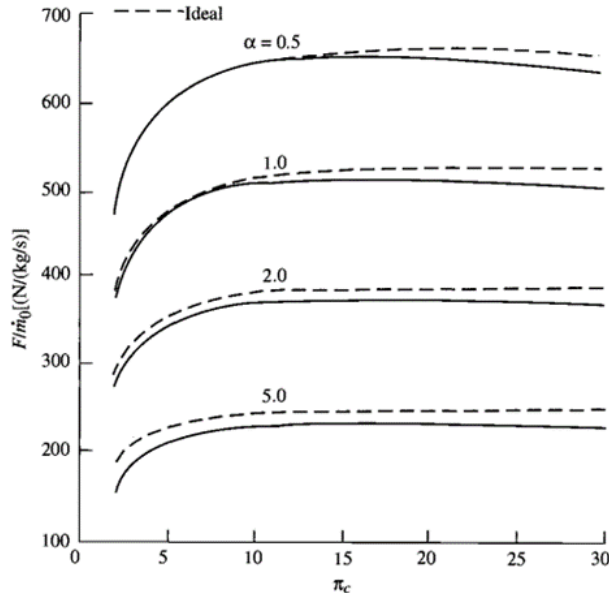


Figure 116 HBPTFE Ideal α vs π_c for $\pi_f = 2, M_0 = 0.9$: Specific Thrust [8]

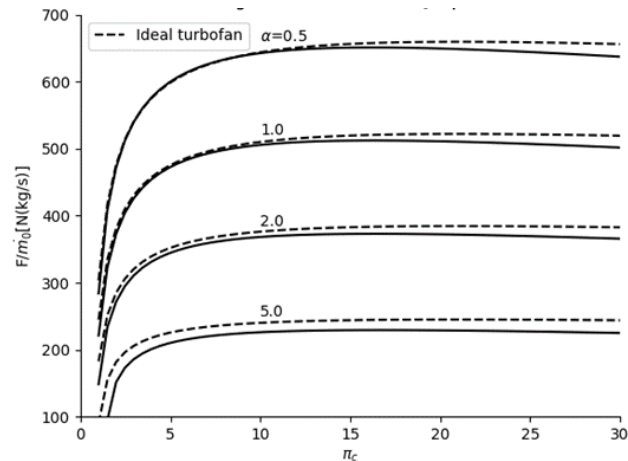


Figure 117 HBPTFE Ideal α vs π_c for $\pi_f = 2, M_0 = 0.9$: Specific Thrust from GTA

From the Figure 116 and 117, it can be seen that the influences of compressor pressure ratio and bypass ratio are taking on the engine performance. As the bypass ratio increases, the difference in specific thrust between the engine cycle with losses and the "ideal" engine cycle increases.

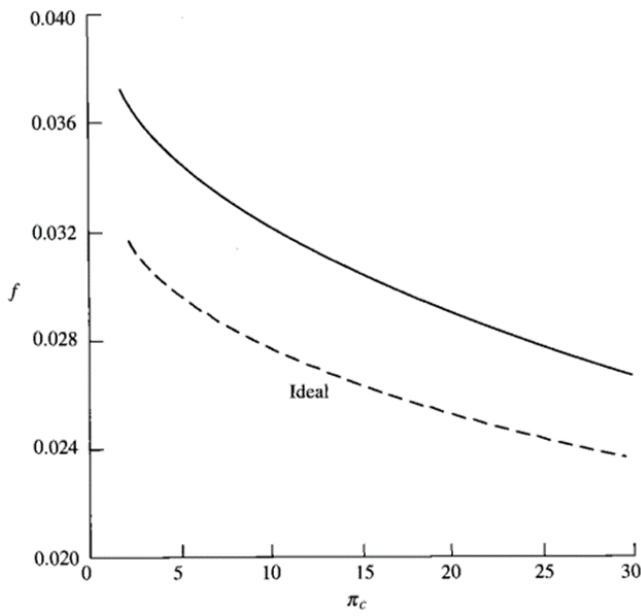


Figure 118 HBPTFE Ideal α vs π_c for $\pi_f = 2, M_0 = 0.9$: fuel/air ratio [8]

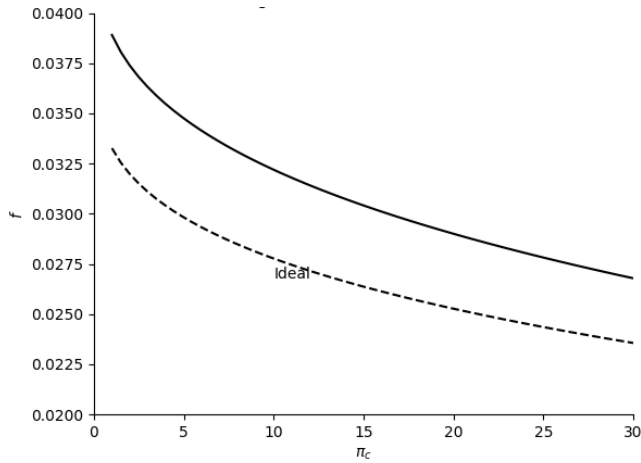


Figure 119 HBPTFE Ideal α vs π_c for $\pi_f = 2, M_0 = 0.9$: fuel/air ratio from GTA

From the Figure 118 and 119, it can be seen that the increasing bypass ratio and variation of compressor pressure ratio will give the decreasing trend in fuel/air ratio respectively and higher than the ideal engine cycle.

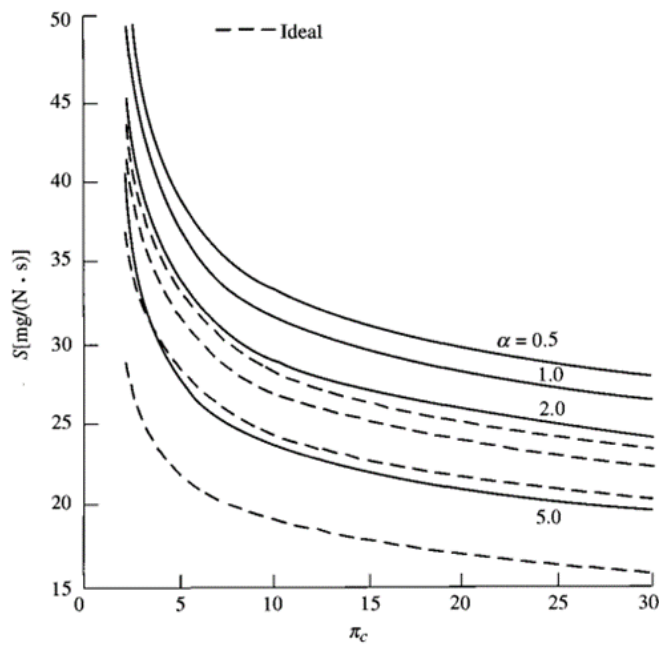


Figure 120 HBPTFE Ideal α vs π_c for $\pi_f = 2, M_0 = 0.9$: Thrust-Specific Fuel Consumption [8]

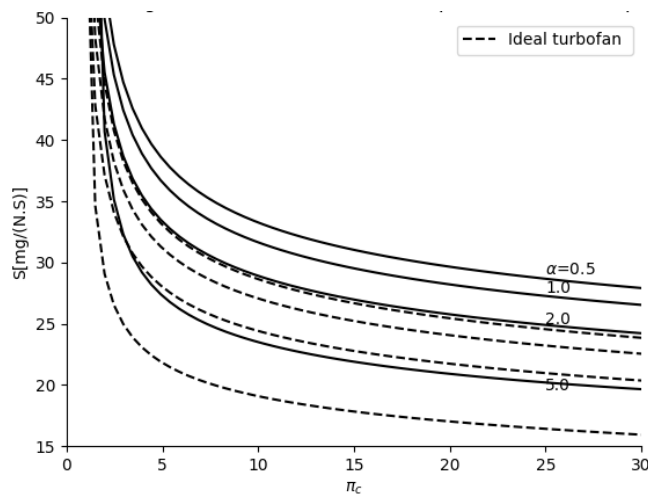


Figure 121 HBPTFE Ideal α vs π_c for $\pi_f = 2, M_0 = 0.9$: Thrust-Specific Fuel Consumption from GTA

From the Figure 120 and 121, it can be seen that the thrust specific fuel consumption for the two models is due to the much higher "fuel/air" ratio for the "real" engine.

Variation of bypass ratio in comparison to flight Mach number with constant fan pressure ratio of 2 and compressor pressure ratio of 24,

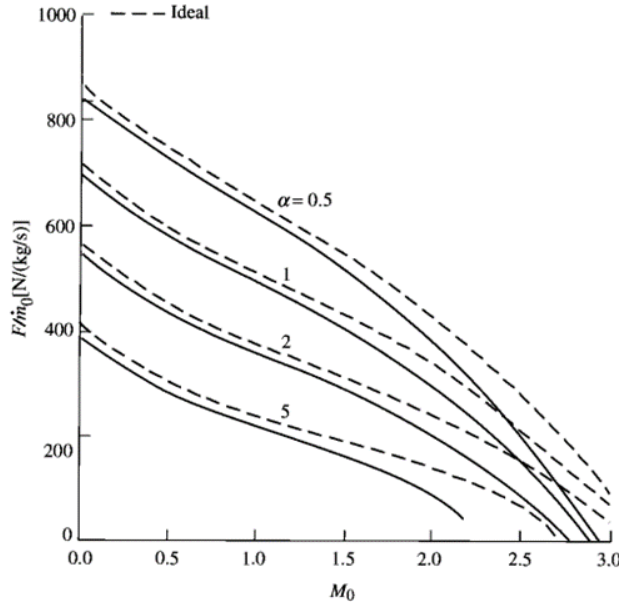


Figure 122 HBPTFE Ideal α vs M_0 for $\pi_f = 2, \pi_c = 24$: Specific Thrust [8]

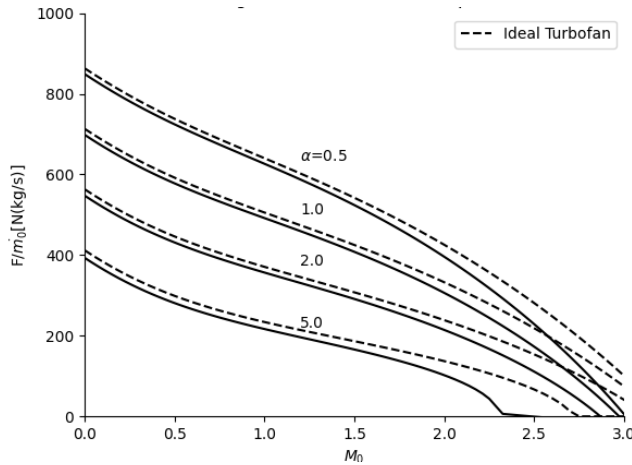


Figure 123 HBPTFE Ideal α vs M_0 for $\pi_f = 2, \pi_c = 24$: Specific Thrust from GTA

From the Figure 122 and 123, it can be seen that the engine's specific thrust is reduced more than that of the ideal engine at high Mach number because of the increasing inlet total pressure loss. The limiting Mach number for the economical operation of a turbofan engine with a specific bypass ratio is much lower for the engine with losses than for the ideal engine.

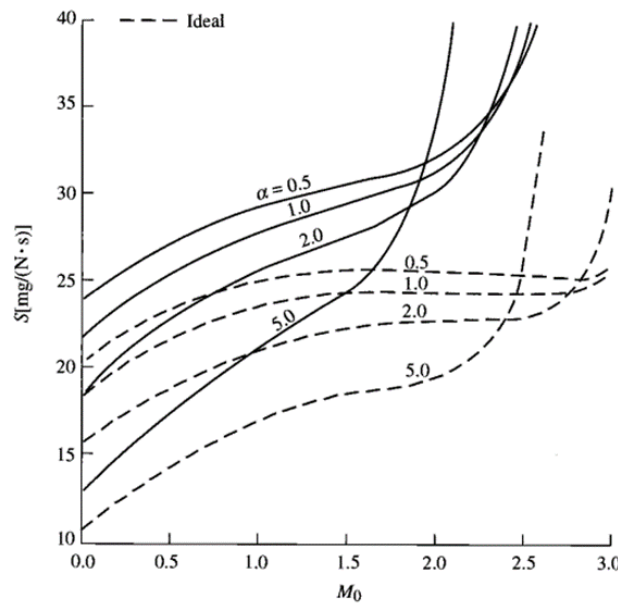


Figure 124 HBPTFE Ideal α vs M_0 for $\pi_f = 2$, $\pi_c = 24$: Thrust-Specific Fuel Consumption [8]

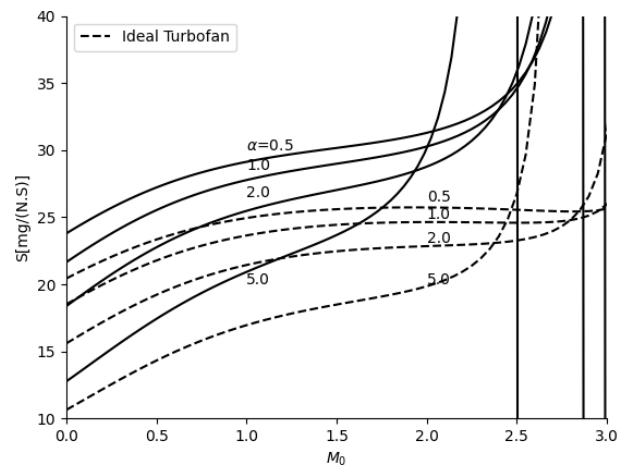


Figure 125 HBPTFE Ideal α vs M_0 for $\pi_f = 2$, $\pi_c = 24$: Thrust-Specific Fuel Consumption from GTA

From the Figure 124 and 125, it can be seen that the increasing bypass ratio and variation of flight Mach number will give the real engine's thrust specific fuel consumption is increase more than that of the ideal engine at high Mach number.

4.2 Case study and validation with AEDsys (ONX)

4.2.1 Single Point Calculation

Single point calculation comparison between GTA and ONX for validation purpose is conducted and shown in the following pages.

The chosen case is the subsonic flight for typical commercial airliners at 10,000 m. It is conducted in SI unit system to compare the result between GTA and ONX, the parameters tables for each case are introduced as well as the results. The inputs parameters are adopted from typical airliners flight except for some specific parameters that are variated for each case.

The input table for single point calculation for this case is presented in table 6 with the parameter comparison between three engines, and their results are presented respectively.

SSTJE = single spool turbojet engine, DSTEJE = double spool turbojet engine,
HBPTFE = high bypass ratio turbofan engine.

Table 6 Input parameters subsonic flight Single point calculation GTA

Parameter, Unit: SI	SSTJE	DSTJE	HBPTFE
\dot{m} (kg/s)	100	100	100
M_0	0.8	0.8	0.8
π_c	24	24	24
α	-	-	5
π_f	-	-	2
h (m)	10000	10000	10000
$g_c ((kg * m) / (N * s^2))$	1	1	1
T_{t4} (K)	1666.67	1666.67	1666.67
γ	1.4	1.4	1.4
c_p ($kJ/(kg * K)$)	1.004	1.004	1.004
h_{PR} (kJ/kg)	42800	42800	42800
T_{t7} (K)	2222.22	2222.22	-
γ_c	1.4	1.4	1.4
c_{pc} ($kJ/(kg * K)$)	1.004	1.004	1.004
γ_t	1.35	1.35	1.35
c_{pt} ($kJ/(kg * K)$)	1.0969	1.0969	1.0969
$\pi_{d_{max}}$	0.98	0.98	0.98
π_b	0.98	0.98	0.98
π_n	0.98	0.98	0.98
π_{fn}	-	-	0.98
π_t	-	-	0.89
e_c	0.92	0.92	0.92
e_f	-	-	0.88
e_t	0.91	0.91	0.91
η_b	0.99	0.99	0.99
η_m	0.98	0.98	0.98
η_{cL}	-	0.8755	-
η_{cH}	-	0.8791	-
P_0/P_9	1	1	1
P_0/P_{19}	-	-	1
γ_{AB}	1.3	1.3	-
c_{pAB} ($kJ/(kg * K)$)	1.24	1.24	-
π_{AB}	0.98	0.98	-
η_{AB}	0.96	0.96	-
P_0 (kPa)	-	101.33	-
π_{tH}	-	0.5466	-
π_{tL}	-	0.6127	-

As mentioned earlier in the input section, some parameters for single point calculation are adopted from the variation calculation section. And as the example case is subsonic flight the Mach number is less than one with the optimum compressor pressure ratio for subsonic flight equal to 24.

```
#####
Results for Real Single Spool Turbojet Engine (Single Point Calculation)

Rc_renmspSSTJE:0.28686          Taut_renmspSSTJE:0.76915
Rt_renmspSSTJE:0.28438          Pit_renmspSSTJE:0.32873
A0_renmspSSTJE:299.363          Nt_renmspSSTJE:0.92134
V0_renmspSSTJE:239.49           Pt9P_renmspSSTJE:11.213
M02_renmspSSTJE:0.64            M9_renmspSSTJE:2.231
Taur_renmspSSTJE:1.128          T9T0_renmspSSTJE:3.07
Pir_renmspSSTJE:1.524           V9A0_renmspSSTJE:3.822
nr_renmspSSTJE:0.991            Tsc_renmspSSTJE:937.135
Pid_renmspSSTJE:0.971           Thrust_renmspSSTJE:93713.5
Tauram_renmspSSTJE:8.16          S_renmspSSTJE:30.273
Tauc_renmspSSTJE:2.683           NT_renmspSSTJE:53.074
Nc_renmspSSTJE:0.879           NP_renmspSSTJE:34.826
f_renmspSSTJE:0.02837          NO_renmspSSTJE:18.484
```

Figure 126 Result single spool turbojet engine single point calculation subsonic flight from GTA

```
On-Design Calcs (ONX V6.102)          Date: 15-Jun-22 2:59:43 PM
File: C:\Users\GOT\Desktop\Projekt GasTurb\Python\project\outputs\Grap
      Turbojet Engine - Single Spool
      using Modified Specific Heat (MSH) Gas Model
***** Input Data *****               *****
Alt (m) = 10000                      Pi c = 24.000
T0 (K) = 223.25                      Pi d (max) = 0.980
P0 (kPa) = 26.500                     Pi b = 0.980
Density (kg/m^3) = .4137928          Pi n = 0.980
Efficiency
Cp c = 1.0040 kJ/kg-K               Burner = 0.990
Cp t = 1.0969 kJ/kg-K                Mechanical = 0.980
Gamma c = 1.4000
Gamma t = 1.3500
Tt4 max = 1666.7 K                  Compressor = 0.920 (ec)
h - fuel = 42800 kJ/kg              Turbine = 0.910 (et)
CTO = 0.0000                         Pwr Mech Eff = 0.980
Cooling Air #1 = 0.000 %
Cooling Air #2 = 0.000 %
***** RESULTS *****                 *****
Tau r (Tt0/T0) = 1.128
Pi r (Pt0/P0) = 1.524
Pi d (Pt2/Pt0) = 0.980
TauL = 8.156
PTO = 0.000 KW
Pi c (Pt3/Pt2) = 24.00
Tau c (Tt3/Tt2) = 2.6831
Eta c = 0.8790
Pi t (Pt5/Pt4) = 0.3295
Eta t = 0.9213
Tau t (Tt5/Tt4) = 0.7695
Pt9/P9 = 11.344
M9 = 2.2386
f = 0.03067
f o = 0.03067
F/mdot = 942.465 N/(kg/s)
S = 32.5432 (g/s)/kN
T9/T0 = 3.0608
V9/V0 = 4.787
M9/M0 = 2.7982
A9/A0 = 0.6534
A9/A8 = 2.1964
Thrust = 94246 N
Thermal Eff = 63.55 %
Propulsive Eff = 34.79 %
Overall Eff = 22.11 %
```

Figure 127 Result single spool turbojet engine single point calculation subsonic flight from ONX

For single-spool turbojet engine single-point calculation results from GTA are as shown above, the specific thrust (T_{sc}), thrust specific fuel consumption (S), and (propulsive (N_p), thermal (N_T), overall (N_O)) efficiency, etc. values are close to ONX but there are still discrepancies. Due to GTA uses constant specific heat (CSH) model and the ONX program is using a modified specific heat (MSH) model which resulted in the different of both programs. In CSH, each component is modeled as perfect gases with constant specific heats, but MSH uses CSH to calculate all properties except the fuel used. In addition, MSH is also using input exit total temperatures (Tt4 and T,7) and C₁₂H₂₃ as the representative fuel to give the better estimates of the fuel used.

```

#####
Results for Real Double Spool Turbojet Engine (Single Point Calculation)

Picrefsp:24.0
PicLrefsp:24.0
PicHrefsp:24.0
Rc_renmspDSTJE:0.2868571428571428
Rt_renmspDSTJE:0.2843814814814815
A0_renmspDSTJE:299.3610529110291
V0_renmspDSTJE:239.4888423288233
M02_renmspDSTJE:0.6400000000000001
Taur_renmspDSTJE:1.1280000000000001
Taueref_renmspDSTJE:1.1280000000000001
Tauclref_renmspDSTJE:2.6897738283623456
Taucl_renmspDSTJE:3.0457476304838975

PicL_renmspDSTJE:36.3235072100892345
Tauchref_renmspDSTJE:2.6828540401902328
Tauch_renmspDSTJE:2.799251095294907
PicH_renmspDSTJE:27.649224280200237
Tauram_renmspDSTJE:8.159922813786308
f_renmspDSTJE:-0.008052358080681632
mdot0_renmspDSTJE:148.31104903680642
Pt9P_renmspDSTJE:478.4356798225575
M9_renmspDSTJE:4.7520630915222
T9T0_renmspDSTJE:2.0110417629479467
V9A0_renmspDSTJE:6.58890781105354
Tsc_renmspDSTJE:1717.090564138637
Thrust_renmspDSTJE:171709.0564138637
S_renmspDSTJE:-4.689536037792523
NT_renmspDSTJE:-551.5776104413352
NP_renmspDSTJE:21.632415150871186
NO_renmspDSTJE:-119.31955856992465

```

Figure 128 Result double spool turbojet engine single point calculation subsonic flight from GTA

```

On-Design Calcs (ONX V6.102) Date: 15-Jun-22 3:26:11 PM
File: C:\Users\GOT\Desktop\Projekt GasTurb\Python\project\outputs\Grap
Turbojet Engine - Dual Spool
using Modified Specific Heat (MSH) Gas Model
***** Input Data *****
Mach No = 0.800
Alt (m) = 10000 Pi cL = 1.000
T0 (K) = 223.25 Pi d (max) = 0.980
P0 (kPa) = 26.500 Pi b = 0.980
Density = .4137928 Pi n = 0.980
(kg/m^3)
Cp c = 1.0040 kJ/kg-K Efficiency
Cp t = 1.0969 kJ/kg-K Burner = 0.990
Gamma c = 1.4000 Mech Hi Pr = 0.879
Gamma t = 1.3500 Mech Lo Pr = 0.876
Tt4 max = 1666.7 K LP Comp = 0.920 (eCL)
h - fuel = 42800 kJ/kg HP Comp = 0.920 (eCH)
CTO Low = 0.0000 HP Turbine = 0.910 (eTH)
CTO High = 0.0000 LP Turbine = 0.910 (eTL)
Cooling Air #1 = 0.000 %
Cooling Air #2 = 0.000 %
P0/P9 = 1.0000 Pwr Mech Eff L = 0.980
P0/P9 = 1.0000 Pwr Mech Eff H = 0.980
Bleed Air = 0.000 %
*****
RESULTS *****
Tau r (Tt0/T0) = 1.128 a0 (m/sec) = 299.5
Pi r (Pt0/P0) = 1.524 V0 (m/sec) = 239.6
Pi d (Pt2/Pt0) = 0.980 Mass Flow = 100.0 kg/sec
TauL = 8.156 Area Zero = 1.009 m^2
PTO Low = 0.00 KW Area Zero* = 0.971 m^2
PTO High = 0.00 KW
Pi c (Pt3/Pt2) = 24.00 Tau ml (Tt41/Tt4) = 1.0000
Pi cL (Pt25/Pt2) = 1.0000 Tau m2 (Tt45/Tt44) = 1.0000
Tau cL (Tt25/Tt2) = 1.0000 Eta cL = 1.0000
Pi cH (Pt3/Pt25) = 24.00 Eta cH = 0.8790
Tau cH (Tt3/Tt25) = 2.6831 Eta tH = 0.9228
Pi tH (Pt45/Pt4) = 0.2841 Tau tL = 1.0000
Tau tH(Tt44/Tt41) = 0.7431 Eta tL = 1.0000
Pi tL (Pt5/Pt45) = 1.0000
Tau tL (Tt5/Tt45) = 1.0000 Pt9/P9 = 9.781 M9 = 2.1464
f = 0.03067
f o = 0.03067
F/mdot = 895.725 N/(kg/s)
S = 34.2413 (g/s)/kN
T9/T0 = 3.0714
V9/V0 = 4.597
M9/M0 = 2.6829
A9/A0 = 0.6826
A9/A8 = 2.0134
Thrust = 89572 N
Thermal Eff = 58.41 %
Propulsive Eff = 35.97 %
Overall Eff = 21.01 %

```

Figure 129 Result double spool turbojet engine single point calculation subsonic flight from ONX

For the double spool turbojet engine single point calculation, from the result, it can be observed that the result from GTA for prior parameters such as the τ_r , π_r , π_d etc. are the same or similar to that of ONX but when determining the desired result such as fuel/air ratio, specific thrust, thrust specific fuel consumption, the results obtained are not the same. Therefore, there is a need to recite the equation for double spool turbojet engine for later phase of calculation to obtain more accurate results.

```
#####
Results for Real High-Bypass Ratio Turbofan Engine (Single Point Calculation)

Rc_resphBPTFE:0.28686
Rt_resphBPTFE:0.28438
A0_resphBPTFE:299.363
V0_resphBPTFE:239.49
M02_resphBPTFE:0.64
TauR_resphBPTFE:1.128
Pir_resphBPTFE:1.524
Nr_resphBPTFE:1
Pid_resphBPTFE:0.98
Tauram_resphBPTFE:8.16
TauC_resphBPTFE:2.683
Nc_resphBPTFE:87.902
TauF_resphBPTFE:1.252
Nf_resphBPTFE:86.91
f_resphBPTFE:0.02837
TauT_resphBPTFE:0.596
Pit_resphBPTFE:0.11152

Nt_resphBPTFE:93.144
Pt9P9_resphBPTFE:30.638
M9_resphBPTFE:2.857
T9T0_resphBPTFE:1.833
V9A0_resphBPTFE:3.782
Pt19P19_resphBPTFE:2.927
M19_resphBPTFE:1.34
T19T0_resphBPTFE:1.039
V19A0_resphBPTFE:1.366
Tsc_resphBPTFE:295.336
Thrust_resphBPTFE:29533.6
S_resphBPTFE:16.01
Fr_resphBPTFE:5.458
NT_resphBPTFE:74.541
NP_resphBPTFE:46.888
NO_resphBPTFE:34.951
*****;*****;
```

Figure 130 Result high bypass ratio turbofan engine single point calculation subsonic flight from GTA

```
On-Design Calcs (ONX V6.102) Date: 16-Jun-22 10:44:32 AM
File: C:\Users\GOT\Desktop\Projekt GasTurb\Python\project\outputs\Graph\SPCC
Turbofan Engine with Two Exhausts & Conv. Nozzles
using Modified Specific Heat (MSH) Gas Model
***** Input Data *****
ie (kg/m^3)
Cp c = 1.0040 kJ/kg-K Burner = 0.990
Cp t = 1.0969 kJ/kg-K Mech Hi Pr = 0.980
Gamma c = 1.4000 Mech Lo Pr = 0.990
Gamma t = 1.3500 Fan/LP Comp = 0.880/0.920 (ef/ecL)
Tt4 max = 1666.7 K HP Comp = 0.920 (ecH)
h - fuel = 42800 kJ/kg HP Turbine = 0.910 (etH)
CTO Low = 0.0000 LP Turbine = 0.910 (etL)
CTO High = 0.0000 Pwr Mech Eff L = 0.980
Cooling Air #1 = 0.000 % Pwr Mech Eff H = 0.980
Cooling Air #2 = 0.000 % Bleed Air = 0.000 %
***** RESULTS *****
Tau r (Tt0/T0) = 1.128 a0 (m/sec) = 299.5
Pi r (Pt0/P0) = 1.524 V0 (m/sec) = 239.6
Pi d (Pt2/Pt0) = 0.980 Mass Flow = 100.0 kg/sec
TauL = 8.156 Area Zero = 1.009 m^2
PTO Low = 0.00 KW Area Zero* = 0.971 m^2
PTO High = 0.00 KW
Tau f (Tt13/Tt2) = 1.2524 Pt19/P0 = 2.988
Eta f = 0.8678 Tt19/T0 = 1.4127
Pt19/P19 = 1.8929 P0/P19 = 0.6465
M19 = 1.0000 V19/V0 = 1.3563
Pi c (Pt3/Pt2) = 24.00 Tau m1 (Tt41/Tt4) = 1.0000
Pi cL (Pt25/Pt2) = 2.000 Tau m2 (Tt45/Tt44) = 1.0000
Tau cL (Tt25/Tt2) = 1.2402 Eta cL = 0.9118
Pi cH (Pt3/Pt25) = 12.000
Tau ch (Tt3/Tt25) = 2.1635 Eta cH = 0.8887
Pi tH (Pt45/Pt4) = 0.3934 Eta tH = 0.9196
Tau tH (Tt44/Tt41) = 0.8024
Pi tL (Pt5/Pt45) = 0.2893 Eta tL = 0.9226
Tau tL (Tt5/Tt45) = 0.7463
P0/P9 = 0.4754
Pt9/P9 = 1.863 M9 = 1.0000
f = 0.03067
f o = 0.00511
F/mdot = 235.834 N/(kg/s)
S = 21.6755 (g/s)/kN
T9/T0 = 3.8047
V9/V0 = 2.384
M9/M0 = 1.250
A9/A0 = 0.1292
Thrust = 23583 N
Thermal Eff = 57.08 %
Propulsive Eff = 58.15 %
Overall Eff = 33.19 %
```

Figure 131 Result high bypass ratio turbofan engine single point calculation subsonic flight from ONX

For high bypass ratio turbofan engine single-point calculation results from GTA are as shown above, the specific thrust (T_{sc}), thrust specific fuel consumption (S), and (propulsive (N_p), thermal (N_T), overall (N_O)) efficiency, etc. values are close to ONX. But there are still discrepancies. Due to GTA uses the constant specific heat (CSH) model and the ONX program uses a modified specific heat (MSH) model which resulted in the different of both programs. In, CSH each component is modeled as perfect gases with constant specific heats, but MSH uses CSH to calculate all properties except the fuel used.

4.2.2 Variation Calculation

For the variation calculation comparison between GTA and ONX, the calculation is conducted and shown in the following pages.

The chosen case is the flight at sea level with the variation of flight Mach number and compressor pressure ratio. It is conducted in SI unit system to compare the result between GTA and ONX, the parameters tables for this case are introduced as well as the results. The inputs parameters are adopted from typical flight except for some specific parameters that are variated for this case.

From the results, the behaviour of each resultant parameter such as specific thrust, thrust specific fuel consumption, etc. is portrayed as well as the effect of the variation of flight Mach number, compressor pressure ratio can be observed.

The input table for variation calculation for this case is presented in Figure 132 with the parameter comparison between three engines, and their results are presented respectively.

SSTJE = single spool turbojet engine, DSTEJE = double spool turbojet engine,
HBPTFE = high bypass ratio turbofan engine.

Case 1: Altitude Variation

Case 1.1: Altitude at sea level

Parameter, Unit: SI	SSTJE	DSTJE	HBPTFE
$g_c ((kg * m)/(N * s^2))$	1	1	1
$h (m)$	0	0	0
$T_{t4} (K)$	1666.67	1666.67	1666.67
γ	1.4	1.4	1.4
$c_p (kJ/(kg * K))$	1.004	1.004	1.004
$h_{PR} (kJ/kg)$	42800	42800	42800
$T_{t7} (K)$	2222.22	2222.22	-
γ_c	1.4	1.4	1.4
$c_{pc} (kJ/(kg * K))$	1.004	1.004	1.004
γ_t	1.35	1.35	1.35
$c_{pt} (kJ/(kg * K))$	1.0969	1.0969	1.0969
$\pi_{d_{max}}$	0.98	0.98	0.98
π_b	0.98	0.98	0.98
π_n	0.98	0.98	0.98
π_{fn}	-	-	0.98
π_t	-	-	0.89
e_c	0.92	0.92	0.92
e_f	-	-	0.88
e_t	0.91	0.91	0.91
η_b	0.99	0.99	0.99
η_m	0.98	0.98	0.98
η_{cL}	-	0.8755	-
η_{cH}	-	0.8791	-
P_0/P_9	1	1	1
P_0/P_{19}	-	-	1
γ_{AB}	1.3	1.3	-
$c_{pAB} (kJ/(kg * K))$	1.24	1.24	-
π_{AB}	0.98	0.98	-
η_{AB}	0.96	0.96	-
$P_0 (kPa)$	-	101.33	-
π_{tH}	-	0.5466	-
π_{tL}	-	0.6127	-
$M_{0,fix}$	-	-	0.5
$\pi_{c,fix}$	-	-	10
α_{fix}	-	-	5
$\pi_{f,fix}$	-	-	2
M_0	0 – 3	0 – 3	0 – 3
Iteration step of M_0	0.5	0.5	0.5
π_c	1 – 40	1 – 40	1 – 40
Iteration step of π_c	1	1	1
α	-	-	0 – 40
Iteration step of α	-	-	0.5
π_f	-	-	0 – 40
Iteration step of π_f	-	-	0.5

Figure 132 Altitude variation calculation at sea level parameter input (SI)

Parameter, Unit: BE	SSTJE	DSTJE	HBPTFE
$g_c (ft/s^2)$	32.174	32.174	32.174
$h (ft)$	0	0	0
$T_{t4} (^{\circ}R)$	3000	3000	3000
γ	1.4	1.4	1.4
$c_p (Btu/(lbm * ^{\circ}R))$	0.24	0.24	0.24
$h_{PR} (Btu/lbm)$	18400	18400	18400
$T_{t7} (^{\circ}R)$	4000	4000	-
γ_c	1.4	1.4	1.4
$c_{pc} (Btu/(lbm * ^{\circ}R))$	0.24	0.24	0.24
γ_t	1.35	1.35	1.35
$c_{pt} (Btu/(lbm * ^{\circ}R))$	0.262	0.262	0.262
$\pi_{d_{max}}$	0.98	0.98	0.98
π_b	0.98	0.98	0.98
π_n	0.98	0.98	0.98
π_{fn}	-	-	0.98
π_t	-	-	0.89
e_c	0.92	0.92	0.92
e_f	-	-	0.88
e_t	0.91	0.91	0.91
η_b	0.99	0.99	0.99
η_m	0.98	0.98	0.98
η_{cL}	-	0.8755	-
η_{cH}	-	0.8791	-
P_0/P_9	1	1	1
P_0/P_{19}	-	-	1
γ_{AB}	1.3	1.3	-
$c_{pAB} (Btu/(lbm * ^{\circ}R))$	0.295	0.295	-
π_{AB}	0.98	0.98	-
η_{AB}	0.96	0.96	-
$P_0 (Psia)$	-	14.696	-
π_{tH}	-	0.5466	-
π_{tL}	-	0.6127	-
$M_{0,fix}$	-	-	0.5
$\pi_{c,fix}$	-	-	10
α_{fix}	-	-	5
$\pi_{f,fix}$	-	-	2
M_0	0 – 3	0 – 3	0 – 3
Iteration step of M_0	0.5	0.5	0.5
π_c	1 – 40	1 – 40	1 – 40
Iteration step of π_c	1	1	1
α	-	-	0 – 40
Iteration step of α	-	-	0.5
π_f	-	-	0 – 40
Iteration step of π_f	-	-	0.5

Figure 133 Altitude variation calculation at sea level parameter input (BE)

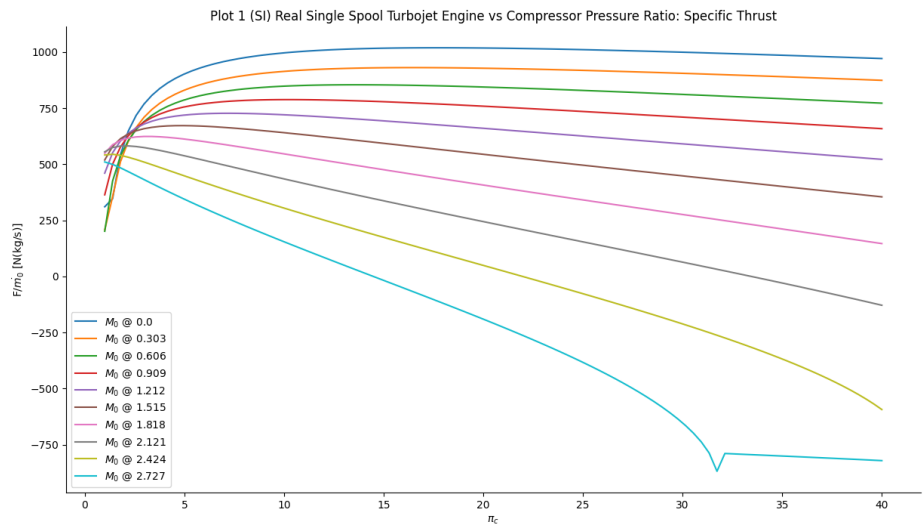


Figure 134 Altitude variation at sea level for Single Spool Turbojet Engine Specific Thrust plot from GTA

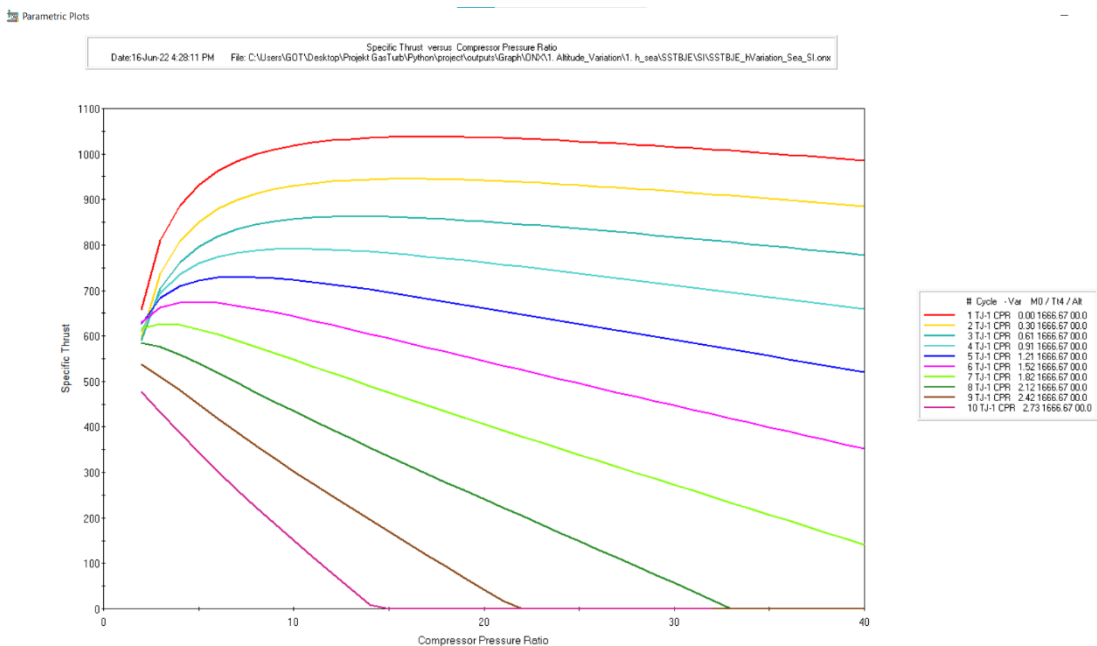


Figure 135 Altitude variation at sea level for Single Spool Turbojet Engine Specific Thrust plot from ONX

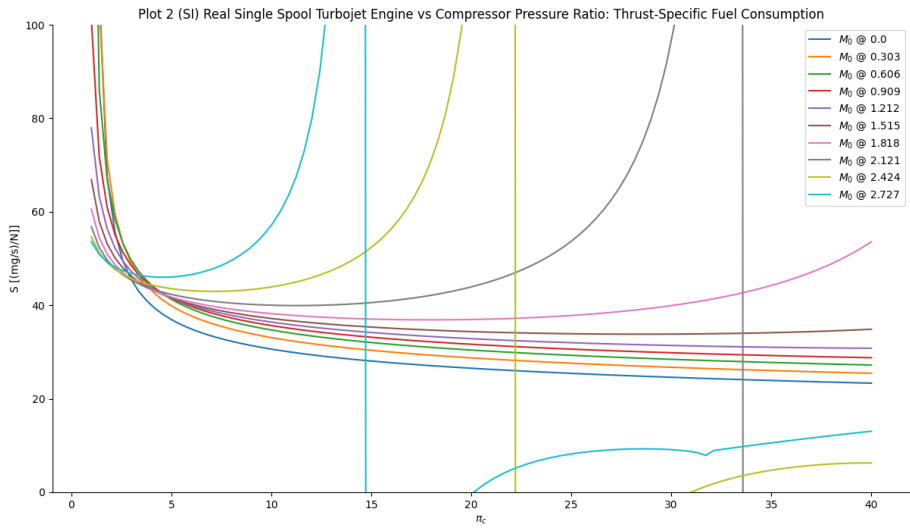


Figure 136 Altitude variation at sea level for Single Spool Turbojet Engine Thrust Specific Fuel Consumption plot from GTA

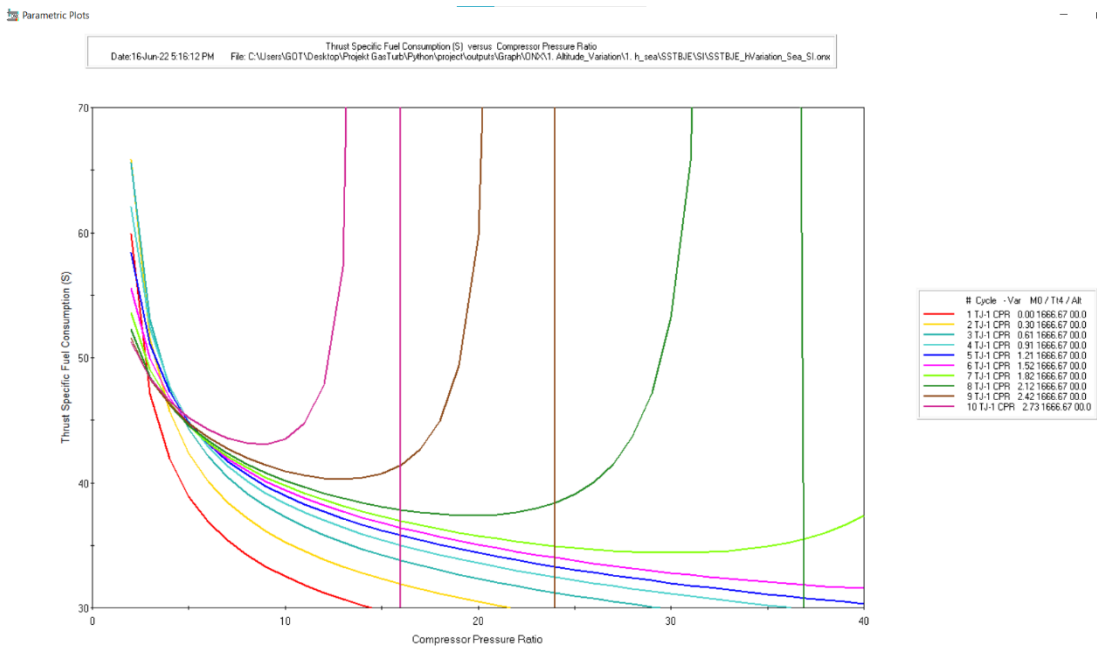


Figure 137 Altitude variation at sea level for Single Spool Turbojet Engine Thrust Specific Fuel Consumption plot from ONX

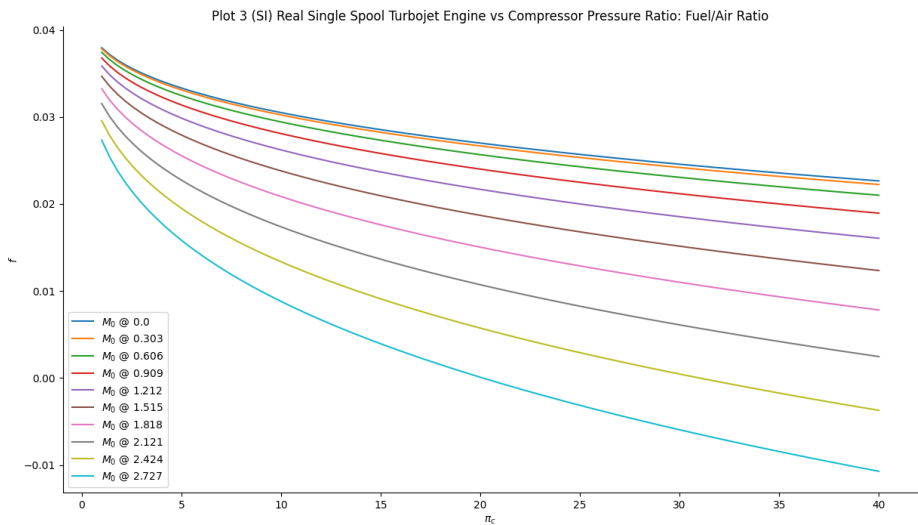


Figure 138 Altitude variation at sea level for Single Spool Turbojet Engine Fuel to Air Ratio plot from GTA

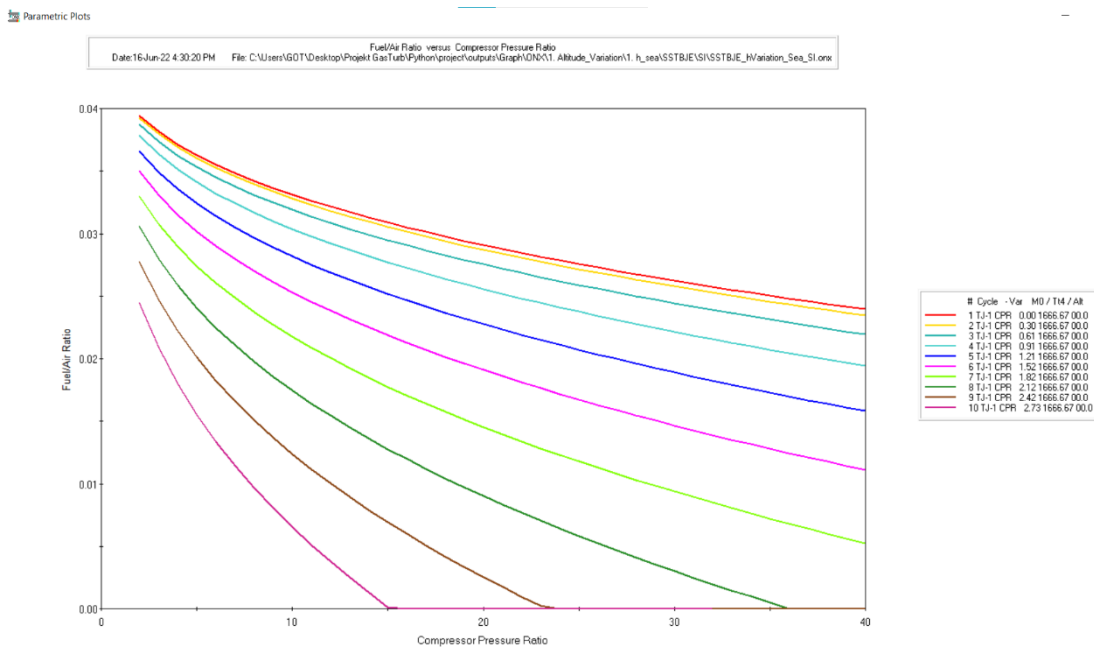


Figure 139 Altitude variation at sea level for Single Spool Turbojet Engine Fuel to Air Ratio plot from ONX

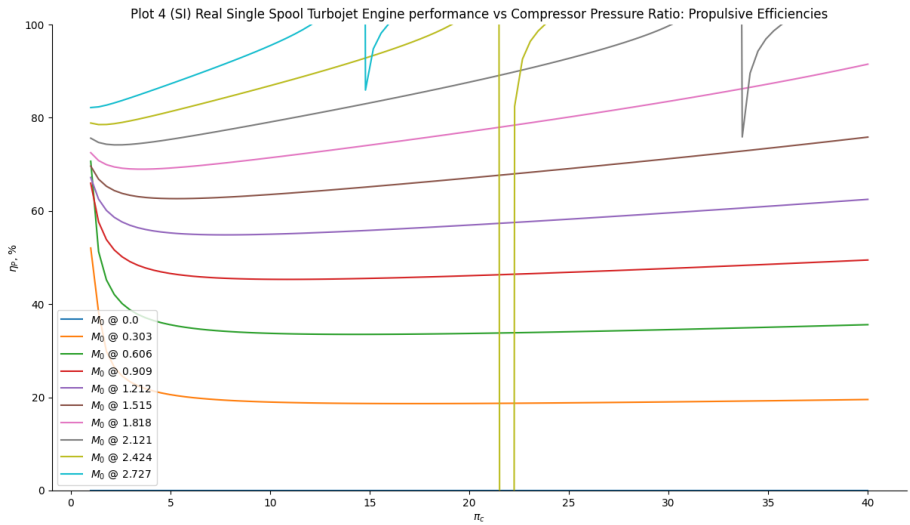


Figure 140 Altitude variation at sea level for Single Spool Turbojet Engine Propulsive Efficiencies plot from GTA

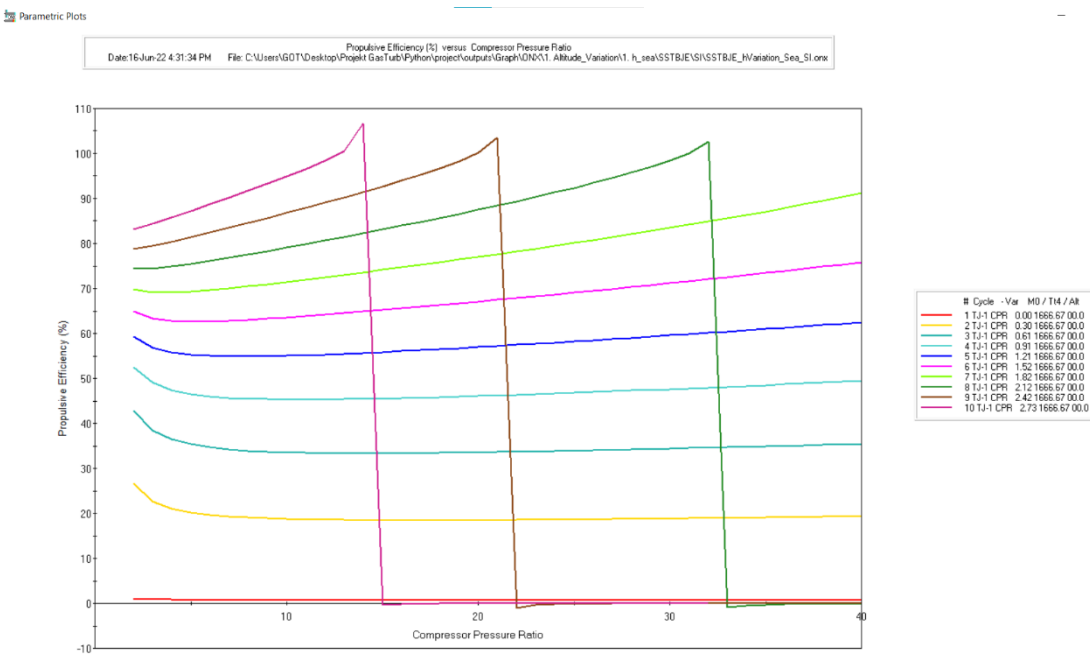


Figure 141 Altitude variation at sea level for Single Spool Turbojet Engine Propulsive Efficiencies plot from ONX

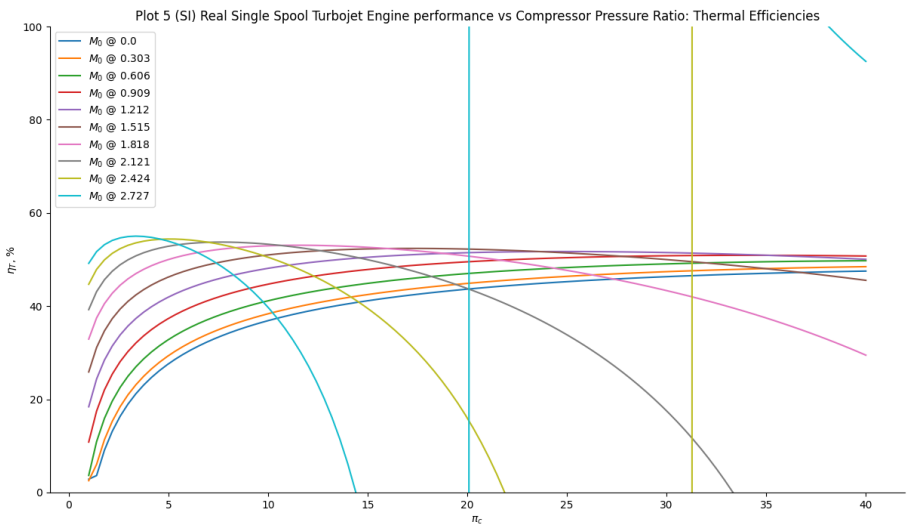


Figure 142 Altitude variation at sea level for Single Spool Turbojet Engine Thermal Efficiencies plot from GTA

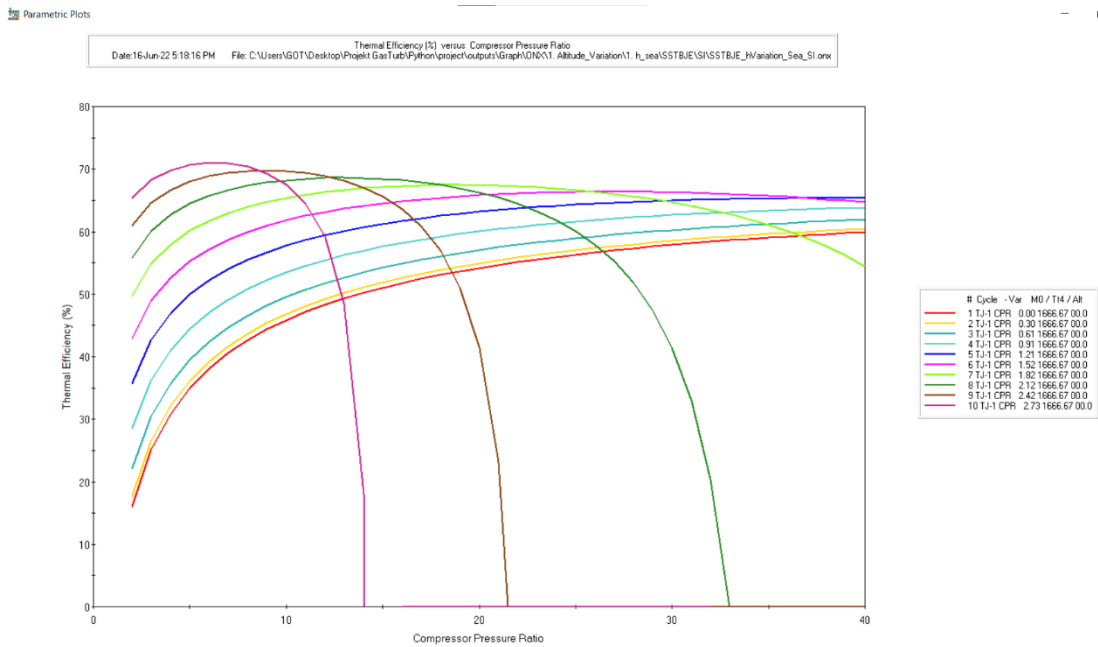


Figure 143 Altitude variation at sea level for Single Spool Turbojet Engine Thermal Efficiencies plot from ONX

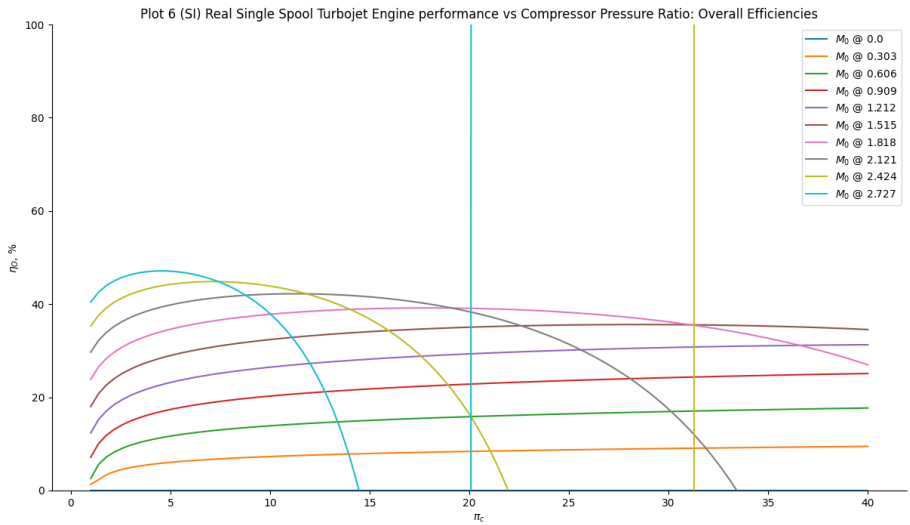


Figure 144 Altitude variation at sea level for Single Spool Turbojet Engine Overall Efficiencies plot from GTA

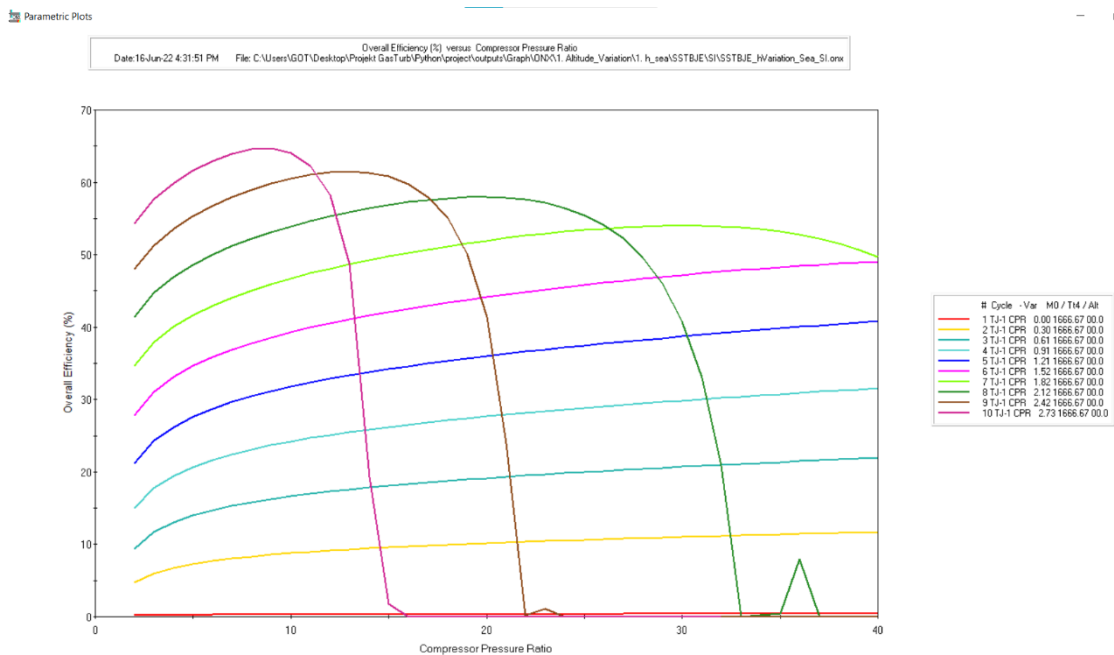


Figure 145 Altitude variation at sea level for Single Spool Turbojet Engine Overall Efficiencies plot from ONX

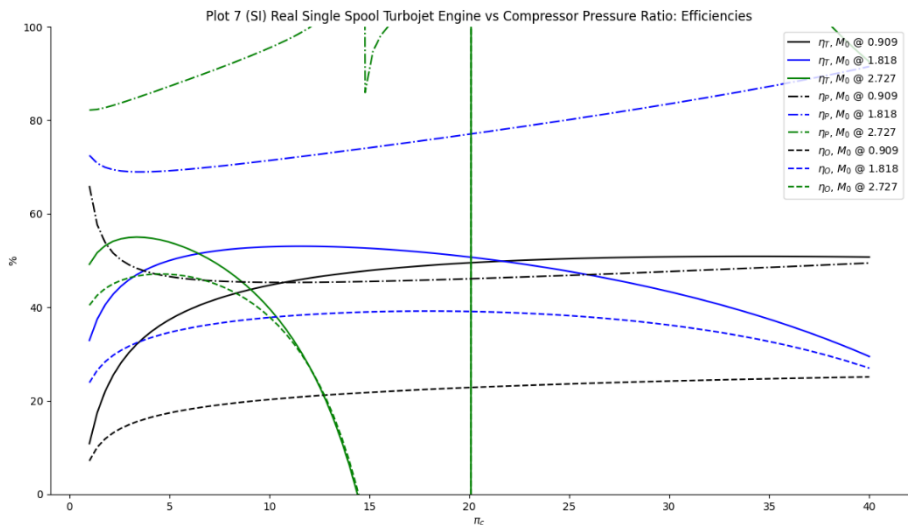


Figure 146 Altitude variation at sea level for Single Spool Turbojet Engine Efficiencies comparison plot from GTA

From the Figure 134 – 146, as mentioned earlier from the single-point calculation result, the GTA implemented constant specific heat (CSH) for ideal gas model and the ONX program implemented a modified specific heat (MSH) model which is different in CSH. Each component is modeled as perfect gases with constant specific heats, but MSH uses CSH to calculate all properties initially but also taken in an account of the fuel used. Therefore, the results for both looks similar but not exactly the same. The effect can be easily observed as the Mach number more than one and approach hypersonic.

The same as the case of specific thrust, with the different ideal gas model, the trending of the lines can be observed that both programs exhibit the same phenomena but due to the different fuel usage assumption, there is a need for better fuel usage estimate for GTA.

For the fuel to air ratio comparison, both programs exhibit as expected to be as the Mach number increase, the fuel to air ratio tends to decrease as shown in the figure above. The ideal gas model (CSH and MSH) does not affect the fuel to air ratio calculation. Therefore, the result comparison for both programs are identical.

As mentioned earlier, some plots exhibit unusual phenomena due to the reason of limitation that needs to be implement in the future phase.

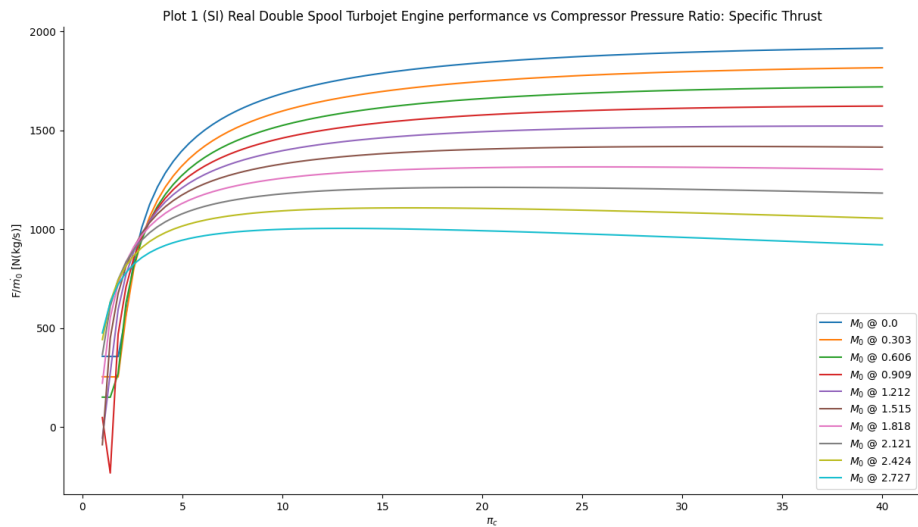


Figure 147 Altitude variation at sea level for Double Spool Turbojet Engine Specific Thrust plot from GTA

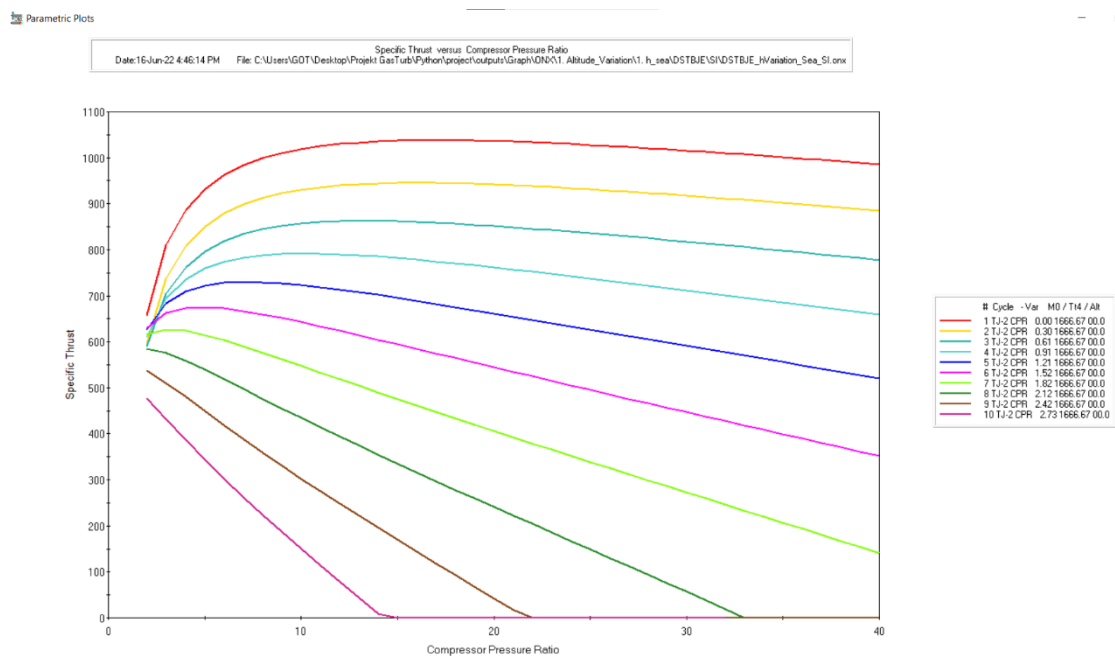


Figure 148 Altitude variation at sea level for Double Spool Turbojet Engine Specific Thrust plot from ONX

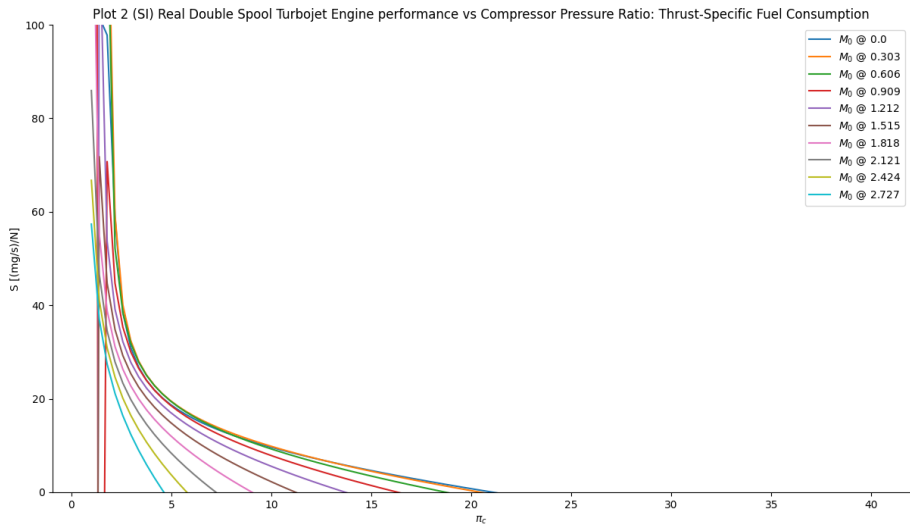


Figure 149 Altitude variation at sea level for Double Spool Turbojet Engine Thrust Specific Fuel Consumption plot from GTA

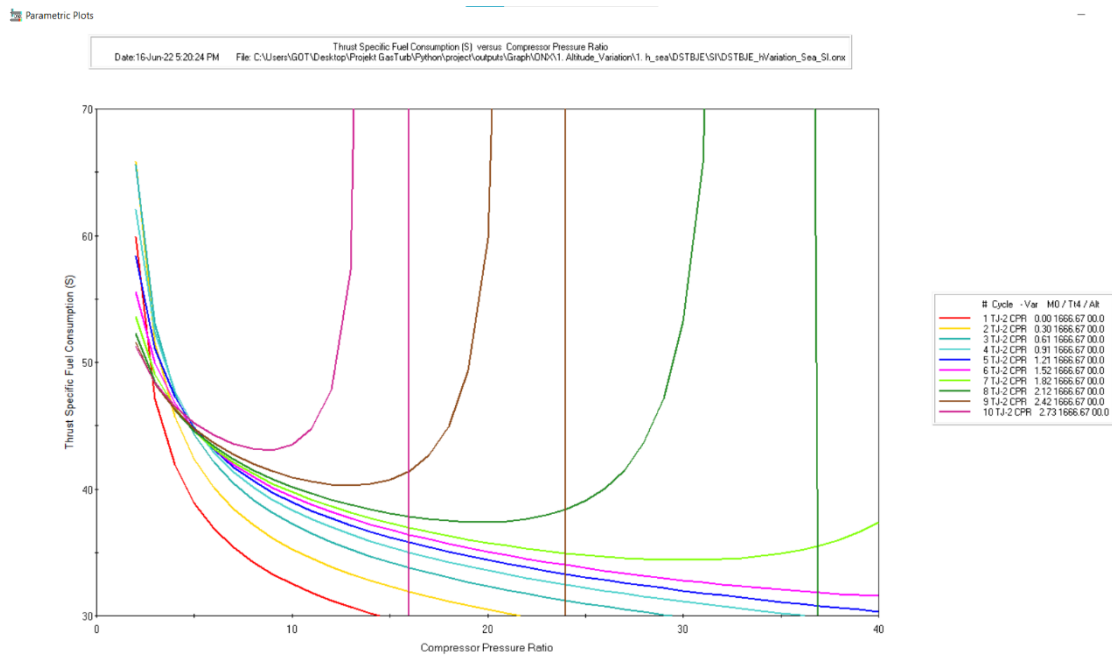


Figure 150 Altitude variation at sea level for Double Spool Turbojet Engine Thrust Specific Fuel Consumption plot from ONX

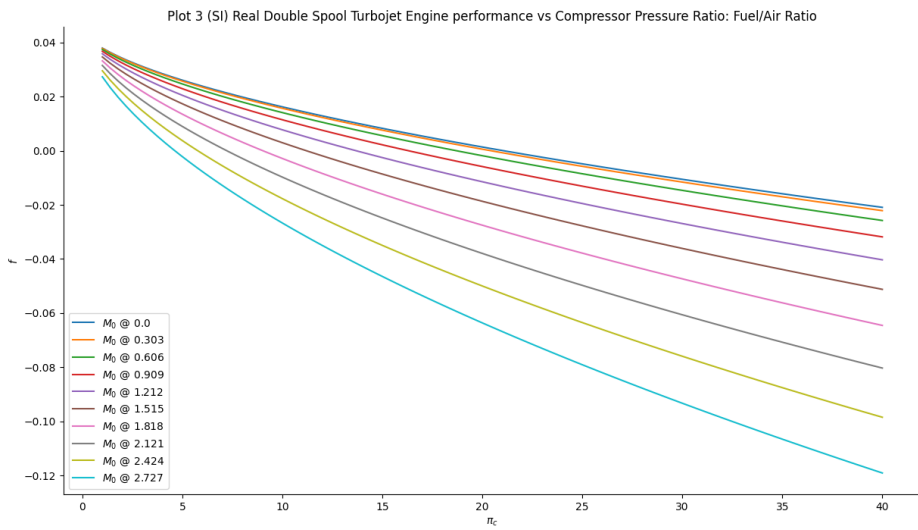


Figure 151 Altitude variation at sea level for Double Spool Turbojet Engine Fuel to Air Ratio plot from GTA

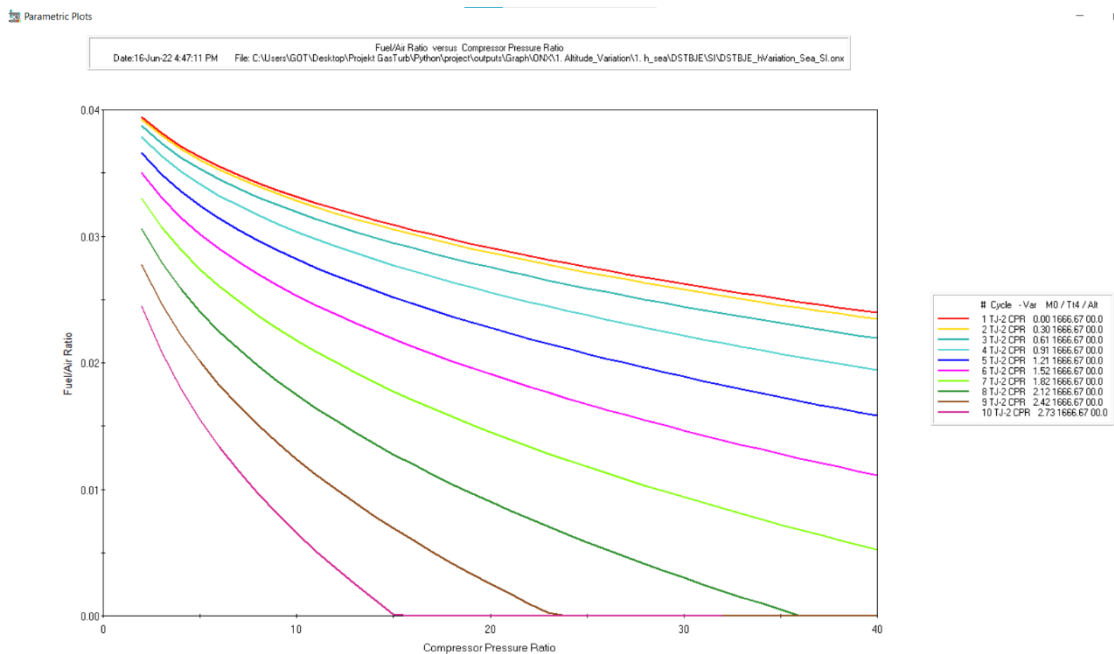


Figure 152 Altitude variation at sea level for Double Spool Turbojet Engine Fuel to Air Ratio plot from ONX

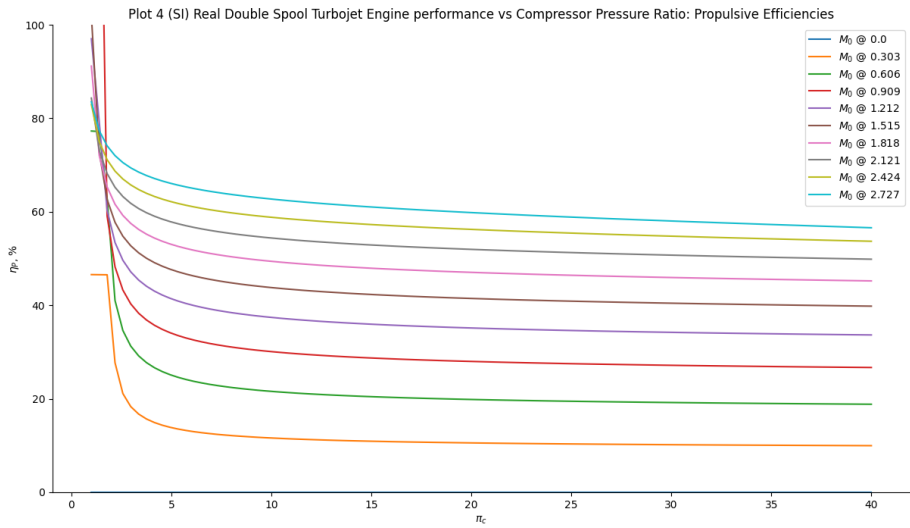


Figure 153 Altitude variation at sea level for Double Spool Turbojet Engine Propulsive Efficiencies plot from GTA

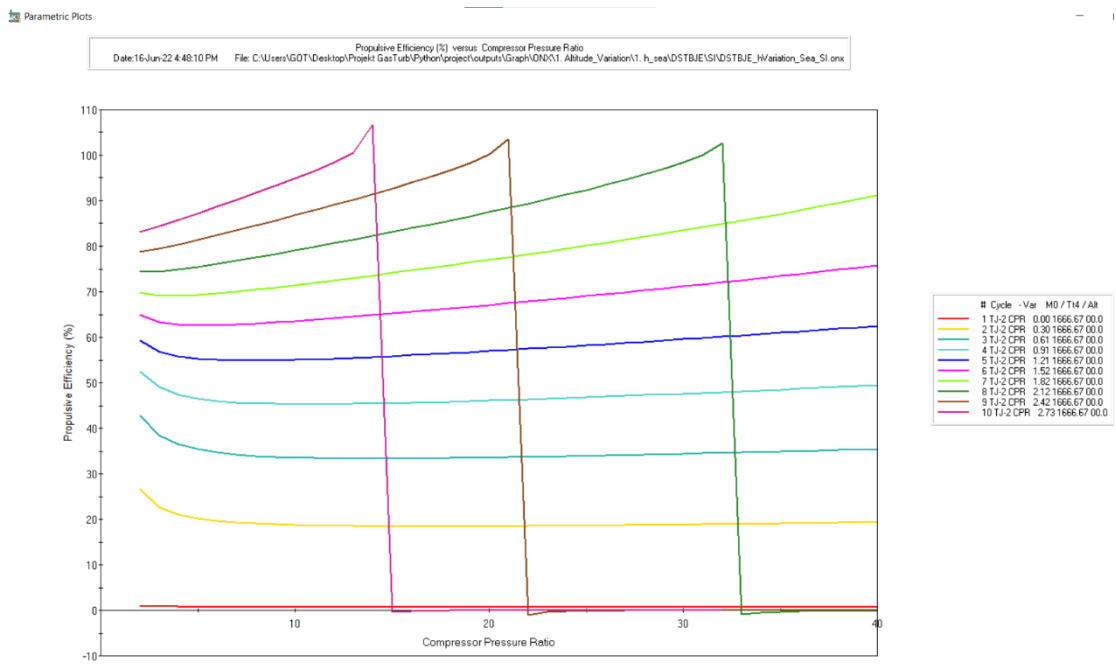


Figure 154 Altitude variation at sea level for Double Spool Turbojet Engine Propulsive Efficiencies plot from ONX

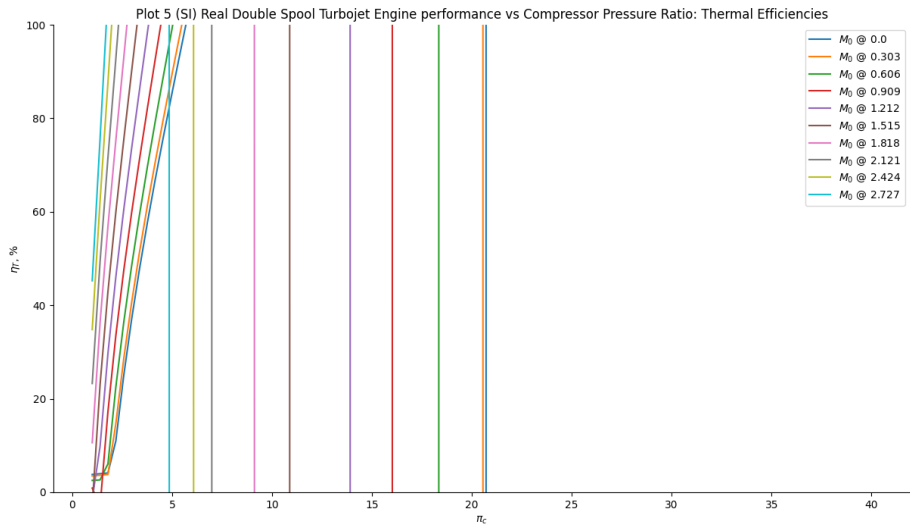


Figure 155 Altitude variation at sea level for Double Spool Turbojet Engine Thermal Efficiencies plot from GTA

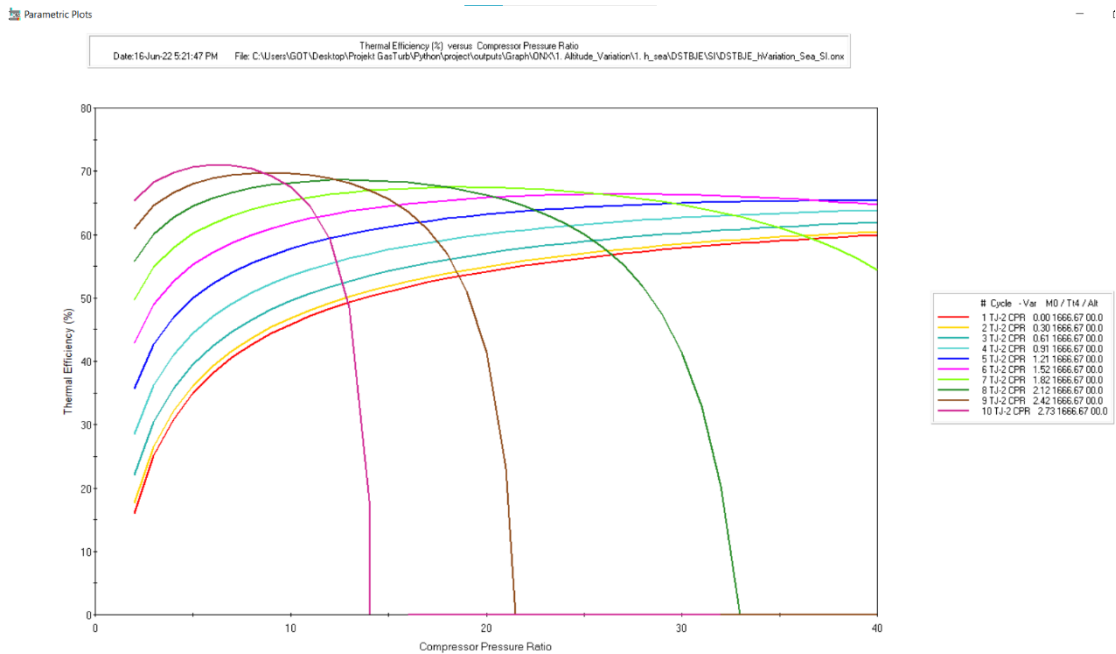


Figure 156 Altitude variation at sea level for Double Spool Turbojet Engine Thermal Efficiencies plot from ONX

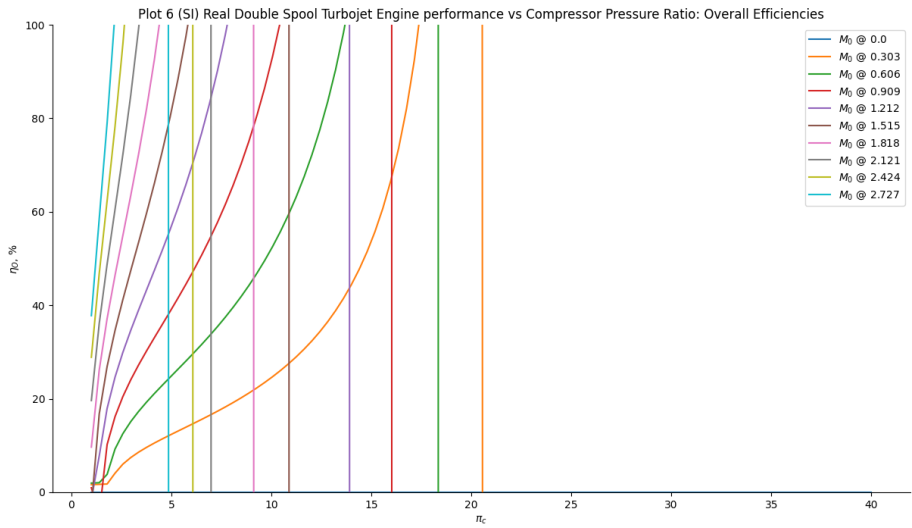


Figure 157 Altitude variation at sea level for Double Spool Turbojet Engine Overall Efficiencies plot from GTA

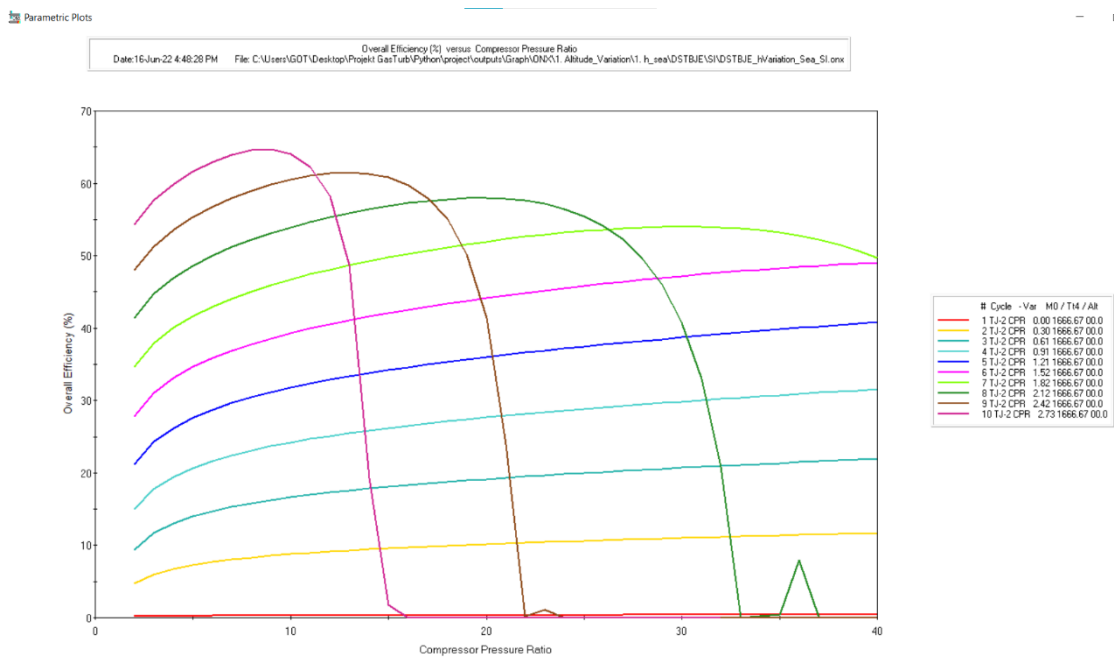


Figure 158 Altitude variation at sea level for Double Spool Turbojet Engine Overall Efficiencies plot from ONX

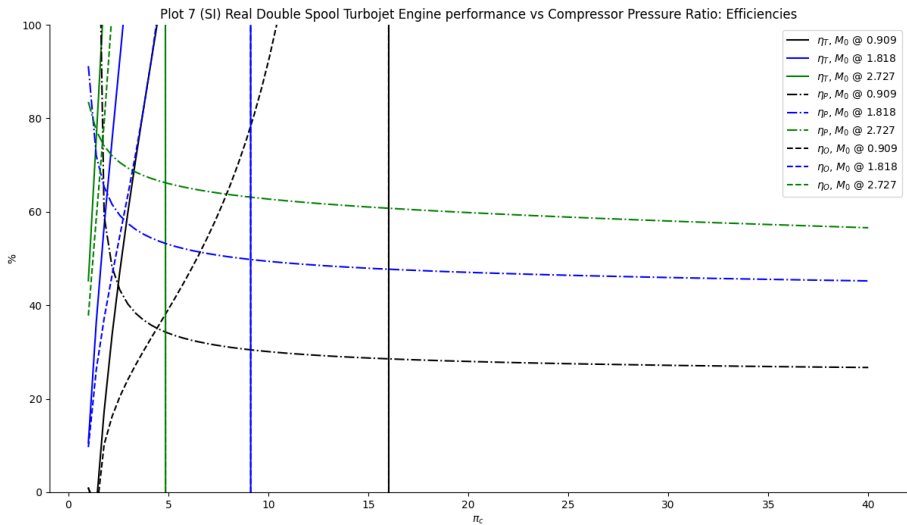


Figure 159 Altitude variation at sea level for Double Spool Turbojet Engine Efficiencies comparison plot from GTA

From the Figure 147 – 159, as mentioned earlier from the single-point calculation result, the GTA is implementing constant specific heat (CSH) for ideal gas model and the ONX program is using a Modified specific heat (MSH) model which is different in CSH each component is modeled as perfect gases with constant specific heats, but MSH uses CSH to calculate all properties initially but also taken in an account of the fuel used. Therefore, the results for both looks similar but not exactly the same. The effect can be easily observed as the Mach number more than one and approach hypersonic.

For the case of double spool turbojet engine, it can be observed that the results from GTA are as twice (or nearly) as that of ONX. The main reason may come from the compressor pressure ratio implementation in GTA that the relationship between the parameter and mixture ratio needs to be declared to obtain an accurate result. The relationship of design choices parameters. For GTA is considered using different dual spool turbojet engine equations calculation from ONX and still considered in the combination of both a low-pressure compressor and a high-pressure compressor ratio whereas in ONX the parameters are separately applied in the calculation. And considered using in combination the relationship of polytropic efficiencies as low-pressure compressor efficiency and high-pressure compressor efficiency. Therefore, the results for both look different. In short, from the obtained results, it can be concluded

that for the double spool turbojet engine, there is a need for further study to alleviate this problem that occurred.

As mentioned earlier, some plots exhibit unusual phenomena due to the reason of limitation that need to be implemented in the future phase for studying double spool turbojet engine equations and the relation of the low-pressure compressor and a high-pressure compressor ratio which effect to double spool turbojet engine performance further.

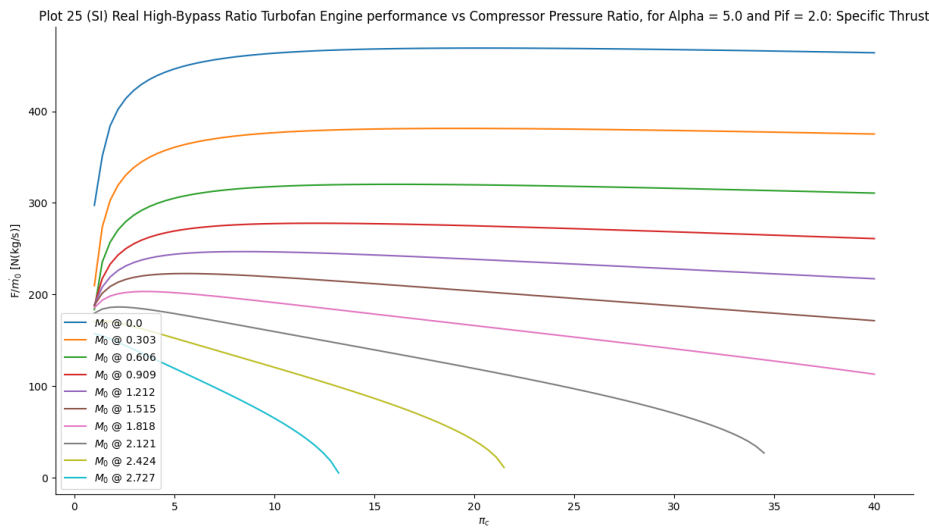


Figure 160 Altitude variation at sea level for High – Bypass Ratio Turbofan Engine Specific Thrust plot from GTA

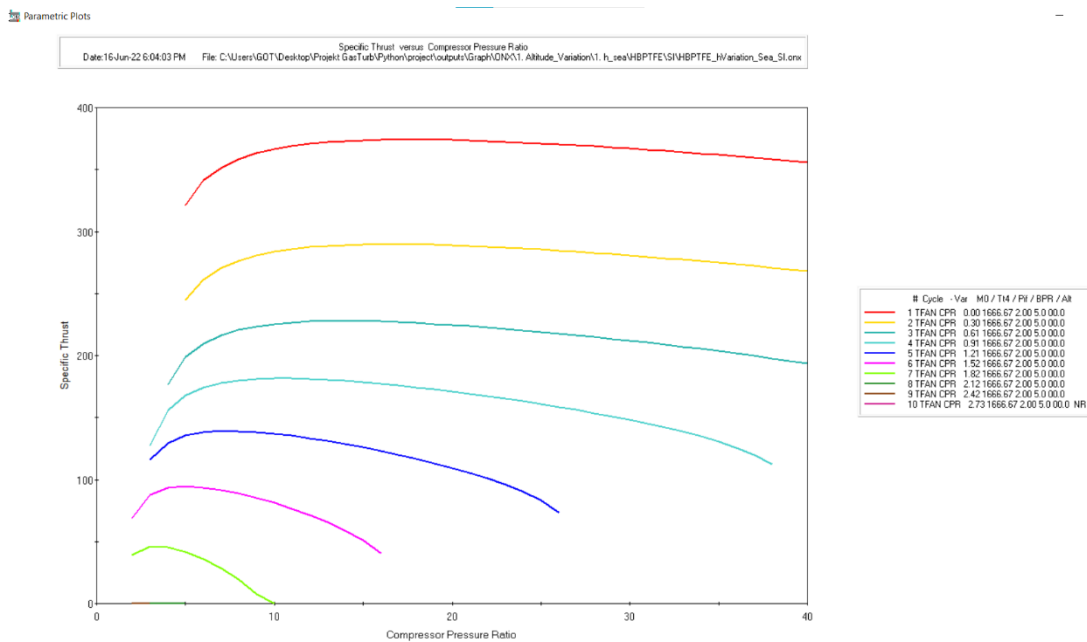


Figure 161 Altitude variation at sea level for High – Bypass Ratio Turbofan Engine Specific Thrust plot from ONX

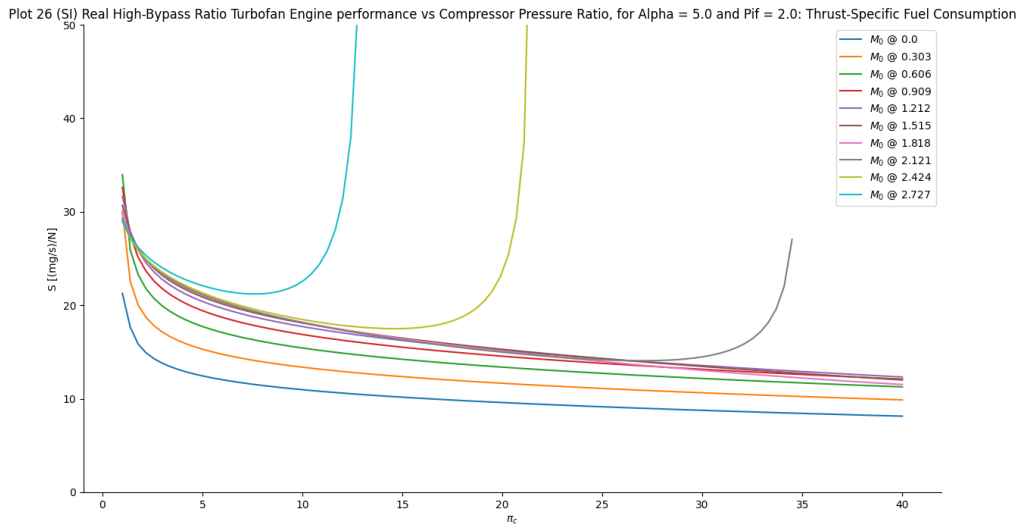


Figure 162 Altitude variation at sea level for High – Bypass Ratio Turbofan Engine Thrust Specific Fuel Consumption plot from GTA

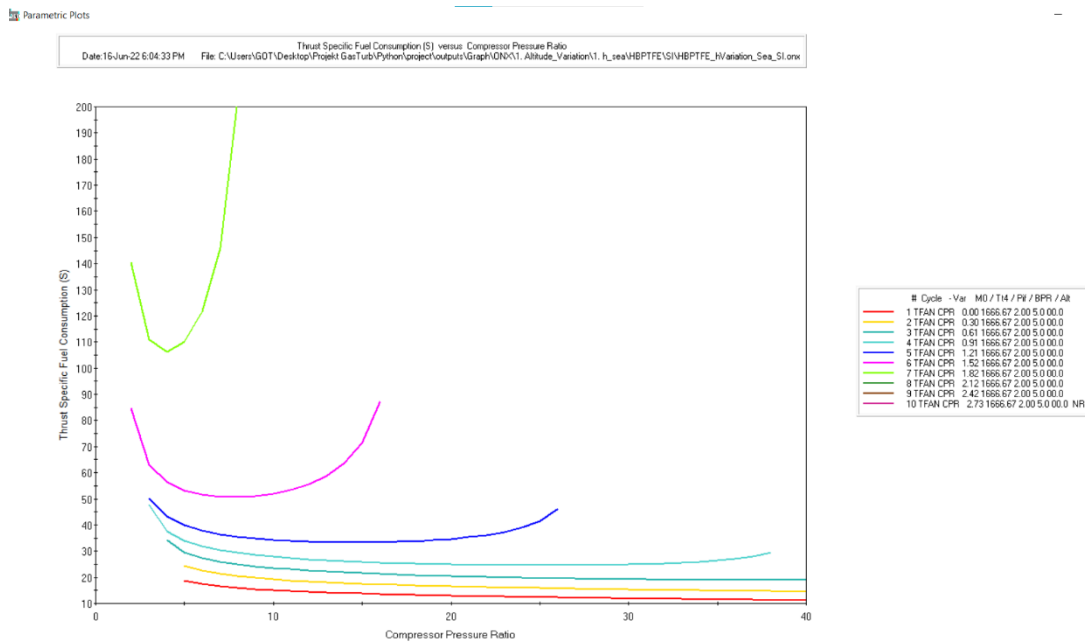


Figure 163 Altitude variation at sea level for High – Bypass Ratio Turbofan Engine Thrust Specific Fuel Consumption plot from ONX

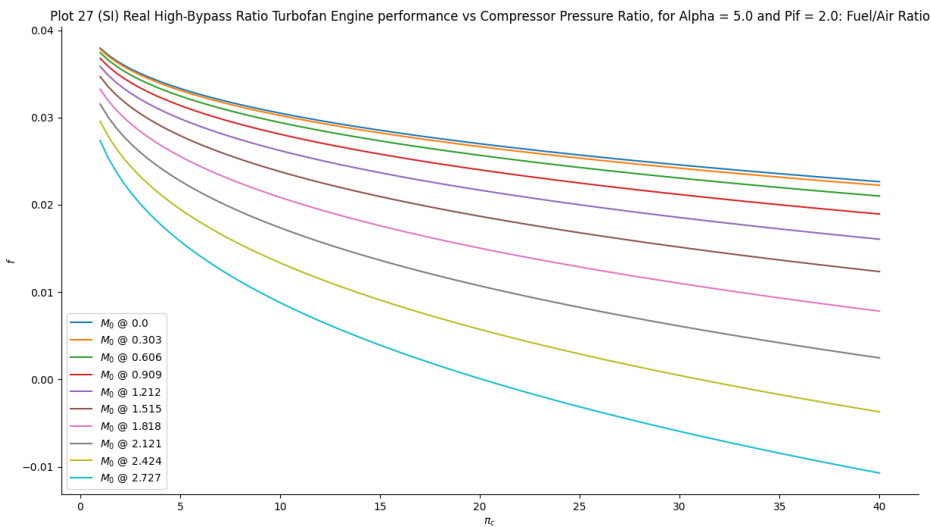


Figure 164 Altitude variation at sea level for High – Bypass Ratio Turbofan Engine Fuel to Air Ratio plot from GTA

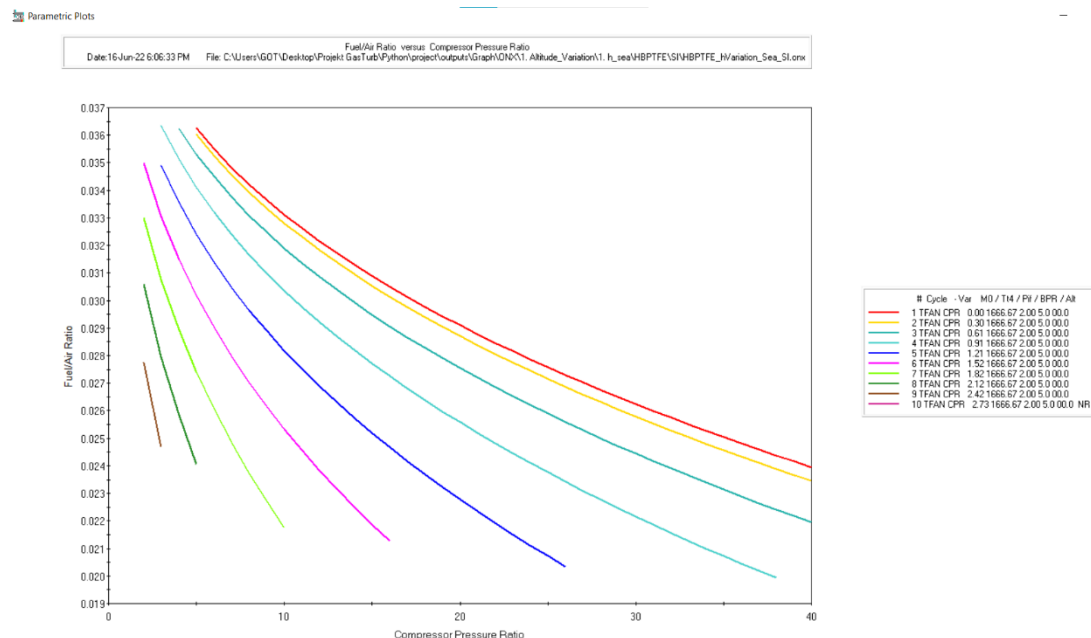


Figure 165 Altitude variation at sea level for High – Bypass Ratio Turbofan Engine Fuel to Air Ratio plot from ONX

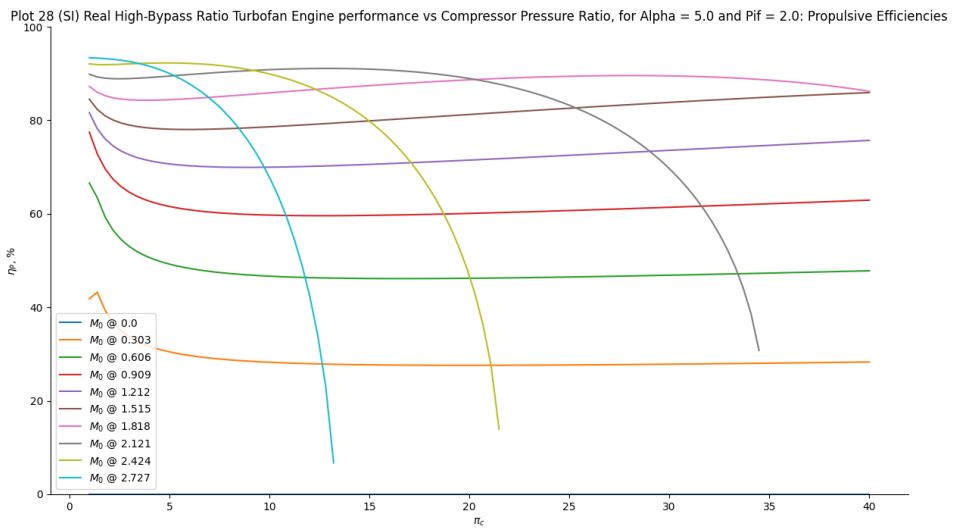


Figure 166 Altitude variation at sea level for High – Bypass Ratio Turbofan Engine Propulsive Efficiencies plot from GTA

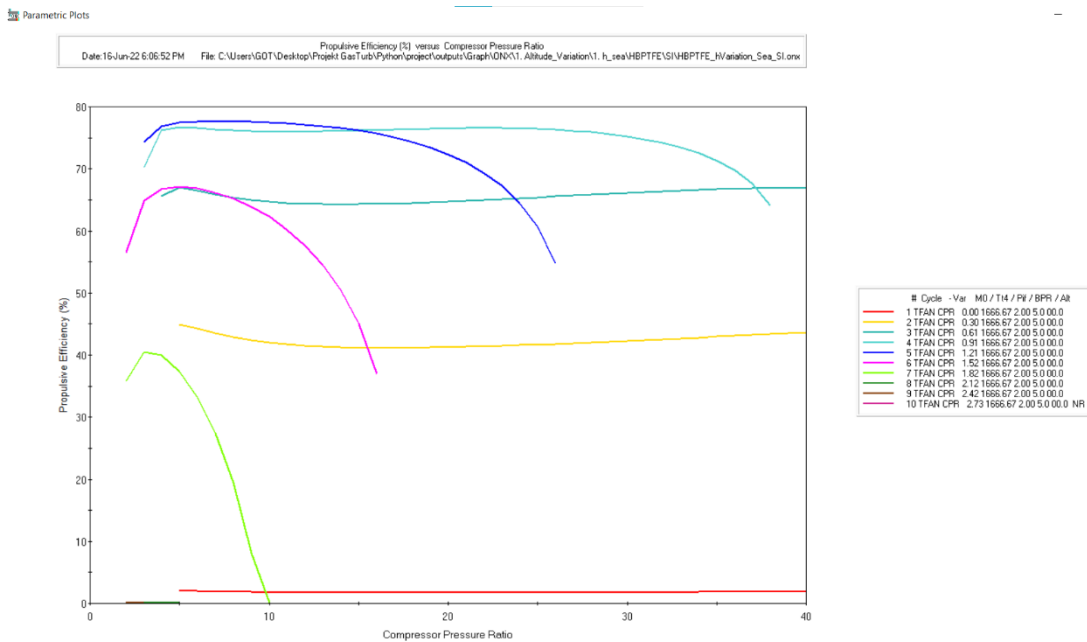


Figure 167 Altitude variation at sea level for High – Bypass Ratio Turbofan Engine Propulsive Efficiencies plot from ONX

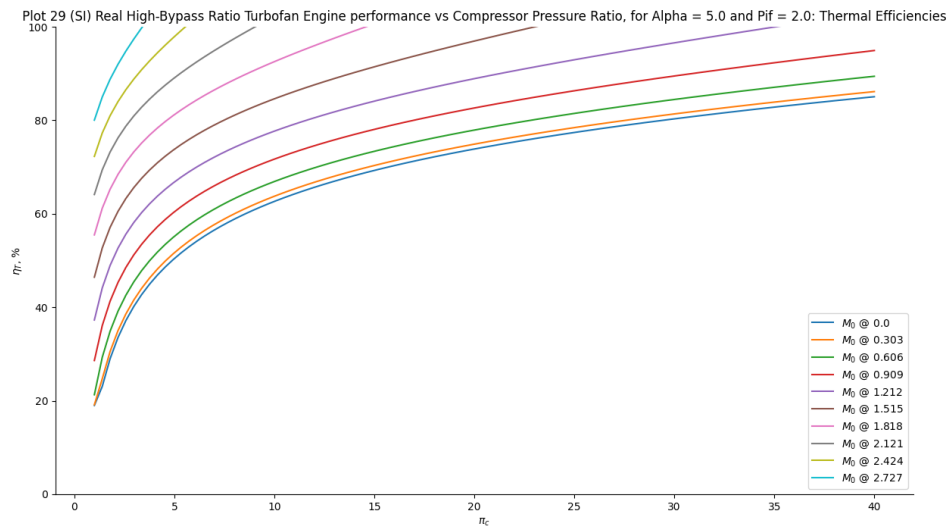


Figure 168 Altitude variation at sea level for High – Bypass Ratio Turbofan Engine Thermal Efficiencies plot from GTA

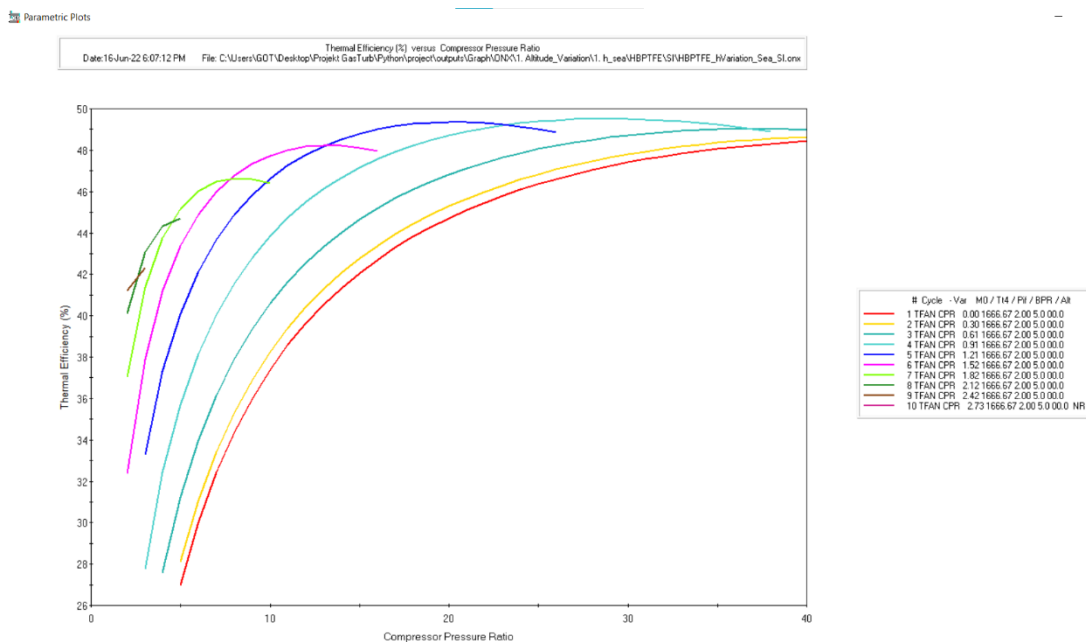


Figure 169 Altitude variation at sea level for High – Bypass Ratio Turbofan Engine Thermal Efficiencies plot from ONX

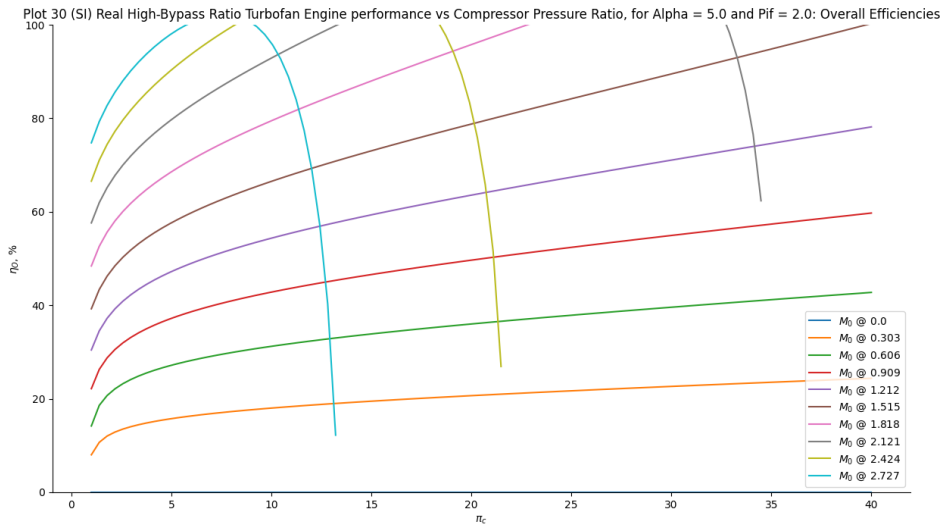


Figure 170 Altitude variation at sea level for High – Bypass Ratio Turbofan Engine Overall Efficiencies plot from GTA

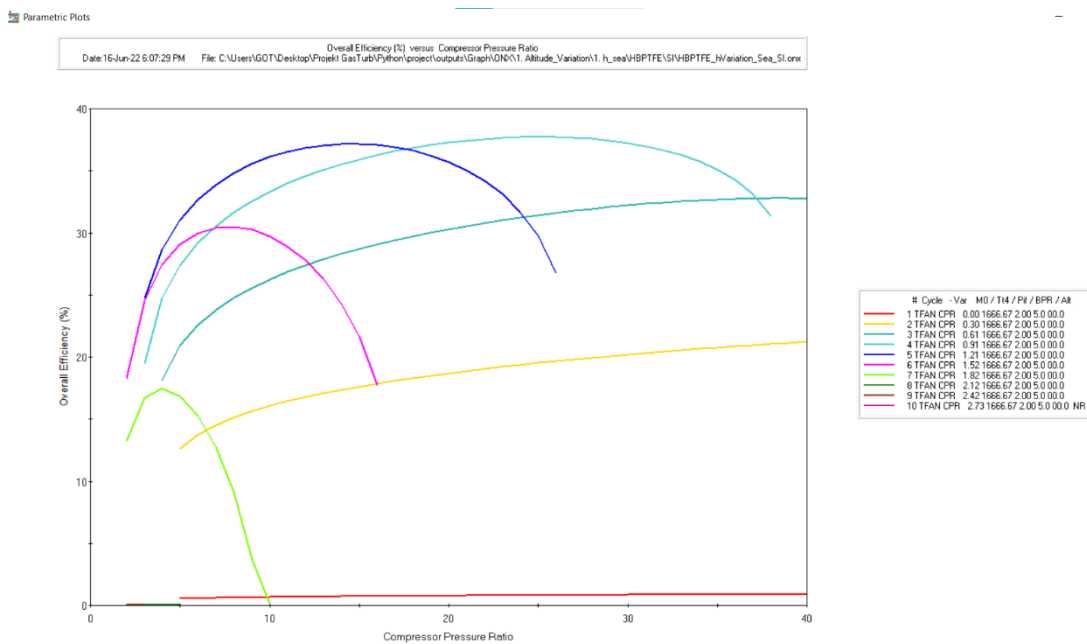


Figure 171 Altitude variation at sea level for High – Bypass Ratio Turbofan Engine Overall Efficiencies plot from ONX

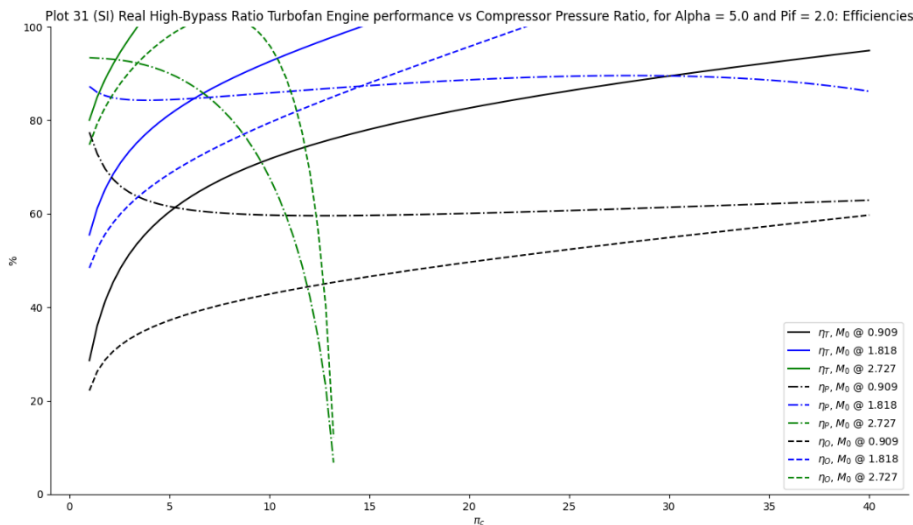


Figure 172 Altitude variation at sea level for High – Bypass Ratio Turbofan Engine Efficiencies comparison plot from GTA

From the Figure 160 – 172, as mentioned earlier from the single-point calculation result, the GTA implemented constant specific heat (CSH) for ideal gas model and the ONX program implemented a modified specific heat (MSH) model which is different in CSH. Each component is modeled as perfect gases with constant specific heats, but MSH uses CSH to calculate all properties initially but also taken in an account of the fuel used. Therefore, the results for both looks similar but not exactly the same. The effect can be easily observed as the Mach number more than one and approach hypersonic.

For the compressor pressure ratio, the parameter that is now implemented for GTA still taken in account of combination of both LPC and HPC pressure ratio whereas in ONX the parameters are separately apply in calculation. Therefore, there is a need of modification regarding that of the compressor pressure ratio.

It can be observed that the trending of lines in each resultant graph from GTA are similar to that of an ONX but with the shifting in value because of the CSH-MSH effect.

As mentioned earlier, some plots exhibit unusual phenomena due to the reason of limitation that needs to be implemented in the future phase.

5. Conclusion and Perspectives

5.1 Conclusions

To conclude, GTA software is developed with a fundamental study approach based on the Mattingly [8] with Python - based source code by implementing the NumPy, Matplotlib modules. All the engine performance equations have been introduced for parametric cycle design and analysis of turbojet and turbofan engines as in the introduction section. The engine analysis will be considered in two cases: ideal case and real case. For the ideal case, isentropic assumptions are applied and for the real case, polytropic equations are taken into consideration as the component efficiency effect is taken into consideration. GTA can perform parametric cycle analysis (on-design) to determine the performance of aircraft engines and component design characteristics best satisfy design requirements under different flight conditions and design choices for three engine layouts namely 1. single spool turbojet engine 2. dual spool turbojet engine 3. high bypass ratio turbofan engine. GTA can work with either the BE (British Empirical) and SI (International System) system units. Also, GTA can conduct single-point calculation and resulted in output text file with aircraft engine performance parameters expressed for ideal and real case such as thrust, specific thrust, etc. For variation calculation, user can vary the altitude h , compressor pressor ratio π_c , Mach number M_0 , bypass ratio α , fan pressure ratio π_f , and component efficiency η to observe the changing behaviour of parameters in the output files in the form of plots and text files. Output plots for variation calculation including the performance parameters, namely, specific thrust F / \dot{m} , thrust specific fuel consumption S , fuel to air ratio f , propulsive, thermal, overall efficiency can be studied by user for both ideal and real case. The results from GTA are compared with the available software, namely AEDsys (ONX). From the validation, the single spool turbojet engine GTA can achieve a fairly accurate result, but there are slight discrepancies due to the main calculation based on a constant specific heat module (CSH). For high bypass ratio turbofan, the results comparison between both programs

shows that the discrepancies are reasonable due to the usage of the compressor pressure ratio, which is currently not separately applied in the calculation, as the high-and low-compressor pressure ratios. For double spool turbojet engine, similarly to the high bypass ratio turbofan engine, there is a need to study further into the equations and the effect of the relation between low and high compressor pressure ratios. To conclude, GTA can perform a parametric cycle analysis for three engines, namely, 1. single spool turbojet engine 2. double spool turbojet engine, and 3. high bypass ratio turbofan engine for both single and variation point calculation. The results obtained when compared to AEDsys (ONX) are considerably accurate for the single spool turbojet engine, but there is a moderate amount of improvement to be done for the double spool turbojet engine and high bypass ratio turbofan engine to achieve more accurate results.

5.2 Perspectives

There are several topics worth discussion as there are many improvements that could be done for GTA.

The ideal gas model implemented in GTA for this phase is constant specific heat model (CSH) and for the better fuel usage calculation, the modified specific heat model (MSH) needs to be implemented as AEDsys (ONX) implemented MSH model calculation. Therefore, in order to gain better results, MSH needs to be implemented in the later phase.

The turbofan engine analysis model(equations) in GTA is different from that of ONX regarding the application of compressor pressure ratio (π_c).

GUI (Graphic – User Interface) could be developed for user-friendly purpose which could help user to interact with the program easier.

Mission analysis to identify required thrust and specific fuel consumption for each mission segment for subsonic aircraft should be carried out in the next phase.

References

- [1] Venedikt S. Kuz'michev, Yaroslav A. Ostapyuk, Andrey Y. Tkachenko, Ilia N. Krupenich, and Evgeniy P. Filinov, “Comparative Analysis of the Computer-Aided Systems of Gas Turbine Engine Designing”, *Samara National Research University*, 2017
- [2] K. H. Liew, E. Urip, and S. L. Yang, “Parametric Cycle Analysis of a Turbofan Engine with an Interstage Turbine Burner”, *Michigan Technological University*, 2005
- [3] Balaji Sankar, Brijeshkumar Shah, Thennavarajan S, Vijayendranath Vanam, and Soumendu Jana, “On Gas Turbine Simulation Model Development, Propulsion division CSIR-NAL”, 2013
- [4] GAO Jian-hua and HUANG Ying-yun, “Modeling and Simulation of an Aero Turbojet Engine with GasTurb”, *Naval University of Engineering*, 2011
- [5] Ozgur Balli, “Afterburning effect on the energetic and exergetic performance of an experimental turbojet engine (TJE)”, *Turkish Air Forces (TurAF)*, 2014
- [6] Feijia Yin, Arvind G. Rao, “Off-Design Performance of an Interstage Turbine Burner Turbofan Engine”, *Delft University of Technology*, 2017
- [7] Ahmed F. El-Sayed, “Aircraft Propulsion and Gas Turbine Engines”, *CRC Press*, 2017
- [8] Jack D. Mattingly, “Elements of Propulsion: Gas Turbines and Rockets”, *American Institute of Aeronautics and Astronautics*, 2006
- [9] Aaron R. Byerley, Kurt P. Rouser, Devin O. O'Dowd, “Exploring GasTurb 12 for supplementary use on an introductory propulsion design project”, *Proceedings of ASME Turbo Expo 2017: Turbomachinery Technical Conference and Exposition*, 2017
- [10] Rayne Sung, “A comparative study of the gas turbine simulation program (GSP) 11 and GasTurb 11 on their respective simulations for a single-spool turbojet”, *University of Tennessee*, 2013

Appendix A: Example case for subsonic flight

Example input table for single point calculation and variation calculation

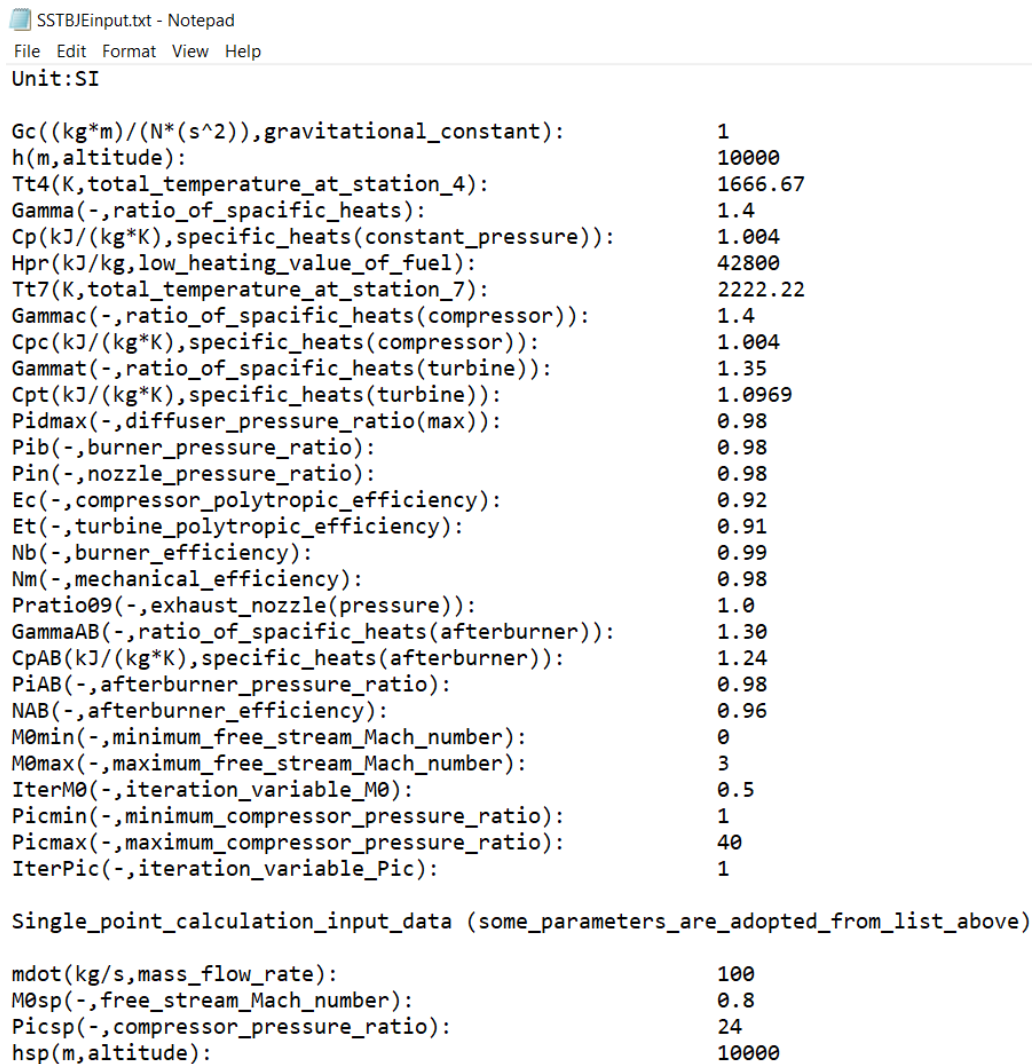
SSTJE = single spool turbojet engine, DSTJE = double spool turbojet engine,
HBPTFE = high bypass ratio turbofan engine

Case 1: Height variation for subsonic flight, commercial airliners

Parameter, Unit: SI	SSTJE	DSTJE	HBPTFE
\dot{m} (kg/s)	100	100	100
M_0	0.8	0.8	0.8
π_c	24	24	24
α	-	-	5
π_f	-	-	2
h (m)	10000	10000	10000
g_c ($(kg * m)/(N * s^2)$)	1	1	1
T_{t4} (K)	1666.67	1666.67	1666.67
γ	1.4	1.4	1.4
c_p ($kJ/(kg * K)$)	1.004	1.004	1.004
h_{PR} (kJ/kg)	42800	42800	42800
T_{t7} (K)	2222.22	2222.22	-
γ_c	1.4	1.4	1.4
c_{pc} ($kJ/(kg * K)$)	1.004	1.004	1.004
γ_t (-)	1.35	1.35	1.35
c_{pt} ($kJ/(kg * K)$)	1.0969	1.0969	1.0969
$\pi_{d_{max}}$	0.98	0.98	0.98
π_b	0.98	0.98	0.98
π_n	0.98	0.98	0.98
π_{fn}	-	-	0.98
π_t	-	-	0.89
e_c	0.92	0.92	0.92
e_f	-	-	0.88
e_t	0.91	0.91	0.91
η_b	0.99	0.99	0.99
η_m	0.98	0.98	0.98
η_{cL}	-	0.8755	-
η_{cH}	-	0.8791	-
P_0/P_9	1	1	1
P_0/P_{19}	-	-	1
γ_{AB}	1.3	1.3	-
c_{pAB} ($kJ/(kg * K)$)	1.24	1.24	-
π_{AB}	0.98	0.98	-
η_{AB}	0.96	0.96	-
P_0 (kPa)	-	101.33	-
π_{tH}	-	0.5466	-
π_{tL}	-	0.6127	-

Input data for GTA

The input file name of the GTA is specified by the names of engine layouts as SSTBJEinput, DSTBJEinput, and HBPTBFEinput. Input parameters are declared then followed by the data which the user defines. These input files are applied for both single point and variation calculation process. The example input text files are as shown below



SSTBJEinput.txt - Notepad
File Edit Format View Help
Unit:SI

Gc((kg*m)/(N*(s^2)),gravitational_constant):	1
h(m,altitude):	10000
Tt4(K,total_temperature_at_station_4):	1666.67
Gamma(-,ratio_of_specific_heats):	1.4
Cp(kJ/(kg*K),specific_heats(constant_pressure)):	1.004
Hpr(kJ/kg,low_heating_value_of_fuel):	42800
Tt7(K,total_temperature_at_station_7):	2222.22
Gammac(-,ratio_of_specific_heats(compressor)):	1.4
Cpc(kJ/(kg*K),specific_heats(compressor)):	1.004
Gamat(-,ratio_of_specific_heats(turbine)):	1.35
Cpt(kJ/(kg*K),specific_heats(turbine)):	1.0969
Pidmax(-,diffuser_pressure_ratio(max)):	0.98
Pib(-,burner_pressure_ratio):	0.98
Pin(-,nozzle_pressure_ratio):	0.98
Ec(-,compressor_polytropic_efficiency):	0.92
Et(-,turbine_polytropic_efficiency):	0.91
Nb(-,burner_efficiency):	0.99
Nm(-,mechanical_efficiency):	0.98
Pratio09(-,exhaust_nozzle(pressure)):	1.0
GammaAB(-,ratio_of_specific_heats(afterburner)):	1.30
CpAB(kJ/(kg*K),specific_heats(afterburner)):	1.24
PiAB(-,afterburner_pressure_ratio):	0.98
NAB(-,afterburner_efficiency):	0.96
M0min(-,minimum_free_stream_Mach_number):	0
M0max(-,maximum_free_stream_Mach_number):	3
IterM0(-,iteration_variable_M0):	0.5
Picmin(-,minimum_compressor_pressure_ratio):	1
Picmax(-,maximum_compressor_pressure_ratio):	40
IterPic(-,iteration_variable_Pic):	1
Single_point_calculation_input_data (some_parameters_are_adopted_from_list_above)	
mdot(kg/s,mass_flow_rate):	100
M0sp(-,free_stream_Mach_number):	0.8
Picsp(-,compressor_pressure_ratio):	24
hsp(m,altitude):	10000

DSTBEEinput.txt - Notepad

File Edit Format View Help

Unit:SI

```

Gc(((kg*m)/(N*(s^2))),Gravitational_constant):           1
h(m,Altitude):                                         10000
Tt4(K,Total_Temperature_at_station_4_Combustor):        1666.67
Gamma(-,Ratio_of_specific_heats):                         1.4
Cp((kJ/(kg*K)),Specific_heats_(constant_pressure)):     1.004
Hpr((kJ/kg),Low_heating_value_of_fuel):                  42800
Tt7(K,Total_Temperature_at_station_7):                   2222.22
Gammac(-,Ratio_of_specific_heats(compressor)):          1.4
Cpc(kJ/(kg*K),Specific_heats(compressor)):             1.004
Gammat(-,Ratio_of_specific_heats(turbine)):            1.35
Cpt((kJ/(kg*K)),Specific_heats(turbine)):              1.0969
Pidmax(-,Diffuser_pressure_ratio_(Max)):                0.98
Pib(-,Burner_pressure_ratio):                           0.98
Pin(-,Nozzle_pressure_ratio):                          0.98
Ec(-,Polytropic_efficiency_Compressor):               0.92
Et(-,Polytropic_efficiency_Turbine):                  0.91
Nb(-,Component_efficiency_Burner):                    0.99
Nm(-,Component_efficiency_Mechanical_Shift_Spool):   0.98
NcL(-,Component_efficiency_low_pressure_compressor): 0.8755
NcH(-,Component_efficiency_high_pressure_compressor): 0.8791
Pratio09(-,Exhaust_Nozzle(pressure)):                1
GammaAB(-,Ratio_of_specific_heats(Afterburner)):       1.30
CpAB((kJ/(kg*K)),Specific_heats(Afterburner)):        1.24
PiAB(-,Afterburner_pressure_ratio):                   0.98
NAB(-,Aterburner_efficiency):                         0.96
P0((kPa),Pressure):                                  101.33
PitH(-,High_turbine_pressure_ratio):                 0.5466
PitL(-,Low_turbine_pressure_ratio):                  0.6127
M0min(-,Minimum_free_stream_Mach_number):           0
M0max(-,Maximum_free_stream_Mach_number):            3
IterM0(-,Iteration_variable_M0):                     0.5
Picmin(-,Minimum_compressor_pressure_ratio):         1
Picmax(-,Maximum_compressor_pressure_ratio):          40
IterPic(-,Iteration_variable_M0):                     1

Single_point_calculation_input_data (some_parameters_are_adopted_from_list_above)

mdot(kg/s,mass_flow_rate):                            100
M0sp(-,free_stream_Mach_number):                      0.8
Picsp(-,compressor_pressure_ratio):                  24
hsp(m,altitude):                                     10000

```

HBPTBFEinput.txt - Notepad

File Edit Format View Help

Unit:SI

Gc((kg*m)/(N*(s^2))),Gravitational_constant):	1
h(m,Altitude):	10000
Tt4(K,total_Temperature_at_station_4):	1666.67
Gamma(-,Ratio_of_specific_heats):	1.4
Cp(kJ/(kg*K)),Specific_heats(constant_pressure):	1.004
Hpr((kJ/kg),Low_heating_value_of_fuel):	42800
Gammac(-,Ratio_of_specific_heats(compressor)):	1.4
Cpc(kJ/(kg*K)),Specific_heats(compressor):	1.004
Gammat(-,Ratio_of_specific_heats(turbine)):	1.35
Cpt((kJ/(kg*K)),Specific_heats(turbine)):	1.0969
Pidmax(-,Diffuser_pressure_ratio_(Max)):	0.98
Pib(-,Burner_pressure_ratio):	0.98
Pin(-,Nozzle_pressure_ratio):	0.98
Pifn(-,Fan_Nozzle_pressure_ratio):	0.98
Pit(-,Turbine_pressure_ratio):	0.89
Ec(-,Polytropic_efficiency_Compressor):	0.92
Ef(-,Polytropic_efficiency_fan):	0.88
Et(-,Polytropic_efficiency_Turbine):	0.91
Nb(-,Component_efficiency_Burner):	0.99
Nm(-,Component_efficiency_Mechanical):	0.98
Pratio09(-,Exhaust_Nozzle(pressure_0_9)):	1.0
Pratio19(-,Exhaust_Nozzle(pressure_1_9)):	1.0
M0fix(-,free_stream_Mach_number):	0.5
Picfix(-,compressor_pressure_ratio):	10
Alphafix(-,Bypass_ratio):	5
Piffix(-,Fan_pressure_ratio):	2
M0min(-,Minimum_free_stream_Mach_number):	0
M0max(-,Maximum_free_stream_Mach_number):	3
IterM0(-,Iteration_variable_M0):	0.5
Picmin(-,Minimum_compressor_pressure_ratio):	1
Picmax(-,Maximum_compressor_pressure_ratio):	40
IterPic(-,Iteration_variable_Pic):	1
Pifmin(-,Minimum_fan_pressure_ratio):	0
Pifmax(-,Maximum_fan_pressure_ratio):	40
IterPif(-,Iteration_variable_Pif):	0.5
Alphamin(-,Minimum_bypass_ratio):	0
Alphamax(-,Maximum_bypass_ratio):	40
IterAlpha(-,Iteration_variable_Alpha):	0.5

Single_point_calculation_input_data (some_parameters_are_adopted_from_list_above)

mdot(kg/s,mass_flow_rate):	100
M0sp(-,free_stream_Mach_number):	0.8
Picsp(-,compressor_pressure_ratio):	24
hsp(m,altitude):	10000
Pifsp(-,fan_pressure_ratio):	2
Alphasp(-,bypass_ratio):	5

Output file name from GTA

The output files from GTA are named after their engine layouts and added with the unit system, namely, SSTBJEoutputSI for single spool turbojet engine with SI unit, DSTBJEoutputSI for double spool turbojet engine with SI unit, and HBPTBFEoutputSI for high bypass ratio turbofan engine with SI unit, as shown below,



DSTBJEoutputSI.txt.txt



HBPTBFEoutputSI.txt.txt



SSTBJEoutputSI.txt.txt

Output from GTA

Outputs from GTA can be classified into two types:

1. single point calculation
2. variation point calculation

The outputs are printed out in two forms:

1. text files
2. plots

GTA's single point calculation output

```
#####
Results for Real Single Spool Turbojet Engine (Single Point Calculation)

Rc_renmspSSTJE:0.28686          Taut_renmspSSTJE:0.76915
Rt_renmspSSTJE:0.28438          Pit_renmspSSTJE:0.32873
A0_renmspSSTJE:299.363          Nt_renmspSSTJE:0.92134
V0_renmspSSTJE:239.49           Pt9P_renmspSSTJE:11.213
M02_renmspSSTJE:0.64            M9_renmspSSTJE:2.231
Taur_renmspSSTJE:1.128          T9T0_renmspSSTJE:3.07
Pir_renmspSSTJE:1.524           V9A0_renmspSSTJE:3.822
nr_renmspSSTJE:0.991            Tsc_renmspSSTJE:937.135
Pid_renmspSSTJE:0.971           Thrust_renmspSSTJE:93713.5
Tauram_renmspSSTJE:8.16         S_renmspSSTJE:30.273
Taucl_renmspSSTJE:2.683          NT_renmspSSTJE:53.074
Nc_renmspSSTJE:0.879           NP_renmspSSTJE:34.826
f_renmspSSTJE:0.02837          NO_renmspSSTJE:18.484

#####
Results for Real Double Spool Turbojet Engine (Single Point Calculation)

Picrefsp:24.0                   PicL_renmspDSTJE:36.323507210892345
PicLrefsp:24.0                  TauchHref_renmspDSTJE:2.6828540401902328
PicHrefsp:24.0                  TauchH_renmspDSTJE:2.799251095294907
Rc_renmspDSTJE:0.2868571428571428 PicH_renmspDSTJE:27.64922428200237
Rt_renmspDSTJE:0.2843814814815   Tauram_renmspDSTJE:8.159922813786308
A0_renmspDSTJE:299.3610529110291 f_renmspDSTJE: -0.008052358089681632
V0_renmspDSTJE:239.4888423288233 mdot0_renmspDSTJE:148.31104903680642
M02_renmspDSTJE:0.6400000000000001 Pt9P_renmspDSTJE:478.4356798225575
Taur_renmspDSTJE:1.1280000000000001 M9_renmspDSTJE:4.7520630915222
Taurref_renmspDSTJE:1.1280000000000001 T9T0_renmspDSTJE:2.0110417629479467
Pir_renmspDSTJE:1.5243400095586486 V9A0_renmspDSTJE:6.58890781105354
Pirref_renmspDSTJE:1.5243400095586486 Tsc_renmspDSTJE:1717.090564138637
nr_renmspDSTJE:0.9914601202086227 Thrust_renmspDSTJE:171709.0564138637
Pid_renmspDSTJE:0.9716309178044502 S_renmspDSTJE: -4.689536037792523
Pidref_renmspDSTJE:0.9716309178044502 NT_renmspDSTJE: -551.5776104413352
Tauclref_renmspDSTJE:2.6897738283623456 NP_renmspDSTJE:21.632415150871186
Taucl_renmspDSTJE:3.0457476304838975 NO_renmspDSTJE: -119.31955856992465

#####
Results for Real High-Bypass Ratio Turbofan Engine (Single Point Calculation)

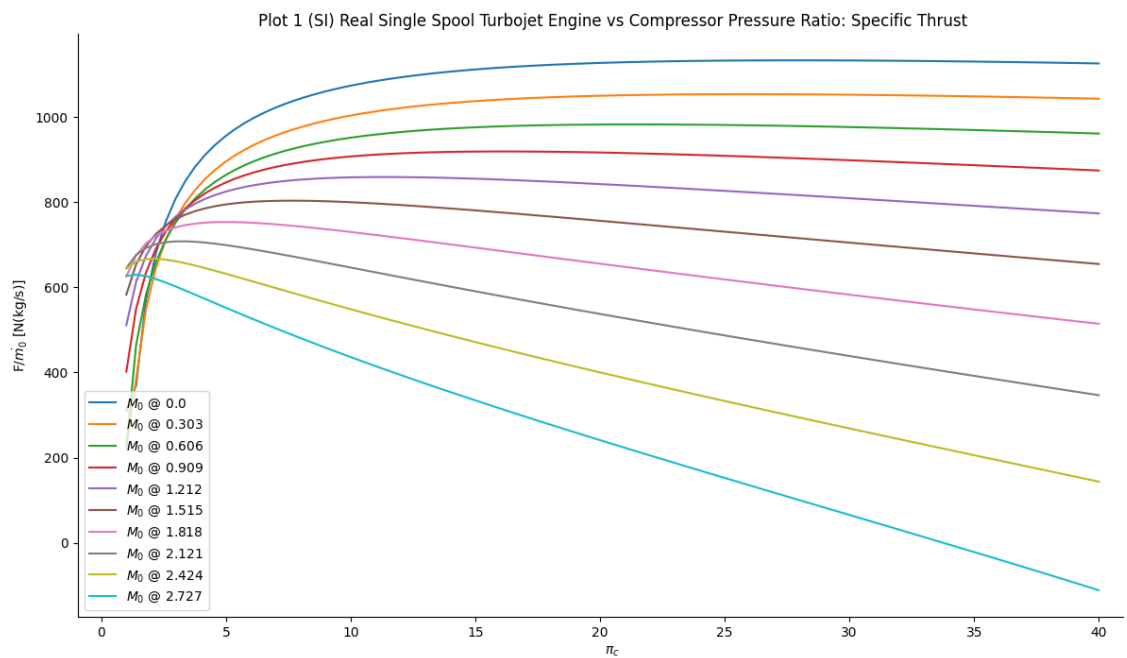
Rc_resphBPTFE:0.28686          Nt_resphBPTFE:93.144
Rt_resphBPTFE:0.28438          Pt9P9_resphBPTFE:30.638
A0_resphBPTFE:299.363          M9_resphBPTFE:2.857
V0_resphBPTFE:239.49           T9T0_resphBPTFE:1.833
M02_resphBPTFE:0.64            V9A0_resphBPTFE:3.782
TauR_resphBPTFE:1.128          Pt19P19_resphBPTFE:2.927
Pir_resphBPTFE:1.524           M19_resphBPTFE:1.34
Nr_resphBPTFE:1                T19T0_resphBPTFE:1.039
Pid_resphBPTFE:0.98            V19A0_resphBPTFE:1.366
Tauram_resphBPTFE:8.16         Tsc_resphBPTFE:295.336
Taucl_resphBPTFE:2.683          Thrust_resphBPTFE:29533.6
Nc_resphBPTFE:87.902           S_resphBPTFE:16.01
Tauf_resphBPTFE:1.252          FR_resphBPTFE:5.458
Nf_resphBPTFE:86.91            NT_resphBPTFE:74.541
f_resphBPTFE:0.02837          NP_resphBPTFE:46.888
Taut_resphBPTFE:0.596          NO_resphBPTFE:34.951
Pit_resphBPTFE:0.11152         ****

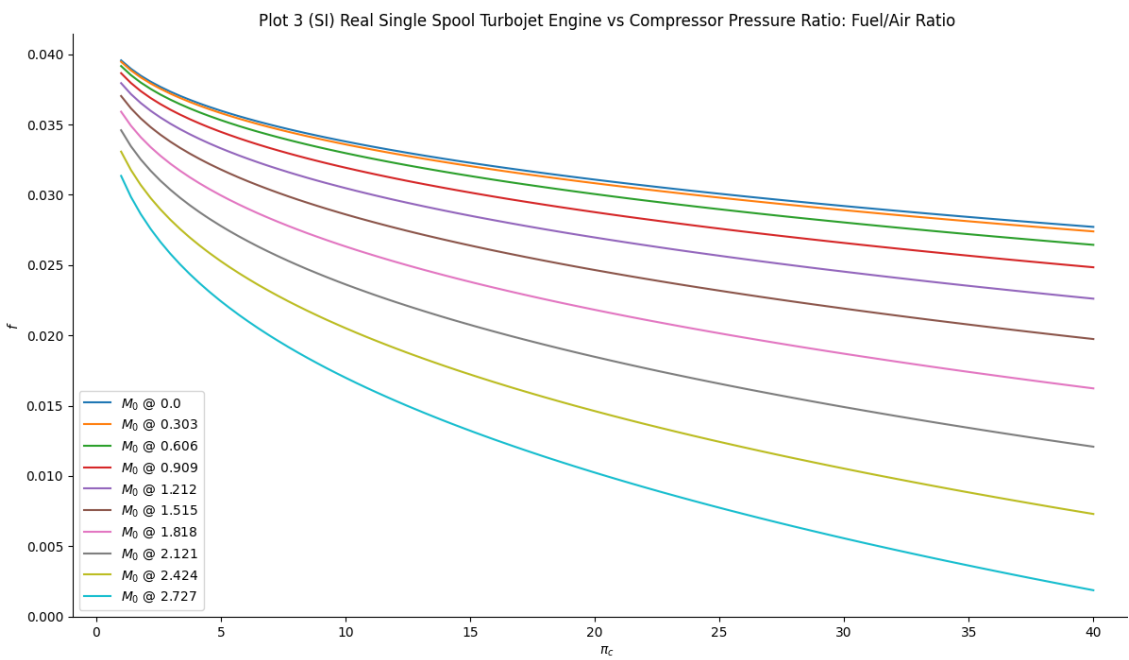
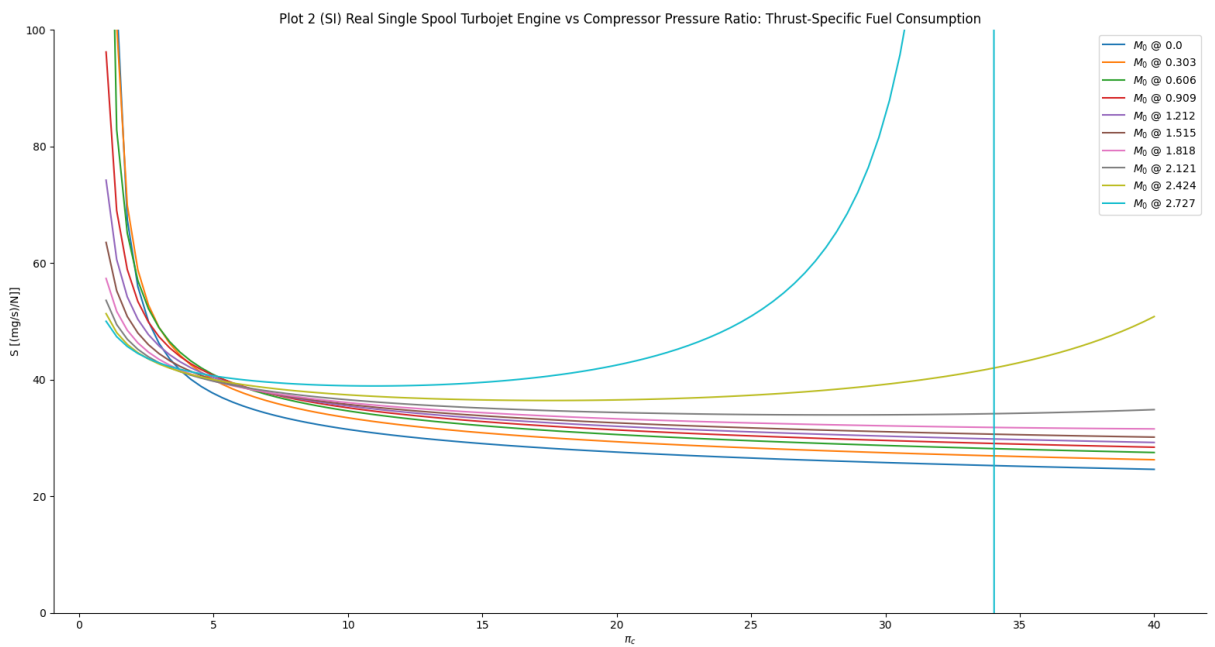
```

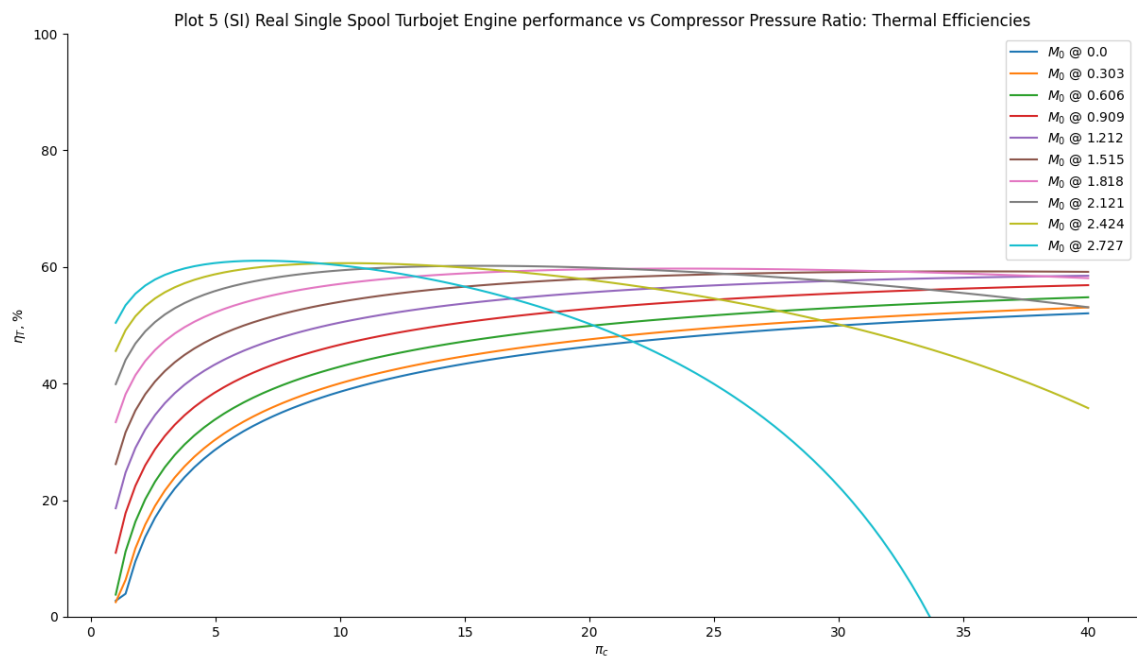
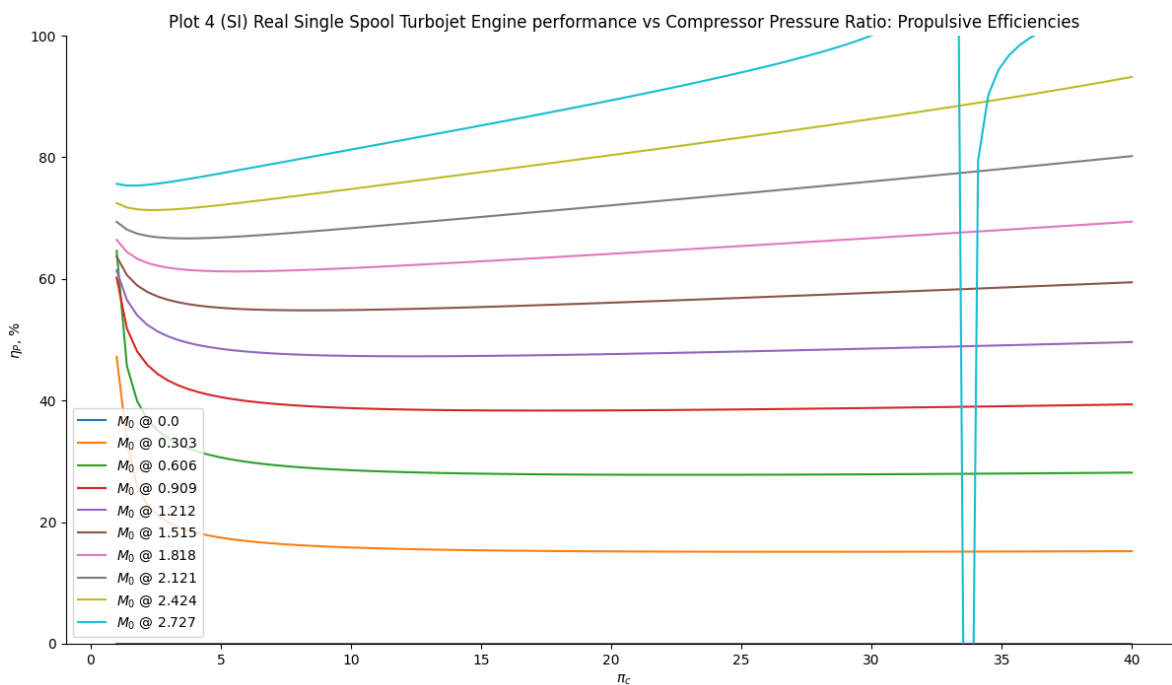
GTA's variation calculation output

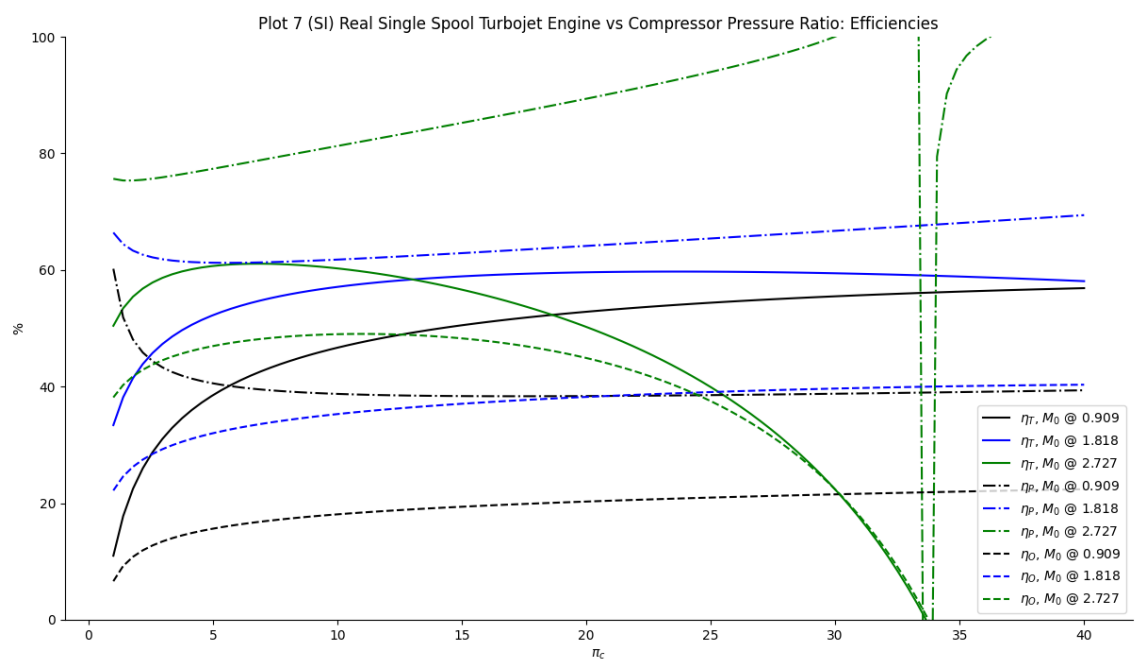
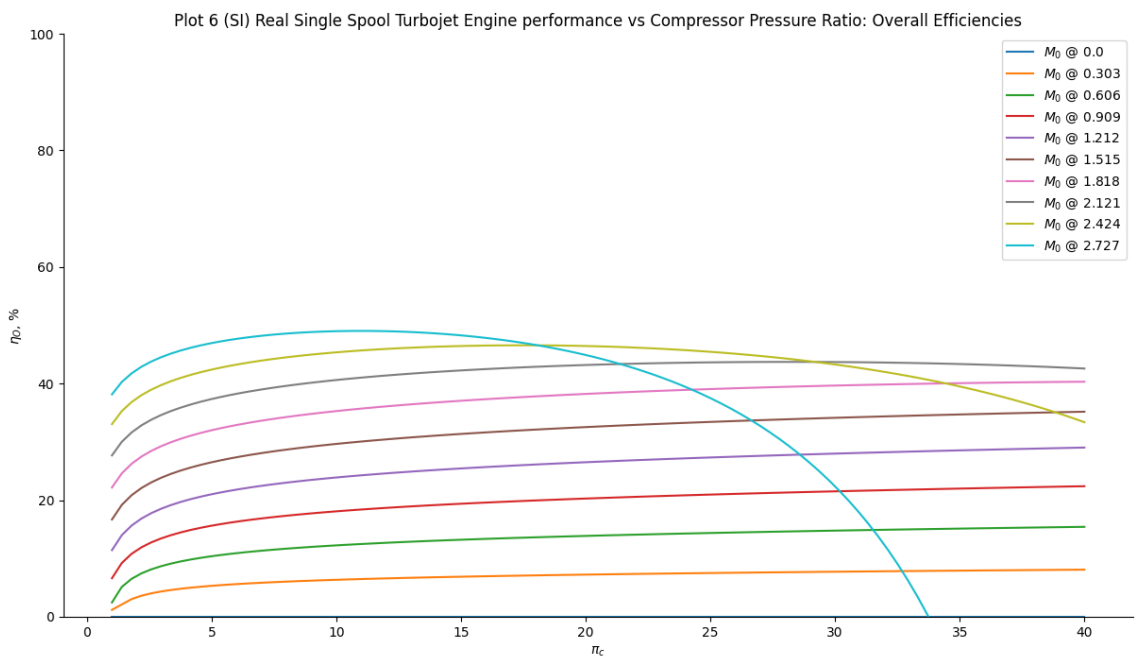
For variation calculation, GTA represents the plot results for three types of engine layouts as Thrust-specific fuel consumption, fuel-to-air ratio, Propulsive, Thermal, Overall efficiency, efficiency comparison, and Thrust ratio (from a high bypass ratio engine).

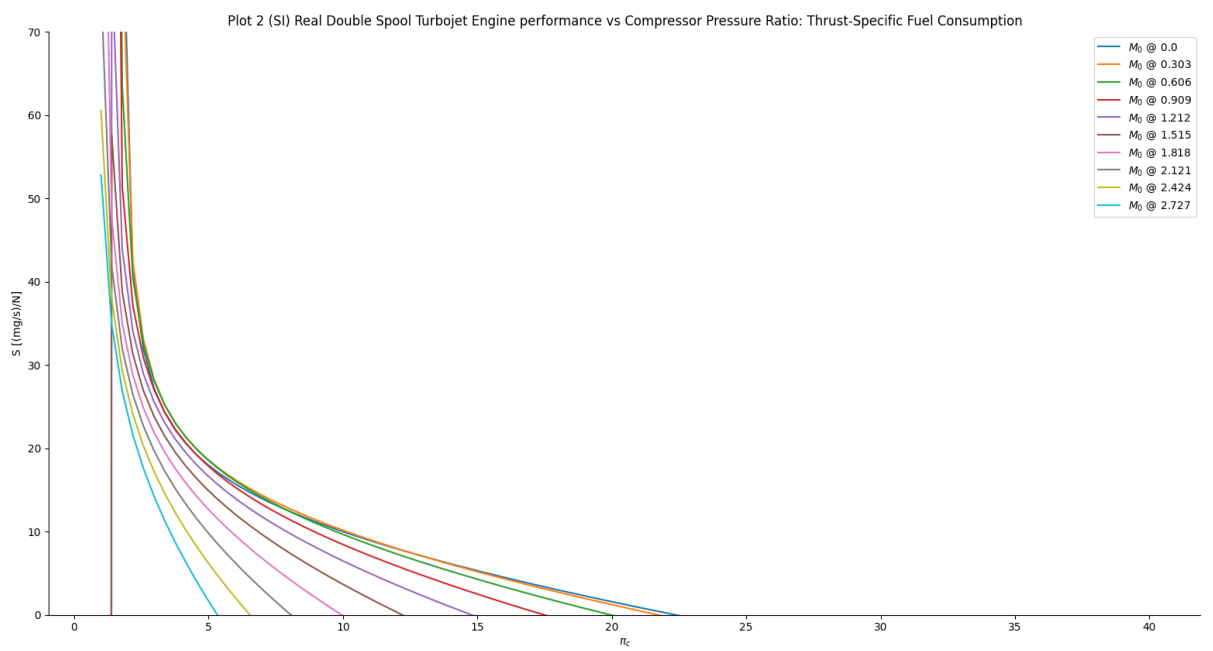
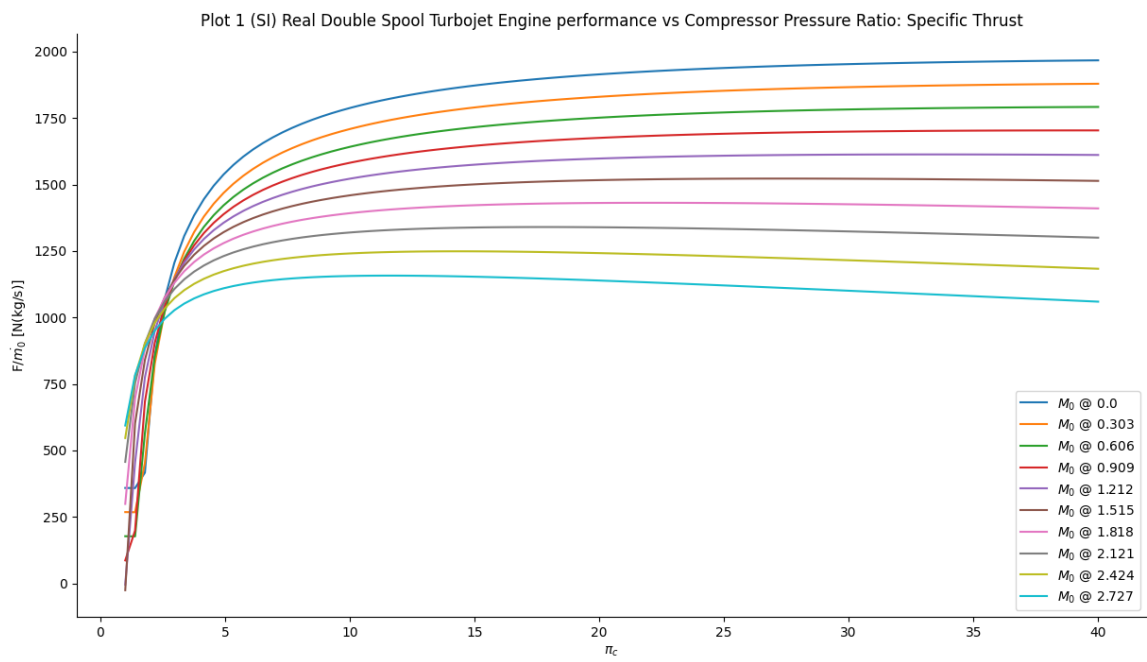
The example output plots are as shown below,

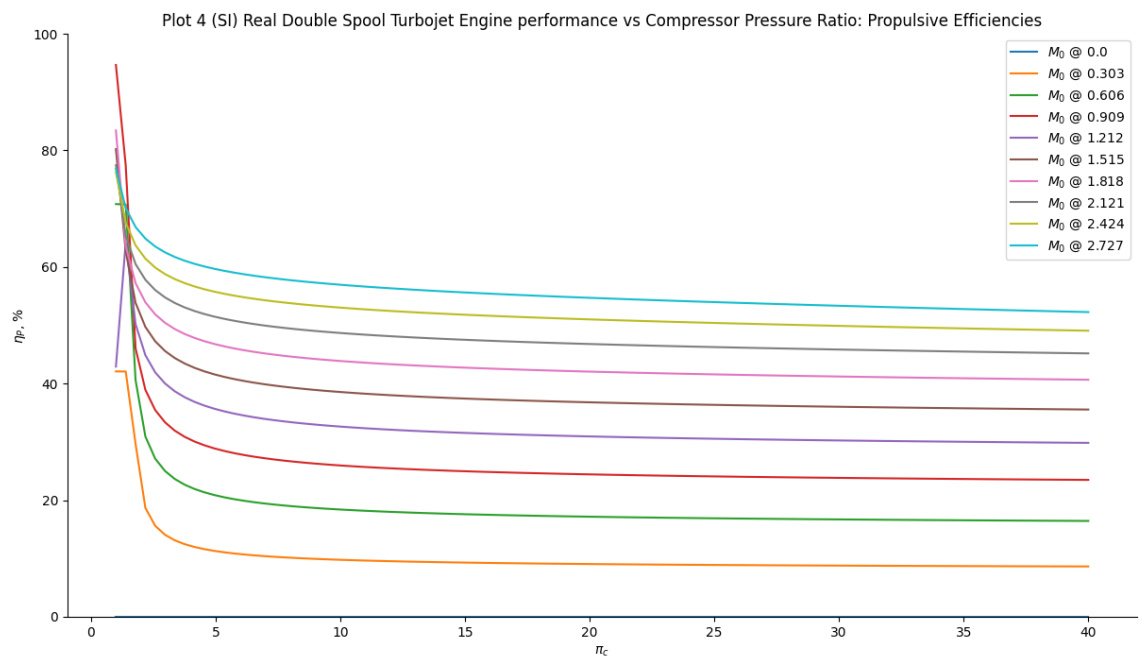
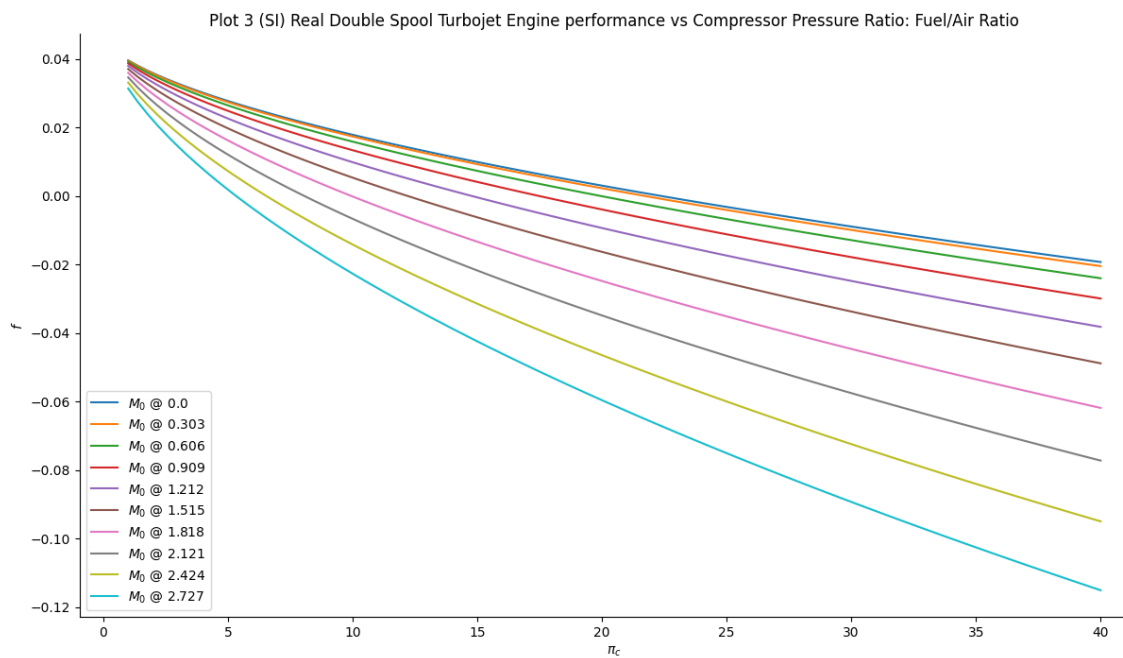


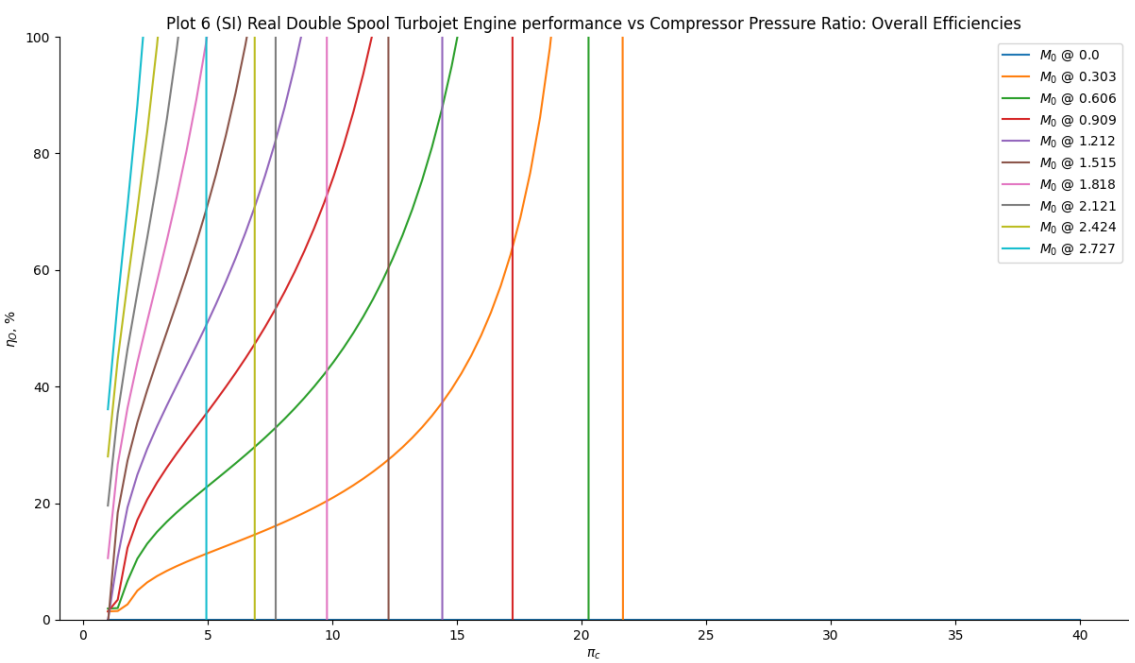
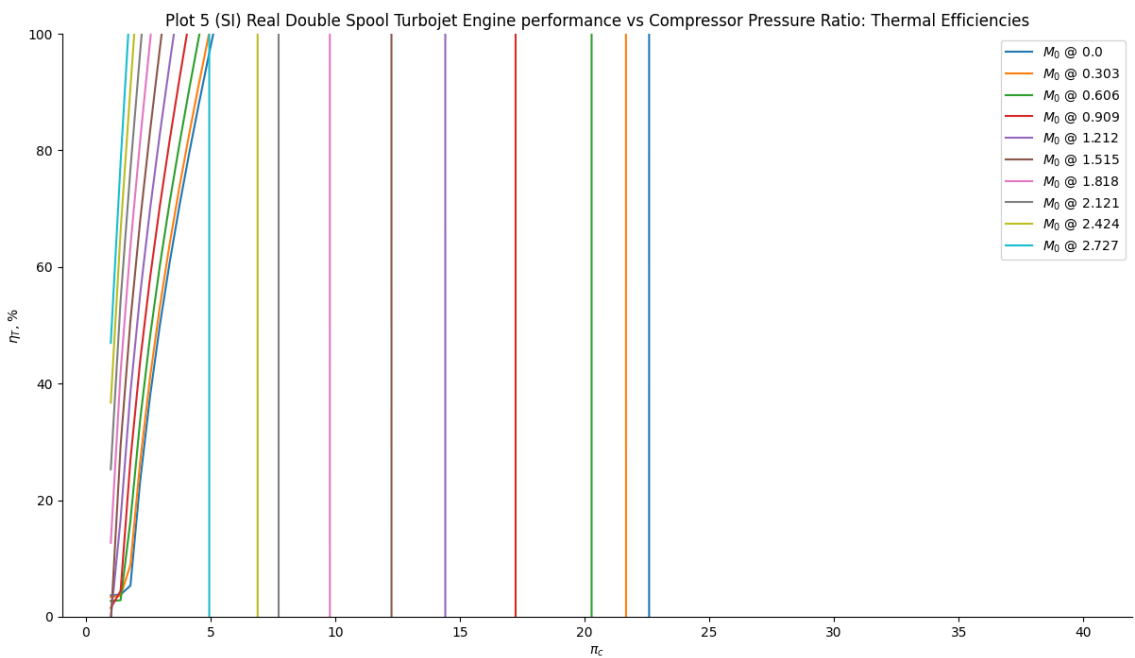


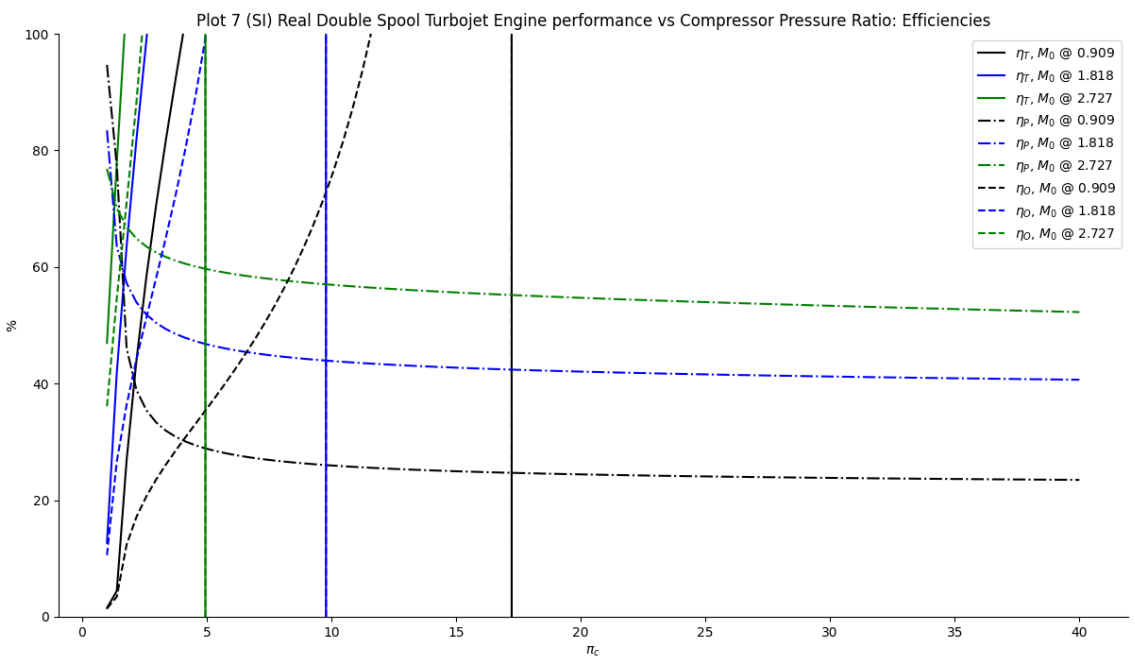




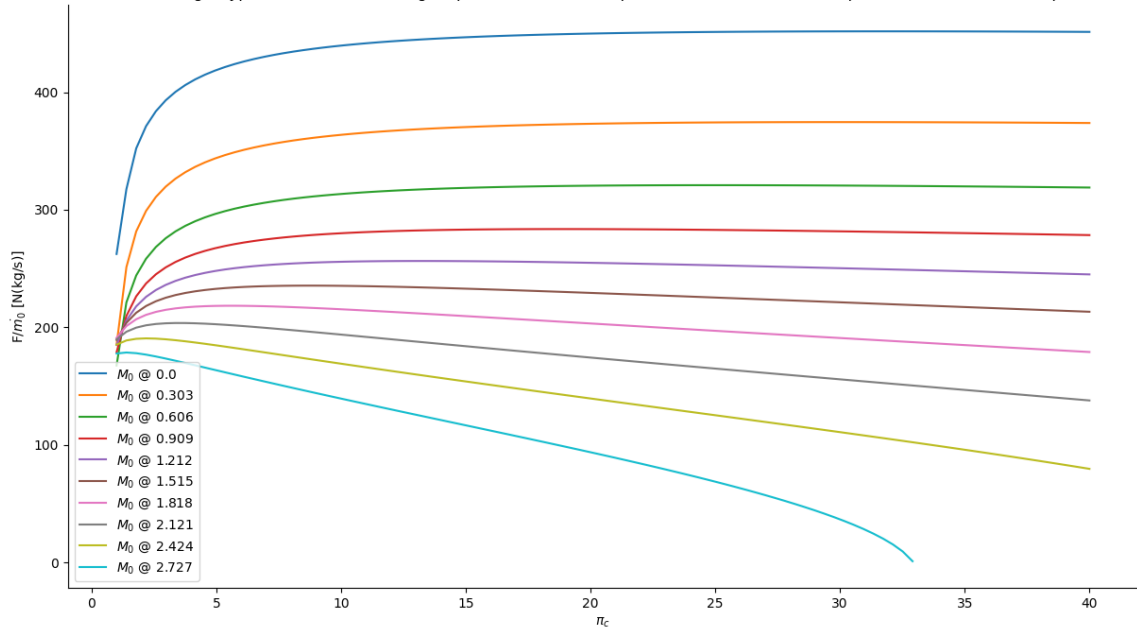








Plot 25 (SI) Real High-Bypass Ratio Turbofan Engine performance vs Compressor Pressure Ratio, for Alpha = 5.0 and Pif = 2.0: Specific Thrust



Plot 26 (SI) Real High-Bypass Ratio Turbofan Engine performance vs Compressor Pressure Ratio, for Alpha = 5.0 and Pif = 2.0: Thrust-Specific Fuel Consumption

